

OPTIMIZATION OF SOLAR RANKINE-CYCLE SYSTEMS

by

Kaushik Chaudhary

Submitted in Partial Fulfillment of the Requirements

for the Degree of

Master of Science

in the

Mechanical Engineering

Program

Prakash A. Damshale  
Adviser

5/12/81  
Date

Lee Rand  
Dean of the Graduate School

5/14/81  
Date

YOUNGSTOWN STATE UNIVERSITY

June, 1981

## ABSTRACT

## OPTIMIZATION OF SOLAR RANKINE-CYCLE SYSTEMS

Kaushik Chaudhary

Master of Science

Youngstown State University, 1981

Solar energy can be converted into electricity very effectively through a Rankine-Cycle operating at high temperatures. The main parameters that affect the overall solar-to-electrical conversion efficiency are studied in detail and the optimum sets of conditions that provide the best efficiency are obtained for a small sized solar plant having a peak power capacity of 100 KW.

The main factors studied in detail are: type of solar collector, Rankine-cycle working fluid and operating temperatures of the solar collector and the Rankine-cycle. The problem is set up such that the influence of these factors can be analyzed simultaneously to arrive at the optimum sets of combinations. Temperatures range from 140 to 1100°F. It was envisaged that at lower temperatures, some of the organic fluids, rather than commonly used water, would generate higher Rankine-cycle efficiencies.

Seven organic fluids that are most desirable for use in a Rankine-cycle are considered. They are: R-11, R-12, R-113, Toluene, Chlorobenzene, Thiophene and Pyridine. Water is included as a reference fluid. Organic fluids, because they are generally found to be in superheated state after expansion through turbine are well suited to take advantage of

regeneration which enhances cycle efficiency significantly. Reheat cycle improves the performance of water/steam power cycle. Thus, two types of cycles are considered: 1) Rankine-Cycle and 2) Rankine-Cycle with regeneration using organic fluids or Rankine-Cycle with reheat using water.

Different types of solar collectors can be used to generate temperatures ranging from 150°F up to 1100°F. The total energy collected per year per unit area using four different generic types of collectors — flat plate, stationary compound parabolic concentrating (CPC), one axis tracking - parabolic trough and two axes tracking - paraboloid disc collector — at different operating temperatures is computed by the use of hourly solar insolation data.

The results of the energy collected by solar collectors and the efficiencies obtained by Rankine-cycles operating at the corresponding temperatures are coupled to arrive at the net electrical energy conversion per year for three climatically different locations — Madison, Wisconsin, Miami, Florida and Albuquerque, New Mexico. It was found that paraboloid disc collector using water as a Rankine-cycle fluid operating at a temperature of 1030°F provides the maximum energy per unit area and also has the least capital cost per unit power output for all three different locations. Analysis indicated that at optimum conditions, for a given collector and power cycle, the choice of Rankine fluid and the corresponding operating temperatures are practically same for all the locations. In a Rankine-cycle, at low temperature, water is found to be far inferior to organic fluids. However, when reheat cycle is used, water gives the efficiency results very comparable to that obtained by organic fluids in a Rankine-cycle with 80% regeneration. The additional energy obtained in Rankine-Cycles with regeneration or reheat cycles at optimum temperatures ranges from 2.5 to 30%.

ACKNOWLEDGEMENTS

I would like to express my deep and sincere thanks to Dr. Prakash Rao Damshala whose valuable suggestions and encouragement made completion of this thesis possible. His patience and guidance are greatly appreciated.

My special thanks to Mrs. Anna Mae Serrecchio for her excellent job in typing and to Mr. Girish Shah for his related help in the area.

CHAPTER

I	INTRODUCTION	1
	Statement of the Problem	5
	Related Work in the Field	6
	Problem Statement	8
	Approach	17
II	RANKINE CYCLE PERFORMANCE	23
III	PERFORMANCE OF RANKINE CYCLE WITH REGENERATION AND REHEAT LOOP	42
IV	PERFORMANCE OF SOLAR COLLECTORS	51
V	COMBINED PERFORMANCE OF SOLAR COLLECTORS AND RANKINE-CYCLE	68
VI	COMBINED PERFORMANCE OF SOLAR COLLECTORS AND RANKINE-CYCLE WITH REGENERATION OF REHEAT LOOP	146
VII	RESULTS AND OPTIMIZATION	199
VIII	DISCUSSIONS AND CONCLUSIONS	208
APPENDIX A		216
APPENDIX B		225
BIBLIOGRAPHY		235
REFERENCES		235

## TABLE OF CONTENTS

	PAGE
ABSTRACT. . . . .	i
ACKNOWLEDGEMENTS. . . . .	iii
TABLE OF CONTENTS . . . . .	iv
LIST OF SYMBOLS . . . . .	v
LIST OF FIGURES . . . . .	ix
LIST OF TABLES. . . . .	xv
CHAPTER	
I    INTRODUCTION. . . . .	1
Statement of the Problem. . . . .	5
Related Work in the Field . . . . .	6
Problem Setup . . . . .	8
Approach. . . . .	17
II   RANKINE-CYCLE PERFORMANCE . . . . .	23
III  PERFORMANCE OF RANKINE-CYCLE WITH REGENERATION OR REHEAT LOOP. . . . .	42
IV   PERFORMANCE OF SOLAR COLLECTORS . . . . .	61
V    COMBINED PERFORMANCE OF SOLAR COLLECTORS AND RANKINE-CYCLE.	88
VI   COMBINED PERFORMANCE OF SOLAR COLLECTORS AND RANKINE-CYCLE WITH REGENERATION OR REHEAT LOOP. . . . .	146
VII  RESULTS AND OPTIMIZATION. . . . .	199
VIII DISCUSSIONS AND CONCLUSIONS . . . . .	209
APPENDIX A. . . . .	216
APPENDIX B. . . . .	225
BIBLIOGRAPHY. . . . .	238
REFERENCES. . . . .	239

## LIST OF SYMBOLS

SYMBOL	DEFINITION	UNITS OR REFERENCE
A	Area	ft <sup>2</sup>
A <sub>C</sub>	Concentrator Aperature Area	ft <sup>2</sup>
A <sub>L</sub>	Fraction of the total collector area from where radiation is not collected	None
C	Concentration Ratio	None
C <sub>PR</sub>	Specific Heat of the Rankine-Cycle Fluid	BTU/lb-°F
C <sub>Pc</sub>	Specific Heat of the Solar Collector Fluid	BTU/lb°F
CPC	Compound Parabolic Concentrating Collector	None
e	Base of Natural Logarithm	None
F	Control Function	None
h	Enthalpy	BTU/lb
h	Convective heat transfer coefficient	BTU/ft <sup>2</sup> -hr-°F
I	Hourly Solar Insolation	BTU/ft <sup>2</sup> -hr
I <sub>coll</sub>	Total Solar Insolation on a collector plane	BTU/ft <sup>2</sup> -hr
I <sub>CPC</sub>	Total Solar Insolation on a CPC collector	BTU/ft <sup>2</sup> -hr
I <sub>d,c</sub>	Direct Solar Insolation on a collector plane	BTU/ft <sup>2</sup> -hr
I <sub>d,CPC</sub>	Direct Solar Insolation on a CPC collector plane	BTU/ft <sup>2</sup> -hr
I <sub>d,h</sub>	Direct Solar Insolation on a horizonial surface	BTU/ft <sup>2</sup> -hr
I <sub>d,n</sub>	Direct Solar Insolation on a surface normal to sunrays	BTU/ft <sup>2</sup> -hr
I <sub>disc</sub>	Direct Solar Insolation on the paraboloid disc collector	BTU/ft <sup>2</sup> -hr

$I_{s,c}$	Scattered solar insolation on a collector surface	BTU/ft <sup>2</sup> -hr
$I_{s,CPC}$	Scattered solar insolation on CPC plane	BTU/ft <sup>2</sup> -hr
$I_{s,h}$	Scattered solar insolation on a horizontal surface	BTU/ft <sup>2</sup> -hr
$I_{t,h}$	Total solar insolation on a horizontal surface	BTU/ft <sup>2</sup> -hr
$I_{trough}$	Direct solar insolation on the parabolic trough collector	BTU/ft <sup>2</sup> -hr
$K_1, K_2$	Constants of proportionality	None
$K_b$	Disc structure blockage factor	None
$K_d$	Dust correction factor	None
$K_T$	Clearness index	None
$\dot{m}$	Mass flow rate	lb/hr
$\dot{m}_R$	Mass flow rate of the Rankine-Cycle fluid	lb/hr
$\dot{m}_c$	Mass flow rate of the solar collector fluid	lb/hr
$n$	day of the year	None
NTU	Number of transfer units	None
$P$	Pressure	lbf/in <sup>2</sup>
$Q_c$	Heat rejected at the condenser	BTU/lb
$Q_{cond}$	Thermal conduction heat losses	BTU/hr
$Q_h$	Heat transferred to the Rankine-Cycle fluid at the boiler	BTU/lb
$Q_s$	Energy content of superheated turbine exhaust	BTU/lb
$Q_{trough}$	Energy absorbed by the parabolic trough collector fluid	BTU/ft <sup>2</sup> -hr
$s$	State along the ideal path	None
$S$	Entropy	BTU/lb-°F

S.R	Product of solar energy collected and Rankine-Cycle efficiency	BTU/ft <sup>2</sup> -yr
S.R <sub>e</sub>	Product of solar energy collected and efficiency of a Rankine-Cycle with regeneration or reheat	BTU/ft <sup>2</sup> -yr
T	Temperature	°F
T <sub>a</sub> or T <sub>∞</sub>	Ambient temperature	°F or °R
T <sub>avg</sub>	Collector fluid average temperature	°F
T <sub>c1</sub>	Temperature of the fluid coming out of the solar collector array	°F
T <sub>c2</sub>	Temperature of the fluid going into the solar collector array	°F
T <sub>f,in</sub>	Temperature of the fluid going into the collector module	°F
T <sub>f,out</sub>	Temperature of the fluid coming out of the collector module	°F
T <sub>r</sub>	Receiver inner surface temperature	°F
T <sub>R</sub>	Rankine-Cycle fluid maximum temperature	°F
T <sub>s</sub>	Temperature at the saturated state	°F
v	Specific volume	ft <sup>3</sup> /lb
V <sub>s</sub>	Solar azimuth angle	degrees of arc
Z	Zenith angle	degrees of arc
α <sub>e</sub>	Absorptivity	None
β	Slope angle	degrees of arc
γ	Intercept factor	None
δ	Declination angle	degrees of arc
ε	Effectiveness of a heat exchanger	None
ε <sub>B</sub>	Effectiveness of a boiler heat exchanger	None
ε <sub>e</sub>	Emissivity	None
η	Efficiency	None
η <sub>avg, coll</sub>	Average efficiency of the collector	None



$\eta_{\text{avg,CPC}}$	Average efficiency of the CPC collector	None
$\eta_{\text{coll}}$	Efficiency of the collector	None
$\eta_{\text{CPC}}$	Instantaneous efficiency of the CPC Collector	None
$\eta_{\text{p}}$	Efficiency of the pump	None
$\eta_{\text{R}}$	Rankine-cycle efficiency	None
$\eta_{\text{Re}}$	Efficiency of a Rankine-cycle with regeneration or reheat loop	None
$\eta_{\text{t}}$	Efficiency of a turbine	None
$\eta_{\text{trough}}$	Efficiency of the parabolic trough collector	None
$\theta$	Angle between the collector normal and sunrays	degrees of arc
$\theta_{\text{c}}$	Half acceptance angle of a CPC collector	degrees of arc
$\theta_{\text{i}}$	Acceptance angle of a CPC collector	degrees of arc
$\rho$	Reflectivity of concentrator surface	None
$\sigma$	Stefan-Boltzmann constant $0.1714 \times 10^{-8}$	BTU/ft <sup>2</sup> -°R <sup>4</sup> -hr
$\phi$	Latitude angle of the location	degrees of arc
$\omega$	Hour angle	degrees of arc
$\omega_{\text{p}}$	Work input in the pump	BTU/lb
$\omega_{\text{t}}$	Work output of the turbine	BTU/lb

## LIST OF FIGURES

FIGURE		PAGE
1.	Schematic Diagram of a Simple Rankine-Cycle. . . . .	4
2.	Schematic Diagram of a Basic Solar Rankine-Cycle . . . . .	8
3.	Saturation - State Vapor line and Rankine-Cycle on a Temperature-Entropy Diagram for Water/Steam . . . . .	11
4.	Saturation - State Vapor line and Rankine-Cycle on a Temperature-Entropy Diagram for a Typical Organic Fluid . . . . .	12
5.	Rankine-Cycle Efficiency vs. Rankine-Cycle Maximum Temperature Curves for Different Fluids . . . . .	17
6.	Solar Collector Efficiency Curves for Different Types of Collectors . . . . .	18
7.	Energy collected Per Year Per Unit Area vs. Collector Fluid Average Temperature Curves for Different Types of Collector. . . . .	19
8.	Net Energy Conversion vs. Operating Temperature Curve for One Possible Combination . . . . .	21
9.	Schematic Diagram of a Rankine-Cycle . . . . .	23
10.	A Curve of Rankine-Cycle Efficiency vs. Rankine-Cycle Maximum Temperature for R-11 . . . . .	34
11.	A Curve of Rankine-Cycle Efficiency vs. Rankine-Cycle Maximum Temperature for R-12 . . . . .	35
12.	A Curve of Rankine-Cycle Efficiency vs. Rankine-Cycle Maximum Temperature for R-113. . . . .	36
13.	A Curve of Rankine-Cycle Efficiency vs. Rankine-Cycle Maximum Temperature for Toluene. . . . .	37
14.	A Curve of Rankine-Cycle Efficiency vs. Rankine-Cycle Maximum Temperature for Chlorobenzene. . . . .	38
15.	A Curve of Rankine-Cycle Efficiency vs. Rankine-Cycle Maximum Temperature for Thiophene. . . . .	39
16.	A Curve of Rankine-Cycle Efficiency vs. Rankine-Cycle Maximum Temperature for Pridine. . . . .	40
17.	A Curve of Rankine-Cycle Efficiency vs. Rankine-Cycle Maximum Temperature for Water. . . . .	41
18.	Schematic Diagram of a Rankine-Cycle with Simple Regeneration. . . . .	42

	PAGE
19. Schematic Diagram of a Rankine-Cycle with One-Step Reheat. . .	44
20. Efficiency of a Rankine-Cycle with 80% Regeneration vs. Cycle Maximum Temperature for R-11 . . . . .	49
21. Efficiency of a Rankine-Cycle with 80% Regeneration vs. Cycle Maximum Temperature for R-12 . . . . .	50
22. Efficiency of a Rankine-Cycle with 80% Regeneration vs. Cycle Maximum Temperature for R-113. . . . .	51
23. Efficiency of a Rankine-Cycle with 80% Regeneration vs. Cycle Maximum Temperature for Toluene. . . . .	52
24. Efficiency of a Rankine-Cycle with 80% Regeneration vs. Cycle Maximum Temperature for Chlorobenzene. . . . .	53
25. Efficiency of a Rankine-Cycle with 80% Regeneration vs. Cycle Maximum Temperature for Thiophene. . . . .	54
26. Efficiency of a Rankine-Cycle with 80% Regeneration vs. Cycle Maximum Temperature for Pyridine . . . . .	55
27. Reheat Cycle Efficiency vs. Maximum Cycle Temperature Curve for Water/Steam. . . . .	60
28. Schematics of a Solar Collector Loop . . . . .	61
29. A Flat Plate Solar Collector . . . . .	62
30. Flat Plate Collector Performance Curve . . . . .	64
31. Typical CPC Collector. . . . .	69
32. Cross-Section of a CPC . . . . .	69
33. CPC Performance Curve. . . . .	71
34. (a) Plan Showing Solar Azimuth Angle- $V_s$ . . . . .	71
(b) Projection on a North-South Plane of CPC Acceptance Angles and Slope. . . . .	71
35. Parabolic Trough Collector . . . . .	75
36. Performance of a Parabolic Trough Solar Collector. . . . .	75
37. Point-Focusing Paraboloid Disc Collector . . . . .	79
38. Graph of Solar Energy Collected by Different Collectors Per ft <sup>2</sup> Area vs. Collector Fluid Average Temperature for Madison, WI . . . . .	83

39.	Graph of Solar Energy Collected by Different Collectors per ft <sup>2</sup> Area vs. Collector Fluid Average Temperature for Miami, FL . .	84
40.	Graph of Solar Energy Collected by Different Collectors per ft <sup>2</sup> Area vs. Collector Fluid Average Temperature for Albuquerque, NM	85
41.	Boiler-Heat Exchanger with Two Heat Transfer Processes Separated. . . . .	89
42.	Boiler-Heat Exchanger in a Water/Steam Rankine-Cycle with Heat Transfer Processes Separated . . . . .	94
43.	Curves of S.R Values vs. Operating Temperature for a Combination of a Flat Plate Collector and R-11 for Three Locations .	99
44.	Curves of S.R Values vs. Operating Temperature for a Combination of a Flat Plate Collector and R-12 for Three Locations.	101
45.	Curves of S.R Values vs. Operating Temperature for a Combination of a Flat Plate Collector and R-113 for Three Locations. . . . .	103
46.	Curves of S.R Values vs. Operating Temperature for a Combination of a CPC Collector and R-11 for Three Locations . . . .	105
47.	Curves of S.R Values vs. Operating Temperature for a Combination of a CPC Collector and R-12 for Three Locations . . . .	107
48.	Curves of S.R Values vs. Operating Temperature for a Combination of a CPC Collector and R-113 for Three Locations. . . .	109
49.	Curves of S.R Values vs. Operating Temperature for a Combination of a CPC Collector and Toluene for Three Locations. . .	111
50.	Curves of S.R Values vs. Operating Temperature for a Combination of a CPC Collector and Chlorobenzene for Three Locations. . . . .	113
51.	Curves of S.R Values vs. Operating Temperature for a Combination of a CPC Collector and Thiophene for Three Locations. .	115
52.	Curves of S.R Values vs. Operating Temperature for a Combination of a CPC Collector and Pyridine for Three Locations . .	117
53.	Curves of S.R Values vs. Operating Temperature for a Combination of a CPC Collector and Water for Three Locations. . . .	119
54.	Curves of S.R Values vs. Operating Temperature for a Combination of a Parabolic Trough Collector and R-11 for Three Locations. . . . .	121

	PAGE
55. Curves of S.R Values vs. Operating Temperature for a Combination of Parabolic Trough Collector and R-12 for Three Locations. . . . .	123
56. Curves of S.R Values vs. Operating Temperature for a Combination of a Parabolic Trough Collector and R-113 for Three Locations. . . . .	125
57. Curves of S.R Values vs. Operating Temperature for a Combination of a Parabolic Trough Collector and Toluene for Three Locations. . . . .	127
58. Curves of S.R Values vs. Operating Temperature for a Combination of a Parabolic Trough Collector and Chlorobenzene for Three Locations. . . . .	129
59. Curves of S.R Values vs. Operating Temperature for a Combination of a Parabolic Trough Collector and Thiophene for Three Locations. . . . .	131
60. Curves of S.R Values vs. Operating Temperature for a Combination of a Parabolic Trough Collector and Pyridine for Three Locations. . . . .	133
61. Curves of S.R Values vs. Operating Temperature for a Combination of a Parabolic Trough Collector and Water for Three Locations. . . . .	135
62. Curves of S.R Values vs. Operating Temperature for a Combination of a Paraboloid Disc Collector and Toluene for Three Locations. . . . .	137
63. Curves of S.R Values vs. Operating Temperature for a Combination of a Paraboloid Disc Collector and Chlorobenzene for Three Locations. . . . .	139
64. Curves of S.R Values vs. Operating Temperature for a Combination of a Paraboloid Disc Collector and Thiophene for Three Locations. . . . .	141
65. Curves of S.R Values vs. Operating Temperature for a Combination of a Paraboloid Disc Collector and Pyridine for Three Locations. . . . .	143
66. Curves of S.R Values vs. Operating Temperature for a Combination of a Paraboloid Disc Collector and Water for Three Locations. . . . .	145
67. Boiler Heat Exchanger in a Water/Steam Reheat Cycle with Different Heat Transfer Processes Separated. . . . .	147

68.	Curves of $S.R_e$ Values vs. Operating Temperature for a Combination of a Flat Plate Collector and R-11 for Three Locations .	152
69.	Curves of $S.R_e$ Values vs. Operating Temperature for a Combination of a Flat Plate Collector and R-12 for Three Locations .	154
70.	Curves of $S.R_e$ Values vs. Operating Temperature for a Combination of a Flat Plate Collector and R-113 for Three Locations.	156
71.	Curves of $S.R_e$ Values vs. Operating Temperature for a Combination of a CPC Collector and R-11 for Three Locations. . . . .	158
72.	Curves of $S.R_e$ Values vs. Operating Temperature for a Combination of a CPC Collector and R-12 for Three Locations. . . . .	160
73.	Curves of $S.R_e$ Values vs. Operating Temperature for a Combination of a CPC Collector and R-113 for Three Locations . . . . .	162
74.	Curves of $S.R_e$ Values vs. Operating Temperature for a Combination of a CPC Collector and Toluene for Three Locations . . .	164
75.	Curves of $S.R_e$ Values vs. Operating Temperature for a Combination of a CPC Collector and Chlorobenzene for Three Locations	166
76.	Curves of $S.R_e$ Values vs. Operating Temperature for a Combination of a CPC Collector and Thiophene for Three Locations . .	168
77.	Curves of $S.R_e$ Values vs. Operating Temperature for a Combination of a CPC Collector and Pyridine for Three Locations. . .	170
78.	Curves of $S.R_e$ Values vs. Operating Temperature for a Combination of a CPC Collector and Water for Three Locations . . . . .	172
79.	Curves of $S.R_e$ Values vs. Operating Temperature for a Combination of a Parabolic Trough Collector and R-11 for Three Locations. . . . .	174
80.	Curves of $S.R_e$ Values vs. Operating Temperature for a Combination of a Parabolic Trough Collector and R-12 for Three Locations . . . . .	176
81.	Curves of $S.R_e$ Values vs. Operating Temperature for a Combination of a Parabolic Trough Collector and R-113 for Three Locations . . . . .	178
82.	Curves of $S.R_e$ Values vs. Operating Temperature for a Combination of a Parabolic Trough Collector and Toluene for Three Locations . . . . .	180

83.	Curves of $S.R_e$ Values vs. Operating Temperature for a Combination of a Parabolic Trough Collector and Chlorobenzene for Three Locations. . . . .	182
84.	Curves of $S.R_e$ Values vs. Operating Temperature for a Combination of a Parabolic Trough Collector and Thiophene for Three Locations. . . . .	184
85.	Curves of $S.R_e$ Values vs. Operating Temperature for a Combination of a Parabolic Trough Collector and Pyridine for Three Locations. . . . .	186
86.	Curves of $S.R_e$ Values vs. Operating Temperature for a Combination of a Parabolic Trough Collector and Water for Three Locations. . . . .	188
87.	Curves of $S.R_e$ Values vs. Operating Temperature for a Combination of a Paraboloid Disc Collector and Toluene for Three Locations. . . . .	190
88.	Curves of $S.R_e$ Values vs. Operating Temperature for a Combination of a Paraboloid Disc Collector and Chlorobenzene for Three Locations. . . . .	192
89.	Curves of $S.R_e$ Values vs. Operating Temperature for a Combination of a Paraboloid Disc Collector and Thiophene for Three Locations. . . . .	194
90.	Curves of $S.R_e$ Values vs. Operating Temperature for a Combination of a Paraboloid Disc Collector and Pyridine for Three Locations. . . . .	196
91.	Curves of $S.R_e$ Values vs. Operating Temperature for a Combination of a Paraboloid Disc Collector and Water for Three Locations. . . . .	198

## LIST OF TABLES

TABLE	PAGE
1. Rankine-Cycle Efficiencies at Several Different Rankine-Cycle Maximum Temperatures Using R-11. . . . .	34
2. Rankine-Cycle Efficiencies at Several Different Rankine-Cycle Maximum Temperatures Using R-12. . . . .	35
3. Rankine-Cycle Efficiencies at Several Different Rankine-Cycle Maximum Temperatures Using R-113 . . . . .	36
4. Rankine-Cycle Efficiencies at Several Different Rankine-Cycle Maximum Temperatures Using Toluene . . . . .	37
5. Rankine-Cycle Efficiencies at Several Different Rankine-Cycle Maximum Temperatures Using Chlorobenzene . . . . .	38
6. Rankine-cycle Efficiencies at Several Different Rankine-Cycle Maximum Temperatures Using Thiophene . . . . .	39
7. Rankine-Cycle Efficiencies at Several Different Rankine-Cycle Maximum Temperatures Using Pyridine. . . . .	40
8. Rankine-Cycle Efficiencies at Several Different Rankine-Cycle Maximum Temperatures Using Water . . . . .	41
9. Efficiency of a Rankine-Cycle with 80% Regeneration at Several Different Heat Source Temperatures Using R-11. . . . .	49
10. Efficiency of a Rankine-Cycle with 80% Regeneration at Several Different Heat Source Temperatures Using R-12. . . . .	50
11. Efficiency of a Rankine-Cycle with 80% Regeneration at Several Different Heat Source Temperatures Using R-113 . . . . .	51
12. Efficiency of a Rankine-Cycle with 80% Regeneration at Several Different Heat Source Temperatures Using Toluene . . . . .	52
13. Efficiency of a Rankine-Cycle with 80% Regeneration at Several Different Heat Source Temperatures Using Cholobenzene. . . . .	53
14. Efficiency of a Rankine-Cycle with 80% Regeneration at Several Different Heat Source Temperatures Using Thiophene . . . . .	54
15. Efficiency of a Rankine-Cycle with 80% Regeneration at Several Different Heat Source Temperatures Using Pyridine. . . . .	55
16. Water/Steam Reheat Cycle Efficiencies at Several Different Heat Source Temperatures. . . . .	60
17. Solar Energy Collected by Flat Plate Collector per ft <sup>2</sup> Area Per Year for Three Locations (BTU/ft <sup>2</sup> -Year). . . . .	69



	PAGE
18. Solar Energy Collected by CPC Collector Per ft <sup>2</sup> Area Per Year for Three Locations. (BTU/ft <sup>2</sup> .Year). . . . .	74
19. Solar Energy Collected by Parabolic Trough Collector Per ft <sup>2</sup> Area Per Year for Three Locations. (BTU/ft <sup>2</sup> .Year). . . . .	78
20. Solar Energy Collected by Paraboloid Disc Collector Per ft <sup>2</sup> Area Per Year for Three Locations. (BTU/ft <sup>2</sup> .Year). . . . .	82
21. S.R Values at Several Temperatures for a Combination of a Flat Plate Collector and R-11 for Three Different Locations . . . .	98
22. S.R Values at Several Temperatures for a Combination of a Flat Plate Collector and R-12 for Three Different Locations . . . .	100
23. S.R Values at Several Temperatures for a Combination of a Flat Plate Collector and R-113 for Three Different Locations. . . .	102
24. S.R. Values at Several Temperatures for a Combination of a CPC Collector and R-11 for Three Different Locations . . . . .	104
25. S.R Values at Several Temperatures for a Combination of a CPC Collector and R-12 for Three Different Locations . . . . .	106
26. S.R Values at Several Temperatures for a Combination of a CPC Collector and R-113 for Three Different Locations. . . . .	108
27. S.R Values at Several Temperatures for a Combination of a CPC Collector and Toluene for Three Different Locations. . . . .	110
28. S.R Values at Several Temperatures for a Combination of a CPC Collector and Chlorobenzene for Three Different Locations. . . .	112
29. S.R Values at Several Temperatures for a Combination of a CPC Collector and Thiophene for Three Different Locations. . . . .	114
30. S.R Values at Several Temperatures for a Combination of a CPC Collector and Pyridine for Three Different Locations . . . . .	116
31. S.R Values at Several Temperatures for a Combination of a CPC Collector and Water for Three Different Locations. . . . .	118
32. S.R Values at Several Temperatures for a Combination of a Parabolic Trough Collector and R-11 for Three Different Locations. . . . .	120
33. S.R Values at Several Temperatures for a Combination of a Parabolic Trough Collector and R-12 for Three Different Locations. . . . .	122

	PAGE
34. S.R Values at Several Temperatures for a Combination of a Parabolic Trough Collector and R-113 for Three Different Locations. . . . .	124
35. S.R Values at Several Temperatures for a Combination of a Parabolic Trough Collector and Toluene for Three Different Locations. . . . .	126
36. S.R Values at Several Temperatures for a Combination of a Parabolic Trough Collector and Chlorobenzene for Three Different Locations. . . . .	128
37. S.R Values at Several Temperatures for a Combination of a Parabolic Trough Collector and Thiophene for Three Different Locations. . . . .	130
38. S.R Values at Several Temperatures for a Combination of a Parabolic Trough Collector and Pyridine for Three Different Locations. . . . .	132
39. S.R Values at Several Temperatures for a Combination of a Parabolic Trough Collector and Water for Three Different Locations. . . . .	134
40. S.R Values at Several Temperatures for a Combination of a Paraboloid Disc Collector and Toluene for Three Different Locations. . . . .	136
41. S.R Values at Several Temperatures for a Combination of a Paraboloid Disc Collector and Chlorobenzene for Three Different Locations. . . . .	138
42. S.R Values at Several Temperatures for a Combination of a Paraboloid Disc Collector and Thiophene for Three Different Locations. . . . .	140
43. S.R Values at Several Temperatures for a Combination of a Paraboloid Disc Collector and Pyridine for Three Different Locations. . . . .	142
44. S.R Values at Several Temperatures for a Combination of a Paraboloid Disc Collector and Water for Three Different Locations. . . . .	144
45. $S.R_e$ Values at Several Temperatures for a Combination of a Flat Plate Collector and R-11 for Three Different Locations . . . .	151
46. $S.R_e$ Values at Several Temperatures for a Combination of a Flat Plate Collector and R-12 for Three Different Locations . . . .	153
47. $S.R_e$ Values at Several Temperatures for a Combination of a Flat Plate Collector and R-113 for Three Different Locations. . . .	155

	PAGE
48. S. <sub>Re</sub> Values at Several Temperatures for a Combination of a CPC Collector and R-11 for Three Different Locations. . . . .	157
49. S. <sub>Re</sub> Values at Several Temperatures for a Combination of a CPC Collector and R-12 for Three Different Locations. . . . .	159
50. S. <sub>Re</sub> Values at Several Temperatures for a Combination of a CPC Collector and R-113 for Three Different Locations . . . . .	161
51. S. <sub>Re</sub> Values at Several Temperatures for a Combination of a CPC Collector and Toluene for Three Different Locations . . . . .	163
52. S. <sub>Re</sub> Values at Several Temperatures for a Combination of a CPC Collector and Chlorobenzene for Three Different Locations . .	165
53. S. <sub>Re</sub> Values at Several Temperatures for a Combination of a CPC Collector and Thiophene for Three Different Locations . . . . .	167
54. S. <sub>Re</sub> Values at Several Temperatures for a Combination of a CPC Collector and Pyridine for Three Different Locations. . . . .	169
55. S. <sub>Re</sub> Values at Several Temperatures for a Combination of a CPC Collector and Water for Three Different Locations . . . . .	171
56. S. <sub>Re</sub> Values at Several Temperatures for a Combination of a Parabolic Trough Collector and R-11 for Three Different Locations . . . . .	173
57. S. <sub>Re</sub> Values at Several Temperatures for a Combination of a Parabolic Trough Collector and R-12 for Three Different Locations . . . . .	175
58. S. <sub>Re</sub> Values at Several Temperatures for a Combination of a Parabolic Trough Collector and R-113 for Three Different Locations . . . . .	177
59. S. <sub>Re</sub> Values at Several Temperatures for a Combination of a Parabolic Trough Collector and Toluene for Three Different Locations . . . . .	179
60. S. <sub>Re</sub> Values at Several Temperatures for a Combination of a Parabolic Trough Collector and Chlorobenzene for Three Different Locations . . . . .	181
61. S. <sub>Re</sub> Values at Several Temperatures for a Combination of a Parabolic Trough Collector and Thiophene for Three Different Locations . . . . .	183
62. S. <sub>Re</sub> Values at Several Temperatures for a Combination of a Parabolic Trough Collector and Pyridine for Three Different Locations . . . . .	185

	PAGE
63. S. <sub>e</sub> Values at Several Temperatures for a Combination of a Parabolic Trough Collector and Water for Three Different Locations. . . . .	187
64. S. <sub>e</sub> Values at Several Temperatures for a Combination of a Paraboloid Disc Collector and Toluene for Three Different Locations. . . . .	189
65. S. <sub>e</sub> Values at Several Temperatures for a Combination of a Paraboloid Disc Collector and Chlorobenzene for Three Different Locations. . . . .	191
66. S. <sub>e</sub> Values at Several Temperatures for a Combination of a Paraboloid Disc Collector and Thiophene for Three Different Locations. . . . .	193
67. S. <sub>e</sub> Values at Several Temperatures for a Combination of a Paraboloid Disc Collector and Pyridine for Three Different Locations. . . . .	195
68. S. <sub>e</sub> Values at Several Temperatures for a Combination of a Paraboloid Disc Collector and Water for Three Different Locations. . . . .	197
69. Summary of Maximum S.R Values and Corresponding Optimum Temperature for all Possible Combinations Using Rankine-Cycle.	200
70. Optimum Working Fluid and Corresponding Rankine-Cycle Maximum Temperature for Each Type of Collector Using Rankine-Cycle for Madison, WI. . . . .	201
71. Optimum Working Fluid and Corresponding Rankine-Cycle Maximum Temperature for Each Type of Collector Using Rankine-Cycle for Miami, FL. . . . .	201
72. Optimum Working Fluid and Corresponding Rankine-Cycle Maximum Temperature for Each type of Collector Using Rankine-Cycle for Albuquerque, NM. . . . .	201
73. Summary of Maximum S. <sub>e</sub> Values and Corresponding Optimum Temperature for all Possible Combinations Using Rankine-Cycle with Regeneration or Reheat Loop . . . . .	202
74. Optimum Working Fluid and Corresponding Power Cycle Maximum Temperature for Each Type of Collector Using Rankine-Cycle with Regeneration or Reheat Loop for Madison, WI . . . . .	203
75. Optimum Working Fluid and Corresponding Power Cycle Maximum Temperature for Each Type of Collector Using a Rankine-Cycle with Regeneration or Reheat Loop for Miami, FL . . . . .	203

76. Optimum Working Fluid and Corresponding Power Cycle Maximum Temperature for Each Type of Collector Using Rankine-Cycle with Regeneration or Reheat Loop for Albuquerque, NM. . . . . 203

77. First Cost of Different Types of Collectors Using Rankine-Cycle for 5000 KWH Output Per Year at Three Different Locations . . . . . 206

78. First Cost of Different Types of Collectors Using Rankine-Cycle with Regeneration or Reheat Loop for 5000 KWH Output Per Year at Three Different Locations (\$) . . . . . 207

energy is used for the same amount of work as before. At all the energy sources in the United States, in 1974, 41% was derived from three fossil fuels - oil, coal and gas - which together with about 45% of the total energy consumption. Unfortunately, the supply of the fossil fuels is not infinite. In less than a century, about 14% of the world's potential oil has been used and the reserves of gas have been about half. The coal reserves are still large but most of the oil and natural gas reserves are in the hands of a few countries. Demand for energy is exponentially increasing. The rate has not only a sharp rise in energy costs which is experienced in recent years, but a definite possibility of decreasing oil and natural gas in a matter of a few decades. Energy is vital to present civilization. The alternatives must be developed. Possible alternatives are few in number, above all coal, nuclear, solar and wind. Single one of these will not solve the problem. The answer to the whole problem is a combination of these.

<sup>1</sup>Federal Energy Administration, Energy Outlook, FEA-75/713 (Washington, D.C., Government Printing Office, 1975), p. xiii.

<sup>2</sup>Douglas M. Goswami, Energy Technology Handbook, (McGraw-Hill Book Company, 1977), p. 1.

## CHAPTER I

### INTRODUCTION

Present civilization is heavily dependent on energy and mainly energy derived from few sources, above all oil, gas and coal. Of all the energy used in the United States in 1974, 94% was derived from these three fossil fuels — oil making up about 46% of the total energy consumption.<sup>1</sup> Unfortunately, the supply of the fossil fuels is dwindling. In less than a century, about 14% of the earth's petroleum has been used up — the resource which took more than half a billion years to build up.<sup>2</sup> Rest of the oil and natural gas reserve is fixed in quantity while demand for energy is exponentially increasing. The result is not only a sharp rise in energy costs which is experienced in recent years, but a definite possibility of depleting oil and natural gas in a matter of few decades. Energy is vital to present civilization. The alternatives must be developed. Potential alternatives are few in number, above all coal, nuclear, solar and wind. Single one of these does not seem to hold the answer to the whole problem.

---

<sup>1</sup>Federal Energy Administration, National Energy Outlook, FEA-N-75/713 (Washington D.C.: Government Printing Office, 1976), p. xxii.

<sup>2</sup>Douglas M. Considine, Energy Technology Handbook, (McGraw-Hill Book Company, 1977), p. xxvi.

Solar energy has a potential to play a significant role. Unlike nuclear, it does not face mass acceptance problem. In fact, it has a great mass appeal because it is simple; unlike coal, it is pollution free and it is everywhere and in abundance. For example, the amount of solar energy incident on a 120 miles by 120 miles area at a reasonably sunny location even if harvested at an average efficiency of 20%, the amount will exceed the total energy consumption of the entire world in 1980. Conversion efficiencies of up to 40% for applications, such as, space heating and service water heating have been widely demonstrated. Solar economics have also been becoming favorable, especially, in recent years when prices of fossil fuels have risen by several folds. Thus, solar energy has the necessary potential to contribute toward future energy needs of the world. It holds a good promise especially for some underdeveloped and developing nations which have a good resource — high solar insolation and low labor costs.

However, solar energy is in diffuse form and it is uncertain and intermittent in its availability. In order to use it as a significant energy source, it has to be collected over a wide area and stored, thus involving a large capital cost of collecting and storage hardware. As such, there are no technical barriers other than trying to make the hardware involved for solar collection and conversion inexpensive. Considerable efforts have been guided in this direction by private and public sectors in recent years.

Solar energy is basically an electromagnetic radiation. Outside the earth's air space, it carries the energy at an almost constant rate

of 429.2 Btu per hour per square foot known as a solar constant.<sup>3</sup> On a clear sunny day, more than 320 Btu per square foot per hour manage to reach earth's surface when measured on a plane normal to sunrays.<sup>4</sup> Average solar insolation can vary anywhere from 320,000 Btu/ft<sup>2</sup>/year for a cloudy location, such as, a place in the northeast United States to 650,000 Btu/ft<sup>2</sup>/year in the southwest United States region.<sup>[6]</sup> This energy can be converted into any desirable form. However, solar energy being thermodynamically closer to thermal form, its most efficient and economical application is heating — either space heating or service water heating.

Electricity is one of the mainly used energy forms. Of all the energy used in the United States in 1974, 28% was in the form of electricity.<sup>5</sup> Solar Energy can be converted into electricity either by photovoltaics or through mechanical power cycle. Conversion through photovoltaics, although more desirable, must wait for the development of technology of making solar cells at significantly lower prices. One of several mechanical power cycles, such as, Rankine, Reheat, Regeneration, Stirling, Ericson and Brayton cycle can also be used for solar to electrical power conversion. Among these, Rankine cycle (along with Reheat and Regeneration loops) is widely used in the great majority of the electric power plants. This cycle has a very high work ratio of turbine

---

<sup>3</sup>Adden B. Meinel and Marjorie P. Meinel, Applied Solar Energy, (Massachusetts: Addison-Wesley Publishing Company, 1977), p. 41.

<sup>4</sup>Meinel and Meinel, Applied Solar Energy, p. 47.

<sup>5</sup>Federal Energy Administration, National Energy Outlook, FEA-N-75/173 (Washington D.C.: Government Printing Office, 1976), p. xxxii.



power output and pump power input. Because of a high work ratio, small variations in the pump and turbine efficiencies do not dramatically affect the overall cycle efficiency. So the pump and turbine used in the cycle need not be highly efficient which could be cost prohibitive in a small scale solar power plant. So Rankine-cycle is the best suited power cycle for solar energy among all power cycles. This thesis deals with solar-to-electrical conversion through a Rankine-cycle.

The schematics of hardware involved in a Rankine-cycle and its cyclic path on a temperature-entropy diagram are shown in Figure 1.

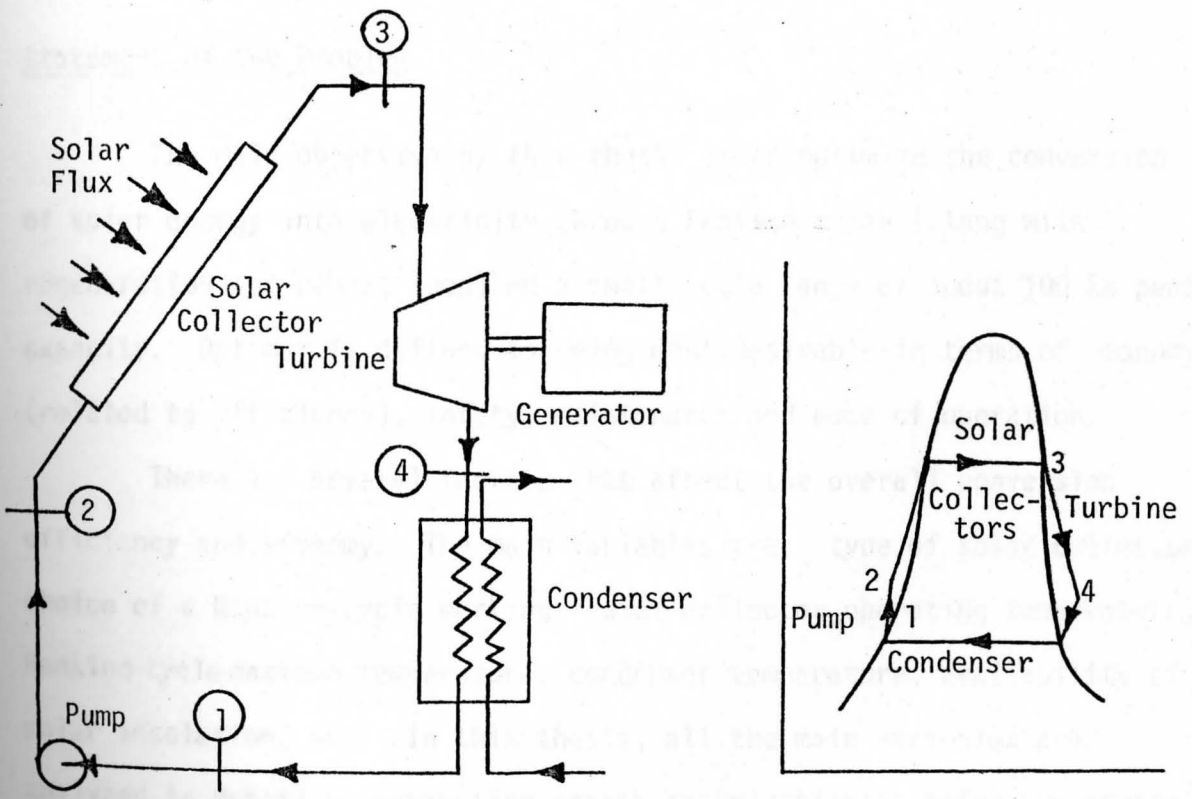


FIGURE 1. Schematic Diagram of a Simple Rankine-Cycle.

The ideal Rankine-cycle consists of four thermodynamic processes, starting with,

1. isentropic pressurization of saturated liquid,
2. constant pressure heat addition to vaporize the fluid by a heat source, such as, solar collectors,
3. isentropic expansion to a low pressure in the prime mover, such as, turbine which in turn drives a generator to produce electricity, and
4. constant pressure heat rejection (condensation) in condenser, thus completing a cycle.

#### Statement of the Problem

The main objective of this thesis is to optimize the conversion of solar energy into electricity through Rankine-cycle (along with regeneration and reheat loop) on a small scale range of about 100 KW peak capacity. Optimum is defined as being most desirable in terms of economy (related to efficiency), safety, maintenance and ease of operation.

There are several factors that affect the overall conversion efficiency and economy. The main variables are: type of solar collector, choice of a Rankine-cycle working fluid, collector operating temperature, Rankine-cycle maximum temperature, condenser temperature, availability of solar insolation, etc. In this thesis, all the main variables are analyzed in detail by exhaustive search optimization technique to arrive at the optimum sets of combinations for overall solar-to-electrical conversion.

## Related Work in the Field

In recent years, the subject of solar energy is going through a very popular and technical revival. There has been quite an activity going on in the private and public sector in the area of small scale solar-to-mechanical (or electrical) power conversion in recent years.

The pioneering work in this area in recent years has been done by Barber and Nichols of Barber-Nichols Engineering Company. This company designed, built and tested several solar operated Rankine-cycle engines using organic fluids as a Rankine-cycle working fluid. The first unit the company built was in 1973. Flat plate solar collectors were used for solar collection; R-113 as a Rankine-cycle working fluid and system was operated at a collector temperature of 200°F and Rankine-cycle maximum temperature of 188°F.<sup>6</sup> Efficiency of 6% was noted. The unit is used for operating a 3-ton air conditioning equipment. This company also built a solar powered Rankine cycle to supply shaft power to drive a conventional 351 KW water chiller for Honeywell, Inc. This unit used parabolic trough concentrating-tracking solar collectors; it used R-113 as a Rankine-cycle working fluid and was operated at a temperature of 275°F. Rankine-cycle efficiency of 15.9 was realized.<sup>7</sup> Another 25-hp solar engine was installed at the DOE demonstration site in Willard, NM for irrigation.<sup>8</sup> This unit

---

<sup>6</sup>R.E. Barber, "Solar Rankine Engines Examples and Projected Costs," An ASME Publication, 79-Sol-3, p.3.

<sup>7</sup>Douglas K. Werner, "Design and Test Results of a 643 KW(85 HP) Solar Powered Rankine Cycle," Present at the 1978 Annual Meeting of the American Section of International Solar Energy Society, Aug. 28-31, Denver, CO.

<sup>8</sup>R.L. Alvis, "Solar Irrigation Program Status Report," Oct., 1977, Sandia Report SAND 78-0049.

was operated at 325°F. Barber and Nichols mainly considered three fluids: R-11, R-12, and R-113, and two types of solar collectors: flat plate and parabolic trough. They mainly dealt with practical and economics side of the problem; simultaneous optimization was not considered.

D.R. Miller of Monsanto Research Corporation analyzed the theoretical performance of several organic fluids as Rankine-cycle working fluids.<sup>9</sup> His study dealt mainly with the performance of the Rankine-cycle; solar collectors were not analyzed; overall solar-to-electrical performance was not considered.

The technical aspects of small scale solar powered engines have also been studied by Biancardi of United Aircraft Research Laboratories,<sup>10</sup> and also by Davis.<sup>11</sup> There are a few complete solar-powered package systems are also commercially available. Among them Omnium-G's system is noteworthy. The system consists of:

- 1) a 20 feet diameter concentrating-tracking parabolic disc having a concentration ratio of 10,000;
- 2) thermal-to-electrical power conversion engine using steam or air as a working fluid-operating at an average temperature of 1400°F, and
- 3) compressed air capsules for storage.

---

<sup>9</sup>D.R. Miller, "Rankine Cycle Working Fluids for Solar-to Electrical Energy Conversion," Jan., 1974, Sandia Report 58-5556.

<sup>10</sup>F.R. Biancardi, "Solar Cooling for Buildings," Workshop Proceedings, Solar Cooling for Buildings, Feb. 6-8, 1974, Los Angeles, California, (Washington: Government Printing Office, 1974), p. 193.

<sup>11</sup>Jerry Davis, "Solar Rankine Powered Cooling Systems," Workshop Proceedings, Solar Cooling for Buildings, Feb. 6-8, 1974, p. 200.

Nominal electrical power output is 7.5 KW and thermal output is 30,000 Btu/hr.

There have also been several studies done to determine the possibility of solar thermal power plants for small communities. [See Reference 3 ]

Most of the work done in the area of small scale solar-to-electrical conversion has mainly dealt with effect of one particular variable on the overall conversion efficiency.

In this thesis, the problem is setup such that all the main variables involved can be analyzed simultaneously and all possible combinations are considered.

### Problem Setup

The schematic diagram of one of the possible arrangements of hardware involved for solar to electrical conversion through Rankine-cycle is shown in Figure 2.

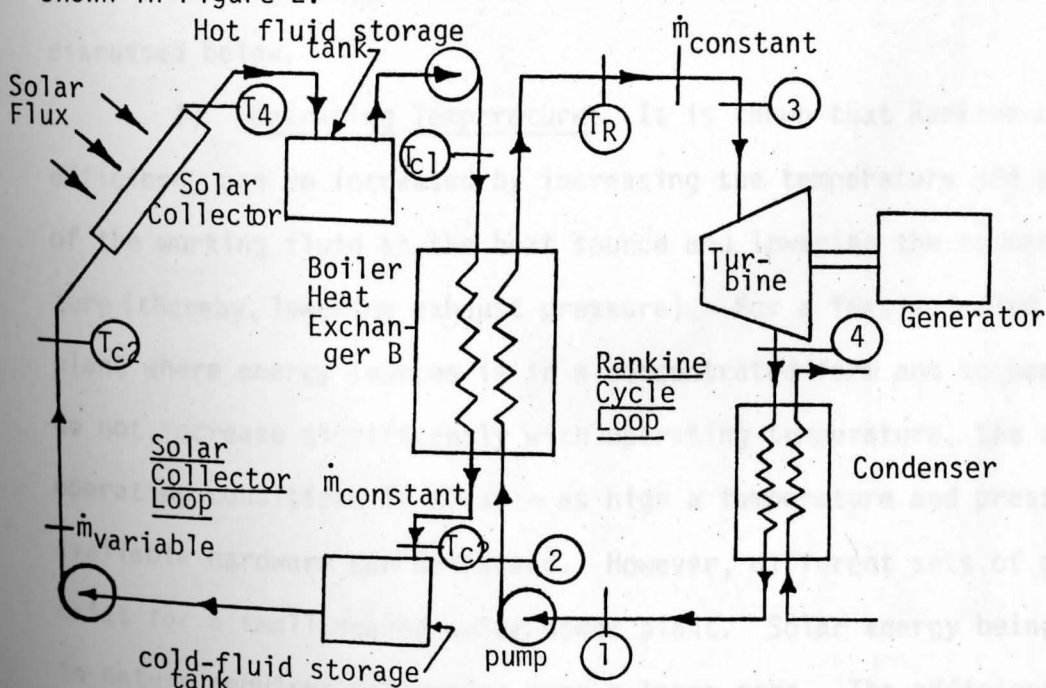


FIGURE 2. Schematic Diagram of a Basic Solar-Rankine Cycle.

In the solar loop, solar collectors collect and transfer solar energy to the circulating fluid. Energy in turn is transferred to the Rankine-cycle working fluid. Solar collector fluid is pumped back to the solar collectors. In a Rankine-cycle loop, thermal energy is converted into electricity.

There are several possible operating arrangements. The philosophy followed in determining the arrangement of hardware involved as shown in Figure 2, was to make both — solar loop and Rankine-cycle loop — operating at a constant temperatures, thereby, making simultaneous optimization a little simpler.

As indicated earlier, there are many factors involved here that affect the overall conversion efficiency. In this study, all the main factors that affect the overall efficiency and economy significantly are analyzed in detail. Certain assumptions are made regarding the other variables, such that, optimum solution is not significantly affected.

All the factors involved and the necessary assumptions are discussed below.

1) Operating Temperature: It is known that Rankine-cycle efficiency can be increased by increasing the temperature and pressure of the working fluid at the heat source and lowering the condenser temperature (thereby, lowering exhaust pressure). For a fossil fueled power plant where energy sources is in a concentrated form and so heat losses do not increase significantly with operating temperature, the choice of operating conditions is clear — as high a temperature and pressure as the available hardware can withstand. However, different sets of conditions exist for a small scaled solar power plant. Solar energy being diffuse in nature requires collection over a large area. The efficiency of the

collector decreases as its operating temperature increases because of high heat losses associated with large collection area. The optimum temperature would be the one that maximizes the product of solar collector efficiency and Rankine-cycle efficiency. In this study, maximum temperature will be limited to 1050°F as this would be a limit in terms corrosion resistance of alloy steels of moderate cost (e.g. ASTM A217).<sup>12</sup>

2) Rankine-Cycle Working Fluid: The fossil-fueled power plants use water/steam as a Rankine-cycle working fluid. Some of the reasons for the choice of the water/steam are that water is a highly stable compound capable of withstanding up to 3000 psi pressure and temperatures above 1300°F without disintegrating; it has low peak temperature requirements for very high thermal efficiency; it is safe, nontoxic and almost free. However, water, as such, does not have desirable thermodynamic and turbomachinery characteristics. The vapor dome and a typical Rankine-cycle path traced on a T-S diagram are shown in Figure 3.

---

<sup>12</sup>D.R. Miller, "Rankine-Cycle Working Fluids for Solar-to-Electrical Energy Conversion," Jan. 1974, Sandia Report 58-5556, p. 12.

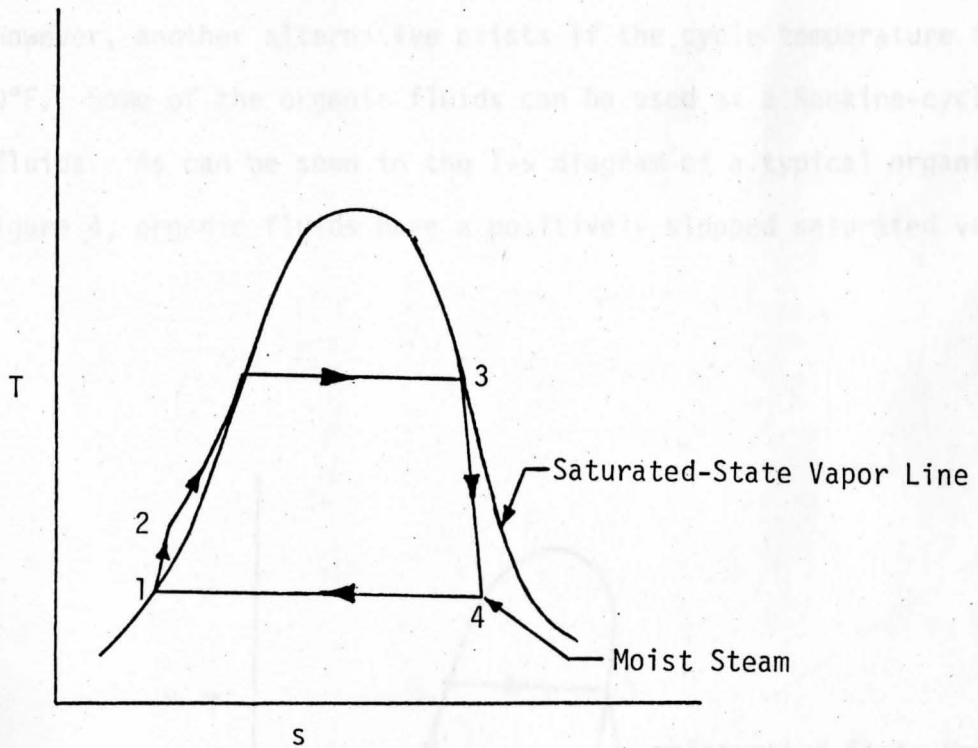


FIGURE 3. Saturation-State Vapor Line and Rankine-Cycle on a Temperature-Entropy Diagram for Water/Steam.

As can be seen in Figure 3, water has a negatively sloped saturated vapor line. During expansion of steam across the turbine, which is almost an isentropic process, steam starts condensing inside the turbine and this causes erosion which is highly undesirable since turbine is one of the most costly and delicate parts of the system. In a fossil-fueled power plants, this problem is taken care of by adding a number of re-heat loops and using multistage turbines. However, this demands large expenditure and therefore, only very large scale electric production becomes economically feasible. For a small solar power plant, where cost has to be limited, multistage turbines and many number of re-heat loops become



cost prohibitive.

However, another alternative exists if the cycle temperature is below 700°F. Some of the organic fluids can be used as a Rankine-cycle working fluids. As can be seen in the T-s diagram of a typical organic fluid, Figure 4, organic fluids have a positively sloped saturated vapor line.

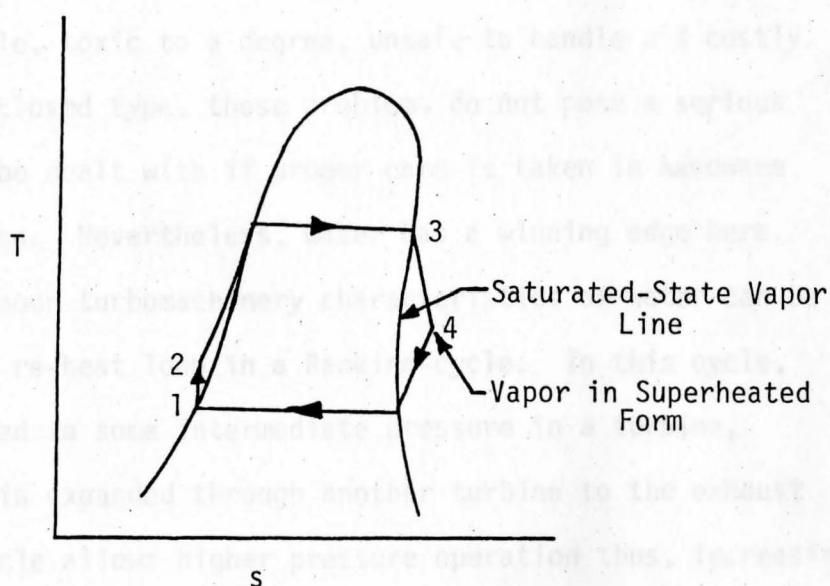


FIGURE 4. Saturation-State Vapor Line and Rankine-Cycle on a Temperature-Entropy Diagram for a Typical Organic Fluid.

During expansion through the turbine, the fluid tends to superheat eliminating turbine erosion problems.

Besides, at a low available temperature, (<300°F) the vapor pressure of water is too low to provide adequate working pressure for a real turbine. Some of the organic fluids (e.g. R-11, R-12, R-113) boil at high pressures even at low available temperature (<200°F). Also,

organic fluids have a low specific heat which is a desirable turbomachinery characteristic. Also, because organic fluids superheat during expansion through turbine, the vapor coming out of the turbine is at higher temperature than condenser liquid temperature and so simple regeneration (by an ordinary heat exchanger — not a costly item) becomes feasible which increases cycle efficiency significantly. Thus, using organic fluids as a working fluid could offer very high efficiency, even at low available temperatures and with a single stage inexpensive turbine. However, most of the organic fluids have poor physical properties: many of them are inflammable, toxic to a degree, unsafe to handle and costly. Since the cycle is a closed type, these problems do not pose a serious problem and they can be dealt with if proper care is taken in hardware design and construction. Nevertheless, water has a winning edge here. One of the ways that poor turbomachinery characteristics of water can be solved is by adding a re-heat loop in a Rankine-cycle. In this cycle, vapor is first expanded to some intermediate pressure in a turbine, reheated and then again expanded through another turbine to the exhaust pressure. Re-heat cycle allows higher pressure operation thus, increasing cycle efficiency yet decreasing or eliminating the condensation in the turbine. In this study, both — regeneration cycle for organics and one-step re-heat loop for water are also considered.

There are many organic fluids that can be used. However, only very few are suitable for use in the Rankine-cycle. Detailed considerations for choice of candidate fluids are discussed in Chapter II. The names of the fluids considered are: R-11, R-12, R-113, Toluene, Thiophene, Pyridine, Chlorobenzene and water.

3) Type of Solar Collector: The choice of an operating temperature desired determines the choice of the solar collector. Different types of solar collectors can be used. There are four main types of solar collectors: flat plate, compound parabolic concentrating (CPC), one axis tracking-concentrating parabolic trough and two axes tracking-concentrating paraboloid disc collector. In a certain temperature range, some types of collectors perform better than others. For example, flat plate collectors perform better in the temperature range from 150°F to 200°F than other collectors while disc type two axes tracking paraboloid collectors are more suitable for temperature above 500°F than other types of collectors. Collectors differ widely in their cost, maintenance requirements and in ease of operation. Above mentioned four types of collectors are considered in this study.

4) Climate (as Related to Solar Insolation and Ambient Temperature): The solar radiation at earth's surface comes in two forms: direct radiation – radiation whose direction has not been changed by atmosphere – and scattered radiation – radiation whose direction has been changed by the atmosphere. Solar collectors differ in their ability to utilize scattered radiation. The efficiency of a solar collector which is a fraction of energy absorbed by collector over that incident on it, is dependent upon the quantity of usable solar radiation incident on its plane and ambient temperature. Different places differ considerably in the amount of each form of solar insolation they receive and in average ambient temperature. So, an optimum choice of a solar collector may very well change from a parabolic trough collector for a sunny location to a flat plate collector for a cloudy location. In this study, the analysis is carried out for three climatically different locations

namely, Madison WI; Alburquerque NM; and Miami FL. Results can be used for any other location by comparing the average amount of each form of solar insolation and average ambient temperature.

5) Condenser Temperature: If environment is used as a heat sink either by air cooled condenser or cooling tower, the condenser temperature will depend upon ambient dry or wet bulb temperature which in turn will depend upon the location. If a constant temperature sink such as well water is used, condenser temperature will almost be constant. Condenser temperature will also depend upon the design characteristics of a condenser heat exchanger, such as its surface area, types of metal used, flow rates, etc. In this study, it is decided not to go into the hardware design factors. Here, a condenser design and flow rates are assumed to be such, that a constant temperature of 90°F of the Rankine-cycle fluid exists at the condenser throughout the year.

6) Hardware Design and Operation Factors: The design characteristics of the hardware, such as, surface area, types of materials, thickness of materials, amount of insulation used, flow rate, etc. affect the pressure drop, thermal losses, etc. which in turn affect overall efficiency. Ideal analysis must include all these factors and optimize the hardware involved in each case. But, consideration of the hardware design factors is beyond the intended scope of this study. Based on the experience, certain assumptions are made regarding hardware design factors – as close as it would be in practical situations and such that simultaneous optimization of solar collection loop and Rankine-cycle loop is possible. These assumptions are as follows.

Mass flow rate of Rankine-cycle fluid is constant and it is such that fluid is vaporized to a constant temperature of Rankine-cycle

operating temperature,  $T_3$  (See Figure 2). Mass flow rate of solar collector fluid across the heat exchanger B, is constant. For a given value of  $T_3$ ,  $T_2$  is known. The physical parameters of the boiler-heat exchanger such as its effectiveness and number of heat transfer units (NTU) and hourly heat capacity ratio of both fluids relate the collector fluid outlet and inlet temperatures  $T_{c1}$  and  $T_{c2}$  to  $T_3$  and  $T_2$ . These parameters are set such that  $T_{c1}$  is minimized. Thus, for a particular  $T_3$ ,  $T_{c1}$  and  $T_{c2}$  are computed. The equations involved and the procedure followed is discussed in detail in Chapters V and VI. Since the difference between  $T_{c1}$  and  $T_{c2}$  is small, a term, collector fluid average temperature,  $T_{avg}$ , is introduced as an average temperature of  $T_{c1}$  and  $T_{c2}$ . Thus, a certain value of  $T_3$  corresponds to a particular value of  $T_{avg}$ .

The pump that circulates fluid to the solar collector is a variable flow rate pump. The flow rate gets adjusted according to the instantaneous solar insolation. The mass flow rate is such that the collector fluid heats up from  $T_{c2}$  to a constant required temperature,  $T_{c1}$ . Here, several collector modules are assumed to be connected in a series. Since the mass flow rate of solar collector fluid is constant across the heat exchanger B but, variable across the solar collector, two small temporary storage tanks are introduced. All components are assumed to be well insulated and thus heat losses through pipes and tanks are neglected. However, this will have no significant effect on the optimum since the same assumption is used throughout in all cases and the errors involved will be relative. Fluids in the tanks are assumed to be thoroughly mixed. Rankine-cycle pump efficiency is assumed to be 50% and turbine efficiency to be 75% in all cases. Turbine supply pressure is not allowed to be less than atmospheric pressure.

### Approach

The problem is divided into two parts: 1) Rankine-cycle loop (or Rankine-cycle with regeneration or re-heat loop), and 2) solar collection loop. Both loops are treated separately and then results are combined to get net results. Exhaustive search optimization technique is used.

First, Rankine-cycle efficiencies at several different temperatures are calculated for each candidate working fluid. The graphs of efficiency vs. Rankine-cycle maximum temperature,  $T_R$ , is to be prepared for each fluid. The qualitative nature of the graphs is as shown in Figure 5. This is the subject covered in Chapter II.

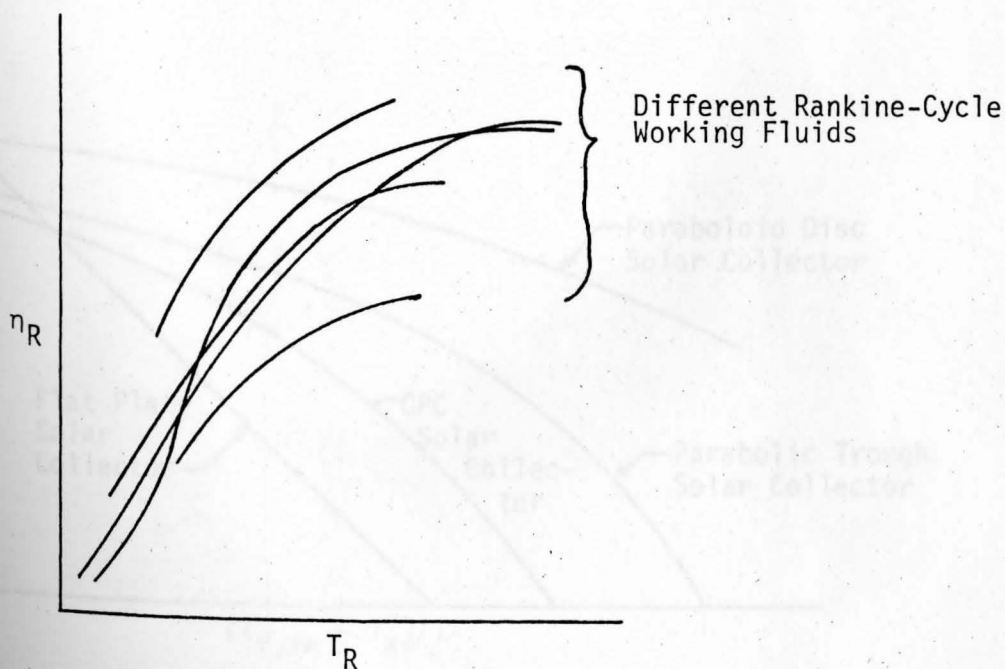


FIGURE 5. Rankine-Cycle Efficiency vs. Rankine-Cycle Maximum Temperature Curves for Different Fluids.

Similar results are to be obtained using Rankine-cycle with regeneration loop in case of organic fluids and Rankine-cycle with one-step re-heat loop in case of water. This is covered in Chapter III. For all calculations Temperature-Entropy charts or property tables are used.

The efficiency of a solar collector depends upon the operating temperature, instantaneous solar insolation and ambient temperature,  $T_a$ . The variation of solar collector efficiency is displayed in several ways. The standard ASHRAE recommended practice is to show the results as collector efficiency,  $\eta_{coll}$ , vs.  $\frac{T_{f,in} - T_a}{I}$ , where  $I$  is the instantaneous solar insolation on the collector plane and  $T_{f,in}$  is the temperature of the fluid going into the collector. Average mass flow rates and a solar collector fluid used is mentioned along with these results. A typical qualitative curve is shown in Figure 6.

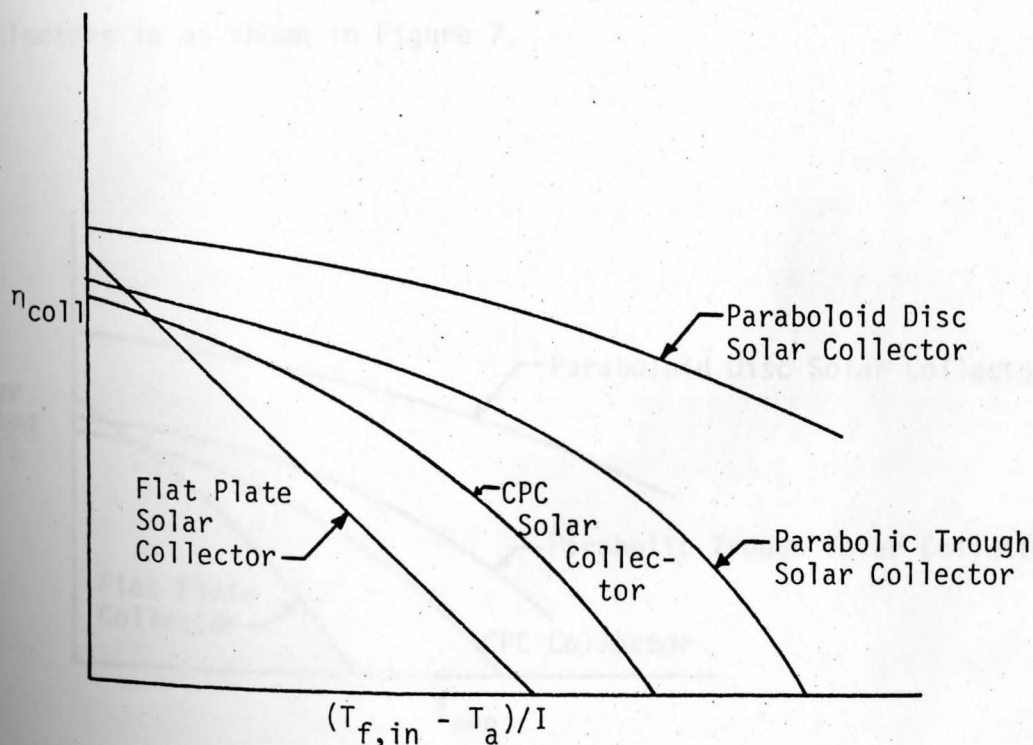


FIGURE 6. Solar Collector Efficiency Curves for Different Types of Collectors.

Even for the same type of collector, these curves differ slightly from one manufacturer's collector to the other. Better efficiency is generally associated with higher cost. In this study, a representative average curve for each type of collector is chosen and used. Equations are derived to curve fit these curves.

An hourly solar insolation and ambient temperature data for a location for a typical year are applied to these equations to calculate the energy collected every hour and then the total energy collected throughout the year is established. Calculations are carried out for three climatically different locations mentioned earlier. This is covered in Chapter IV. A computer and the magnetic weather data tape having hourly solar insolation and ambient temperature are used. The qualitative nature of the graph of total energy collected per year per unit area vs. collector fluid average temperature,  $T_{avg}$ , for different types of collectors is as shown in Figure 7.

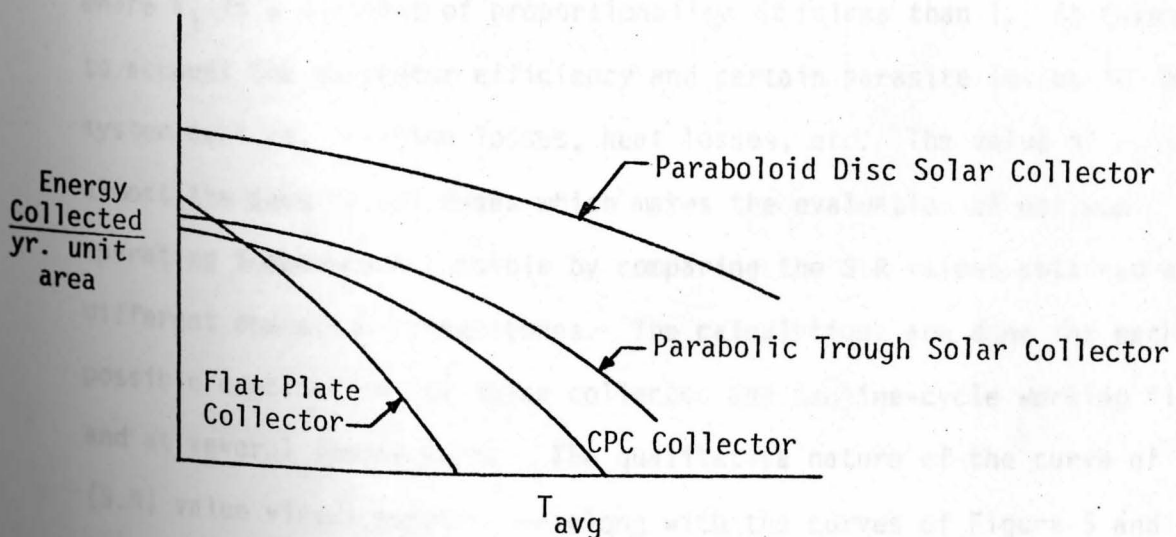


FIGURE 7. Energy Collected Per Year Per Unit Area vs. Collector Fluid Outlet Temperature Curves for Different Types of Collectors.



The results from both loops – solar and Rankine-cycle loop – are combined. The product of solar energy collected/(yr. unit area) at a particular collector fluid outlet temperature ( $T_{avg}$ ) and Rankine-cycle efficiency at the corresponding Rankine-cycle maximum temperature (calling this product as S.R Value) is obtained. This is directly proportional to the net electrical production/yr unit area at a certain operating temperature ( $T_{avg} \equiv T_R$ ).

$$\left( \frac{\text{Solar Energy Collected by the Collector}}{\text{Yr. unit area}} \times \text{Rankine-Cycle Efficiency} \right)_{\text{Operating Temperature}} \propto \left( \frac{\text{Net Electrical Energy Production}}{\text{Yr. unit area}} \right)_{\text{Operating Temperature}} \quad (1)$$

$$\text{(S.R)}_{\text{Operating Temperature}} = k_1 \cdot \left( \frac{\text{Net Electrical Energy Production}}{\text{Yr. unit area}} \right)_{\text{Operating Temperature}} \quad (2)$$

where  $k_1$  is a constant of proportionality. It is less than 1. It takes into account the generator efficiency and certain parasite losses in the system such as, friction losses, heat losses, etc. The value of  $k_1$  is almost the same in all cases which makes the evaluation of optimum operating temperature possible by comparing the S.R values obtained at different operating temperatures. The calculations are done for each possible combination of solar collector and Rankine-cycle working fluid and at several temperatures. The qualitative nature of the curve of an (S.R) value versus temperature along with the curves of Figure 5 and Figure 7, is as shown in Figure 8 for one possible combination of a solar collector and Rankine-cycle working fluid. These types of graphs are prepared

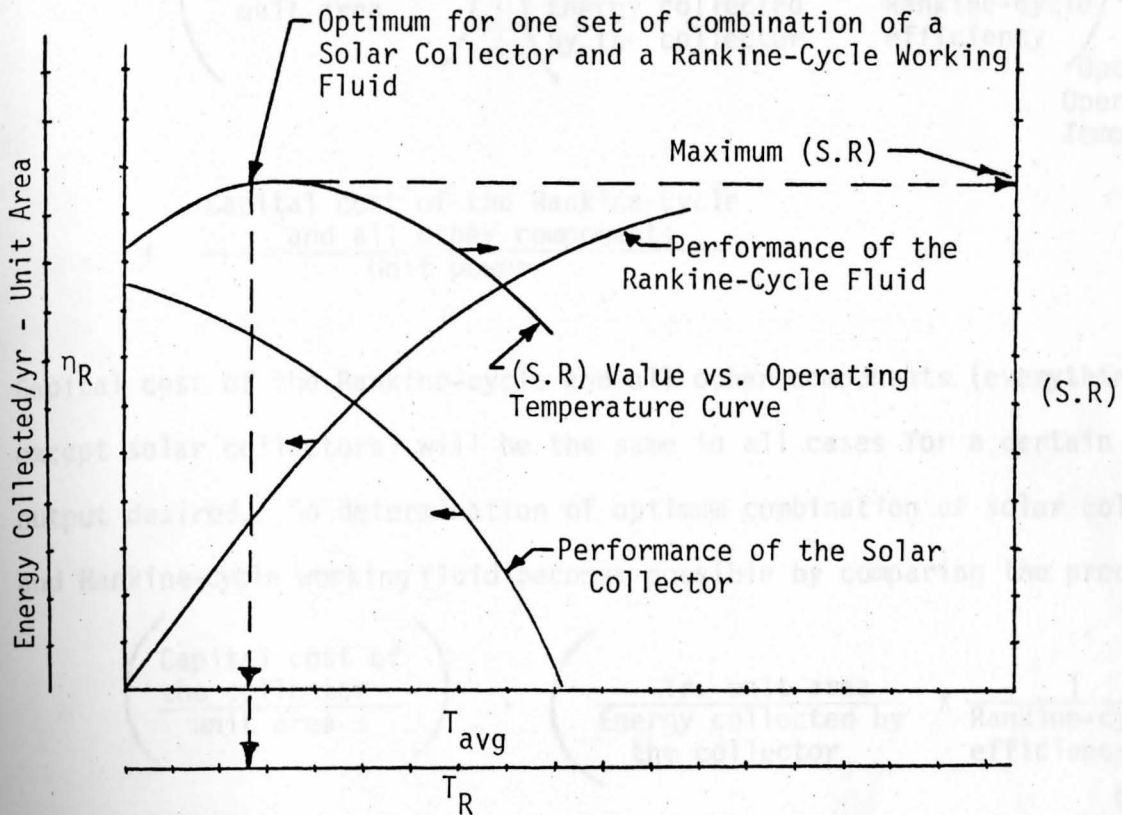


FIGURE 8. Net Energy Conversion vs. Operating Temperature Curve for One Possible Combination.

for every possible combination of solar collector and Rankine-cycle working fluid to determine the optimum operating temperature and maximum possible net energy conversion per year per  $\text{ft}^2$  (i.e., S.R. Value) in each case.

Overall economics would be the most determining factor for a choice of an optimum. In case of solar installation, the main cost is the initial capital cost of the hardware.

$$\frac{\text{Total cost of the system}}{\text{unit power}} = \frac{\text{Capital cost of the collectors}}{\text{unit power}} + \frac{\text{Capital cost of the Rankine-cycle and all other components}}{\text{unit power}}$$

$$= \left( \frac{\text{Capital cost of the collector}}{\text{unit area}} \right) \cdot \left( \frac{\text{yr. unit area}}{\text{Energy collected by the collector}} \times \frac{1}{\text{Rankine-cycle efficiency}} \right) \text{Optimum Operating Temperature}$$

$$+ \frac{\text{Capital cost of the Rankine-cycle and all other components}}{\text{Unit power}}$$

Capital cost of the Rankine-cycle and all other components (everything except solar collectors) will be the same in all cases for a certain power output desired. So determination of optimum combination of solar collector and Rankine-cycle working fluid becomes possible by comparing the product.

$$\left( \frac{\text{Capital cost of the collector}}{\text{unit area}} \right) \cdot \left( \frac{\text{Yr. unit area}}{\text{Energy collected by the collector}} \times \frac{1}{\text{Rankine-cycle efficiency}} \right) \text{Optimum Operating Temperature}$$

Other factors such as, safety, maintenance and ease of operation are also considered along with economics to arrive at the optimum solar collector and Rankine-cycle working fluid for solar-to-electric power conversion.

The thesis concludes with discussion of these results and scope for refinement and further work in this area.

## CHAPTER II

RANKINE-CYCLE PERFORMANCE

Rankine-cycle is the most widely used power cycle for electric generation. The schematic diagram of a Rankine-cycle and its path traced on a temperature-entropy diagram are repeated here for easy reference, (Figure 9).

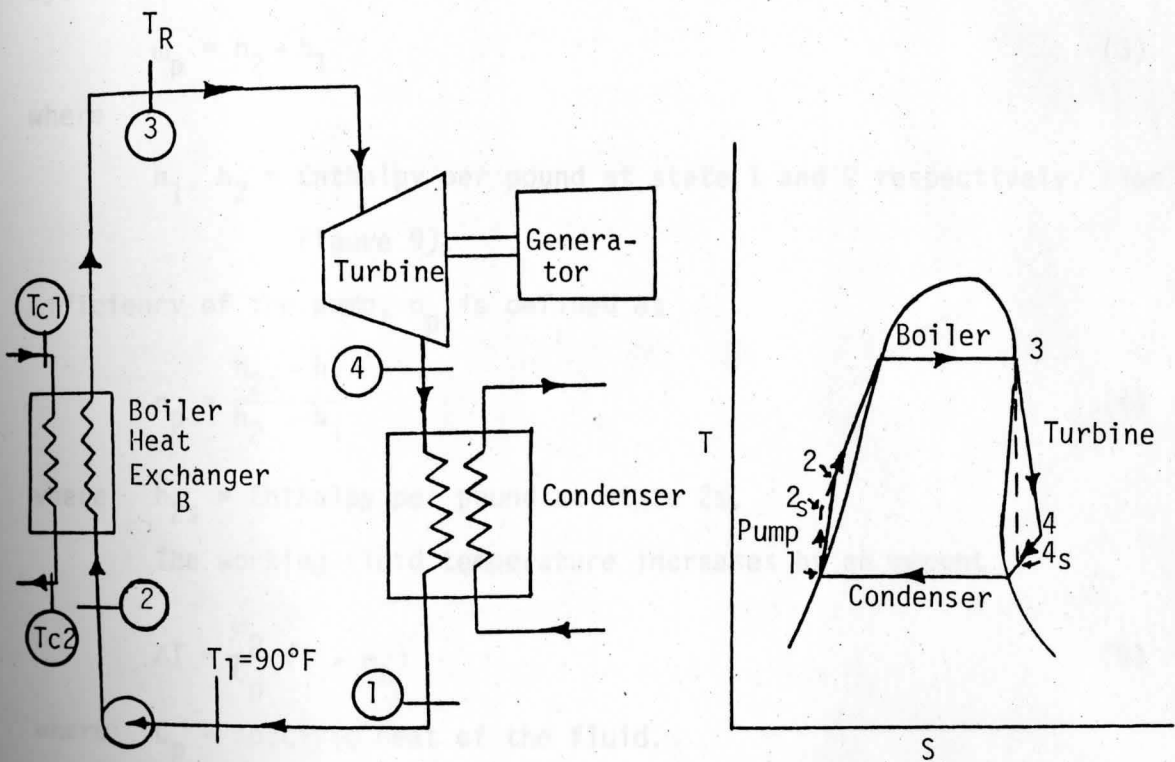


FIGURE 9. Schematic Diagram of a Rankine-Cycle.

There are four main components of the cycle.

1. Pump – Pump pressurises the Rankine-cycle working fluid, which is in the liquid form, from condenser exhaust pressure,  $P_1$ , to the boiler pressure,  $P_2$ . In an ideal cycle, the process is reversible

adiabatic, i.e., entropy remains constant. Ideal process would follow path 1-2s as shown on a T-s diagram, Figure 9. However, in practice, pumping process is non-isentropic; entropy increases slightly following path 1-2 as shown on T-s diagram. For calculations, pump efficiency is assumed to be 50%.

The pump work required per pound of working fluid,  $\omega_p$ , is given by,

$$\omega_p = h_2 - h_1 \quad (3)$$

where

$h_1, h_2$  = Enthalpy per pound at state 1 and 2 respectively, (See Figure 9).

Efficiency of the pump,  $\eta_p$  is defined as

$$\eta_p = \frac{h_{2s} - h_1}{h_2 - h_1} \quad (4)$$

where  $h_{2s}$  = Enthalpy per pound at state 2s.

The working fluid temperature increases by an amount

$$\Delta T = \frac{\omega_p}{C_p} (1 - \eta_p) \quad (5)$$

where  $C_p$  = specific heat of the fluid.

This temperature rise is generally very small — fraction of a degree F — for normal pressure operations.

2. Boiler — Here, heat is transferred at a constant pressure,  $P_2$ , from the solar collector fluid to the Rankine-cycle working fluid, boiling it to a temperature,  $T_R$ . As mentioned in Chapter I, the maximum Rankine-cycle temperature,  $T_R$  is related to the solar collector fluid inlet and outlet temperatures through the characteristics of a boiler heat exchanger — such as its effectiveness and number of transfer units.

Heat input per pound of working fluid,  $Q_h$ , is given by,

$$Q_h = h_3 - h_2 \quad (6)$$

where  $h_2, h_3$  = Enthalpy per pound of fluid at state 2 and 3 respectively.

3. Turbine — Saturated or superheated vapor expands from high pressure,  $P_2$ , to a condenser exhaust pressure,  $P_1$ , across the turbine which is connected to a generator to convert turbine shaft power into electricity. In an ideal cycle, the process is isentropic and would follow the path 3-4s of constant entropy. However the process is less than ideal. The actual expansion follows path 3-4 as shown on T-s diagram, Figure 9.

The efficiency of the turbine is assumed to be 75% in all cases.

The work output of the turbine per pound of working fluid,  $\omega_t$  is given by

$$\omega_t = h_3 - h_4 \quad (7)$$

where  $h_4$  = Enthalpy per pound at state 4, (Figure 9).

The efficiency of the turbine,  $\eta_t$ , is defined as the ratio of actual work output and work output of an ideal process. That is,

$$\eta_t = \frac{h_3 - h_4}{h_3 - h_{4s}} \quad (8)$$

4. Condenser — Here, the Rankine-cycle fluid rejects heat and condenses at constant pressure,  $P_2$ . Process follows path 4-1 as shown on T-s diagram.

Heat rejected at the condenser per pound of working fluid

$$Q_c = h_4 - h_1 \quad (9)$$

As discussed in Chapter I, organic fluids because of their superb thermodynamic and turbomachinery characteristics are more suited

as a Rankine-cycle working fluid than water in the low temperature range. There are numerous organic fluids. Refrigeration cycles make extensive use of organic fluids. However, only very few organic fluids are suitable for power cycles. The desired characteristics of a Rankine-cycle working fluid are:

- 1) High disintegration temperature and pressure.
- 2) The lower the exhaust (condenser) pressure, generally the higher the cycle efficiency. So fluids having low saturation pressure ( $<$  atmospheric pressure) at an available condenser temperature of  $90^{\circ}\text{F}$  are preferred.
- 3) Safe to handle.
- 4) Non-Toxic
- 5) Non-flammable
- 6) Low cost.

Properties of some thirty refrigerant organic fluids are given in the ASHRAE Fundamentals Handbook.<sup>8</sup> The properties of these fluids were examined to evaluate their suitability in Rankine-cycles. Refrigerant fluids are relatively safe; most of them are non-flammable and have low cost. But, they are generally unstable at high temperature. Also, they have high saturation pressure at  $90^{\circ}\text{F}$  of condenser available temperature; so are likely to be less efficient when used in power cycles. However, they have high saturation pressure at temperatures below  $200^{\circ}\text{F}$  of available heat source temperature — and thus are suitable for use with the flat plate solar collectors. So after some rough calculations and based

---

<sup>8</sup>ASHRAE, Handbook of Fundamentals, (Menasha: George Banta Co. Inc., 1974) p. 575.

on the experience of others in this area, three refrigerants are chosen as candidate working fluids. They are: R-11, R-12, and R-113.

Some of the other organic fluids which some of the chemical companies claim to be good for power cycles were also examined. These fluids are generally flammable and toxic to a degree. However, they have high disintegration temperature (above 500°F) and pressure. Also, they have low saturation pressure at 90°F of available condenser temperature and so are likely to be more efficient when used in power cycles. Also, they can be used at temperatures above 400°F, where refrigerants are not suitable. Four such fluids are chosen as Rankine-cycle candidate fluids from this non-refrigerant group. They are: Toluene, Chlorobenzene, Thiophene and Pyridine. Water is considered, of course, as it has the best physical properties and is the only fluid good at temperatures above 800°F.

The temperature-entropy charts or property tables of these candidate fluids were first obtained which are shown in Appendix A. Some of the important physical properties of these fluids are:

1. Refrigerant<sup>9</sup> 11: Formula: Trichlorofluoromethane  
 Normal Boiling point (@ 1 atm pressure) = 75°F  
 Maximum use temperature = 300°F.  
 Specific heat of liquid = 0.207 BTU/lbm. °F at 68°F  
 Non-flammable, low cost, reasonably safe and non-toxic.
2. Refrigerant 12: Formula: Dichlorodifluoromethane  
 Normal Boiling Point = -19°F.  
 Maximum use temperature = 250°F

---

<sup>9</sup>ASHRAE, Handbook of Fundamentals, (Menasha: George Banta Co., Inc., 1974) p. 581.



Specific heat of liquid = 0.229 BTU/lbm  $^{\circ}$ F at 90 $^{\circ}$ F

Non-flammable, low cost, reasonably safe and non-toxic.

3. R-113: Formula: Trichlorotrifluoroethane

Normal Boiling Point = 118 $^{\circ}$ F

Maximum use temperature = 300F

Specific heat = 0.44 BTU/lbm. $^{\circ}$ F

Non-flammable, low cost, reasonably safe and non-toxic.

4. Toluene<sup>10</sup>: Formula: CH<sub>3</sub> C<sub>6</sub>H<sub>5</sub>

Normal Boiling Point = 231 $^{\circ}$ F

Maximum use temperature = 750 $^{\circ}$ F

Specific heat = 0.392 BTU/lbm. $^{\circ}$ F

Low cost, flammable, toxic to a degree.

5. Chlorobenzene: Formula: C<sub>6</sub>H<sub>5</sub>Cl

Normal Boiling Point = 269 $^{\circ}$ F

Maximum use temperature = 630 $^{\circ}$ F

Specific heat = 0.303 BTU/lbm. $^{\circ}$ F

Low in cost, flammable, toxic to a degree.

6. Thiophene: Formula: C<sub>4</sub> H<sub>4</sub> S

Normal Boiling Point = 183.5 $^{\circ}$ F

Maximum use temperature = 550 $^{\circ}$ F

Specific heat = 0.345 BTU/lbm $^{\circ}$ F

Low in cost, flammable, toxic to a degree.

---

<sup>10</sup>D.R. Miller, "Rankine-Cycle Working Fluids for Solar-to-Electrical Energy Conversion", Report for Sandia Laboratory Contract No. 58-5556, Jan. 1974, p. 14, 15, 18.

7. Pyridine<sup>11</sup>: Formula:  $C_5H_5N$   
 Normal Boiling Point = 239°F  
 Maximum use temperature = 670°F  
 Specific heat = 0.367 BTU/lb.°F  
 Low in cost, flammable, toxic to a degree.

8. Water: Formula:  $H_2O$   
 Normal Boiling Point = 212°F  
 Maximum use temperature = 1050°F  
 Specific heat = 1 BTU/lbm °F  
 Non-flammable, non-toxic, safe and almost cost-free.

Maximum use temperature of 1050°F is not limited by the thermal stability of water, but by corrosion resistance of alloy steels of moderate cost (e.g. ASTM A217)

For each fluid, Rankine-cycle efficiencies are calculated for about 7 to 10 different heat source temperatures at an appropriate temperature intervals, starting from a normal boiling point temperature or 140°F whichever is higher up to a temperature of 20°F below maximum use temperature. Turbine supply pressure is not to be less than atmospheric pressure.

In each case, at a particular available temperature, Rankine-cycle is operated such that the maximum possible efficiency is obtained. It is known that as the pressure at the heat source is increased, the cycle efficiency increases. So boiler pressure is taken maximum possible limited by the constraints of available boiler temperature ( $T_R$ ) and that no condensation is to occur in the turbine during actual expansion.

---

<sup>11</sup>Miller, "Rankine-Cycle Working Fluids for Solar-to-Electrical Energy Conversion", p. 20.

The calculation procedure followed is illustrated through two sample calculations given below for toluene and water as working fluids operating at boiler temperature of 400°F and 500°F, respectively,

1. Rankine cycle efficiency calculations using toluene at a heat source temperature of 400°F:

Across the turbine, toluene superheats. So the maximum possible pressure,  $P_2$ , in this case is saturation pressure corresponding to 400°F temperature. From T-S diagram, it is 120 psia.

$$\text{i.e. } P_2 = P_3 = 120 \text{ psia}^*$$

$$h_3 = -36.5 \text{ BTU/lbm}^*$$

$$S_3 = -0.015 \text{ BTU/lbm-}^\circ\text{F}^*$$

where  $S_3$  is the entropy per pound of the fluid at state point 3.

$$\text{Therefore, } S_{4S} = S_3 = -0.015 \text{ BTU/lbm-}^\circ\text{F}$$

$$h_{4S} = -114 \text{ BTU/lbm}^*$$

$$\text{Condenser Temperature} = 90^\circ\text{F}$$

$$\text{Corresponding pressure, } P_1 = 0.8 \text{ psia}^*$$

$$h_1 = -315 \text{ BTU/lbm}^*$$

Efficiency of turbine,

$$\eta_t = \frac{h_3 - h_4}{h_3 - h_{4S}} = 0.75$$

Therefore,

$$h_4 = h_3 - 0.75 \times (h_3 - h_{4S})$$

$$= -36.5 - 0.75 \times (-36.5 + 114)$$

$$= -94.6 \text{ BTU/lbm}$$

Consider a control surface around the pump.

$$\text{First Law: } \omega_p = h_2 - h_1$$

where  $\omega_p$  is the work done by the pump per pound of fluid.

\*Data read from T-S diagrams or tables.

$$\omega_p = \frac{v(P_2 - P_1)}{\text{Efficiency of pump}} = 0.01848 (120 - 0.8) \times \frac{114}{778} \times \frac{1}{0.5}$$

$$= 0.65 \text{ BTU/lbm}$$

$$\therefore h_2 = -315 + 0.65 = -314.35 \text{ BTU/lbm}$$

Consider a control surface around the turbine.

$$\text{First Law: Work done by turbine, } \omega_t = h_3 - h_4$$

$$\therefore \omega_t = -36.5 + 94.6 = 58.1 \text{ BTU/lbm}$$

Consider a control surface around the boiler.

$$q_H = h_3 - h_2$$

$$= -36.5 + 314.35$$

$$= 277.85 \text{ BTU/lbm}$$

Network output,

$$\omega_{\text{net}} = \omega_t - \omega_p$$

$$= 58.1 - 0.65$$

$$= 57.45 \text{ BTU/lbm}$$

Rankine-cycle efficiency,

$$\eta_R = \frac{\omega_{\text{net}}}{q_H}$$

$$= \frac{57.45}{277.85}$$

$$= 20.7\%$$

2. Rankine-cycle efficiency calculations using water at a heat source temperature of 500°F

$$T_3 = 500^\circ\text{F}$$

$$\text{Condenser Temperature} = 90^\circ\text{F}$$

$$\text{Corresponding pressure, } P_1 = 0.6988 \text{ psia}^*$$

$$h_1 = 58.07 \text{ BTU/lbm}^*$$

\*Data read from T-S tables

$$s_1 = 0.11165 \text{ BTU/lbm}^\circ\text{F}^*$$

point 1 is on saturated vapor line.

Consider a control surface around the turbine.

$$\text{First Law: } \omega_t = h_3 - h_4$$

$$\text{Second Law: } s_3 = s_{4S}$$

$$h_4 = 1100.7 \text{ BTU/lbm}^*$$

Turbine efficiency,

$$\eta_t = \frac{h_3 - h_4}{h_3 - h_{4S}} = 0.75$$

Different pressures are assumed;  $h_3$  is obtained from the T-S tables corresponding to the assumed pressure and  $T_3 = 400^\circ\text{F}$ ; the ratio,  $(h_3 - h_4)/(h_3 - h_{4S})$  is calculated and match it to 0.75.

Thus, by trial and error,

$$h_3 = 1287 \frac{\text{BTU}}{\text{lbm}}^*$$

Consider a control surface around the pump.

$$\text{First Law: } \omega_p = h_2 - h_1$$

$$\omega_p = \frac{v(P_2 - P_1)}{\eta_p} = 0.01614 (22 - 0.7) \times \frac{144}{778} \times \frac{1}{0.5}$$

$$= 0.127 \text{ BTU/lbm}$$

$$\therefore h_2 = h_1 + \omega_p$$

$$= 58.07 + 0.127$$

$$= 58.197 \text{ BTU/lbm}$$

Consider a control surface around the turbine.

$$\text{First Law: Work done by turbine, } \omega_t = h_3 - h_4$$

---

\*Data read from T-S tables

$$\begin{aligned}\therefore \omega_t &= 1287 - 1100.7 \\ &= 186.3 \text{ BTU/lbm}\end{aligned}$$

Consider a control surface around the boiler.

$$\begin{aligned}q_H &= h_3 - h_2 \\ &= 1287 - 58.134 \\ &= 1228.87 \text{ BTU/lbm}\end{aligned}$$

$$\begin{aligned}\text{Net work output, } \omega_{\text{net}} &= \omega_t - \omega_p \\ &= 186.3 - 0.127 \\ &= 186.173 \text{ BTU/lbm}\end{aligned}$$

Rankine-cycle efficiency,

$$\begin{aligned}\eta_R &= \frac{\omega_{\text{net}}}{q_H} \\ &= \frac{186.173}{1228.87} \\ &= 15.15\%\end{aligned}$$

Rankine-cycle efficiency results at several different temperatures with all fluids are tabulated in the Tables 1 to 8. Results are also shown on Temperature vs. Efficiency graphs, Figures 10 thru 17.

RANKINE-CYCLE MAX. TEMP. (DEG. F.)

FIG. 10. A Graph of Rankine-Cycle Efficiency vs. Rankine-Cycle Maximum Temperature for R-11.

TABLE 1. Rankine-Cycle Efficiencies at Several Different Rankine-Cycle Maximum Temperatures Using R-11.

Rankine-Cycle Maximum Temperature, $T_R$ °F	Rankine-Cycle Efficiency $\eta_R$ %
150	6.8
180	9.4
200	10.8
220	12.1
250	13.8
280	15.2

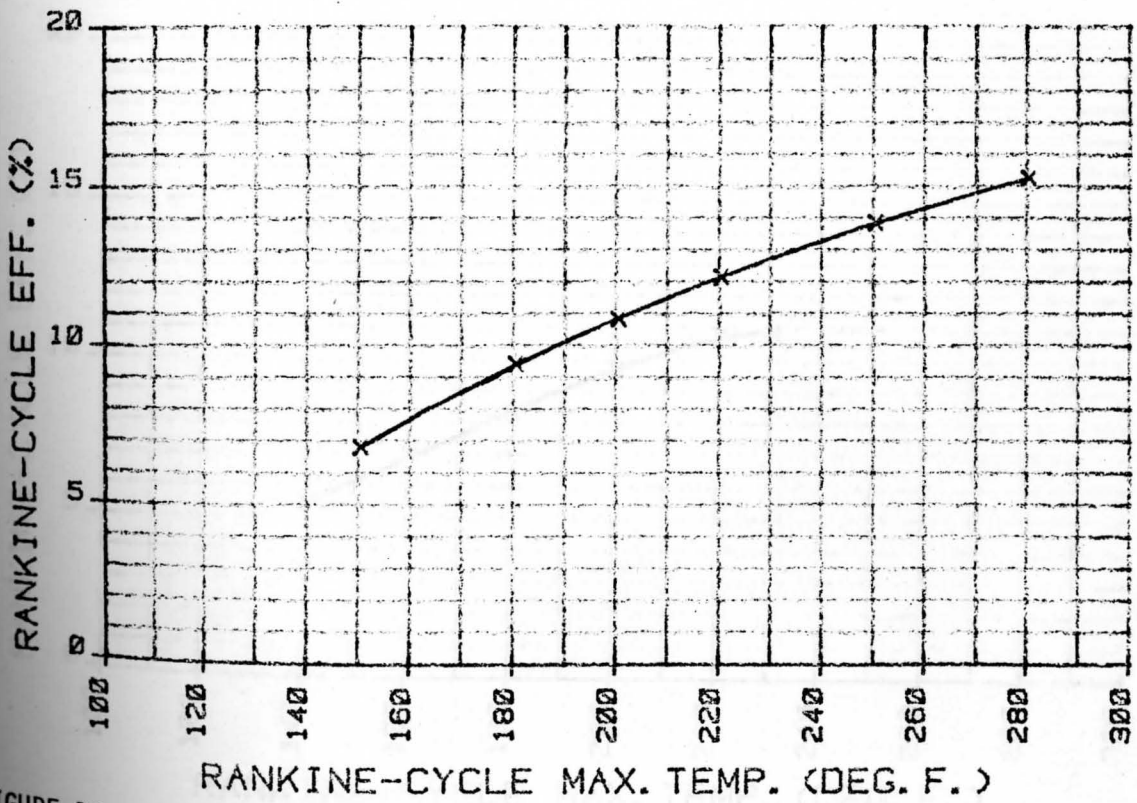


FIGURE 10. A Curve of Rankine-Cycle Efficiency vs. Rankine-Cycle Maximum Temperature for R-11.

TABLE 2. Rankine Cycle Efficiencies at Several Different Rankine-Cycle Maximum Temperatures Using R-12.

Rankine-Cycle Maximum Temperature, $T_R$ °F	Rankine-Cycle Efficiency $\eta_R$ %
140	5.4
160	6.9
180	8.2
200	9.6
220	10.7
230	10.8

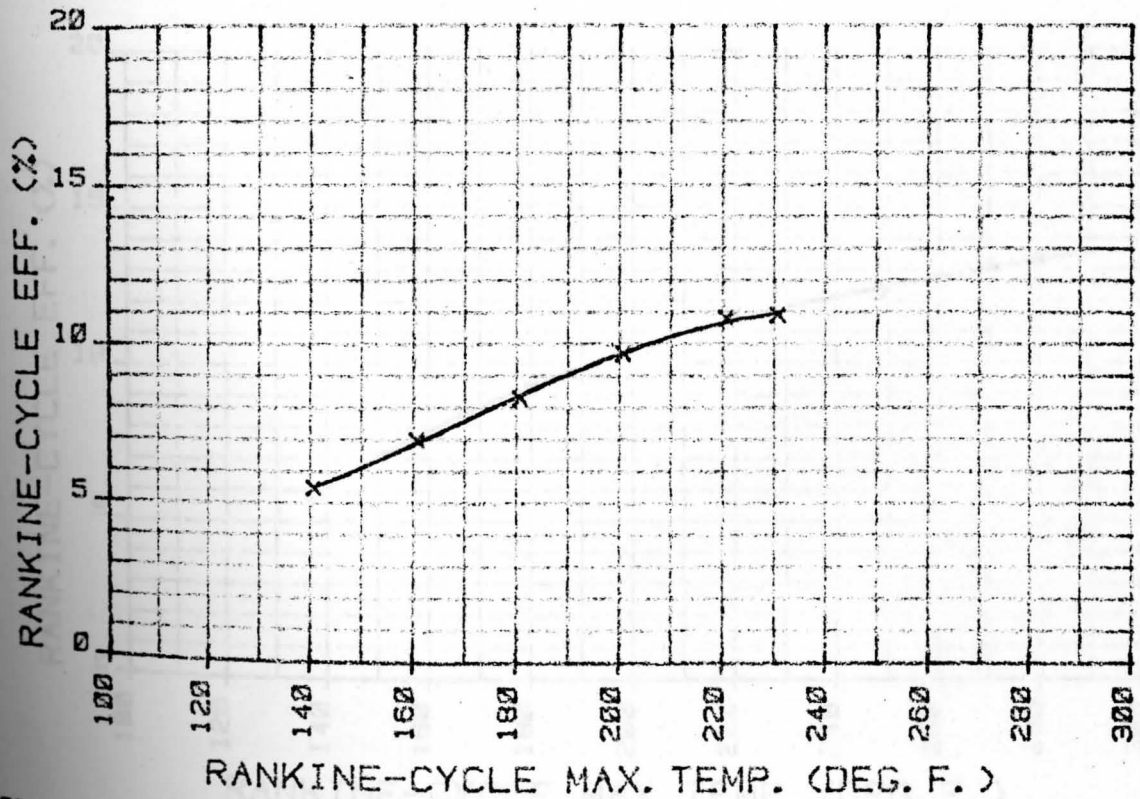


FIGURE 11. A Curve of Rankine-Cycle Efficiency vs. Rankine-Cycle Maximum Temperature for R-12.



TABLE 3. Rankine-Cycle Efficiencies at Several Different Rankine-Cycle Maximum Temperatures Using R-113.

Rankine-Cycle Maximum Temperature $T_R$ °F	Rankine-Cycle Efficiency, $\eta_R$ %
150	7.2
180	9.4
200	10.6
220	11.7
250	12.5
280	13.5

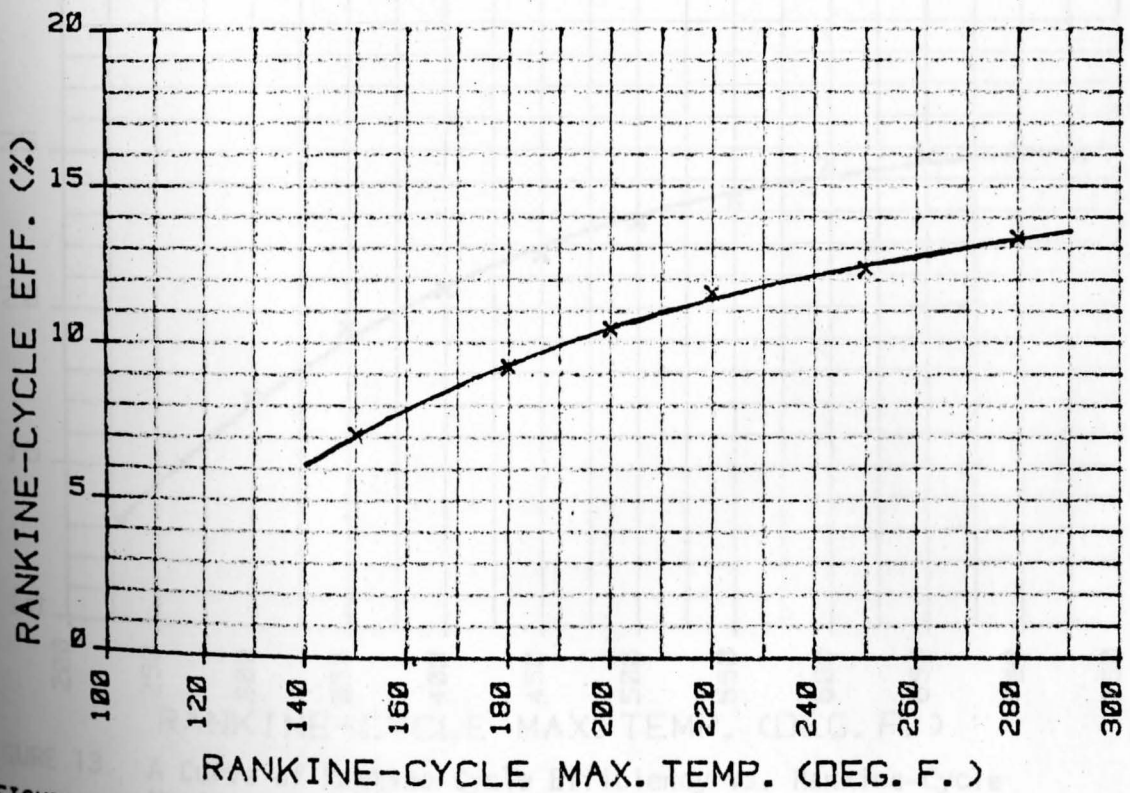


FIGURE 12. A Curve of Rankine-Cycle Efficiency vs. Rankine-Cycle Maximum Temperature for R-113.

TABLE 4. Rankine-Cycle Efficiencies at Several Different Rankine-Cycle Maximum Temperatures Using Toluene.

Rankine-Cycle Maximum Temperature °F	Rankine-Cycle Efficiency, $\eta_R$ %
230	13.2
300	17.2
350	19.4
400	20.6
450	21.7
500	22.7
550	23.4
600	24.5
650	24.7
730	24.8

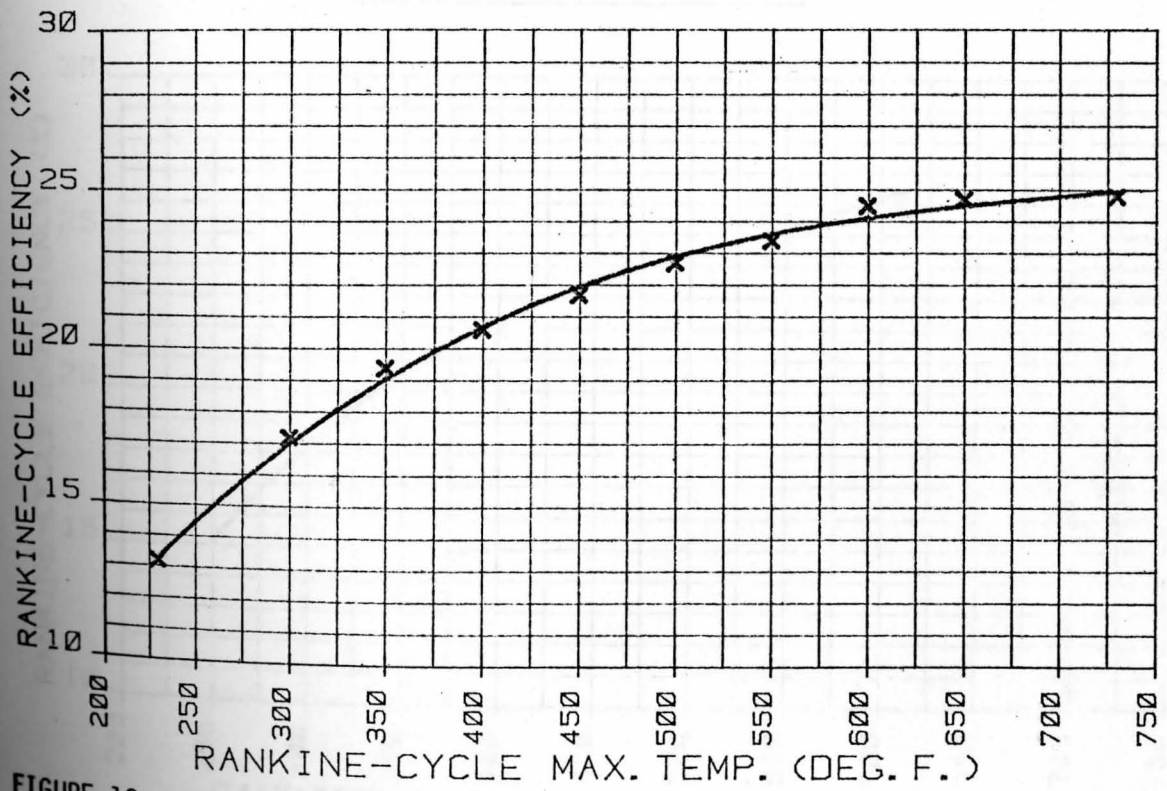


FIGURE 13. A Curve of Rankine-Cycle Efficiency vs. Rankine-Cycle Maximum Temperature for Toluene.

TABLE 5. Rankine-Cycle Efficiencies at Several Different Rankine-Cycle Maximum Temperatures Using Chlorobenzene.

Rankine-Cycle Maximum Temperature °F	Rankine-Cycle Efficiency, $\eta_R$ %
270	16.4
300	18.4
350	20.7
400	21.9
450	23.5
500	24.2
550	25.6
610	26.3

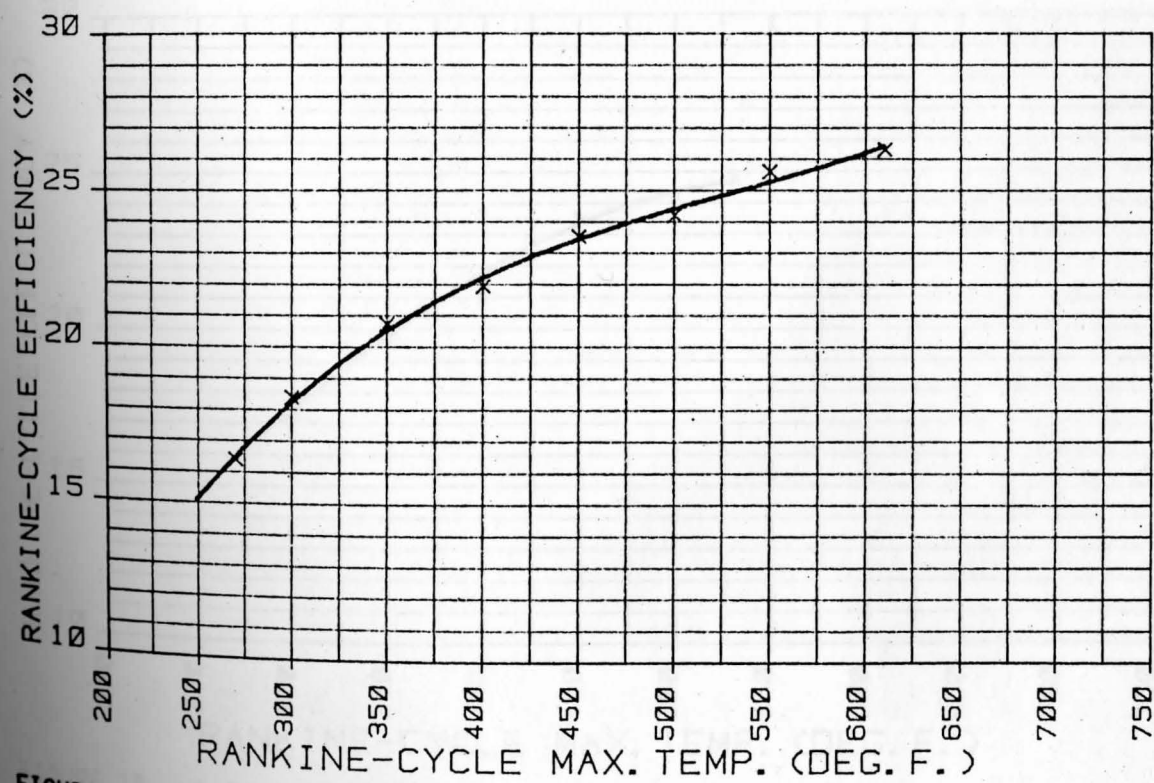


FIGURE 14. A Curve of Rankine-Cycle Efficiency vs. Rankine-Cycle Maximum Temperature for Chlorobenzene.

TABLE 6. Rankine-Cycle Efficiencies at Several Different Rankine-Cycle Maximum Temperatures Using Thiophene.

Rankine-Cycle Maximum Temperature °F	Rankine-Cycle Efficiency, $\eta_R$ %
250	14.9
300	17.3
350	19.9
400	21.8
450	23.5
500	24.2
530	24.8

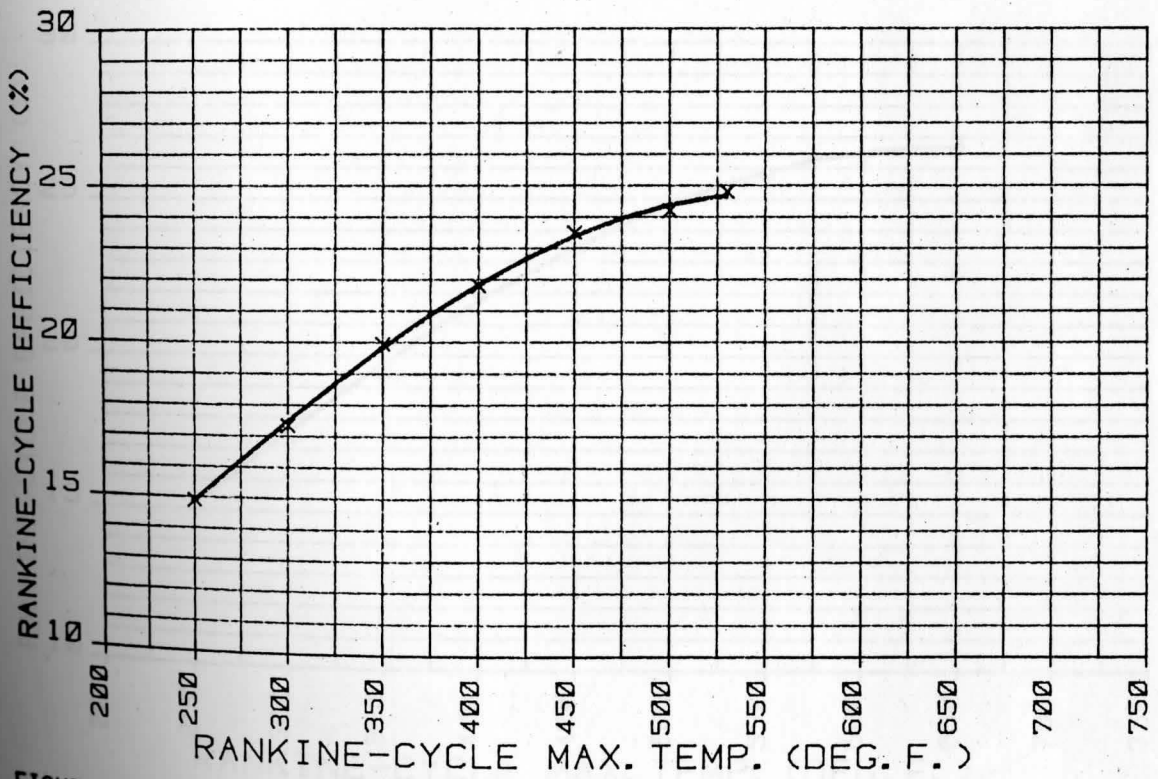


FIGURE 15. A Curve of Rankine-Cycle Efficiency vs. Rankine-Cycle Maximum Temperature for Thiophene.

TABLE 7. Rankine-Cycle Efficiencies at Several Different Rankine-Cycle Maximum Temperatures Using Pyridine.

Rankine-Cycle Maximum Temperature °F	Rankine-Cycle Efficiency, $\eta_R$ %
250	15.2
300	17.4
350	19.4
400	22.1
450	23.5
500	24.9
550	25.8
600	26.3
650	26.8

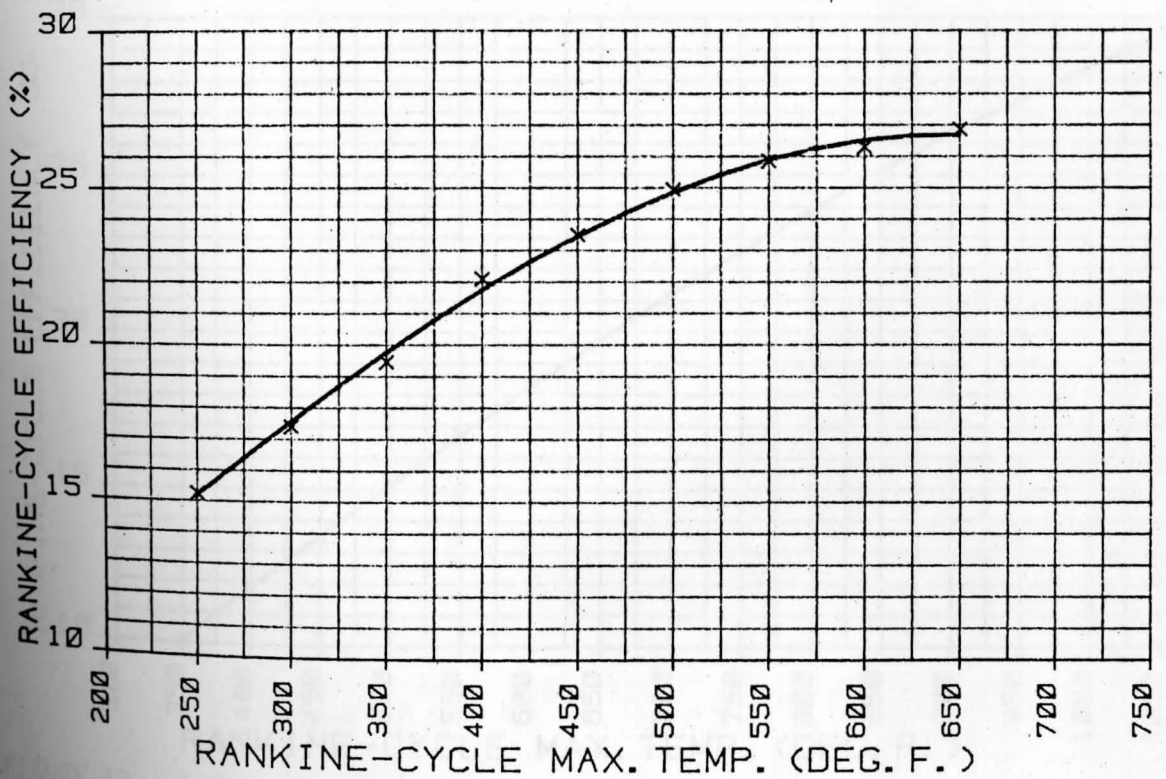


FIGURE 16. A Curve of Rankine-Cycle Efficiency vs. Rankine-Cycle Maximum Temperature for Pyridine.

TABLE 8. Rankine-Cycle Efficiencies at Several Different Rankine-Cycle Maximum Temperatures Using Water.

Rankine-Cycle Maximum Temperature °F	Rankine-Cycle Efficiency, $\eta_R$ %
350	10.1
400	11.8
450	13.5
500	15.1
550	16.7
600	18.3
700	21.1
800	23.8
900	26.4
1030	29.0

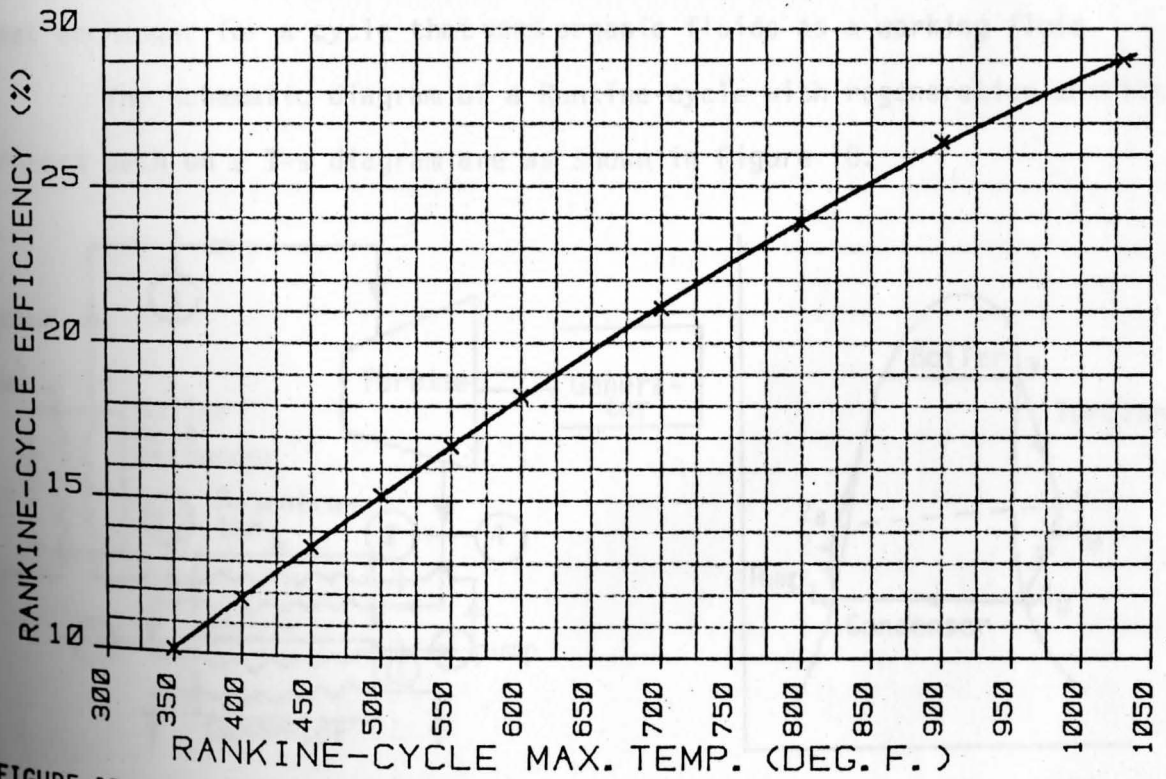


FIGURE 17. A Curve of Rankine-Cycle Efficiency vs. Rankine-Cycle Maximum Temperature for Water.

## CHAPTER III

PERFORMANCE OF RANKINE-CYCLE WITH REGENERATION OR REHEAT LOOP

As discussed in Chapter I, organic fluids superheat during expansion through turbine. So the temperature of the vapor coming out of the turbine is higher than the temperature of the fluid going into the boiler-heat exchanger. This temperature difference allows preheating of the fluid going into the boiler by turbine exhaust, thus, enabling to recover energy which would otherwise be rejected at the condenser. Consequently, the efficiency of the entire cycle would be significantly increased.

This requires an additional hardware component – a heat exchanger which is not an expensive item. The improvement in cycle efficiency due to this regeneration would easily justify the added initial cost of the heat exchanger for a cycle that uses organic fluids as a working fluid.

The schematic diagram of a Rankine-cycle with regeneration and its process path on a T-s diagram are as shown in Figure 18.

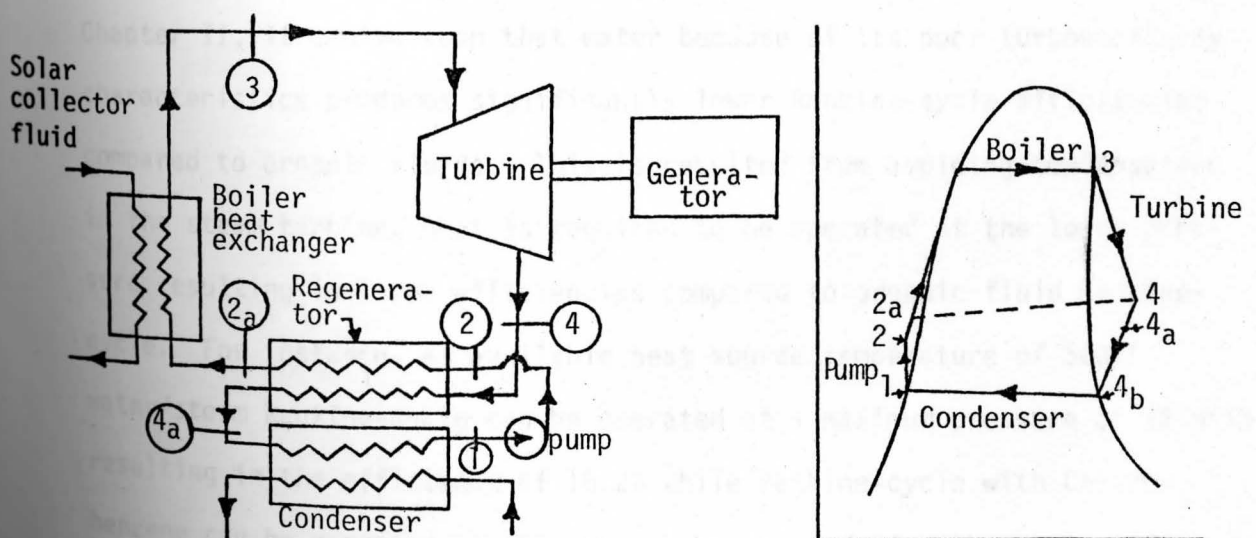


FIGURE 18. Schematic Diagram of a Rankine-Cycle with Simple Regeneration

About 80% of the regeneration is possible, that is, 80% of the energy content of the superheated vapor between states 4 and 4b (Figure 18) can be transferred to the liquid, heating it to a temperature of  $T_{2a}$  from  $T_2$ . Temperature rise across the pump is negligibly small — usually in the order of 1°F for normal pressure operations. Since vapor has higher specific heat than liquid, temperature drop in the vapor is smaller than temperature rise in the liquid for the same amount of heat transfer. Throughout the heat transfer process in a regenerator — heat exchanger, vapor stays at higher temperature than liquid in an organic power cycle. Thus, heat transfer can be easily achieved — and 80% of the maximum possible heat transfer is easily possible. In case of organic fluids, Rankine-cycle with 80% regeneration loop is now considered.

Simple regeneration (that is, transferring heat from the turbine exhaust to the liquid entering the boiler) is not possible in case of water since temperature of the turbine exhaust is lower than the temperature of the water going into the boiler. Evaluating the results obtained in Chapter II, it can be seen that water because of its poor turbomachinery characteristics produces significantly lower Rankine-cycle efficiencies compared to organic fluids. This is resulted from avoiding condensation in the steam turbine, that is required to be operated at the lower pressure resulting in lower efficiencies compared to organic fluid Rankine-cycle. For instance, at available heat source temperature of 500°F water/steam Rankine-cycle can be operated at a maximum pressure of 22 psia resulting in the efficiency of 15.2% while Rankine-cycle with Chlorobenzene can be operated at 185 psia pressure producing the cycle efficiency of 24.2%.



Another alternative to avoid the poor turbomachinery characteristics is to add a reheat loop to the Rankine-cycle. Reheat cycle allows higher pressure operation yet avoiding condensation in the turbine. This cycle is shown schematically and on a T-s diagram in Figure 19.

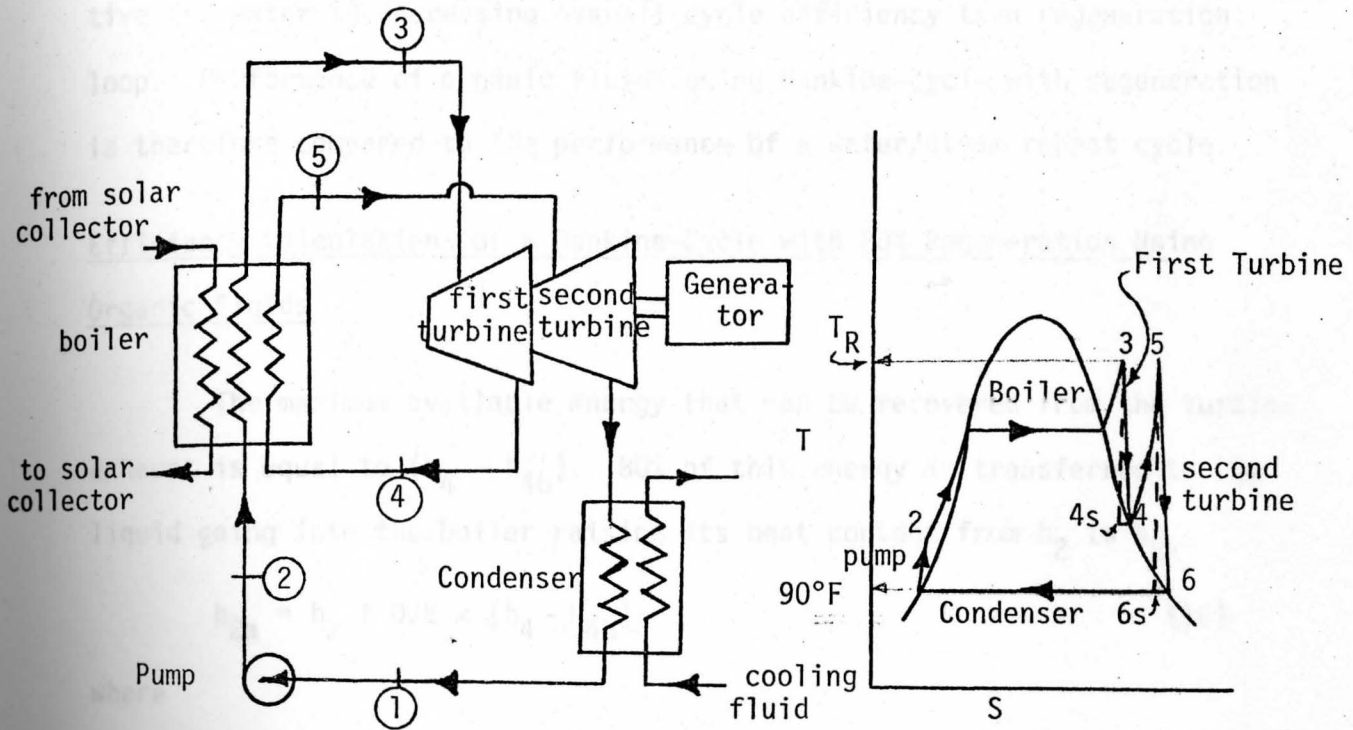


FIGURE 19. Schematic Diagram of a Rankine-Cycle with One-Step Reheat.

In a reheat cycle, vapor is expanded to some intermediate pressure in the turbine and is reheated in the boiler, after which it expands in the turbine to the exhaust pressure.

This cycle is more useful to water/steam power cycle than for organic fluid power cycle. Because organic fluids superheat during turbine expansion, their Rankine-cycles can be operated at maximum allowable pressure (limited only by the available heat source temperature). The average pressure at which heat is added to the organic fluid does not increase in a reheat cycle; in fact, it could decrease. Thus,

reheat cycle does not produce any efficiency improvements in the organic Rankine-cycles.

Addition of a regeneration loop increases overall cycle efficiency significantly in case of organic fluids while reheat loop is more effective for water in increasing overall cycle efficiency than regeneration loop. Performance of organic fluids using Rankine-cycle with regeneration is therefore compared to the performance of a water/steam reheat cycle.

### Efficiency Calculations of a Rankine-Cycle with 80% Regeneration Using Organic Fluids.

The maximum available energy that can be recovered from the turbine exhaust is equal to  $(h_4 - h_{4b})$ . 80% of this energy is transferred to the liquid going into the boiler raising its heat content from  $h_2$  to  $h_{2a}$ .

$$h_{2a} = h_2 + 0.8 \times (h_4 - h_{4b}) \quad (10)$$

where

$h_2, h_{2a}, h_4, h_{4b}$  = Enthalpy per pound of fluid at state points 2, 2a, 4 and 4b (Figure 18).

At this point it is checked to make sure that temperature  $T_4$  is higher than temperature at state point 2a,  $T_{2a}$ .

Thus, regeneration decreases the amount of heat to be added from the heat source to the working fluid ( $Q_h$ ). It is given by an equation,

$$Q_h = h_3 - h_{2a} \quad (11)$$

where

$h_3$  = Enthalpy per pound of the fluid at state point 3.

The procedure followed for efficiency calculations of an organic Rankine-cycle with 80% regeneration is best illustrated by a sample calculation as shown on the next page.

Sample Example: Rankine-cycle with 80% regeneration operating with Toluene at a heat source temperature of 400°F.

Across the turbine, toluene superheats. So the maximum possible pressure,  $P_2$ , in this case is saturation pressure corresponding to 400°F temperature.

From T-s diagram, it is 120 psia.

$$\text{i.e. } P_2 = P_3 = 120 \text{ psia}^*$$

$$h_3 = -37 \text{ BTU/lbm}^*$$

$$S_3 = 0.015 \text{ BTU/lbm } ^\circ\text{F}^*$$

Therefore,

$$S_{4S} = S_3 = -0.015 \text{ BTU/lbm } ^\circ\text{F}$$

$$h_{4S} = -117 \text{ BTU/lbm}^*$$

$$\text{Condenser temperature} = 90^\circ\text{F}$$

$$\text{Corresponding pressure, } P_1 = 0.8 \text{ psia}^*$$

$$h_1 = -315 \text{ BTU/lbm}^*$$

Efficiency of turbine,

$$\eta_t = \frac{h_3 - h_4}{h_3 - h_{4S}} = 0.75$$

Therefore,

$$h_4 = h_3 - 0.75 \times (h_3 - h_{4S})$$

$$= -37 - 0.75 \times (-37 + 117)$$

$$= -97 \text{ BTU/lbm}$$

Considering a control surface around the pump.

$$\text{First Law: } \omega_p = h_2 - h_1$$

---

\* Indicates data read from T-s charts or tables.

Work done by the pump,  $\omega_p$ , is related to pressures  $P_1$ ,  $P_2$ , specific volume of the liquid,  $v$  and efficiency of the pump  $\eta_p$  by an equation,

$$\begin{aligned}\omega_p &= \frac{v(P_2 - P_1)}{\eta_p} = 0.01848 \times (120 - 0.8) \times \frac{144}{778} \times \frac{1}{0.5} \\ &= 0.65 \text{ BTU/lbm}\end{aligned}$$

Therefore,

$$h_2 = h_1 + \omega_p = -315 + 0.65 = -314.35 \text{ BTU/lbm}$$

Consider a control surface around the turbine.

First Law: Work done by the turbine,  $\omega_t = h_3 - h_4$ .

Therefore,

$$\omega_t = -37 + 97 = 60 \text{ BTU/lbm}$$

Energy content of superheated exhaust between state point 4 and 4b,  $Q_S$  is given by

$$\begin{aligned}Q_S &= h_4 - h_{4b} \\ &= -97 + 117 = 20 \text{ BTU/lbm}\end{aligned}$$

80% of this energy is transferred to the fluid coming out of the pump.

$$\begin{aligned}h_{2a} &= h_2 + 0.8(20) \\ &= -314.65 + 16 = -298.65 \text{ BTU/lbm}\end{aligned}$$

Corresponding  $T_{2a} = 132^\circ\text{F}$  which is lower than  $T_4 = 222^\circ\text{F}$

Consider a control surface around the boiler.

External heat added at the boiler,  $Q_h$  is given by

$$\begin{aligned}Q_h &= h_3 - h_{2a} \\ &= -37 + 298.65 \\ &= 261.65 \text{ BTU/lbm}\end{aligned}$$

Network output,  $\omega_{\text{net}} = \omega_t - \omega_p$

$$\begin{aligned}&= 60 - 0.65 \\ &= 59.35 \text{ BTU/lbm}\end{aligned}$$

Efficiency of the cycle,

$$\begin{aligned}\eta_{Re} &= \frac{\omega_{net}}{Q_h} \\ &= \frac{59.35}{261.65} \\ &= 0.227 \\ &= 22.7\%\end{aligned}$$

Efficiency of the Rankine-cycle without regeneration for the same conditions is 21.4%.

The efficiency is calculated at about 7 to 10 different heat source temperatures for all 7 organic fluids. The results are shown in Tables 9 thru 15 and in a graphical form of heat source temperature vs cycle efficiency in Figures 20 thru 26. The turbine supply pressure is not to be less than atmospheric pressure.

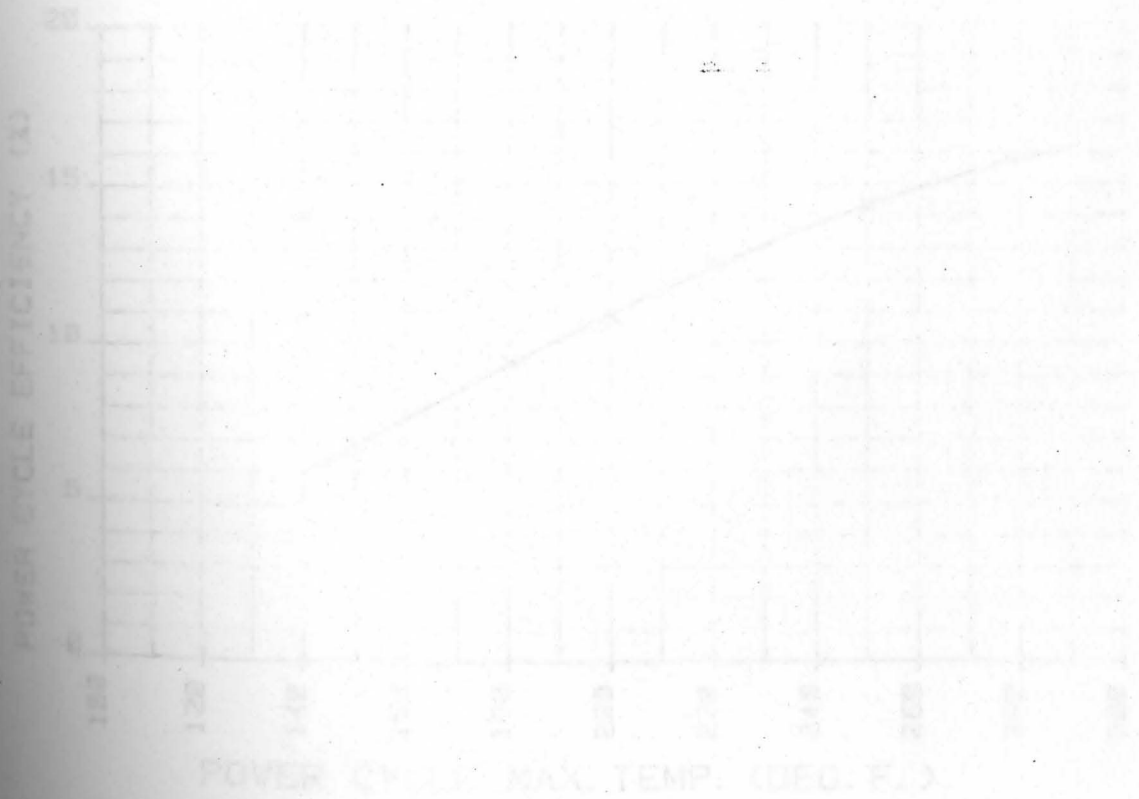


FIGURE 20. Efficiency of a Rankine-cycle with 5% regeneration vs. Cycle maximum temperature (Deg. F.).

TABLE 9. Efficiency of a Rankine-Cycle with 80% Regeneration at Several Different Heat Source Temperatures Using R-11.

Heat Source Temperature $T_{Re}$ °F	Cycle Efficiency, $\eta_{Re}$ %
150	6.8
180	9.4
200	10.8
220	12.5
250	14.3
280	15.8

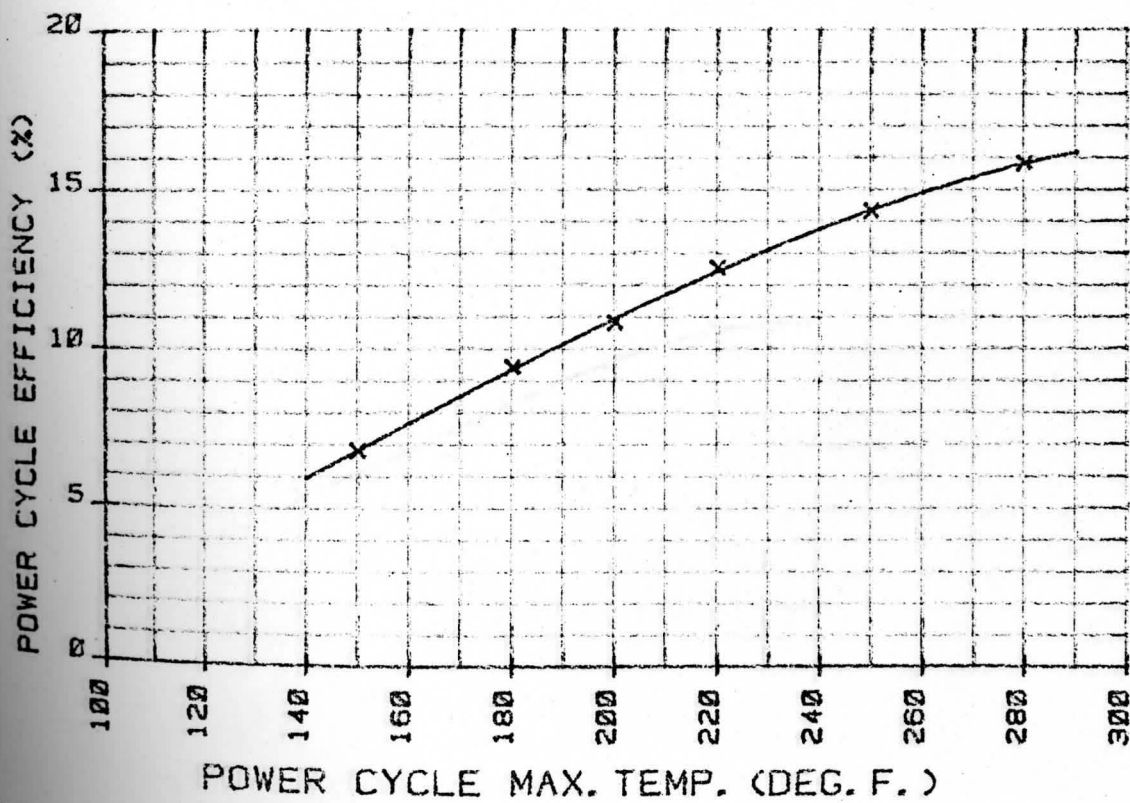


FIGURE 20. Efficiency of a Rankine-Cycle with 80% Regeneration vs. Cycle Maximum Temperature Curve for R-11.

TABLE 10. Efficiency of a Rankine-Cycle with 80% Regeneration at Several Different Heat Source Temperatures Using R-12.

Heat Source Temperature $T_{Re}$ °F	Cycle Efficiency, $\eta_{Re}$ %
140	5.4
160	6.8
180	8.2
200	9.6
220	10.7
230	10.8

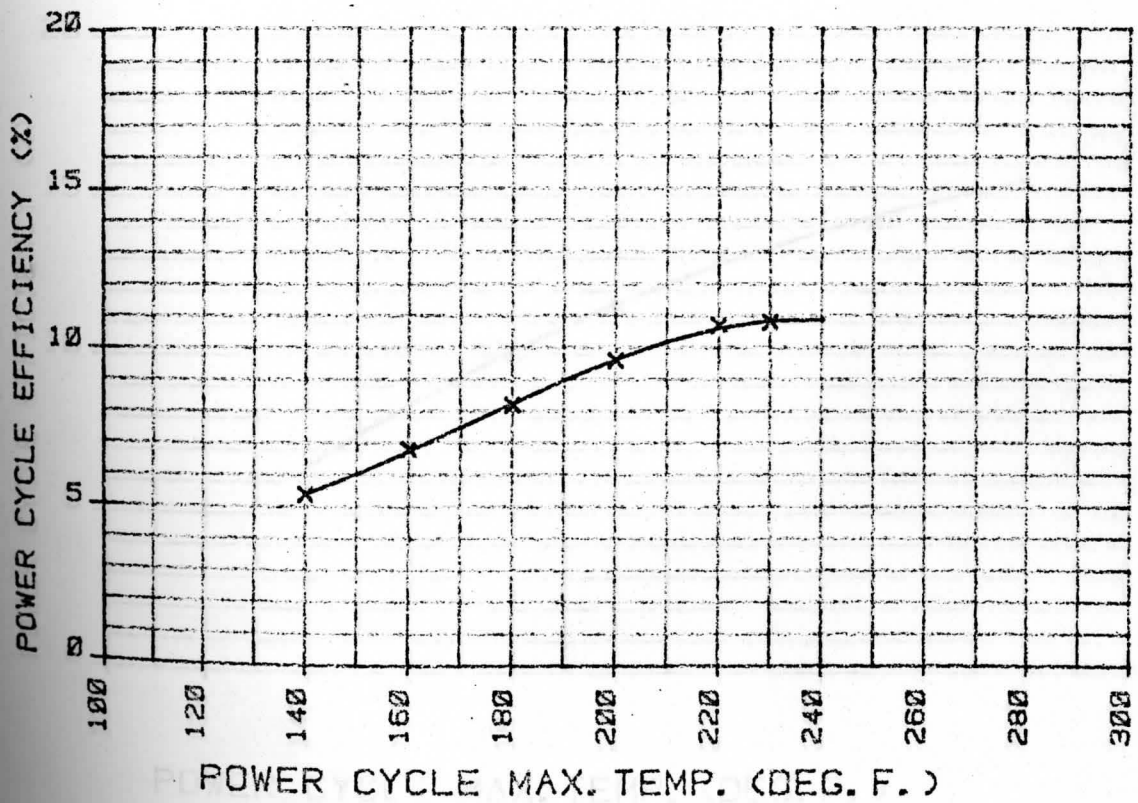


FIGURE 21. Efficiency of a Rankine-Cycle with 80% Regeneration vs. Cycle Maximum Temperature Curve for R-12.

TABLE 11. Efficiency of a Rankine-Cycle with 80% Regeneration at Several Different Heat Source Temperatures Using R-113.

Heat Source Temperature $T_{Re}$ °F	Cycle Efficiency, $\eta_{Re}$ %
150	7.5
180	10.0
200	11.5
220	13.1
250	14.1
280	15.5

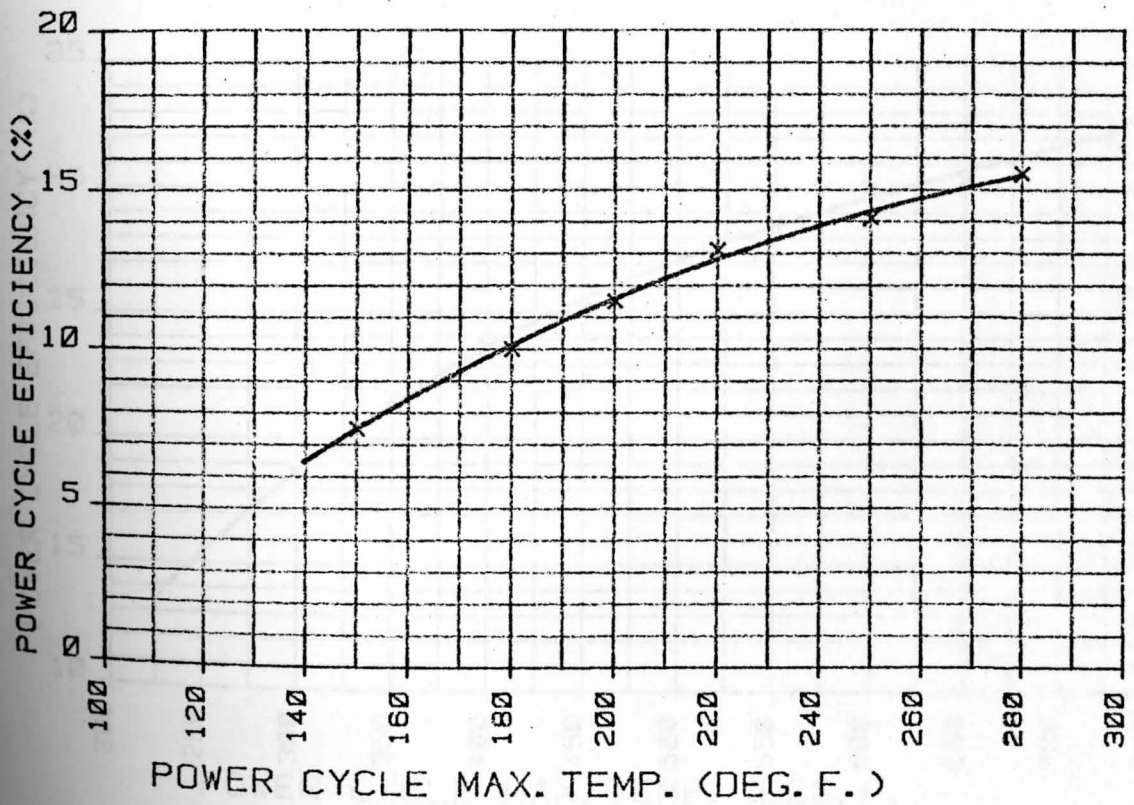


FIGURE 22. Efficiency of a Rankine-Cycle with 80% Regeneration vs. Cycle Maximum Temperature Curve for R-113.



TABLE 12. Efficiency of a Rankine-Cycle with 80% Regeneration at Several Different Heat Source Temperature Using Toluene.

Heat Source Temperature, $T_{Re}$ °F	Cycle Efficiency, $\eta_{Re}$ %
230	13.9
300	18.6
350	21.5
400	23.5
450	25.1
500	27.2
550	28.5
600	30.0
650	30.3
730	32.4

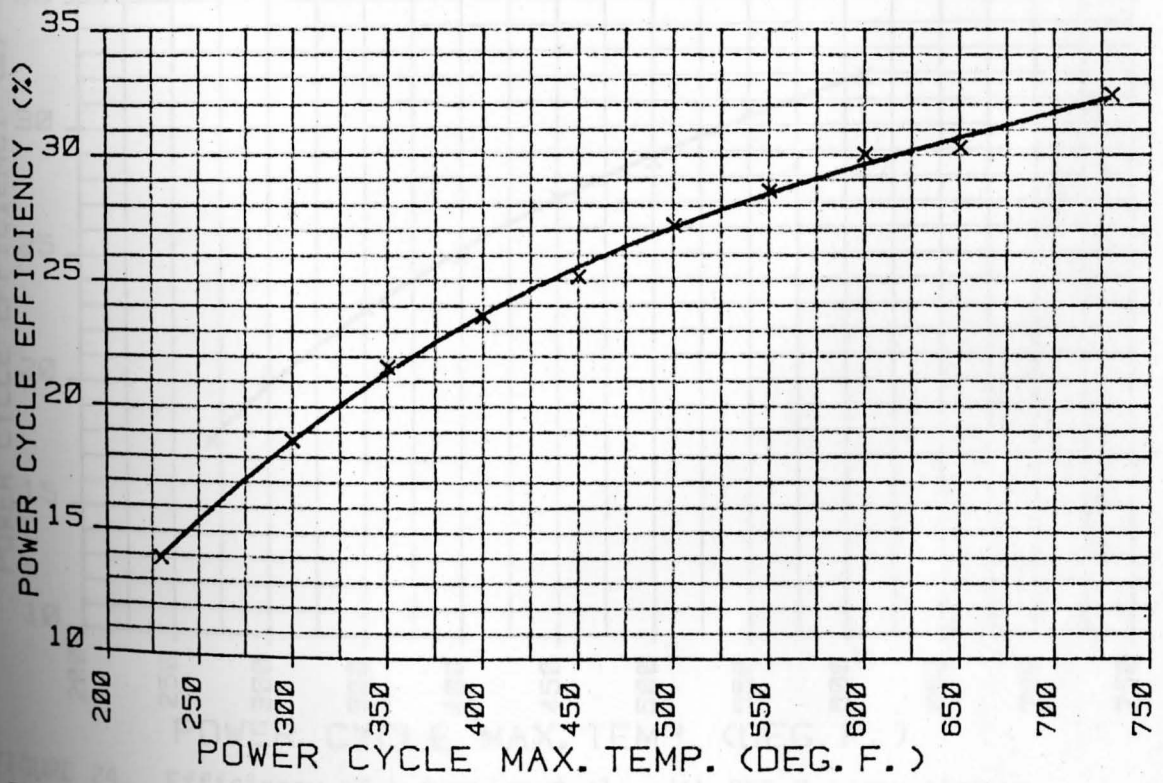


FIGURE 23. Efficiency of a Rankine-Cycle with 80% Regeneration vs. Cycle Maximum Temperature Curve for Toluene.

TABLE 13. Efficiency of a Rankine-Cycle with 80% Regeneration at Several Different Heat Source Temperatures Using Chlorobenzene.

Heat Source Temperature, $T_{Re}$ °F	Cycle Efficiency, $\eta_{Re}$ %
270	17.7
300	20.0
350	22.9
400	24.9
450	27.2
500	28.6
550	30.6
610	31.9

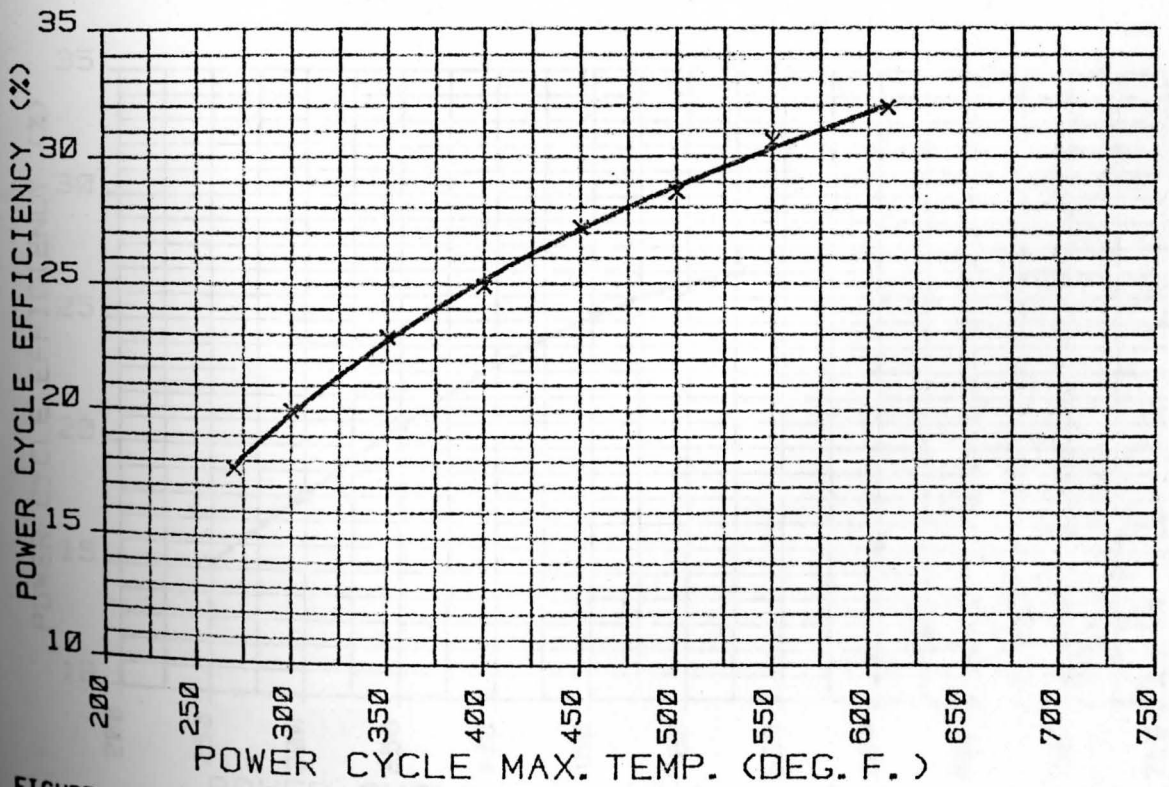


FIGURE 24. Efficiency of a Rankine-Cycle with 80% Regeneration vs. Cycle Maximum Temperature Curve for Chlorobenzene.

TABLE 14. Efficiency of a Rankine-Cycle with 80% Regeneration at Several Different Heat Source Temperatures Using Thiophene.

Heat Source Temperature, $T_{Re}$ °F	Cycle Efficiency, $\eta_{Re}$ %
250	15.2
300	17.9
350	20.9
400	23.2
450	25.3
500	26.3
530	27.1

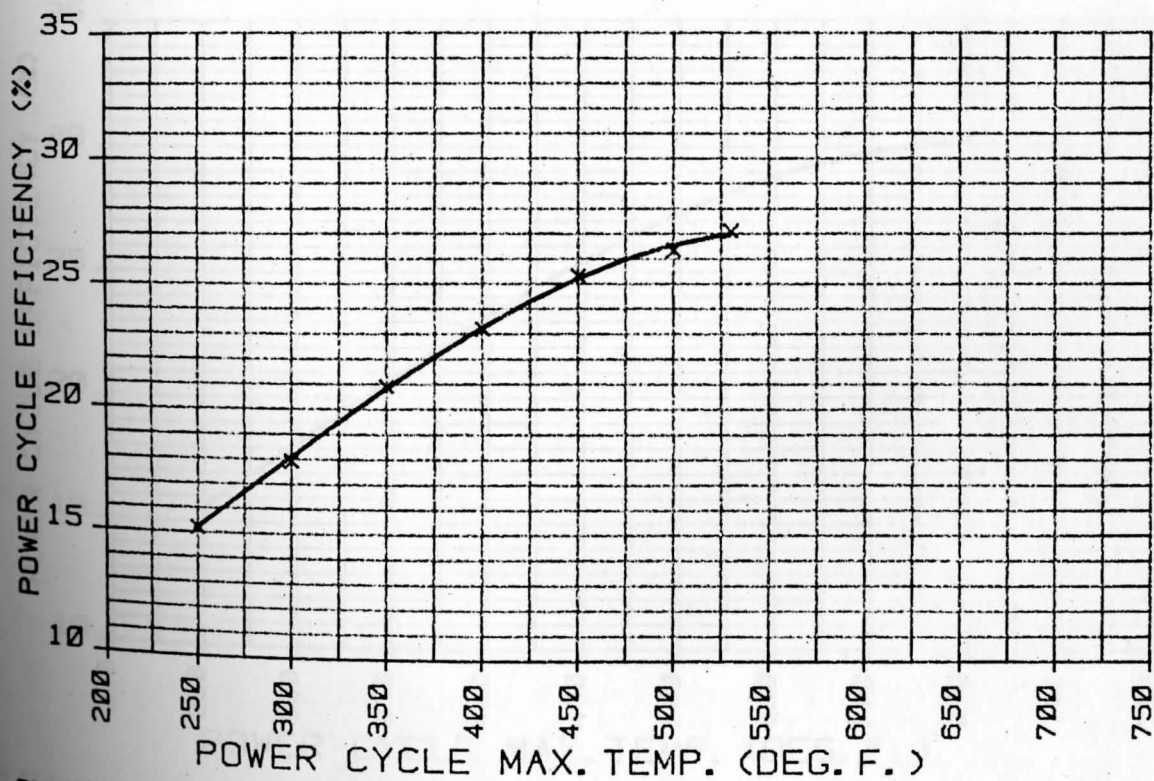


FIGURE 25. Efficiency of a Rankine-Cycle with 80% Regeneration vs. Cycle Maximum Temperature Curve for Thiophene.

TABLE 15. Efficiency of a Rankine-Cycle with 80% Regeneration at Several Different Heat Source Temperatures Using Pyridine.

Heat Source Temperature, $T_{Re}$ °F	Cycle Efficiency, $\eta_{Re}$ %
250	15.5
300	18.2
350	20.3
400	23.5
450	25.4
500	27.4
550	28.8
600	29.5
650	30.3

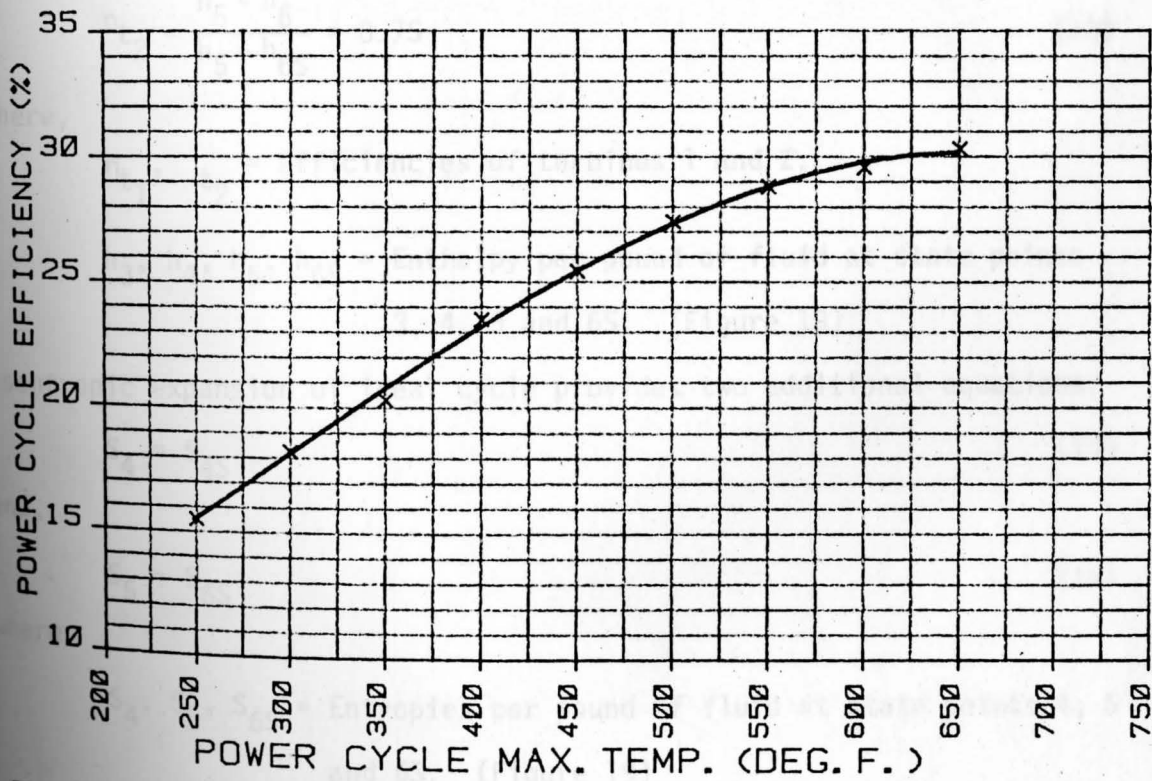


FIGURE 26. Efficiency of a Rankine-Cycle with 80% Regeneration vs. Cycle Maximum Temperature Curve for Pyridine.

### Efficiency Calculations of Reheat Cycle with Water.

The reheat cycle is to be operated such that maximum possible efficiency is obtained with a given available source temperature yet avoiding condensation during any of the turbine expansion process. For this to happen, points 4 and 6 (Figure 19) must fall on the saturated vapor line and point 5 must be at a maximum available temperature – same as temperature  $T_3$ .

The efficiencies of pump and turbines are the same – 50% and 75%, respectively. The efficiency of the turbines relate to enthalpies at several state points by equations:

$$\eta_{t_1} = \frac{h_3 - h_4}{h_3 - h_{4S}} = 0.75 \quad (12)$$

and,

$$\eta_{t_2} = \frac{h_5 - h_6}{h_5 - h_{6S}} = 0.75 \quad (13)$$

where,

$\eta_{t_1}, \eta_{t_2}$  = Efficiencies of turbines 1 and 2.

$h_3, h_4, h_5, h_{6S}$  = Enthalpy per pound of fluid at state points 3, 4, 5 and 6S. (Figure 19)

Isentropic expansion of ideal cycle provides two additional equations:

$$s_4 = s_{4S} \quad (14)$$

and,

$$s_5 = s_{6S} \quad (15)$$

where

$s_4, s_5, s_{6S}$  = Entropies per pound of fluid at state points 4, 5 and 6S. (Figure 19)

These additional equations, along with previous equations (See Chapter II) are used for calculating water/steam reheat cycle efficiency at several different temperatures starting from 300°F up to 1030°F at an interval of 50°F. The procedure followed is best illustrated by sample calculations shown below for an available heat source temperature,  $T_3 = T_5 = 450^\circ\text{F}$ .

Condenser Temperature,  $T_1 = 90^\circ\text{F}$ ,  $P_1 = 0.7 \text{ psia}^*$

$$h_1 = 58.07 \text{ BTU/lbm}^*$$

$$h_6 = 1100.7 \text{ BTU/lbm}^*$$

Consider a control surface around the second turbine.

$$\eta_{t_2} = \frac{h_5 - h_6}{h_5 - h_{6S}} = 0.75$$

Second Law:  $S_5 = S_{6S}$

Consider a control surface around the first turbine.

$$\eta_{t_1} = \frac{h_3 - h_4}{h_3 - h_{4S}} = 0.75$$

Second Law:  $S_3 = S_{4S}$

$$T_3 = T_5 = 450^\circ\text{F}$$

Using these equations and property tables,  $h_3$ ,  $h_5$  and  $P_3$  are obtained by trial and error.

$$h_3 = 1255 \text{ BTU/lbm}$$

$$h_5 = 1263 \text{ BTU/lbm}$$

and

$$P_2 = P_3 = 90 \text{ psia}$$

Then

$$h_4 = 1150.5 \text{ BTU/lbm}^*$$

\*Data read from T-s Charts or Tables.

Consider a control surface around the pump. Work done by the pump,  $\omega_p$ , is related to specific volume of the liquid,  $v$ , pressures at state points 1 and 2 —  $P_1$  and  $P_2$ , respectively — and efficiency of the pump,  $\omega_p$  by an equation,

$$\begin{aligned}\omega_p &= \frac{v(P_2 - P_1)}{\eta_p} \\ &= 0.01615 \times (90 - 0.7) \times \frac{144}{778} \times \frac{1}{0.5} \\ &= 0.53 \text{ BTU/lbm} \\ h_2 &= h_1 + \omega_p \\ &= 58.07 + 0.53 = 58.6 \text{ BTU/lbm}\end{aligned}$$

Consider a control surface around the boiler. Total heat added to the boiler,

$$\begin{aligned}Q_h &= (h_3 - h_2) + (h_5 - h_4) \\ &= (1255 - 58.6) + (1263 - 1150.5) \\ &= 1308.9 \text{ BTU/lbm}\end{aligned}$$

Consider a control surface around the turbines. Total work output of the turbines,  $\omega_t$ , is given by,

$$\begin{aligned}\omega_t &= (h_3 - h_4) + (h_5 - h_6) \\ &= (1255 - 1150.5) + (1263 - 1100.7) \\ &= 266.8 \text{ BTU/lbm}\end{aligned}$$

Net work output,  $\omega_{net} = \omega_t - \omega_p$

Therefore,

$$\begin{aligned}\omega_{net} &= 266.8 - 0.53 \\ &= 266.27 \text{ BTU/lbm}\end{aligned}$$

Cycle Efficiency =  $\frac{\omega_{net}}{Q_h}$

$$= \frac{266.27}{1308.9}$$

= 0.2034 i.e. 20.34%

The efficiency of the cycle without reheat was 13.5%. The results of water/steam reheat cycle efficiencies calculated at several different temperatures are tabulated in Table 16. The graph of efficiency vs. heat source temperature is shown in Figure 27.

Temperature (°F)	Efficiency (%)
370	13.5
380	14.5
390	15.5
400	16.5
410	17.5
420	18.5
430	19.5
440	20.34
450	21.0

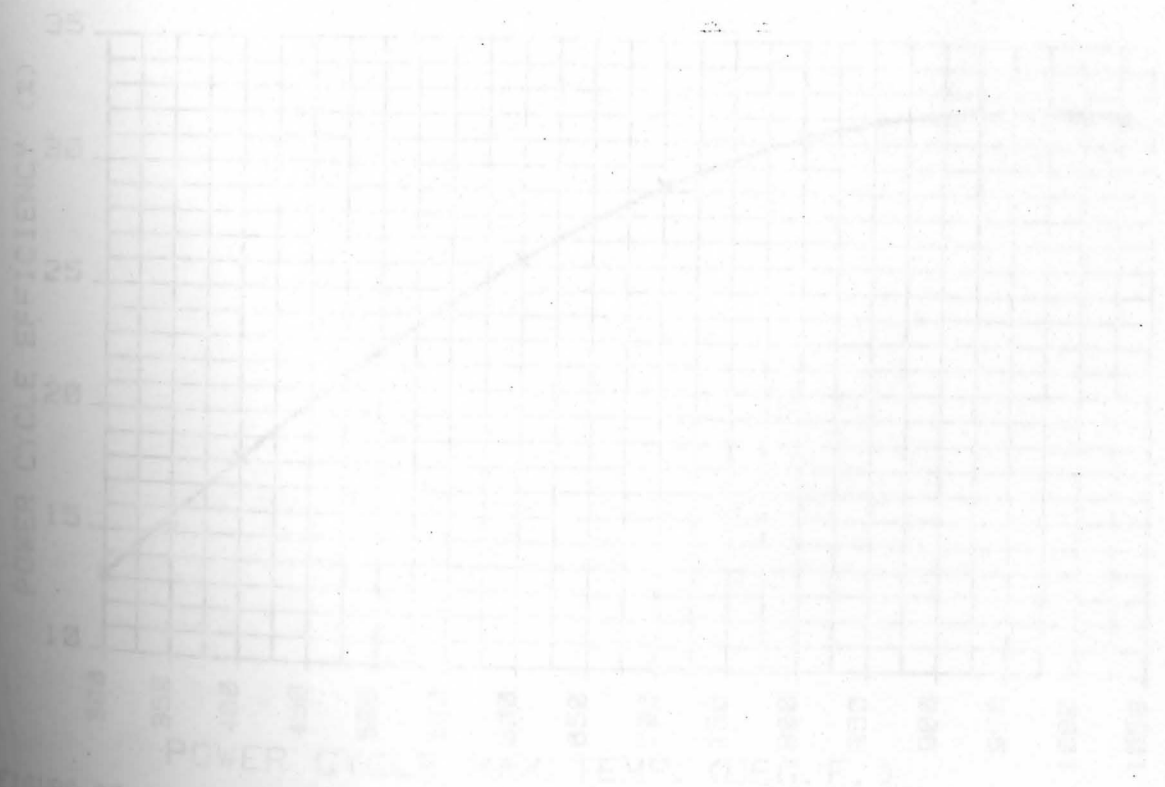


FIGURE 27. Reheat Cycle Efficiency vs. Power Cycle Temperature Curve for Water/Steam



TABLE 16. Water/Steam Reheat Cycle Efficiencies at Several Different Heat Source Temperatures.

Heat Source Temperature, $T_3$ °F	Water/Steam Reheat Cycle Efficiency, $\eta_{Re}$ %
300	13.1
350	15.7
400	18.1
450	20.3
500	22.5
600	26.2
700	29.2
800	31.2
900	32.0
1030	32.0

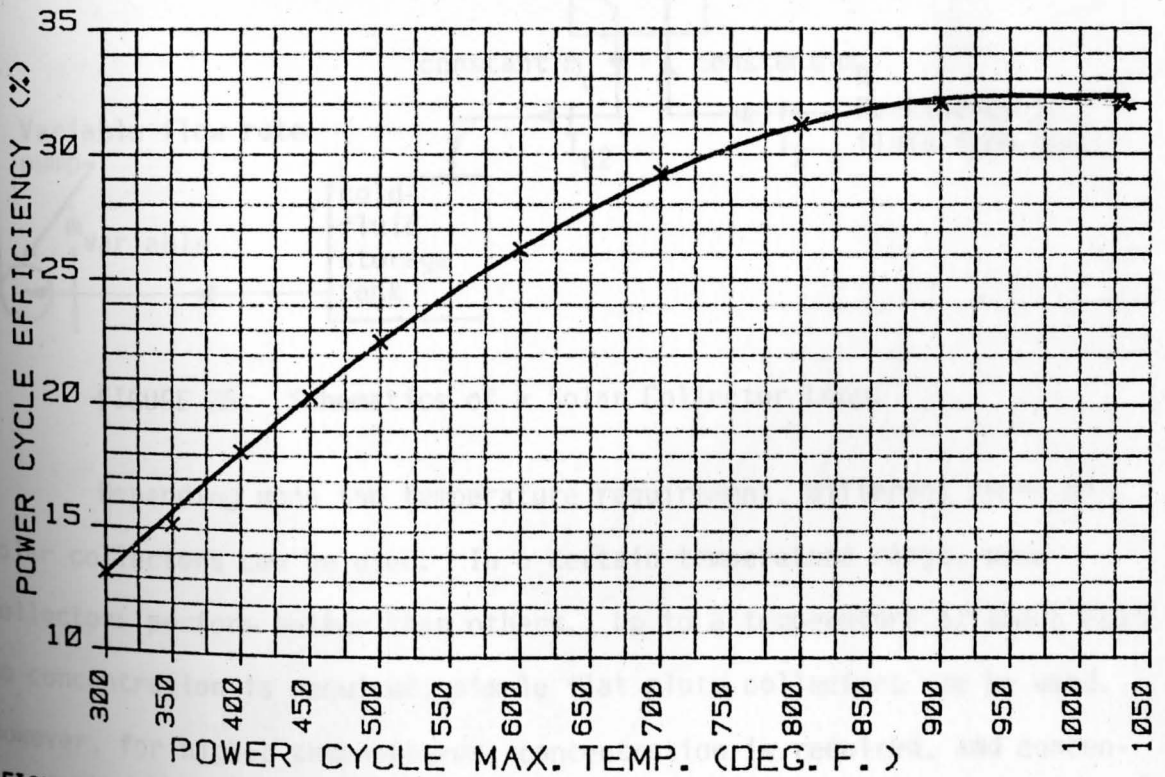


FIGURE 27. Reheat Cycle Efficiency vs. Maximum Cycle Temperature Curve for Water/Steam.

## CHAPTER IV

PERFORMANCE OF SOLAR COLLECTORS

In this chapter, performance of the solar collector loop is analyzed. Its schematic diagram is repeated here for easy reference.

(Figure 28)

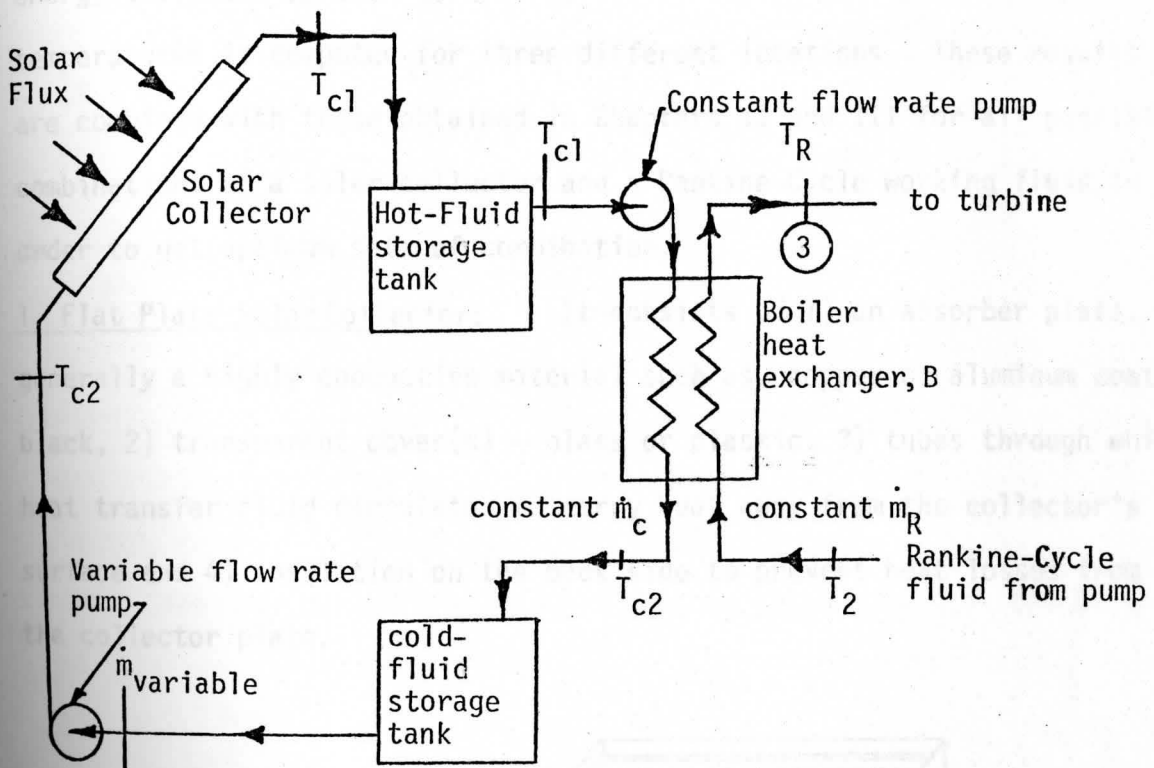


FIGURE 28. Schematics of a Solar Collector Loop.

Depending upon the temperature requirement, different types of solar collectors can be used. In a certain temperature range, some collectors perform better than others. Up to a temperature of about 220°F no concentration is required; simple flat plate collectors can be used. However, for higher temperatures, concentration is required, and concentrating collectors are used. There are four main generic types of solar collectors. In the order of their increasing ability to operate at

higher temperatures, they are:

1. Flat plate collector
2. Compound parabolic concentrating (CPC) collector
3. Line-focusing parabolic trough collector
4. Point-focusing paraboloid disc collector

In this thesis, these four types of collectors are analyzed. Solar energy collected by each type of collector at several different operating temperatures is computed for three different locations. These results are combined with those obtained in Chapters II and III for all possible combinations of a solar collector and a Rankine-Cycle working fluid in order to get optimum sets of combination.

1. Flat Plate Solar Collector: It consists of 1) an absorber plate, generally a highly conductive material such as, copper or aluminum coated black, 2) transparent cover(s) – glass or plastic, 3) tubes through which heat transfer fluid circulates to carry heat away from the collector's surface and 4) insulation on the back side to prevent heat losses from the collector plate.

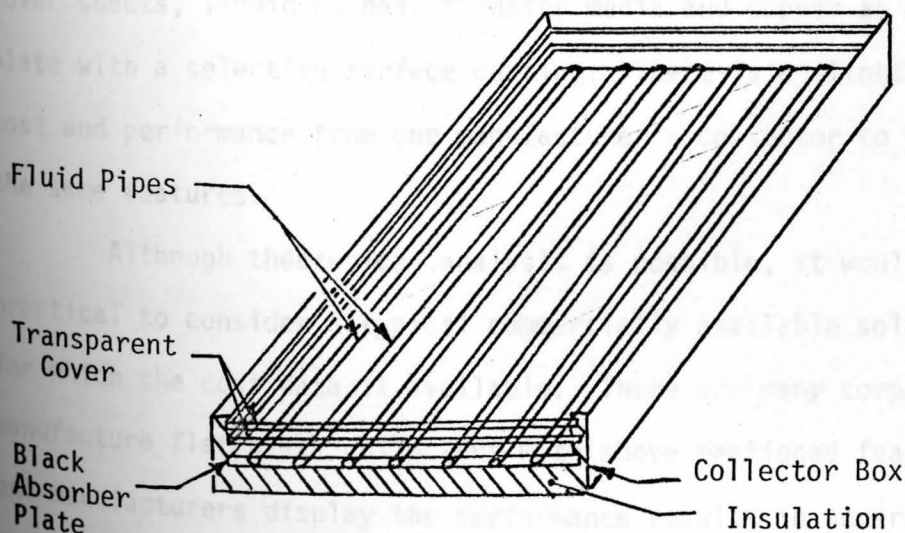


FIGURE 29. A Flat Plate Solar Collector.

Sunlight having shorter wavelength passes through the glass, gets absorbed by the absorber plate, but radiation emitted by the absorber plate having longer wavelength cannot pass through glass since glass is opaque to long wave radiation. Thus, glass besides suppressing conduction and convection losses, also suppresses radiation losses and so absorber plate can easily attain temperatures above 150°F. Flat plate collectors are ideal for low temperature applications requiring temperatures from 100°F up to 250°F. A significant advantage of using flat plate collector is that it can use both the direct and scattered solar energy components.

There are several variations within a flat plate collector, such as, the number of cover plates may vary from 1 to 3, cover plates can be glass or plastic, absorber plate can be copper or aluminum, absorber coating can be black paint or a selective surface such as, black chrome, heat transfer fluid may be air or liquid. The type of application, cost and life expectancy requirements determine the choice of these options. For applications with a Rankine-cycle, where reasonably high temperatures and life expectancy are required, the features needed are: two glass cover sheets, liquid as heat transfer media and copper as an absorber plate with a selective surface coating. There is a slight variation in cost and performance from one manufacturer's collector to the other having the same features.

Although theoretical analysis is possible, it would be more practical to consider a typical commercially available solar collector for which the cost data is available. There are many companies that manufacture flat plate collectors with above mentioned features. Different manufacturers display the performance results in several different forms. The ASHRAE recommended practice is to show flat plate collector

performance results in terms of its efficiency vs.  $(T_{f,in} - T_a)/I_{coll.}$ .

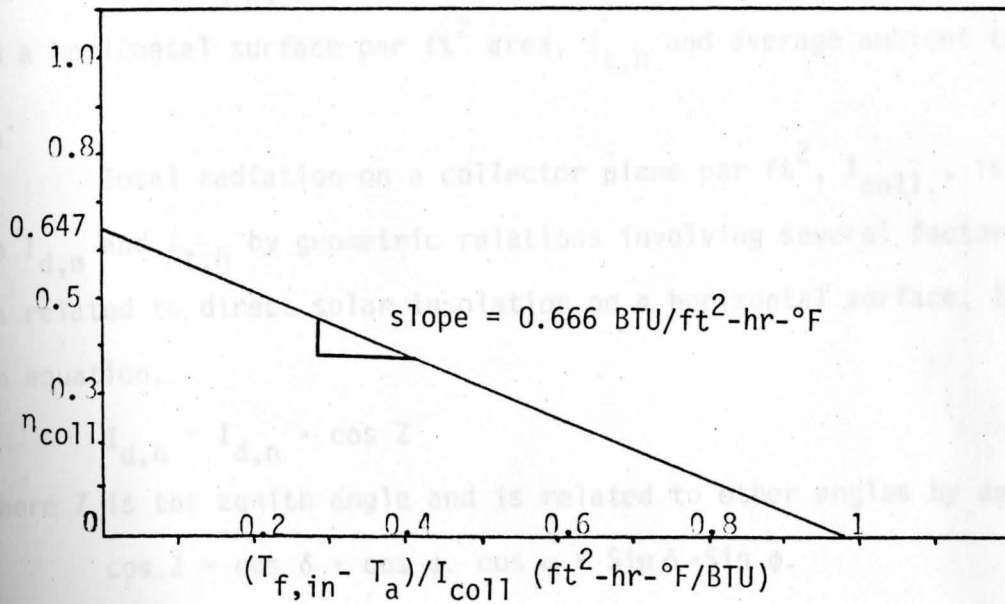


FIGURE 30. Flat Plate Collector Performance Curve.

where  $T_{f,in}$  is the temperature of the fluid entering each collector module,  $T_a$  is the ambient temperature and  $I_{coll.}$  is the instantaneous total (direct + scattered) solar insolation on the collector plane per unit area. The collector fluid used and its mass flow rate through each module are also given. Efficiency of the solar collector is the energy absorbed by the fluid over the solar insolation on its plane.

A typical average performance curve is as shown in Figure 30. The average cost is \$17 per  $ft^2$  as of March 1981. The curve shown in Figure 30 is a straight line. An equation is obtained by curve fitting.

$$\eta_{coll.} = 0.647 - 0.666 \frac{T_{f,in} - T_a}{I_{coll}} \quad (16)$$

Sufficient accuracy is obtained for calculations done for a time segment of one hour. The 'SOLMET' tape-magnetic tape having hourly weather data — contains data of direct solar insolation on a surface normal to sunrays per  $\text{ft}^2$  area,  $I_{d,n}$ , total (direct + scattered) amount of solar insolation on a horizontal surface per  $\text{ft}^2$  area,  $I_{t,h}$  and average ambient temperature,  $T_a$ .

Total radiation on a collector plane per  $\text{ft}^2$ ,  $I_{\text{coll}}$ , is related to  $I_{d,n}$  and  $I_{t,h}$  by geometric relations involving several factors.  $I_{d,n}$  is related to direct solar insolation on a horizontal surface,  $I_{d,h}$ , by an equation,

$$I_{d,h} = I_{d,n} \cdot \cos Z \quad (17)$$

where  $Z$  is the zenith angle and is related to other angles by an equation,

$$\cos Z = \cos \delta \cdot \cos \phi \cdot \cos \omega + \sin \delta \cdot \sin \phi. \quad (18)$$

where  $\delta$  is the declination angle and is related to the number of the day of the year,  $n$ , by an equation,

$$\delta = 23.45 \times \sin \left( 360 \times \frac{284 + n}{365} \right) \quad (19)$$

where,

$\phi$  = latitude of the location in degrees.

$\omega$  = hour angle, that is, the angular displacement of the sun east or west of the local meridian due to the rotation of the earth on its axis at  $15^\circ$  per hour; morning negative, afternoon positive.

Then, scattered radiation on a horizontal surface,  $I_{s,h}$  is

$$I_{s,h} = I_{t,h} - I_{d,h} \quad (20)$$

The direct solar insolation on a collector plane,  $I_{d,c}$ , is related to  $I_{d,n}$  by an equation,

$$I_{d,c} = I_{d,n} \times \cos \theta \quad (21)$$

where  $\theta$  is the angle between sunrays and normal to the collector plane and for a south facing collector, it is related to other angles by an equation,

$$\begin{aligned} \cos \theta &= \sin \delta \cdot \sin \phi \cdot \cos \beta - \sin \delta \cdot \cos \phi \cdot \sin \beta \\ &+ \cos \delta \cdot \cos \phi \cdot \cos \beta \cdot \cos \omega \\ &+ \cos \delta \cdot \sin \phi \cdot \sin \beta \cdot \cos \omega \end{aligned} \quad (22)$$

where,

$\beta$  = slope, angle between the collector plane and the horizontal.

For year round application, the solar collection is maximized when collector is tilted at an angle,  $\beta$ , equal to latitude angle of the location,  $\phi$ .

Substituting  $\beta = \phi$ , Equation (22) reduces to

$$\cos \theta = \cos \delta \cdot \cos \omega. \quad (23)$$

According to Hottel and Woertz, scattered radiation can be assumed to be isotropic i.e. uniformly distributed over the sky.<sup>12</sup>

Hence, the scattered radiation on a flat plate collector plane,  $I_{s,c}$ , is the same as that on the horizontal surface,  $I_{s,h}$ .

$$I_{s,c} = I_{s,h} \quad (24)$$

Thus, the total insolation on a collector plane,  $I_{t,c}$  can be computed every hour by summing  $I_{d,c}$  as obtained by equation (21) and  $I_{s,c}$ , as obtained by Equations (20) and (24).  $I_{t,c}$  is then used in Equation (1)

---

<sup>12</sup>John A. Duffie, et al, Solar Engineering of Thermal Processes, (New York: John Wiley & Sons, 1980) p. 85.

to calculate efficiency of each collector module every hour. Usually, the mass flow rate is such that temperature rise of about 10°F is obtained through each collector module. In order to get desired output temperature, the collector modules are to be connected in a series. Efficiency is calculated at every 10°F interval and is then averaged out. Total useful solar energy collected by the collector per ft<sup>2</sup> every hour is then calculated from the following equation.

$$\text{Solar Energy Collected/hr} = \eta_{\text{avg., coll.}} \times I_{t,c} \quad (25)$$

Hourly results are summed up for the year to establish total energy collected per year. From the practical point of view, anytime solar insolation on the collector is less than 50 BTU per ft<sup>2</sup> per hour or average collector efficiency,  $\eta_{\text{avg.}}$ , is less than 15%, it is assumed that the pump is not turned on and, thus no energy is collected during that hour.

Total energy collected per year is calculated for collector fluid average temperature,  $T_{\text{avg}}$ , starting from 140°F to 220°F at an interval of 20°F for three locations mentioned earlier. 'SOLMET' weather tape is used for solar insolation and ambient temperature data and calculations are performed by use of a computer. The flow chart of the computer program and computer program listing along with the output are shown in Appendix B. Monthly results, that is the solar energy collected per month are tabulated in Table 17 and are shown graphically in Figure 38, 39 and 40.



TABLE 17. Solar Energy Collected by Flat Plate Solar Collector per ft<sup>2</sup> Area Per Year for Three Locations. (BTU/ft<sup>2</sup>-Year)

Collector Fluid Average Temperature (°F)	Madison WI	Miami FL	Albuquerque NM
140	158,864	235,953	315,731
160	130,141	193,832	273,617
180	104,954	157,481	234,909
200	81,248	123,773	199,224
220	60,020	91,594	164,424
240	42,525	65,451	131,496
260	26,695	40,744	101,071
280	13,269	21,020	70,021
300	2,855	6,688	45,497

#### Compound Parabolic Concentrating (CPC) Collectors.

The compound parabolic concentrating (CPC) collectors are a class of non-imaging concentrators which offer medium range concentration — concentration of up to 10 — without tracking requirement and are good for temperature application between 175°F and 350°F. CPC collector is basically made of two parabolic surface — each half a separate parabola, an absorber usually encased in an evacuated glass tube located at the truncated surface and glass cover sheet on top. Figure 31 shows a typical CPC collector.

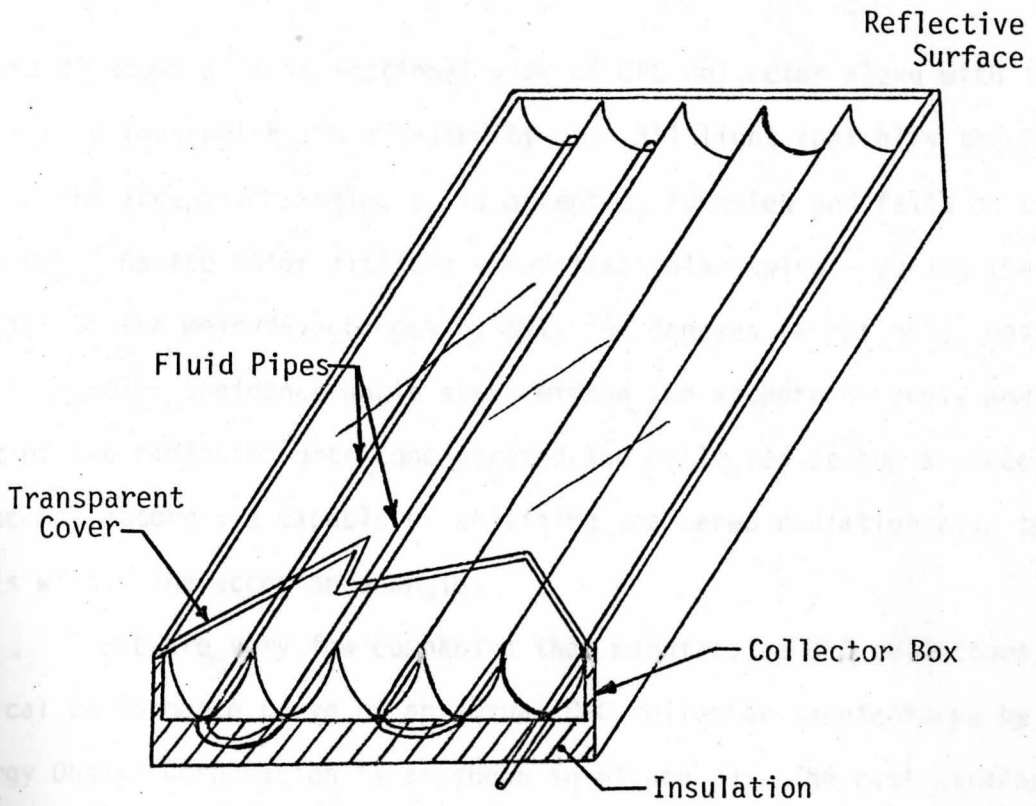


FIGURE 31. Typical CPC Collector

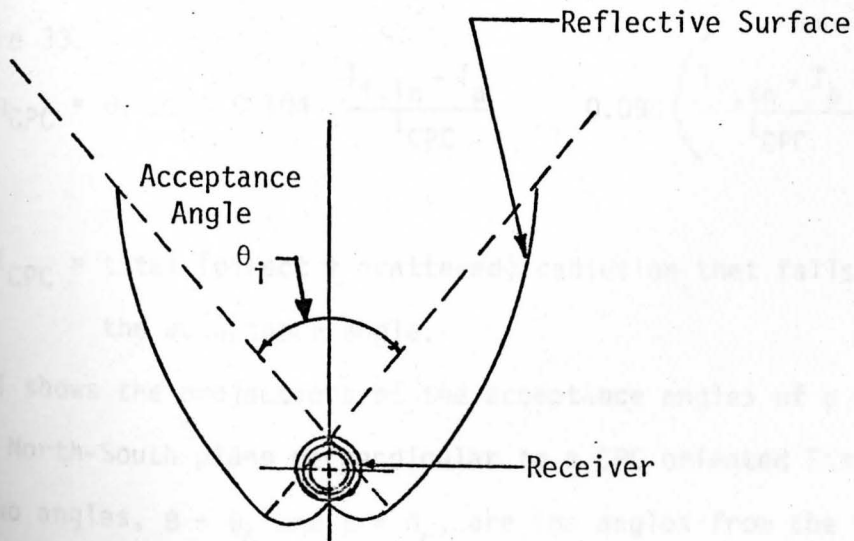


FIGURE 32. Cross-Section of a CPC.

Figure 32 shows a cross sectional view of CPC collector along with the paths of extreme rays which are accepted by it. All light that hits the CPC within the acceptance angle,  $\theta_i$  is accepted, funneled and falls on the absorber. As the solar altitude – vertical solar swing – during the major portion of the mean day changes by only few degrees (about  $\pm 6^\circ$ ), most of the time solar incidence angle stays within the acceptance angle and thus most of the radiation gets concentrated and collected at the absorber. These collectors are capable of utilizing scattered radiation also that falls within the acceptance angle.

There are very few companies that manufacture CPC collectors. A typical performance curve of an actual CPC collector manufactured by Energy Design Corporation is as shown in Figure 33. The cost of this unit is \$28/ft<sup>2</sup> as of March, 1981. The angle of acceptance for this collector is 98° with a concentration ratio of 1.33.

The following quadratic equation is obtained by curvefitting the Figure 33.

$$\eta_{\text{CPC}} = 0.499 - 0.104 \frac{T_{f,\text{in}} - T_a}{I_{\text{CPC}}} - 0.098 \left( \frac{T_{f,\text{in}} - T_a}{I_{\text{CPC}}} \right)^2 \quad (26)$$

where

$I_{\text{CPC}}$  = total (direct + scattered) radiation that falls within the acceptance angle.

Figure 34 shows the projections of the acceptance angles of a CPC on a vertical North-South plane perpendicular to a CPC oriented East-West axis. Two angles,  $\beta - \theta_c$  and  $\beta + \theta_c$ , are the angles from the vertical in this plane to the two limits describing the acceptance angle. Mitchell has shown that the following condition must be met in order for the beam

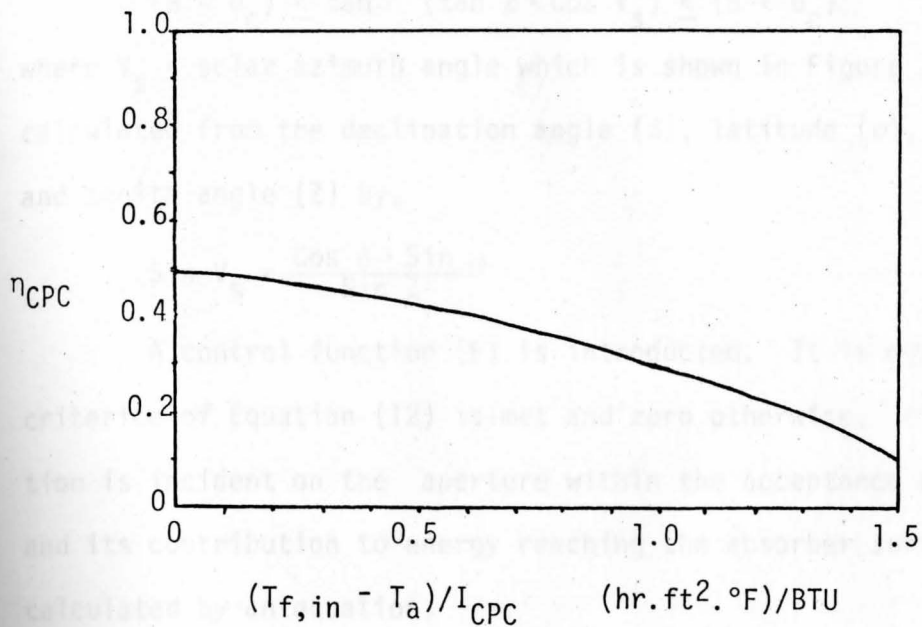


FIGURE 33. CPC Performance Curve.

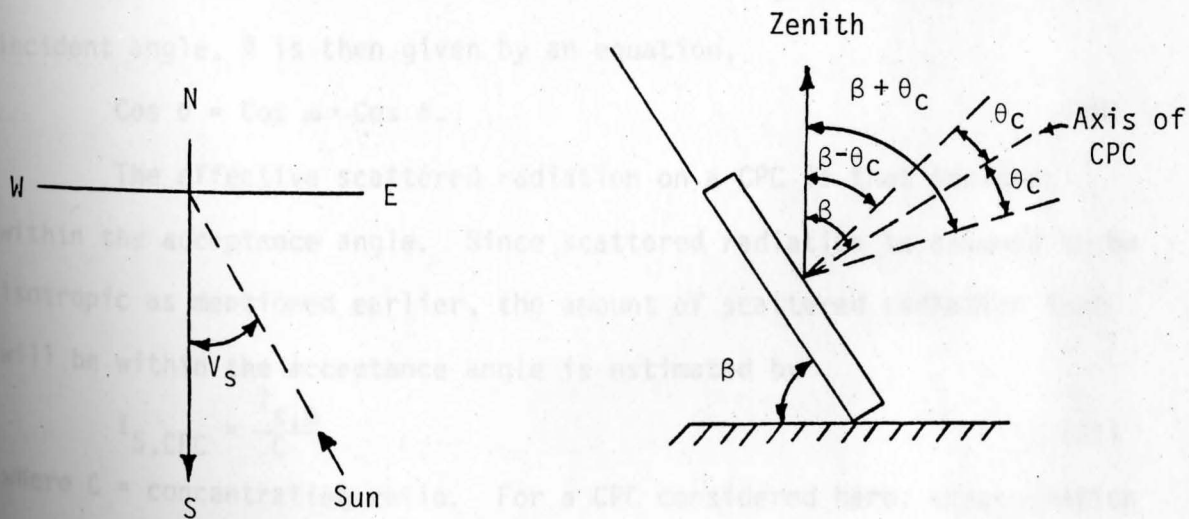


FIGURE 34. (a) Plan Showing Solar Azimuth Angle  $-V_s$ ,  
 (b) Projection on a North-South Plane of CPC Acceptance Angles and Slope.

radiation to be useful.<sup>13</sup>

$$(\beta - \theta_c) \leq \tan^{-1} (\tan Z \cdot \cos V_s) \leq (\beta + \theta_c) \quad (27)$$

where  $V_s$  = solar azimuth angle which is shown in Figure 34a and can be calculated from the declination angle ( $\delta$ ), latitude ( $\phi$ ), hour angle ( $\omega$ ) and zenith angle ( $Z$ ) by,

$$\sin V_s = \frac{\cos \delta \cdot \sin \omega}{\sin Z} \quad (28)$$

A control function ( $F$ ) is introduced. It is equal to 1 if the criterion of Equation (12) is met and zero otherwise. If direct radiation is incident on the aperture within the acceptance angle, then  $F = 1$ , and its contribution to energy reaching the absorber surface can be calculated by an equation,

$$I_{d,CPC} = F \times I_{d,n} \times \cos \theta. \quad (29)$$

where  $\theta$  is the angle between collector normal and sunrays.

Like flat-plate collectors, CPC collectors are also to be tilted at an angle equal to latitude and are fixed throughout the year. The incident angle,  $\theta$  is then given by an equation,

$$\cos \theta = \cos \omega \cdot \cos \delta. \quad (30)$$

The effective scattered radiation on a CPC is that incident within the acceptance angle. Since scattered radiation is assumed to be isotropic as mentioned earlier, the amount of scattered radiation that will be within the acceptance angle is estimated by

$$I_{S,CPC} = \frac{I_{s,h}}{C} \quad (31)$$

where  $C$  = concentration ratio. For a CPC considered here, concentration ratio is 1.33.

---

<sup>13</sup>John A. Duffie, et al, Solar Engineering of Thermal Processes, (New York: John Wiley & Sons, 1980), p. 300.

Therefore,

$$I_{S,CPC} = \frac{I_{S,h}}{1.33}$$

$$= 0.75 \times I_{S,h} \quad (32)$$

That is 75% of the scattered radiation is accepted by the CPC collector considered here. The total solar insolation on a CPC collector,  $I_{CPC}$ , is obtained by summing  $I_{d,CPC}$  as obtained by Equation (29) and  $I_{S,CPC}$  as obtained by Equation (32).  $I_{CPC}$  is then used in Equation (26) to calculate efficiency of each collector module for each hour. Usually, the mass flow rate is such that temperature rise of about 20°F is obtained through each collector module. In order to get desired output temperature, the collector modules are to be connected in a series. Efficiency is calculated at every 40°F interval and is then averaged out. Total useful solar energy collected by the collector per ft<sup>2</sup> every hour is then calculated by

$$\text{Solar Energy Collected/hr} = \eta_{\text{avg.},CPC} \times I_{CPC} \quad (33)$$

Hourly results are summed up to establish total energy collected per year. From the practical point of view, anytime solar insolation on the collector is less than 50 BTU/hr/ft<sup>2</sup> or average collector efficiency,  $\eta_{\text{avg.}}$ , is less than 15% or the efficiency of the last collector module is not positive, it is assumed that the pump is not turned on, and thus no energy is collected during that hour. Total energy collected is calculated for collector fluid average temperature,  $T_{\text{avg}}$  ranging from 150°F to 470°F at an interval of 40°F for three locations mentioned earlier. The 'SOLMET' weather tape is used for solar insolation and ambient temperature data and calculations are performed by use of a computer. The flow chart of the computer program and computer program listing along with output are shown in Appendix B.

Annual results are tabulated in Table 18 and are shown graphically in Figures 38, 39 and 40.

TABLE 18. Solar Energy Collected by CPC Collector per ft<sup>2</sup> Area per Year for Three Locations (BTU/ft<sup>2</sup>/year)

Collector Fluid Average Temperature (°F)	Madison WI	Miami FL	Albuquerque NM
150	166,752	215,272	306,188
190	143,329	185,767	278,695
230	119,739	154,731	248,176
270	98,354	125,674	216,788
310	77,373	95,839	187,519
350	57,752	70,671	155,253
390	38,958	46,922	124,037
430	22,946	25,607	95,409
470	9,315	10,591	62,112

### Line Focusing Parabolic Trough Collectors.

These collectors are basically made of reflecting parabolic surface, a receiver located at the focal axis of a parabola and is structured to constantly track the sun. (Figure 35)

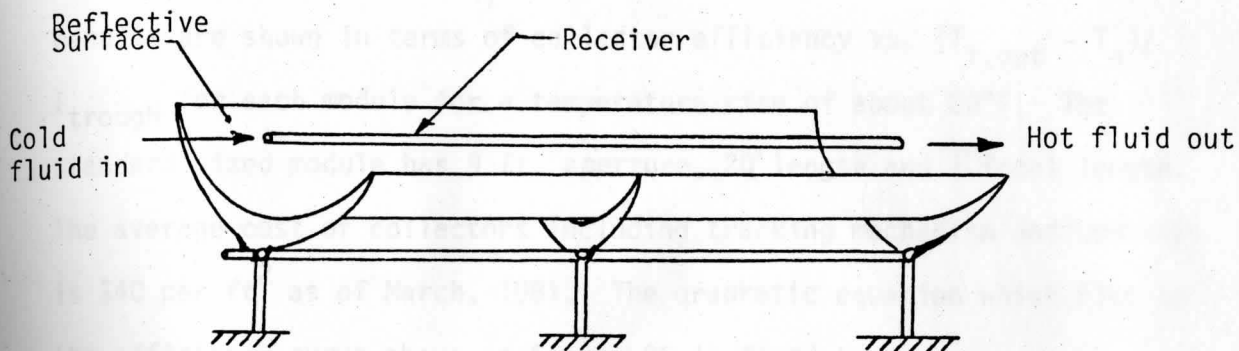


FIGURE 35. Parabolic Trough Collector.

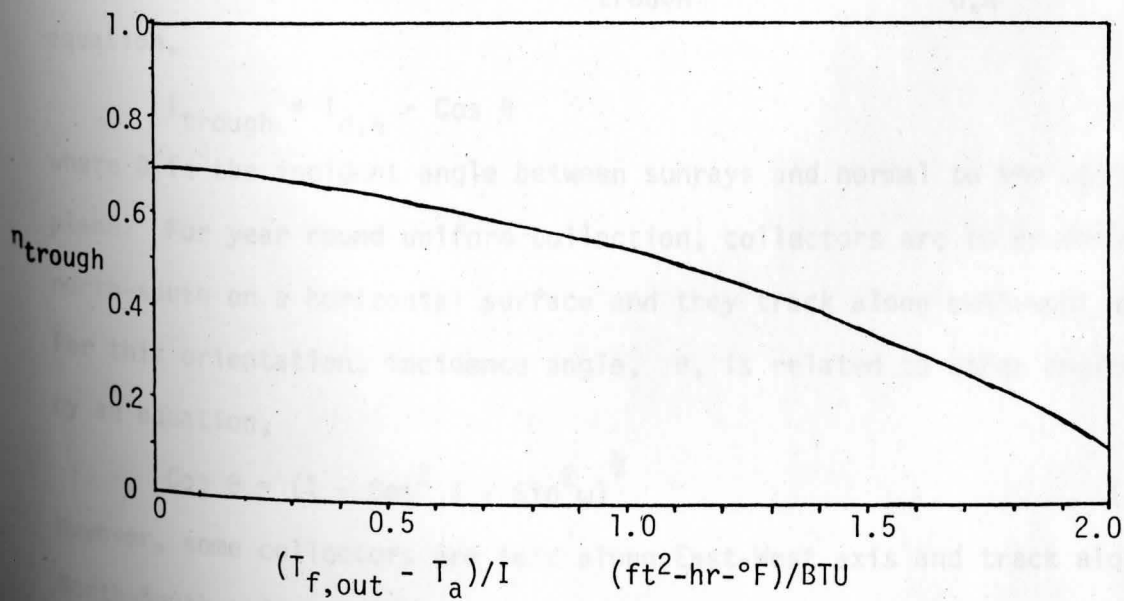


FIGURE 36. Performance of a Parabolic Trough Solar Collector



Reflecting surface concentrates only direct solar rays on the receiver. Receiver is either encased in a vacuumed glass tube or insulated on the back side to suppress heat losses from the receiver.

A typical average performance curve shown in Figure 36, from this group of collectors as manufactured by Suntec is used here. The results are shown in terms of collector efficiency vs.  $(T_{f,out} - T_a) / I_{\text{trough}}$  for each module for a temperature rise of about 20°F. The standard sized module has 9 ft aperture, 20' length and 3' focal length. The average cost of collectors including tracking mechanism and controls is \$40 per ft<sup>2</sup> as of March, 1981. The quadratic equation which fits to the efficiency curve shown in Figure 36 is found to be

$$\eta_{\text{trough}} = 0.694 - 0.052 \left( \frac{T_{f,out} - T_a}{I_{\text{trough}}} \right) - 0.119 \left( \frac{T_{f,out} - T_a}{I_{\text{trough}}} \right)^2 \quad (34)$$

where,  $I_{\text{trough}}$  = Instantaneous direct solar insolation on the collector plane per ft<sup>2</sup>. Sufficient accuracy is obtained for results obtained for a time segment of one hour.  $I_{\text{trough}}$  is related to  $I_{d,n}$  by an equation,

$$I_{\text{trough}} = I_{d,n} \cdot \cos \theta \quad (35)$$

where  $\theta$  is the incident angle between sunrays and normal to the collector plane. For year round uniform collection, collectors are to be oriented north-south on a horizontal surface and they track along east-west axis. For this orientation, incidence angle,  $\theta$ , is related to other angles by an equation,

$$\cos \theta = (1 - \cos^2 \delta \cdot \sin^2 \omega)^{\frac{1}{2}} \quad (36)$$

However, some collectors are laid along East-West axis and track along North-South axis.

$I_{d,n}$  required in Equation (35) is taken from SOLMET weather tape.

In order to get desired output temperature, the collector modules are to be connected in a series. Efficiencies are calculated at every 20°F interval and are then averaged out to get  $\eta_{avg}$ .

In this collector, at the edges, part of the radiation is lost because the collector is not directly facing the sun; its plane makes angle  $\theta$  between its normal and sunrays. In order to minimize end losses, parabolic trough collector modules are installed in a straight line as long as possible. Generally, collectors are installed in a total length of 80'. The fraction of the area per  $\text{ft}^2$  lost,  $A_L$ , in an 80' long orientation and for a collector having 3 feet focal length is

$$A_L = \frac{3}{80} \times \tan \theta \quad (37)$$

The useful energy collected by the collector per hour per  $\text{ft}^2$  area,  $Q_{trough}$ , is given by,

$$Q_{trough} = \eta_{avg} \times \left(1 - \frac{3}{80} \tan \theta\right) \times I_{trough} \quad (38)$$

Hourly useful energy gains are summed up to establish total energy collected per year. Total energy collected per year is calculated for collector fluid average temperature,  $T_{avg}$ , starting from 200°F to 600°F at an interval of 50°F for three locations. The 'SOLMET' weather tape is used for solar insolation and ambient temperature data and calculation are performed by use of a computer. The flow chart of the computer program and computer program listing along with output are shown in Appendix B. Annual results are tabulated in Table 19 and are shown graphically in Figures 38, 39 and 40.

TABLE 19. Solar Energy Collected by Parabolic Trough Collector Per  $\text{ft}^2$  area Per Year for Three Locations (BTU/ $\text{ft}^2$ -Year)

Collector Fluid Average Temperature ( $^{\circ}\text{F}$ )	Madison WI	Miami FL	Albuquerque NM
200	159,357	177,632	360,309
250	134,591	148,197	323,193
300	109,425	118,331	283,601
350	84,076	89,973	241,246
400	60,946	64,273	198,188
450	39,551	41,522	157,242
500	22,663	23,886	115,241
550	9,064	10,769	74,850
600	1,419	3,508	40,202

#### Point-Focusing Paraboloid Disc Collectors

These collectors are basically made of reflecting surface and a receiver located at the focal point. It is structured to constantly track the sun in both directions such that collector is always facing the sun during operating hours. Reflecting surface concentrates only direct solar radiation on the receiver. Generally concentration ratio of more than 1000 is achieved. Since the receiver area is small, thermal losses are low and so these collectors can operate at high efficiency even at high temperatures. These collectors are ideal for applications requiring temperatures above  $500^{\circ}\text{F}$ .

Very few companies manufacture this type of collectors. Omnium-G is the leading manufacturer. Its reflector is a 20' diameter disc with average concentration ratio of 1600.

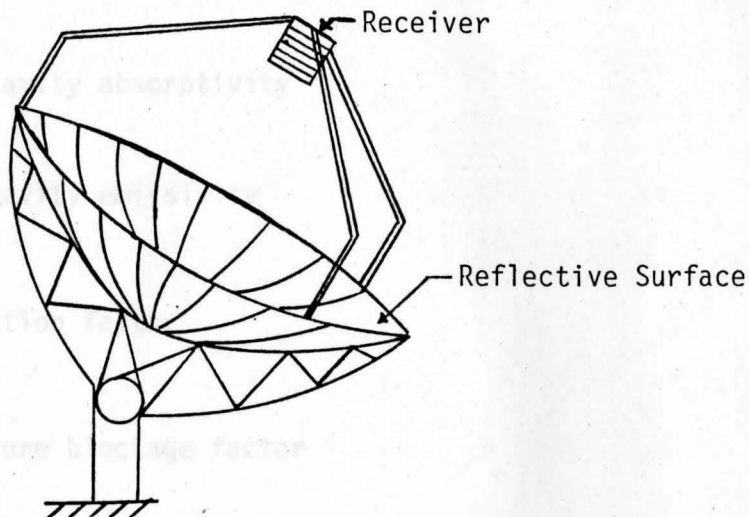


FIGURE 37. Point Focusing Paraboloid Disc Collector

The cost varies greatly depending on the quantity purchased. Average cost is around \$65 per ft<sup>2</sup>. A thorough testing by an established independent testing laboratories have not been done. For the analysis of these collectors, theoretical equations are used and results obtained were confirmed with actual performance of the collector.

An energy balance on the concentrator/receiver combination results in the following expression for collection efficiency.<sup>14</sup>

---

<sup>14</sup>R.L. Sons, "Optimization of a Point-Focusing Distributed Receiver Solar Thermal Electric System" An ASME Publication, 79-WA/Sol-11, Aug, 1979, p. 5.

$$\eta_{\text{coll}} = \rho \alpha_e K_d K_b \gamma - \frac{[\sigma \epsilon_e (T_r^4 - T_\infty^4) + h(T_r - T_\infty)]}{C \cdot I_{\text{disc}}} - \frac{Q_{\text{cond}}}{A_c \cdot I_{\text{disc}}} \quad (39)$$

where

$\rho$  = reflectivity of concentrator surface

$\approx 0.9$

$\alpha_e$  = effective cavity absorptivity

$\approx 0.9$

$\epsilon_e$  = effective cavity emissivity

$\approx 0.9$

$K_d$  = dust correction factor

$\approx 0.95$

$K_b$  = dish structure blockage factor

$\approx 0.92$

$\gamma$  = intercept factor, i.e. fraction of focal plane energy intercepted by the cavity receiver.

$\approx 1$  for a well designed collector.

$\sigma$  = Stefan-Boltzmann constant

$= 0.1714 \times 10^{-8} \text{ BTU/ft}^2 \cdot \text{°R}^4 \cdot \text{hr}$

$T_r$  = receiver inner surface temperature, °R

$T_\infty$  = ambient temperature °R

$h$  = convective heat transfer coefficient at cavity aperture

$\approx 2.82 \text{ BTU/ft}^2 \cdot \text{hr} \cdot \text{°R}$

$Q_{\text{cond}}$  = thermal conduction losses from surface of the receiver

$A_c$  = concentrator aperture area,  $\text{ft}^2$

$$\frac{Q_{\text{cond}}}{A_c} \approx 0.952 \frac{\text{BTU}}{\text{hr} \cdot \text{ft}^2}$$

$C =$  geometric concentration ratio = 1600

Substituting these values, reduces equation to

$$\eta_{coll} = 0.708 - \frac{[0.15426 \times 10^{-8}(T_r^4 - T_\infty^4) + 2.82(T_r - T_\infty)]}{1600 \times I_{disc}} - \frac{0.952}{I_{disc}} \quad (40)$$

$I_{disc}$  = instantaneous direct solar insolation on the collector plane.

Sufficient accuracy is obtained if calculations are done for time segment of 1 hour. As collector is constantly tracking the sun,

$$I_{disc} = I_{d,n} \quad (41)$$

Collector efficiencies are calculated every hour for different receiver temperatures. Solar energy collected by the collector per  $\text{ft}^2$  for each hour is calculated by

$$\text{Solar Energy Collected/hr} = \eta_{coll} \times I_{d,n} \quad (42)$$

Hourly results are summed up to establish total energy collected per year. Total energy collected per year is obtained for collector fluid average temperature,  $T_{avg.}$ , starting from  $400^\circ\text{F}$  to  $1200^\circ\text{F}$  at an interval of  $100^\circ\text{F}$  for three different locations. The calculations are performed by use of the computer. The flow chart of the computer program and computer program listing along with output are shown in Appendix B. Annual results are tabulated in Table 20 and are shown graphically in Figures 38, 39 and 40.

TABLE 20. Solar Energy Collected by Paraboloid Disc Collector Per ft<sup>2</sup> Area Per Year for Three Locations. (BTU/ft<sup>2</sup>-Year)

Collector Fluid Average Temperature (°F)	Madison WI	Miami FL	Albuquerque NM
400	276,902	296,084	571,066
500	275,873	294,868	569,427
600	274,608	293,374	567,415
700	273,057	291,542	564,946
800	271,162	289,304	561,931
900	268,864	286,589	558,272
1000	266,093	283,316	553,863
1100	262,780	279,402	548,590
1200	258,846	274,755	542,329

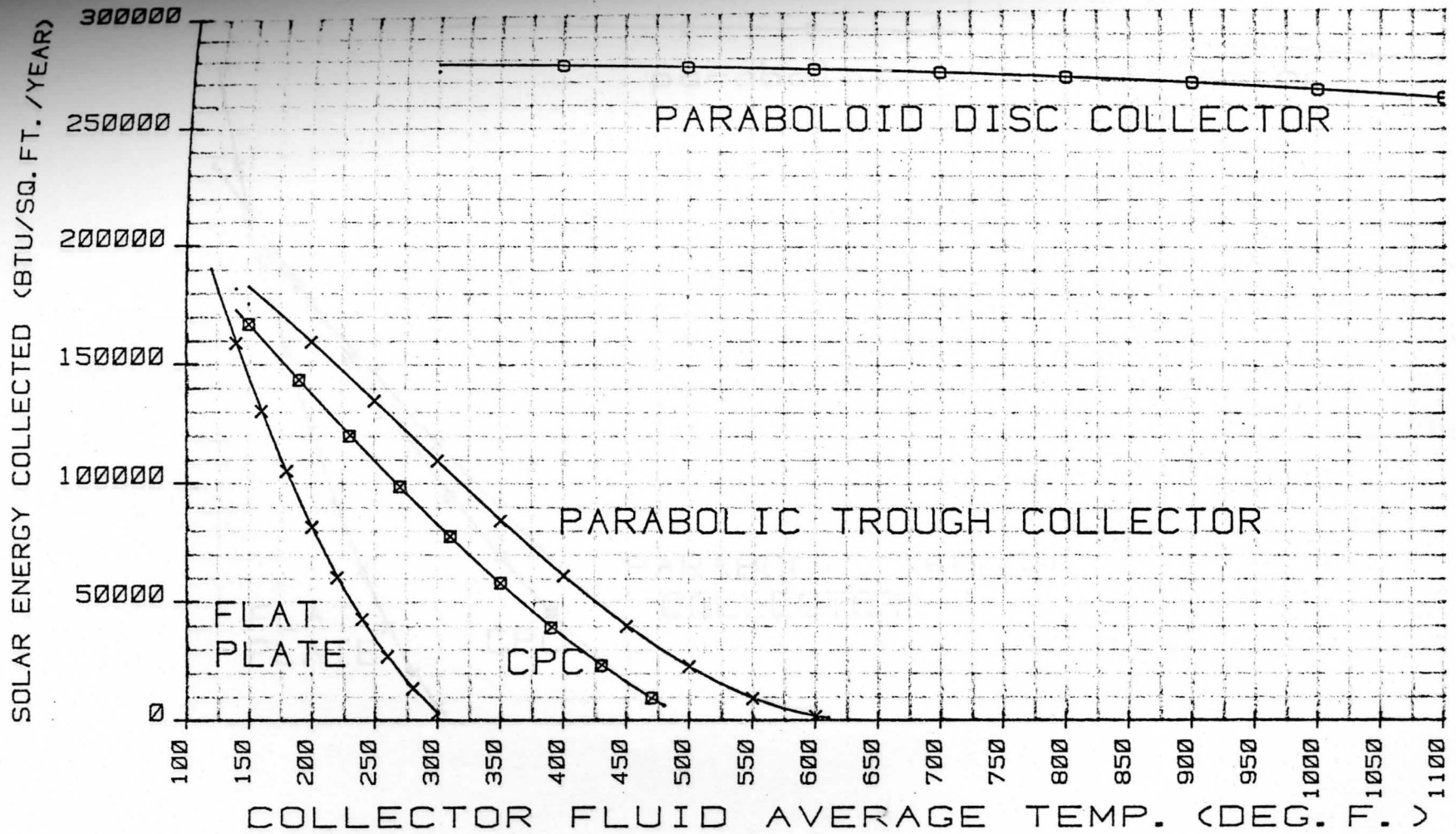


FIGURE 38. Graph of Solar Energy Collected by Different Collectors Per ft<sup>2</sup> Area Per Year vs. Collector Fluid Average Temperature for Madison, WI.



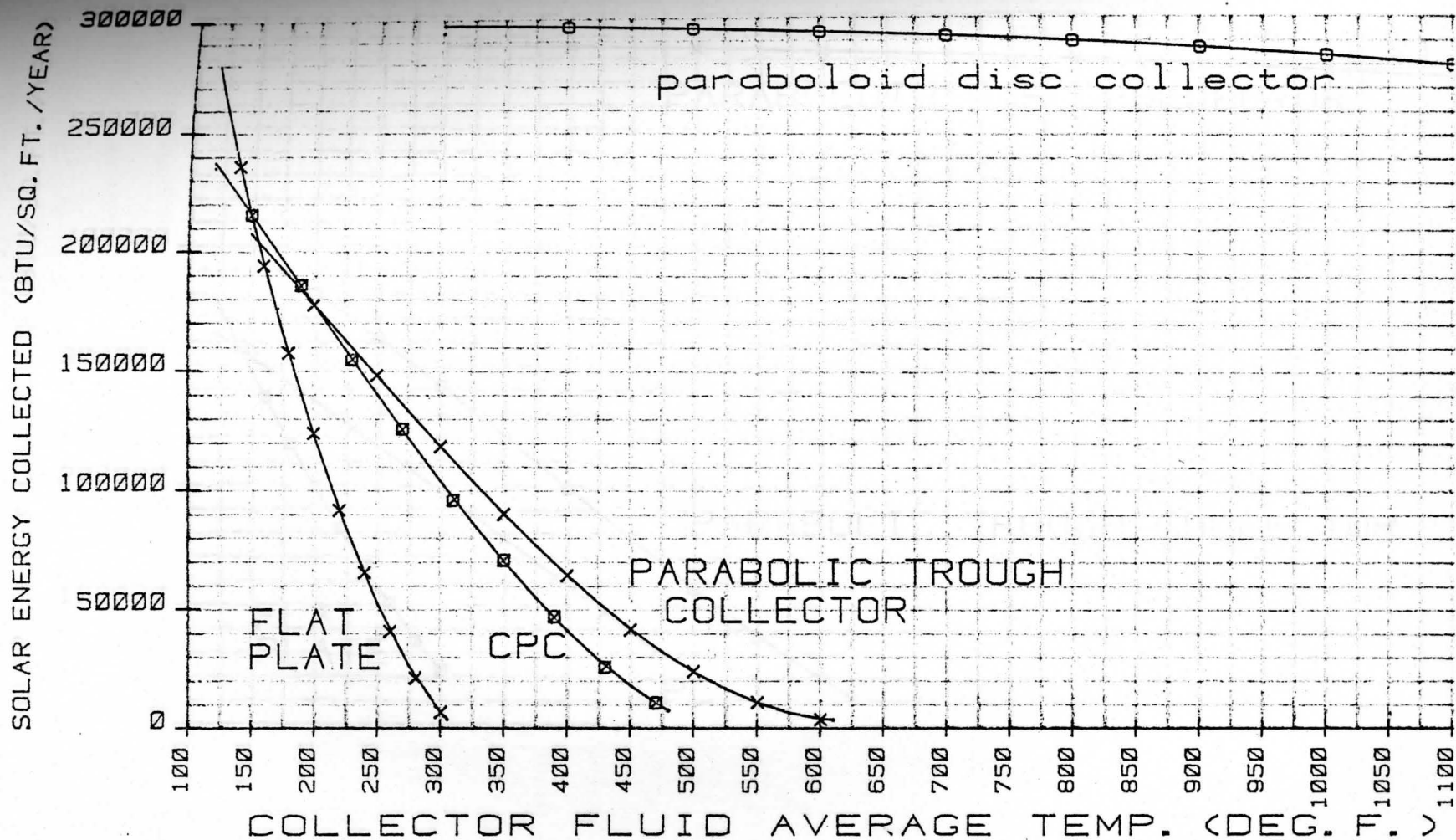


FIGURE 39. Graph of Solar Energy Collected by Different Collectors Per ft<sup>2</sup> Area Per Year vs. Collector Fluid Average Temperature for Miami, FL.

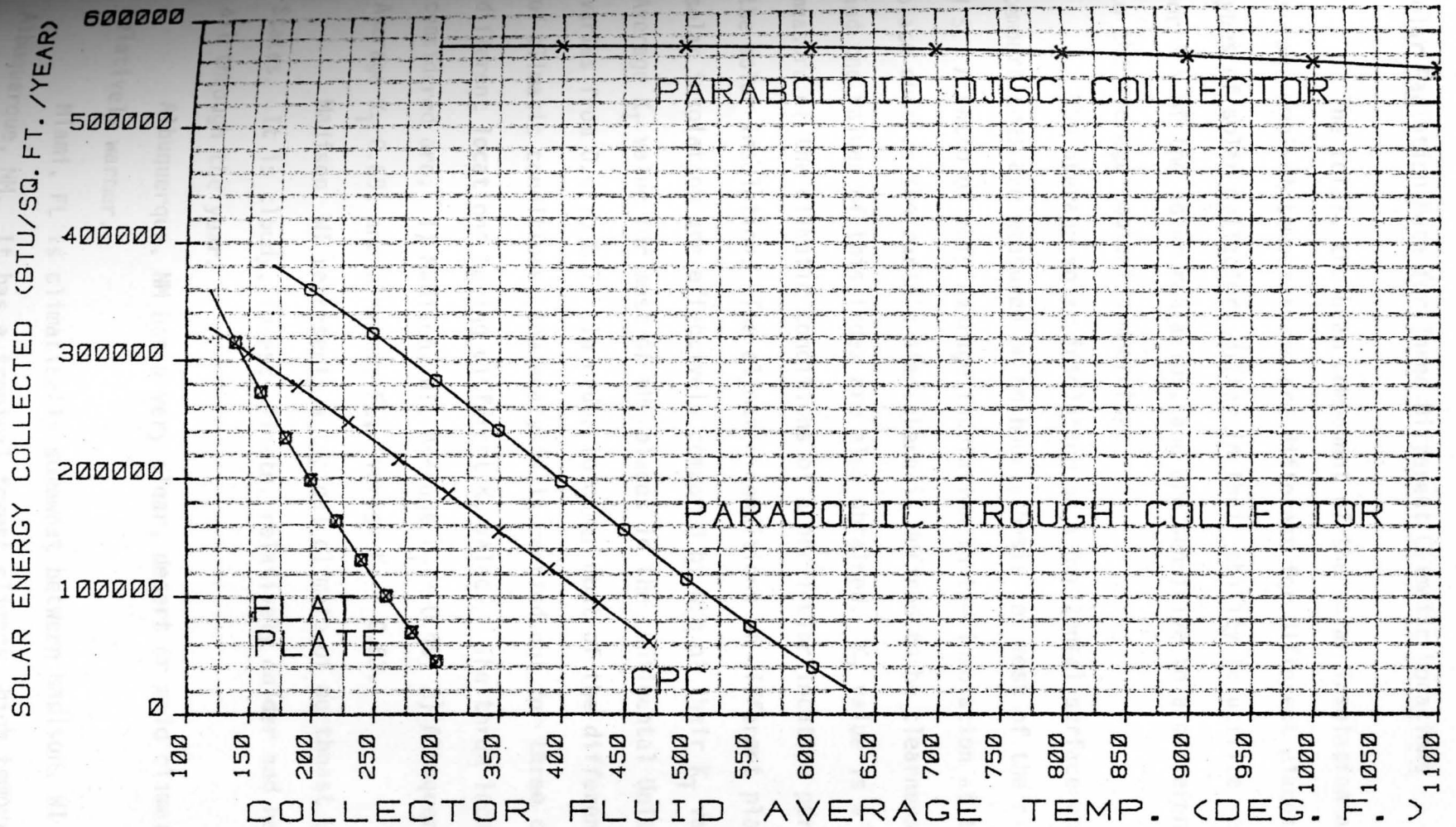


FIGURE 40. Graph of Solar Energy Collected by Different Collectors Per  $\text{ft}^2$  Area Per Year vs. Collector Fluid Average Temperature for Albuquerque, NM.

Solar Radiation Data for Three Different Climatic Locations

The total, the beam component of the solar insolation and the average ambient temperatures are different for different places. Different types of solar collectors differ in their ability to utilize scattered portion of the solar radiation, and are sensitive to a different degree to the average ambient temperature.

The average solar insolation on a horizontal surface and ambient temperatures are measured on an hourly basis for most of the cities in U.S. A ratio of this average insolation to the insolation at the same place outside the earth's atmosphere is defined to be clearness index  $K_T$ , and the values of this index are also obtained.  $K_T$  value is a good measure of the climatic conditions of a particular location pertinent to the solar insolation. The climatic conditions of different places for solar insolation are effectively compared by use of their  $K_T$  values. Average  $K_T$  value for most of the places in the continental United States varies from 0.4 to 0.7. In order to cover most of the different types of climatic conditions, the analysis is carried out for three climatically different locations having different  $K_T$  values. The three locations considered are: 1) Madison, WI, Average  $K_T = 0.49$ , 2) Albuquerque, NM, Average  $K_T = 0.69$ , and 3) Miami, FL, Average  $K_T = 0.52$ .

Madison, WI represents a typical climate of northeast United States. It is cloudy, forest climate, relatively colder and has rainfall all through the year.

Albuquerque, NM has a very clear, desert or arid climate and is relatively warmer.

Miami, FL is climatically somewhat between Madison, WI and Albuquerque, NM. It has a tropical forest climate, high temperatures

but humid and generally sunny.

The results of energy collected per year for different collectors for these locations can be used for any other location by comparing the climate patterns and average  $K_T$  values.

Hourly solar insolation data are available for many cities in the United States. In recent years, the U.S. National Oceanic and Atmospheric Administration (NOAA) has made these data available with all other related meteorological data such as, ambient dry bulb temperature, wet bulb temperature, wind speed, etc. on magnetic tapes for 26 different cities in the United States for an average year averaged over a period of 23 years. These tapes are referred to as 'SOLMET' tapes. Solar insolation data are given in two different forms on these tapes: 1) total solar insolation on a horizontal surface and 2) direct solar insolation on the surface normal to sunrays. These two data are sufficient to compute direct or scattered component of the solar insolation on the plane tilted at any angle as illustrated earlier in this chapter.

Thus, hourly solar insolation data were obtained from these tapes and used with each collector to get solar energy collected per hour and results were summed up to establish solar energy collected per year. In the next chapter, these results are combined with the results obtained in Chapter II to get overall solar-to-electric energy conversion.

## CHAPTER V

COMBINED PERFORMANCE OF SOLAR COLLECTORS AND RANKINE-CYCLE

In Chapter III, Rankine-cycle performance is analyzed. Rankine-cycle efficiencies are calculated at several different temperatures using eight different working fluids. In Chapter IV, solar collector performance is analyzed. Total solar energy collected per year per ft<sup>2</sup> by four types of collectors at several different temperatures for three different locations is computed. In this chapter, the results from both loops — solar collector and Rankine-cycle loops are coupled.

Relationship Between Operating Temperatures of a Rankine-Cycle and Collector Fluid.

The Rankine-cycle operating temperatures are related to solar collector operating temperatures by mass flow rates of the fluids and characteristics of a heat exchanger, B (see Figure 2). As discussed in Chapter II, for a given Rankine-cycle maximum temperature,  $T_3$ , maximum cycle efficiency with organic fluids is obtained when the cycle is operated such that the vapor coming out of the boiler is in saturated state. Thus, two types of heat transfer processes occur in a boiler — heat exchanger, B:

- 1) heat is transferred from solar collector liquid to Rankine-cycle liquid heating it from temperature,  $T_2$  to a saturation temperature,  $T_s$  and,
- 2) further heating is done by the solar collector fluid to boil the Rankine-cycle fluid at a constant temperature of,

$$T_s (T_s = T_3)$$

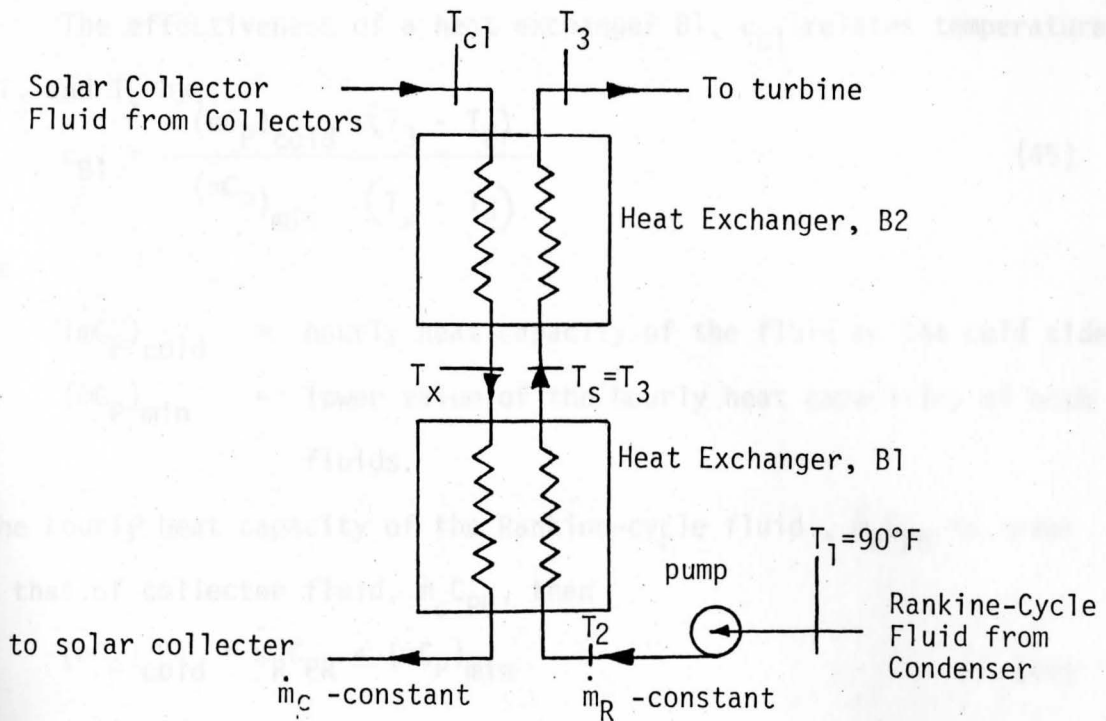


FIGURE 41. Boiler - Heat Exchanger with Two Heat Transfer Processes Separated.

Temperature  $T_2$  of the Rankine-cycle liquid entering the heat exchanger is related to constant fluid temperature,  $T_1$ , entering Rankine-cycle pump by an equation

$$T_2 = T_1 + \frac{\omega_p}{C_{PR}} (1 - \eta_p) \quad (43)$$

$$T_2 = T_1 + \frac{v(P_2 - P_1)}{C_{PR}} (1 - \eta_p) \quad (44)$$

where

$\omega_p$  = work done by the Rankine-cycle pump per pound of liquid.

$v$  = specific volume of a liquid.

$P_2, P_1$  = pressures at state points 1 and 2.

$C_{PR}$  = heat capacity of a Rankine-cycle liquid.

The values of  $P_1$  and  $P_2$  are determined in Chapter II,  $v$  and  $C_{PR}$  are obtained from property tables or diagrams and thus  $T_2$  is calculated.

The effectiveness of a heat exchanger B1,  $\epsilon_{B1}$  relates temperatures  $T_2$ ,  $T_3$  and  $T_x$  by,

$$\epsilon_{B1} = \frac{(\dot{m}C_p)_{cold} (T_3 - T_2)}{(\dot{m}C_p)_{min} (T_x - T_2)} \quad (45)$$

where

$(\dot{m}C_p)_{cold}$  = hourly heat capacity of the fluid on the cold side.

$(\dot{m}C_p)_{min}$  = lower value of the hourly heat capacities of both fluids.

If the hourly heat capacity of the Rankine-cycle fluid,  $\dot{m}_R C_{PR}$  is lower than that of collector fluid,  $\dot{m}_C C_{PC}$ , then

$$(\dot{m}C_p)_{cold} = \dot{m}_R C_{PR} = (\dot{m}C_p)_{min} \quad (46)$$

Equation (3) reduces to,

$$\epsilon_{B1} = \frac{T_3 - T_2}{T_x - T_2} \quad (47)$$

$$T_x = T_2 + \frac{1}{\epsilon_{B1}} (T_3 - T_2) \quad (48)$$

If heat losses from the heat exchanger are neglected, following two equations are obtained.

$$\dot{m}_R (h_3 - h_s) = \dot{m}_C C_{PC} (T_{c1} - T_x) \quad (49)$$

$$\dot{m}_C C_{PC} (T_x - T_{c2}) = \dot{m}_R C_{PR} (T_3 - T_2) \quad (50)$$

Substituting  $\dot{m}_C C_{PC}$  from Equation (50) into Equation (49), we get

$$(h_3 - h_s)(T_x - T_{c2}) = C_{PR} (T_3 - T_2) \times (T_{c1} - T_x)$$

$$\begin{aligned} \therefore h_3 T_x - h_3 T_{c2} - h_s T_x + h_s T_{c2} &= C_{PR} T_3 T_{c1} - C_{PR} T_3 T_x \\ &- C_{PR} T_2 T_{c1} + C_{PR} T_2 T_x \end{aligned}$$

$$\therefore T_{c1} C_{PR} (T_3 - T_2) + T_{c2} (h_3 - h_s) = T_x \{ (h_3 - h_z) + C_{PR} (T_3 - T_2) \} \quad (51)$$

Substituting  $T_x$  from Equation (48) into Equation (51), we get

$$T_{c1} C_{PR} (T_3 - T_2) + T_{c2} (h_3 - h_s) = \left\{ T_2 + \frac{1}{\epsilon_{B1}} (T_3 - T_2) \right\} \{ (h_3 - h_s) + C_{PR} (T_3 - T_2) \} \quad (52)$$

Now from Equation (50),

$$T_{c2} = T_x - \frac{\dot{m}_R C_{PR}}{\dot{m}_C C_{PC}} (T_3 - T_2) \quad (53)$$

Substituting  $T_x$  from Equation (48) into Equation (53), we get

$$T_{c2} = T_2 + \frac{1}{\epsilon_{B1}} (T_3 - T_2) - \frac{\dot{m}_R C_{PR}}{\dot{m}_C C_{PC}} (T_3 - T_2) \quad (54)$$

Substituting  $T_{c2}$  from Equation (54) into Equation (52), we get

$$\begin{aligned} T_{c1} C_{PR} (T_3 - T_2) &= T_2 (h_3 - h_s) + T_2 C_{PR} (T_3 - T_2) + \frac{1}{\epsilon_{B1}} (T_3 - T_2) (h_3 - h_s) \\ &+ \frac{C_{PR}}{\epsilon_{B1}} (T_3 - T_2)^2 - T_2 (h_3 - h_s) - \frac{1}{\epsilon_{B1}} (T_3 - T_2) (h_3 - h_s) \\ &+ \frac{\dot{m}_R C_{PR}}{\dot{m}_C C_{PC}} (T_3 - T_2) (h_3 - h_s) \end{aligned}$$

Therefore,

$$\begin{aligned} T_{c1} &= T_2 + \frac{(T_3 - T_2)}{\epsilon_{B1}} + \frac{\dot{m}_R C_{PR}}{\dot{m}_C C_{PC}} (T_3 - T_2) \left\{ \frac{h_3 - h_s}{C_{PR} (T_3 - T_2)} \right\} \\ T_{c1} &= T_2 + (T_3 - T_2) \left\{ \frac{1}{\epsilon_{B1}} + \frac{\dot{m}_R C_{PR}}{\dot{m}_C C_{PC}} \times \frac{h_3 - h_s}{C_{PR} (T_3 - T_2)} \right\} \quad (55) \end{aligned}$$

Substituting  $C_{PR} (T_3 - T_2) = h_s - h_2$  into Equation (55), we get,

$$T_{c1} = T_2 + (T_3 - T_2) \left\{ \frac{1}{\epsilon_{B1}} + \frac{\dot{m}_R C_{PR}}{\dot{m}_C C_{PC}} \times \frac{h_3 - h_s}{h_s - h_2} \right\} \quad (56)$$



where  $h_s$  = enthalpy per pound of fluid at state 2.

Equation (56) gives  $T_{c1}$  explicitly in terms of known temperatures and enthalpies when  $\dot{m}_R C_{PR} < \dot{m}_C \cdot C_{PC}$ . For case when  $\dot{m}_R C_{PR} > \dot{m}_C C_{PC}$ , proceeding in similar lines as above, the following expression for  $T_{c1}$  is obtained

$$T_{c1} = T_2 + (T_3 - T_2) \cdot \frac{\dot{m}_R C_{PR}}{\dot{m}_C C_{PC}} \left\{ \frac{1}{\epsilon_{B1}} + \frac{h_3 - h_s}{h_s - h_2} \right\} \quad (57)$$

for  $\dot{m}_R C_{PR} > \dot{m}_C C_{PC}$ .

In order to maximize solar energy collection for a given value of  $T_3$ ,  $T_{c1}$  should be minimized. It can be seen from Equations (56) and (57) that  $T_{c1}$  can be minimized by having  $\epsilon_{B1}$  as high as possible and  $\frac{\dot{m}_2 C_{P2}}{\dot{m}_1 C_{P1}}$  as low as possible since  $T_2$  and  $(T_3 - T_2)$  are fixed and positive.

For a counter flow,  $\epsilon_{B1}$  is related to

$$\frac{\dot{m}_R C_{PR}}{\dot{m}_C C_{PC}} \quad \text{by,}$$

$$\epsilon_{B1} = \frac{1 - e^{-\left(1 - \frac{\dot{m}_R C_{PC}}{\dot{m}_C C_{PC}}\right) NTU_{\max}}}{1 - \frac{\dot{m}_R C_{PR}}{\dot{m}_C C_{PC}} \times e^{-\left(1 - \frac{\dot{m}_R C_{PR}}{\dot{m}_C C_{PC}}\right) NTU_{\max}}} \quad (58)$$

where  $(NTU)_{\max}$  = the number of transfer units

$$= \frac{UA}{(\dot{m}C_p)_{\min}} \quad (59)$$

For a given value of

$\frac{\dot{m}_R C_{PR}}{\dot{m}_C C_{PC}}$ , the value of  $(NTU)_{\max}$  greater than 4 produces very

little increase in the value of  $\epsilon_{B1}$ , since the relationship is exponential.

However, the higher the  $(NTU)_{max}$ , the higher the required surface area of the heat exchanger and hence, the higher the cost. This relationship is linear as can be seen in Equation (59). So  $(NTU)_{max}$  is fixed to be equal to 4. This value offers high enough  $\epsilon_{B1}$  for a reasonable size of a heat exchanger.

Equation (58), now reduces to,

$$\epsilon_{B1} = \frac{1 - e^{-4(1 - \frac{\dot{m}_R C_{PR}}{\dot{m}_C C_{PC}})}}{1 - \frac{\dot{m}_R C_{PR}}{\dot{m}_C C_{PC}} \times e^{-4(\frac{\dot{m}_R C_{PR}}{\dot{m}_C C_{PC}})}} \quad (60)$$

It can be seen from Equation (59) that the lower the  $\frac{\dot{m}_R C_{PR}}{\dot{m}_C C_{PC}}$ , the higher the value of  $\epsilon_{B1}$ . As  $\frac{\dot{m}_R C_{PR}}{\dot{m}_C C_{PC}}$  approaches 0,  $\epsilon_{B1}$  approaches 1. Thus,  $\frac{\dot{m}_R C_{PR}}{\dot{m}_C C_{PC}}$  should be as low as possible in order to minimize  $T_{c1}$ . The rough calculations indicate that after  $\frac{\dot{m}_R C_{PR}}{\dot{m}_C C_{PC}}$  goes below 0.1, the decrease in  $T_{c1}$  is very small since the relationship is exponential.

However, the lower the value of  $\frac{\dot{m}_R C_{PR}}{\dot{m}_C C_{PC}}$ , the higher the required pumping energy for a given power output. This relationship is linear.

Consequently,  $\frac{\dot{m}_R C_{PR}}{\dot{m}_C C_{PC}}$  is fixed to be equal to 0.1.

Substituting  $\frac{\dot{m}_R C_{PR}}{\dot{m}_C C_{PC}} = 0.1$  into Equation (60), yields

$$\epsilon_{B1} = 0.975 \quad (61)$$

Substituting the values of  $\epsilon_{B1}$  and  $\frac{\dot{m}_R C_{PC}}{\dot{m}_C C_{PC}}$  into Equations (56) and (53) reduces them to,

$$T_{c1} = T_2 + (T_3 - T_2) \left\{ 1.025 + 0.1 \times \frac{(h_3 - h_s)}{(h_3 - h_2)} \right\} \quad (62)$$

and

$$T_{c2} = T_2 + 1.025 (T_3 - T_2) - 0.1 (T_3 - T_2)$$

or

$$T_{c2} = T_2 + 0.925 (T_3 - T_2) \tag{63}$$

Equations (62) and (63) can only be used with organic fluids. In case of water/steam Rankine-cycle, as discussed in Chapter II, steam is heated to a superheated state. As shown in Figure 42, three types of heat transfer processes occur in the boiler-heat exchanger:

- 1) water gets heated from temperature  $T_2$  to a saturated temperature,  $T_s$ ,
- 2) water boils into steam at constant saturation temperature,  $T_s$  corresponding to pressure,  $P_2$  and finally,
- 3) steam is superheated from temperature  $T_s$  to a temperature of  $T_3$ .

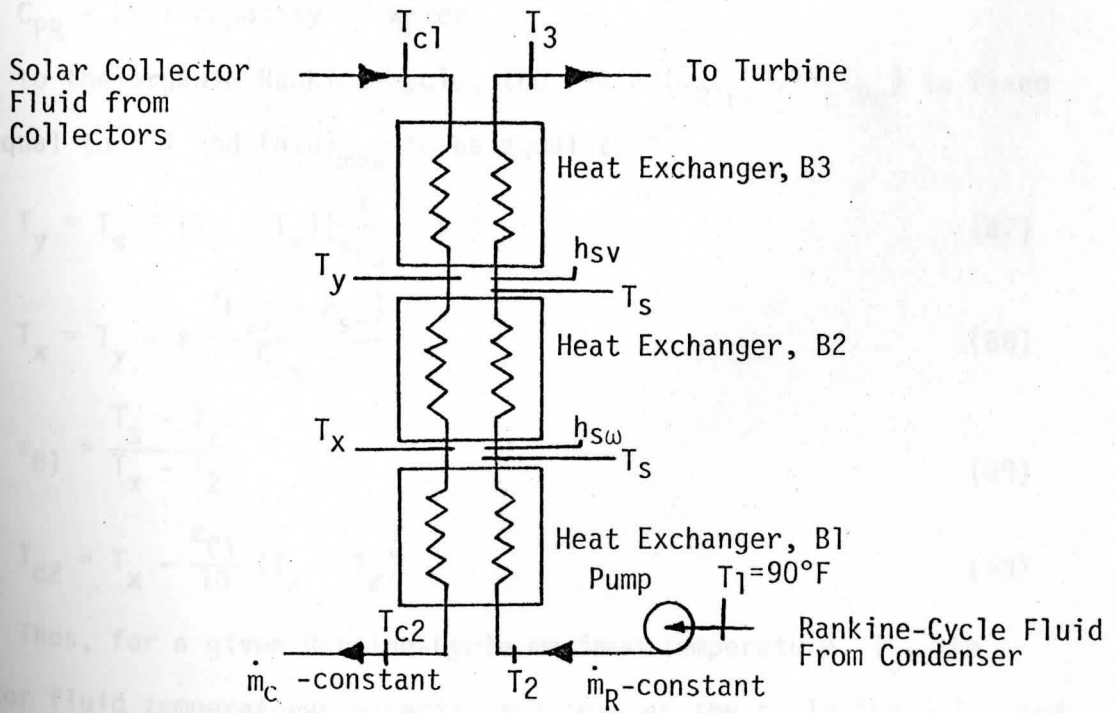


FIGURE 42. Boiler-Heat Exchanger in a Water/Steam Rankine-Cycle with Heat Transfer Processes Separated.

Following the procedure discussed earlier, the expressions for  $T_{c1}$  and  $T_{c2}$  are obtained as shown below:

$$T_{c1} = \frac{1}{\epsilon_{B3}} (T_3 - T_s) + T_s \quad (64)$$

$$\epsilon_{B3} = \frac{1 - e^{-(1-x)NTU_{max}}}{1 - x \cdot e^{-(1-x)NTU_{max}}} \quad (65)$$

where

$$x = \frac{\dot{m}_R C_{Ps}}{\dot{m}_C C_{Pc}} = \frac{\dot{m}_R C_{PR}}{\dot{m}_C C_{Pc}} \times \frac{\dot{m}_R C_{Ps}}{\dot{m}_R C_{PR}} = \left( \frac{\dot{m}_R C_{PR}}{\dot{m}_C C_{Pc}} \right) \left( \frac{C_{Ps}}{C_{PR}} \right) \quad (66)$$

where

$C_{Ps}$  = heat capacity of steam

$C_{PR}$  = Heat capacity of water

Similar to the organic Rankine-cycle, the ratio  $(\dot{m}_R C_{PR})/(\dot{m}_C C_{Pc})$  is fixed to be equal to 0.1 and  $(NTU)_{max}$  to be equal to 4.

$$T_y = T_s + (T_3 - T_s) \left( \frac{1}{\epsilon_{B3}} - x \right) \quad (67)$$

$$T_x = T_y - x \frac{(h_{sv} - h_{sw})}{C_{Ps}} \quad (68)$$

$$\epsilon_{B1} = \frac{T_s - T_2}{T_x - T_2} \quad (69)$$

$$T_{c2} = T_x - \frac{\epsilon_{B1}}{10} (T_x - T_2) \quad (70)$$

Thus, for a given Rankine-Cycle maximum temperature,  $T_3$ , the collector fluid temperatures entering and leaving the collector -  $T_{c2}$  and  $T_{c1}$  respectively - are calculated at several different temperatures using Equations (62) and (63) in case of organic fluids and Equations (64)

through (70) in case of water/steam Rankine-cycle. These values are tabulated in Tables 21 to 40.

It can be seen from Tables 21 to 40 that  $T_{c1}$  and  $T_{c2}$  differ on the average by about 40°F. As can be seen in Figures 38, 39 and 40 (Chapter IV) that over a 40°F temperature range, the curves of solar energy collected per year vs. collector fluid operating temperature are a straight line in all cases. Therefore, solar energy collected for a fluid entering temperature of  $T_{c2}$  and leaving temperature of  $T_{c1}$  is the same as the energy collected for an operating temperature equal to average temperature of  $T_{c1}$  and  $T_{c2}$ . Thus, an average collector fluid temperature,  $T_{avg}$  is introduced.

$$T_{avg} = \frac{T_{c1} + T_{c2}}{2} \quad (71)$$

Thus, for a particular Rankine-cycle maximum temperature, corresponding collector fluid average temperature,  $T_{avg}$  is calculated. Solar energy collected at an average fluid temperature is obtained from results obtained in Chapter IV. A product of Rankine-cycle efficiency at a certain Rankine-cycle maximum temperature and solar energy collected per year per  $ft^2$  at the corresponding collector fluid average temperature is obtained. This product will be called as an S.R value.

The S.R value is directly proportional to the net electrical production per year per unit area of a collector at a certain operating temperature ( $T_{avg} \equiv T_3$ )

$$\left( \frac{\text{Solar Energy Collected by the collector}}{\text{yr. ft}^2} \times \text{Rankine-cycle Efficiency} \right)_{T_{avg}} \propto \left( \frac{\text{Net electrical energy production}}{\text{yr. ft}^2} \right)_{T_{avg}} \quad (72)$$

$$(S.R)_{T_{avg}} = K_1 \cdot \left( \frac{\text{Net Electrical energy production}}{\text{yr. ft}^2} \right)_{T_{avg}} \quad (73)$$

Where  $K_1$  is a constant of proportionality.  $K_1$  takes into account the generator efficiency and certain parasite losses in the system, such as, friction losses, heat losses, etc. The value of  $K_1$  is less than 1. It has approximately the same value in all cases which makes the evaluation of optimum operating temperature possible by comparing the S.R values obtained at several different operating temperatures.

The results of S.R values at different operating temperatures for each possible combination of solar collector and Rankine-cycle fluid are shown graphically indicating the variation of S.R value vs. collector fluid average temperature or Rankine-cycle maximum temperature. A peak corresponds to the maximum net solar-to-electrical conversion. Figures 43 to 66 show the graphs of S.R value vs. collector fluid average temperature and Rankine-cycle maximum temperature for all possible combinations.

Comparing the maximum S.R values obtained in the combinations of each type of collector and all Rankine-cycle working fluids gives the fluid best suited for that collector. Thus, an optimum Rankine-cycle working fluid for each type of solar collector is obtained.

TABLE 27. S.R. Values at Several Different Temperatures for Three Different Collectors

Collector	Rankine-cycle fluid	100	110	120	130	140	150
Flat-plate	Water	6.5	26.7	113	36.1	53.8	100
	Oil	7.1	26.8	113	35.8	53.9	100
	Alcohol	10.8	26.9	115	50.2	91.3	100
Parabolic	Water	19.1	27.9	117	54.7	91.9	100
	Oil	13.8	21.2	120	61.7	92.8	100
	Alcohol	15.2	21.3	112	68.0	93.3	100

TABLE 21. S.R Values at Several Temperatures for a Combination of a Flat Plate Collector and R-11 for Three Different Locations.

$T_3$ (°F)	$\eta_R$ (%)	$h_2$ BTU/Tb	$h_3$ BTU/Tb	$h_s$ BTU/Tb	$T_2$ (°F)	$T_{c1}$ (°F)	$T_{c2}$ (°F)	$T_{avg}$ (°F)	Madison, WI		Miami, FL		Albuquerque, NM	
									Energy Collected BTU/ft <sup>2</sup> yr.	S.R Product BTU/ft <sup>2</sup> yr.	Energy Collected BTU/ft <sup>2</sup> yr.	S.R Product BTU/ft <sup>2</sup> yr.	Energy Collected BTU/ft <sup>2</sup> yr.	S.R Product BTU/ft <sup>2</sup> yr.
150	6.8	26.7	110	39.3	90.4	185	145	165	123,844	8,421	184,744	12,562	263,940	17,948
180	9.4	26.8	113	45.8	90.9	214	173	194	88,360	8,306	133,885	12,585	209,930	19,733
200	10.8	26.9	115	50.2	91.4	233	192	212	68,511	7,399	104,466	11,282	178,344	19,261
220	12.1	27.0	117	54.7	91.9	252	211	231	50,398	6,098	77,215	9,343	146,314	17,704
250	13.8	27.2	120	61.7	92.8	281	239	260	26,695	3,684	40,744	5,623	101,071	13,948
280	15.2	27.3	122	69.0	93.3	308	267	288	9,103	1,384	15,287	2,324	60,211	9,152

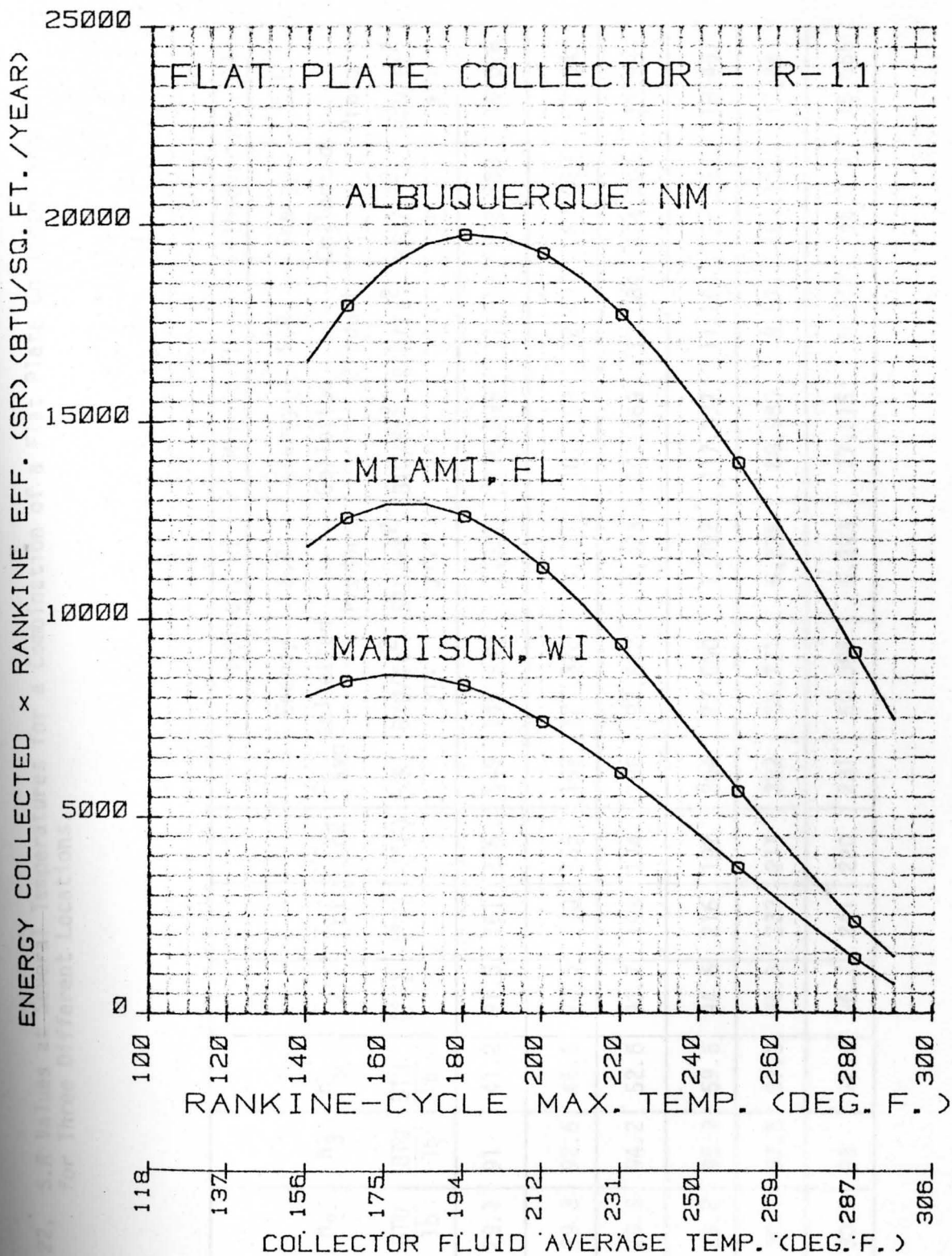


FIGURE 43. Curves of S.R Values vs. Operating Temperature for a Combination of a Flat Plate Collector and R-11 for Three Locations.



TABLE 22, S.R Values at Several Temperatures for a Combination of a Flat Plate Collector and R-12 for Three Different Locations.

$T_3$ (°F)	$\eta_R$ (%)	$h_2$ BTU/lb	$h_3$ BTU/lb	$h_s$ BTU/lb	$T_2$ (°F)	$T_{c1}$ (°F)	$T_{c2}$ (°F)	$T_{avg}$ (°F)	Madison, WI		Miami, FL		Albuquerque, NM	
									Energy Collected BTU/ft <sup>2</sup> yr.	S.R Product BTU/ft <sup>2</sup> yr.	Energy Collected BTU/ft <sup>2</sup> yr.	S.R Product BTU/ft <sup>2</sup> yr.	Energy Collected BTU/ft <sup>2</sup> yr.	S.R Product BTU/ft <sup>2</sup> yr.
140	5.4	29.1	91	41.2	91.6	161	136	149	145,939	7,881	216,999	11,718	296,780	16,026
160	6.9	29.3	92.6	46.6	92.5	180	155	167	121,326	8,371	181,109	12,497	260,069	17,945
180	8.2	29.6	94.2	52.6	93.7	198	174	186	97,842	8,023	147,369	12,084	224,204	18,385
200	9.6	29.8	95.9	59.6	94.6	216	192	204	77,000	7,392	117,337	11,264	192,264	18,457
220	10.7	30.1	97.5	67.3	95.8	233	211	222	58,271	6,235	88,980	9,521	161,131	17,241
230	10.8	30.3	98	72.9	96.7	241	220	231	50,398	5,393	77,215	8,262	146,314	15,656

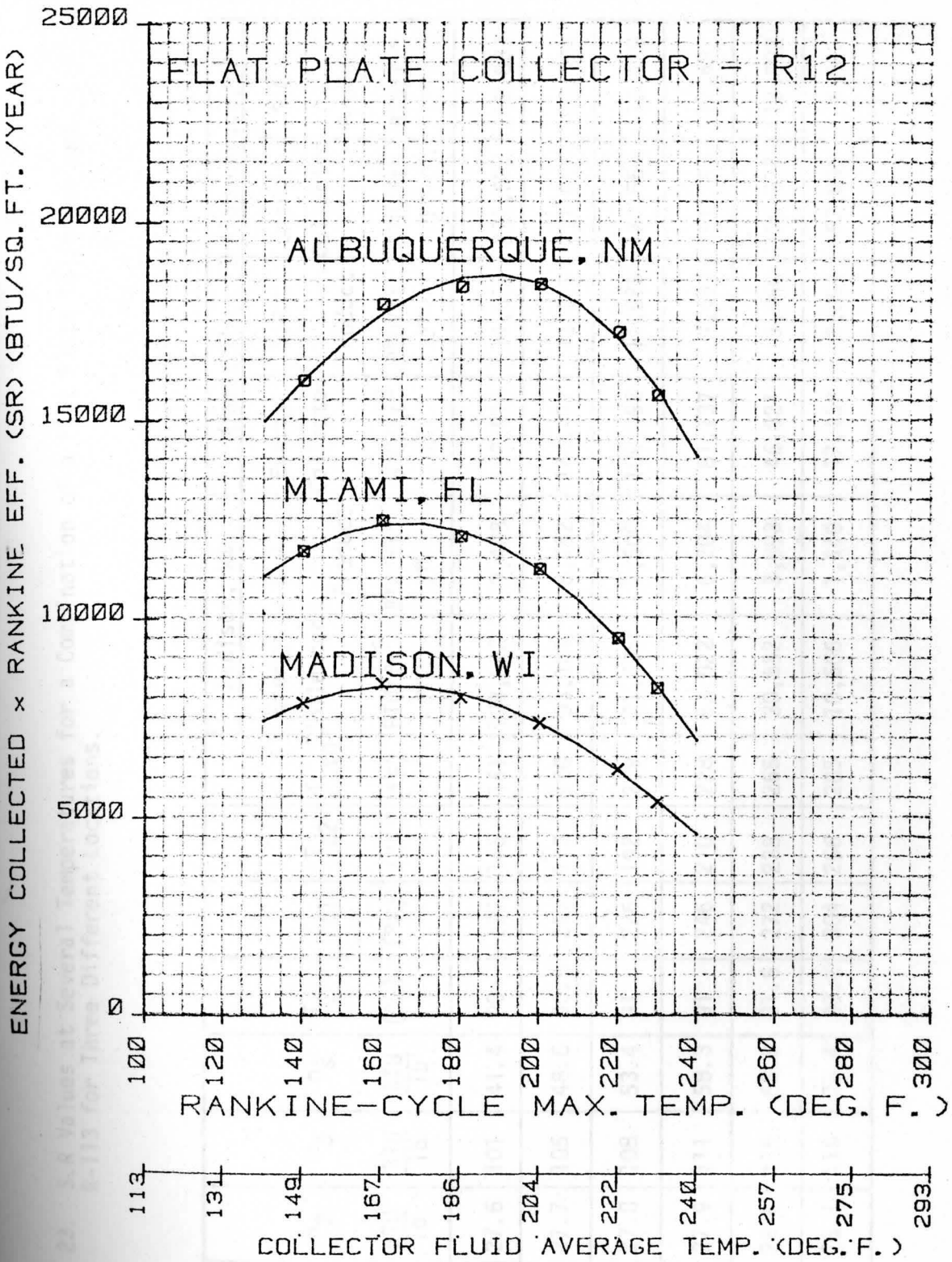


FIGURE 44. Curves of S.R Values vs. Operating Temperature for a Combination of a Flat Plate Collector and R-12 for Three Locations.

TABLE 23. S.R Values at Several Temperatures for a Combination of a Flat Plate Collector and R-113 for Three Different Locations.

T <sub>3</sub> (°F)	η <sub>R</sub> (%)	h <sub>2</sub> BTU/Tb	h <sub>3</sub> BTU/Tb	h <sub>s</sub> BTU/Tb	T <sub>2</sub> (°F)	T <sub>c1</sub> (°F)	T <sub>c2</sub> (°F)	T <sub>avg</sub> (°F)	Madison, WI		Miami, FL		Albuquerque, NM	
									Energy Collected BTU/ft <sup>2</sup> yr.	S.R Product BTU/ft <sup>2</sup> yr.	Energy Collected BTU/ft <sup>2</sup> yr.	S.R Product BTU/ft <sup>2</sup> yr.	Energy Collected BTU/ft <sup>2</sup> yr.	S.E Product BTU/ft <sup>2</sup> yr.
150	7.3	27.6	101	41.4	90	177	145	161	128,882	9,408	192,014	14,017	271,682	19,833
180	9.4	27.7	105	48.6	90.5	207	173	190	93,101	8,752	140,627	13,219	217,067	20,404
200	10.6	27.8	108	53.4	91	226	192	209	71,695	7,600	109,292	11,585	183,564	19,458
220	11.7	27.9	111	58.3	91	246	210	228	53,022	6,204	81,137	9,493	151,253	17,697
250	12.7	28.0	115	68.8	91.5	272	238	255	30,652	3,893	46,921	5,960	108,677	13,802
280	13.5	28.1	119	73.4	92.2	304	266	285	10,666	1,440	17,437	2,354	63,890	8,625

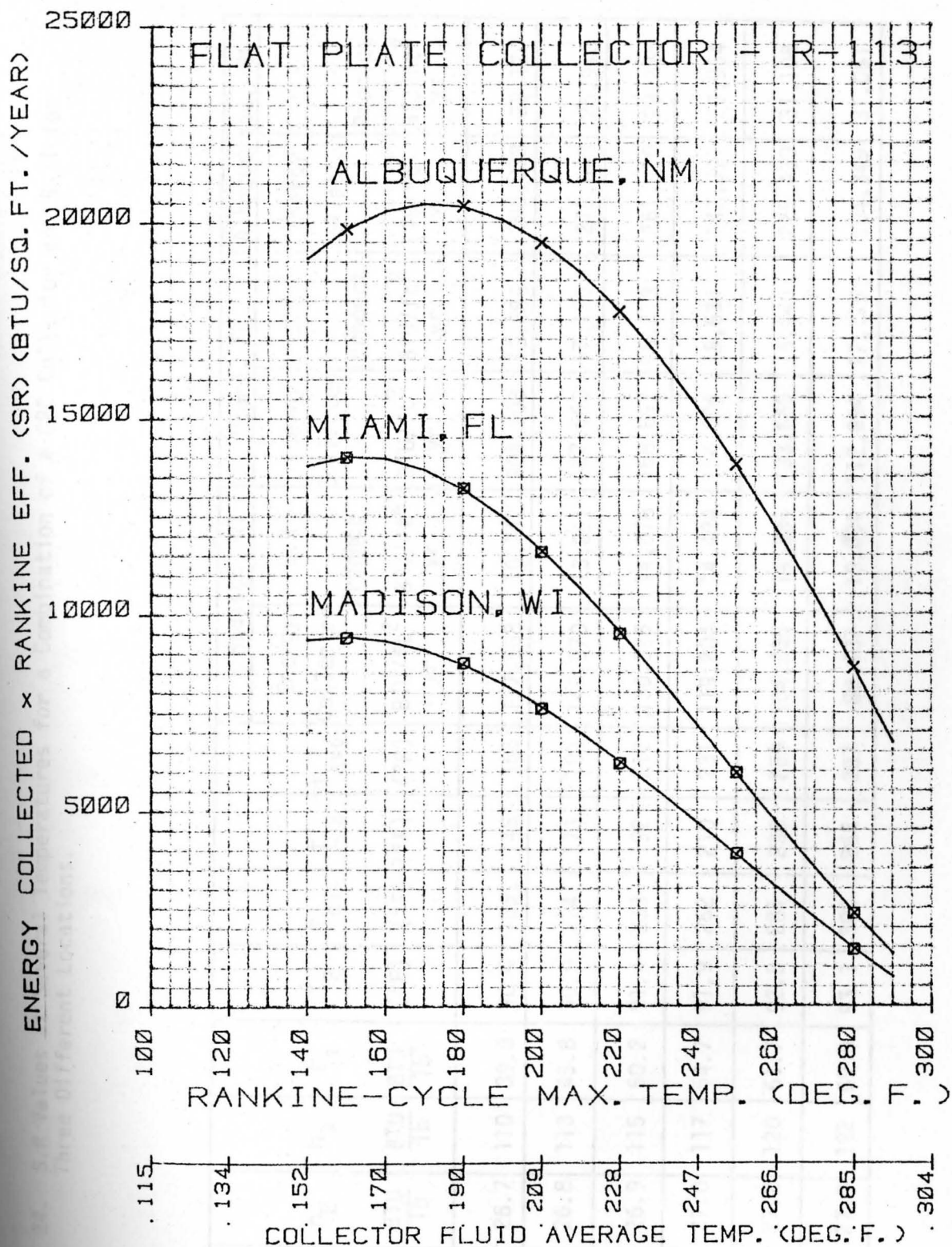


FIGURE 45. Curves of S.R Values vs. Operating Temperature for a Combination of a Flat Plate Collector and R-113 for Three Locations.

TABLE 24. S.R Values at Several Temperatures for a Combination of a CPC Collector and R-11 for Three Different Locations.

$T_3$ (°F)	$\eta_R$ (%)	$h_2$ BTU/lb	$h_3$ BTU/lb	$h_s$ BTU/lb	$T_2$ (°F)	$T_{c1}$ (°F)	$T_{c2}$ (°F)	$T_{avg}$ (°F)	Madison, WI		Miami, FL		Albuquerque, NM	
									Energy Collected BTU/ft <sup>2</sup> yr.	S.R Product BTU/ft <sup>2</sup> yr.	Energy Collected BTU/ft <sup>2</sup> yr.	S.R Product BTU/ft <sup>2</sup> yr.	Energy Collected BTU/ft <sup>2</sup> yr.	S.R Product BTU/ft <sup>2</sup> yr.
150	6.8	26.7	110	39.3	90.4	185	145	165	157,968	10,742	204,208	13,886	295,878	20,120
180	9.4	26.8	113	45.8	90.9	214	173	194	140,970	13,251	182,663	17,170	275,643	25,910
200	10.8	26.9	115	50.2	91.4	233	192	212	130,355	14,078	168,697	18,219	261,910	28,286
220	12.1	27.0	117	54.7	91.9	252	210	231	119,204	14,424	154,005	18,634	247,391	29,934
250	13.8	27.2	120	61.7	92.8	281	238	259	104,235	14,384	133,665	18,446	225,420	31,108
280	15.2	27.3	122	69.0	93.3	308	266	287	89,437	13,594	112,994	17,175	204,349	31,061

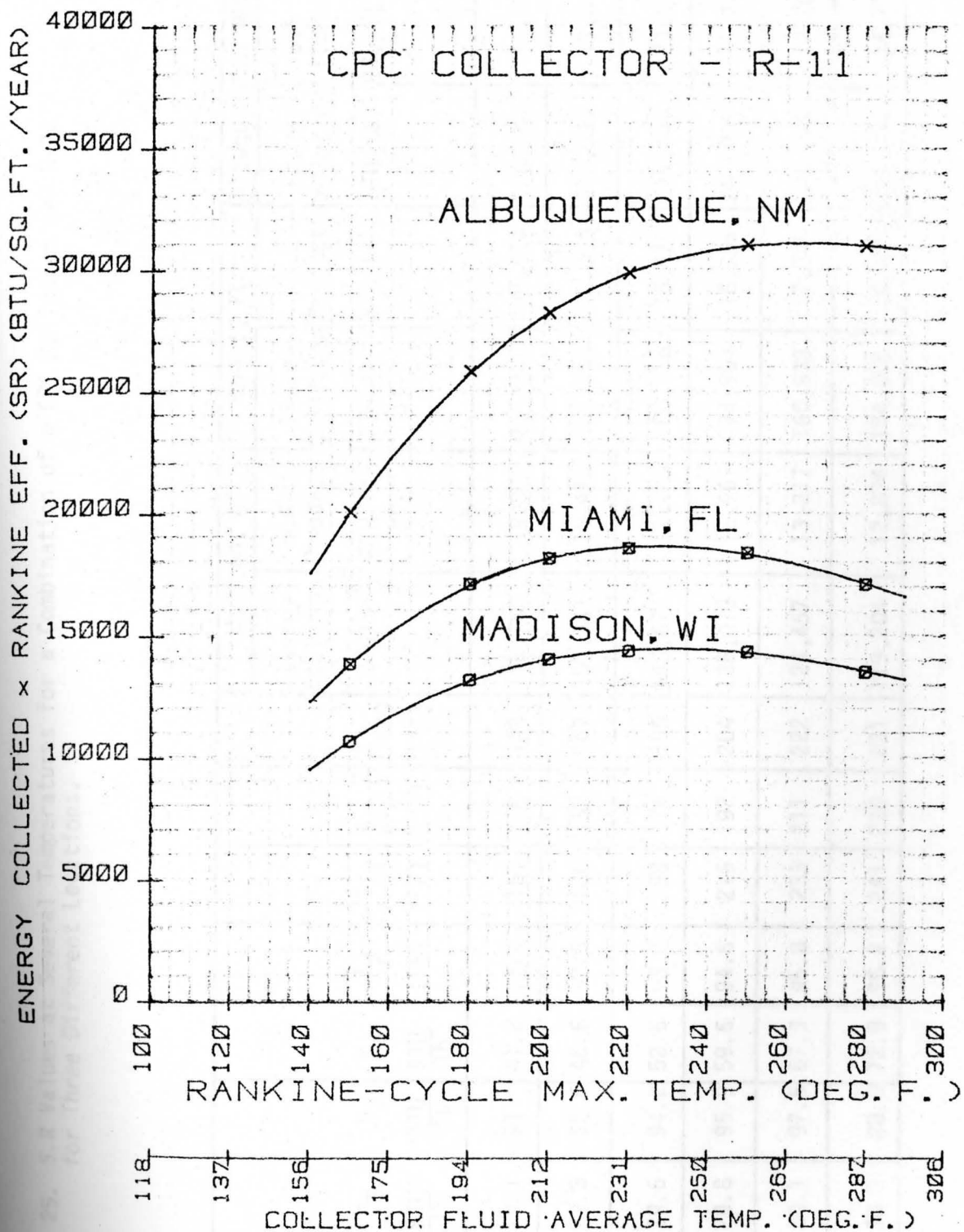


FIGURE 46. Curves of S.R Values vs. Operating Temperature for a Combination of a CPC Collector and R-11 for Three Locations.

TABLE 25. S.R Values at Several Temperatures for a Combination of a CPC Collector and R-12 for Three Different Locations.

$T_3$ (°F)	$\eta_R$ (%)	$h_3$ $\frac{\text{BTU}}{\text{Tb}}$	$h_3$ $\frac{\text{BTU}}{\text{Tb}}$	$h_s$ $\frac{\text{BTU}}{\text{Tb}}$	$T_2$ (°F)	$T_{c1}$ (°F)	$T_{c2}$ (°F)	$T_{\text{avg}}$ (°F)	Madison, WI		Miami, FL		Albuquerque, NM	
									Energy Collected BTU/ft <sup>2</sup> yr.	S.R Product BTU/ft <sup>2</sup> yr.	Energy Collected BTU/ft <sup>2</sup> yr.	S.R Product BTU/ft <sup>2</sup> yr.	Energy Collected BTU/ft <sup>2</sup> yr.	S.R Product BTU/ft <sup>2</sup> yr.
140	5.4	29.1	91	41.2	91.6	161	136	149	166,740	9,004	215,260	11,624	306,180	16,534
160	6.9	29.3	92.6	46.6	92.5	180	155	167	150,941	10,415	195,356	13,480	287,630	19,846
180	8.2	29.6	94.2	52.6	93.7	198	174	186	145,671	11,945	188,718	15,475	281,444	23,078
200	9.6	29.8	95.9	59.6	94.6	216	192	204	135,073	12,967	174,904	16,791	268,013	25,729
220	10.7	30.1	97.5	67.3	95.8	233	211	222	124,457	13,317	160,938	17,220	254,280	27,208
230	10.8	30.3	98.0	72.9	96.7	241	220	231	119,204	12,874	154,005	16,632	247,391	26,718

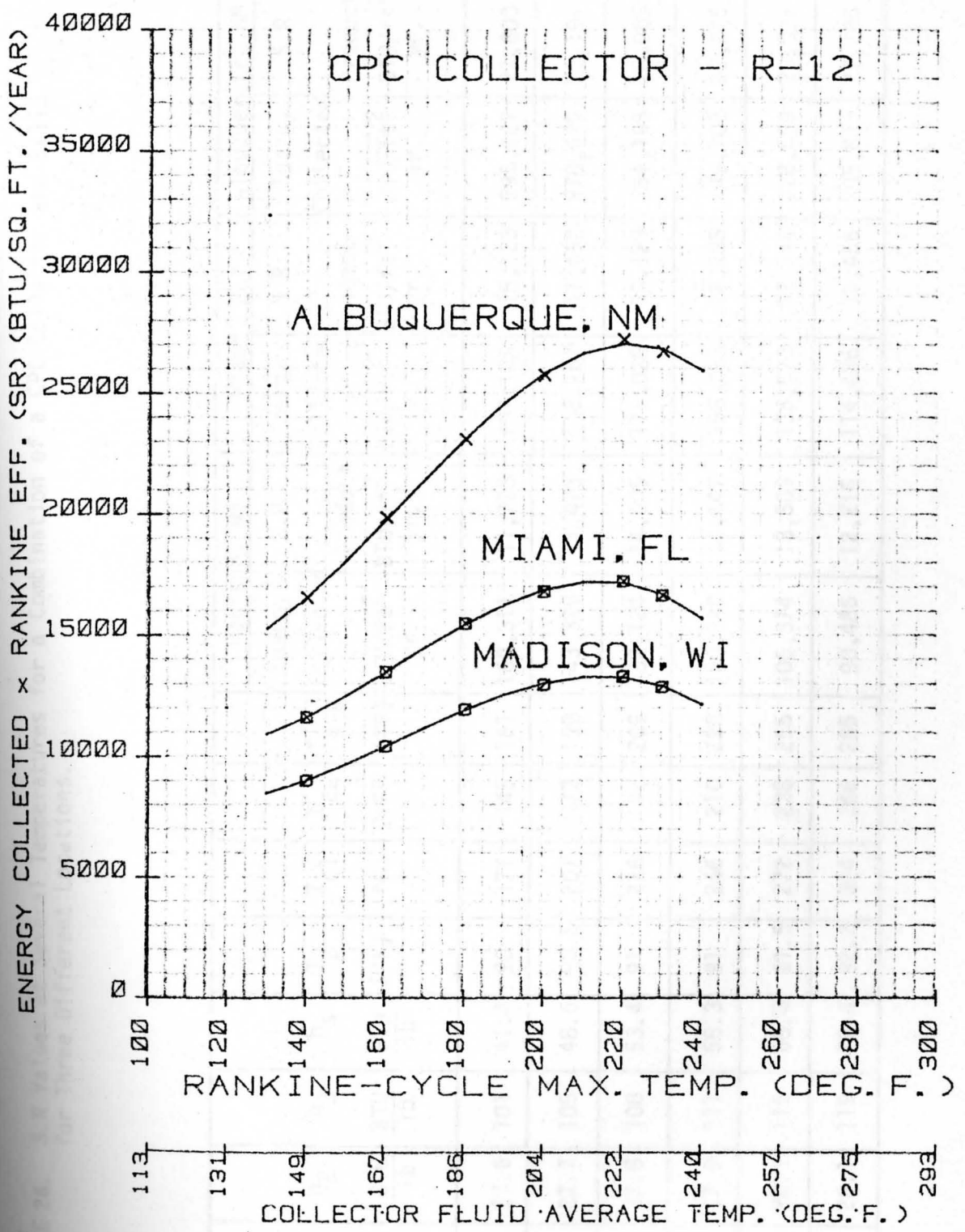


FIGURE 47. Curves of S.R Values vs. Operating Temperature for a Combination of a CPC Collector and R-12 for Three Locations.



TABLE 26. S.R Values at Several Temperatures for a Combination of a CPC Collector and R-113 for Three Different Locations.

$T_3$ (°F)	$\eta_R$ (%)	$h_2$ BTU/lb	$h_3$ BTU/lb	$h_s$ BTU/lb	$T_2$ (°F)	$T_{c1}$ (°F)	$T_{c2}$ (°F)	$T_{avg}$ (°F)	Madison, WI		Miami, FL		Albuquerque, NM	
									Energy Collected BTU/ft <sup>2</sup> yr.	S.R. Product BTU/ft <sup>2</sup> yr.	Energy Collected BTU/ft <sup>2</sup> yr.	S.R. Product BTU/ft <sup>2</sup> yr.	Energy Collected BTU/ft <sup>2</sup> yr.	S.R. Product BTU/ft <sup>2</sup> yr.
150	7.3	27.6	101	41.4	90	177	145	161	160,311	11,703	207,158	15,123	298,627	21,800
180	9.4	27.7	105	48.6	90.5	207	173	190	143,329	13,473	185,767	17,462	278,695	26,197
200	10.6	27.8	108	53.4	91	226	192	209	132,124	14,005	171,025	18,129	264,198	28,005
220	11.7	27.9	111	58.3	91	246	210	228	120,920	14,147	156,283	18,285	249,702	29,215
250	12.7	28.1	115	68.8	91.5	272	238	255	106,374	13,509	136,570	17,344	228,559	29,027
280	13.5	28.1	119	73.4	92.2	304	266	285	90,486	12,216	114,486	15,456	205,812	27,785

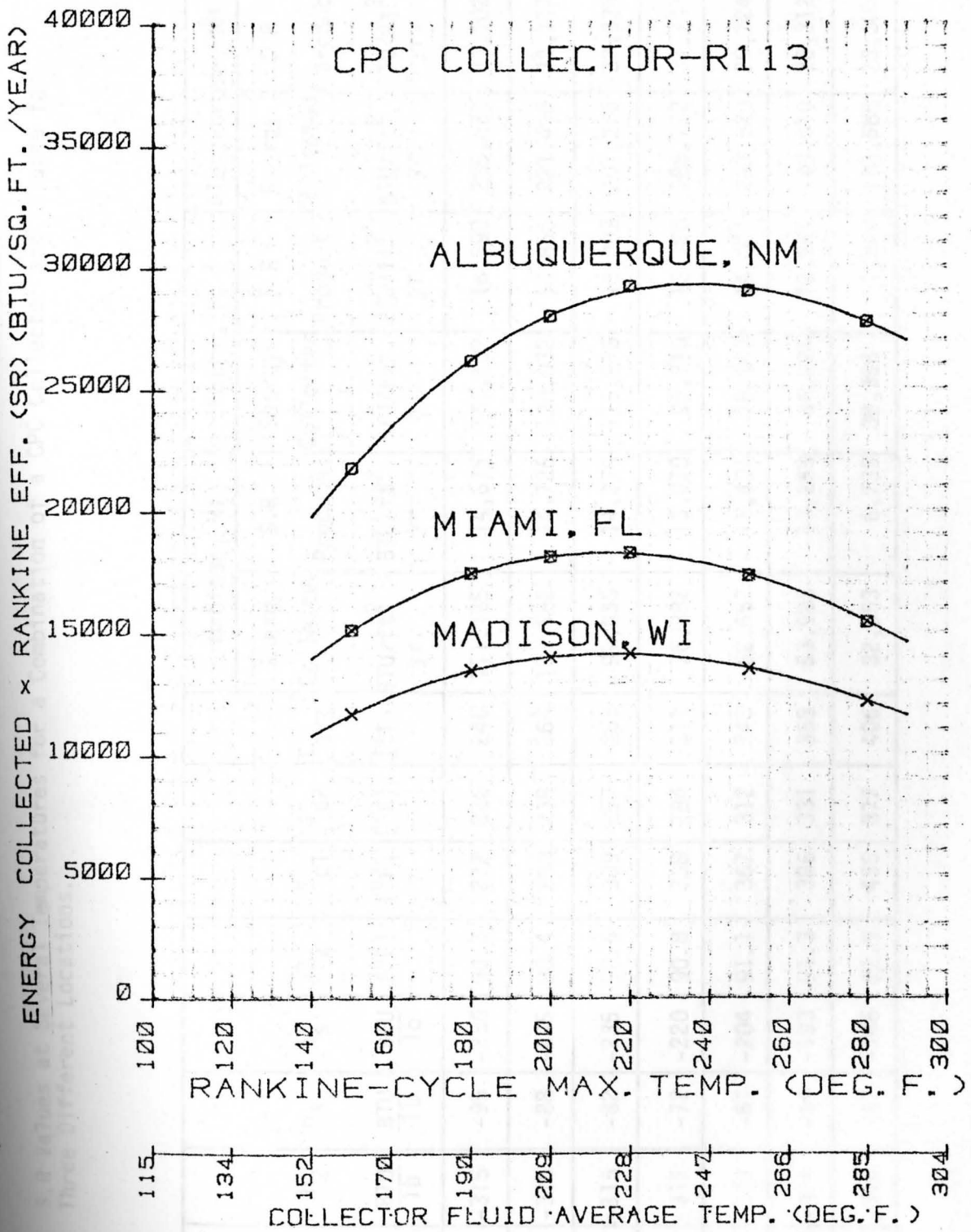


FIGURE 48. Curves of S.R Values vs. Operating Temperature for a Combination of a CPC Collector and R-113 for Three Locations.

TABLE 27. S.R Values at Several Temperatures for a Combination of a CPC Collector and Toluene for Three Different Locations.

T <sub>3</sub> (°F)	η <sub>R</sub> (%)	h <sub>2</sub> BTU/lb	h <sub>3</sub> BTU/lb	h <sub>s</sub> BTU/lb	T <sub>2</sub> (°F)	T <sub>c1</sub> (°F)	T <sub>c2</sub> (°F)	T <sub>avg</sub> (°F)	Madison, WI		Miami, FL		Albuquerque, NM	
									Energy Collected BTU/ft <sup>2</sup> yr.	S.R Produce BTU/ft <sup>2</sup> yr.	Energy Collected BTU/ft <sup>2</sup> yr.	S.R Product BTU/ft <sup>2</sup> yr.	Energy Collected BTU/ft <sup>2</sup> yr.	S.R Product BTU/ft <sup>2</sup> yr.
230	13.2	-315	-95	-256	90.3	272	220	246	111,185	14,676	143,108	18,890	235,621	31,102
250	14.5	-315	-88	-245	90.4	290	238	264	101,562	14,726	130,032	18,855	221,496	32,117
270	15.6	-315	-82	-235	90.6	309	257	283	91,535	14,279	115,978	18,093	207,276	32,335
300	17.0	-315	-72	-220	90.8	338	284	311	76,882	13,070	95,210	16,186	186,712	31,741
330	18.2	-314	-61	-204	91.1	367	312	340	62,657	11,404	76,963	14,007	163,320	29,724
350	19.0	-314	-54	-193	91.3	386	331	358	53,993	10,259	65,921	12,525	149,010	28,312
400	20.7	-314	-37	-166	92.5	435	377	406	32,553	6,739	38,396	7,948	112,586	23,305

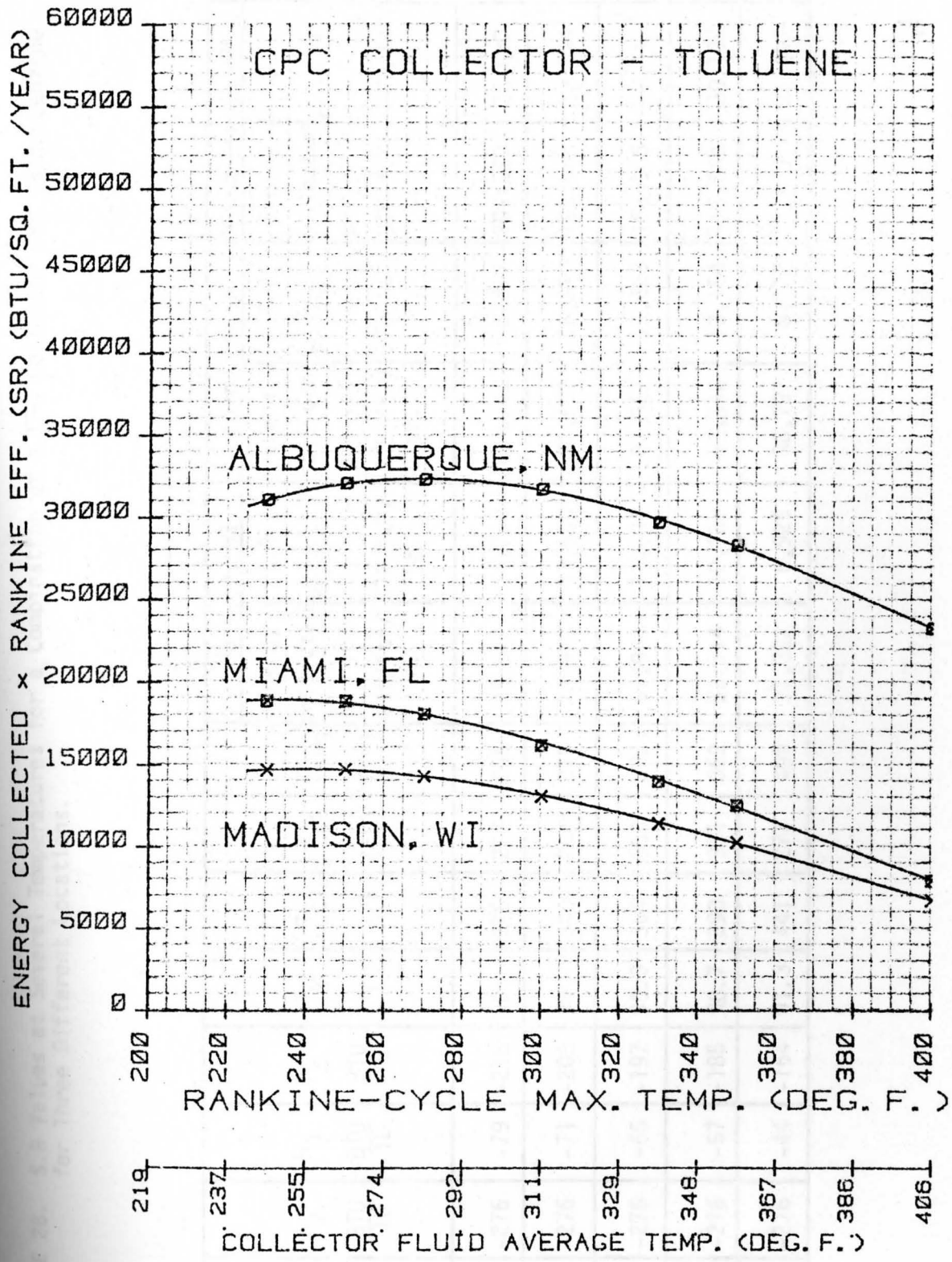


FIGURE 49. Curves of S.R Values vs. Operating Temperature for a Combination of a CPC Collector and Toluene for Three Locations.

TABLE 28. S.R Values at Several Temperatures for a Combination of a CPC Collector and Chlorobenzene for Three Different Locations.

T <sub>3</sub> (°F)	η <sub>R</sub> (%)	h <sub>2</sub> BTU lb	h <sub>3</sub> BTU lb	h <sub>s</sub> BTU lb	T <sub>2</sub> (°F)	T <sub>c1</sub> (°F)	T <sub>c2</sub> (°F)	T <sub>avg</sub> (°F)	Madison, WI		Miami, FL		Albuquerque, NM	
									Energy collected per year BTU/ft <sup>2</sup> / yr.	S.R. Product BTU/ft <sup>2</sup> / yr.	Energy collected per year BTU/ft <sup>2</sup> / yr.	S.R. Product BTU/ft <sup>2</sup> / yr.	Energy collected per year BTU/ft <sup>2</sup> / yr.	S.R. Product BTU/ft <sup>2</sup> / yr.
270	16.4	-276	-79	-216	90	316	257	286	89,962	14,754	113,740	18,653	205,080	33,633
300	18.2	-276	-71	-205	90	345	284	315	74,920	13,635	92,693	16,870	183,486	33,394
320	19.2	-276	-65	-197	90.3	364	303	333	66,048	12,681	81,367	15,623	168,966	32,441
350	20.7	-276	-57	-185	90.7	393	331	362	52,114	10,788	63,546	13,154	145,888	30,199
400	22.1	-276	-44	-164	91.3	441	277	409	31,352	6,929	36,797	8,132	11,439	24,407

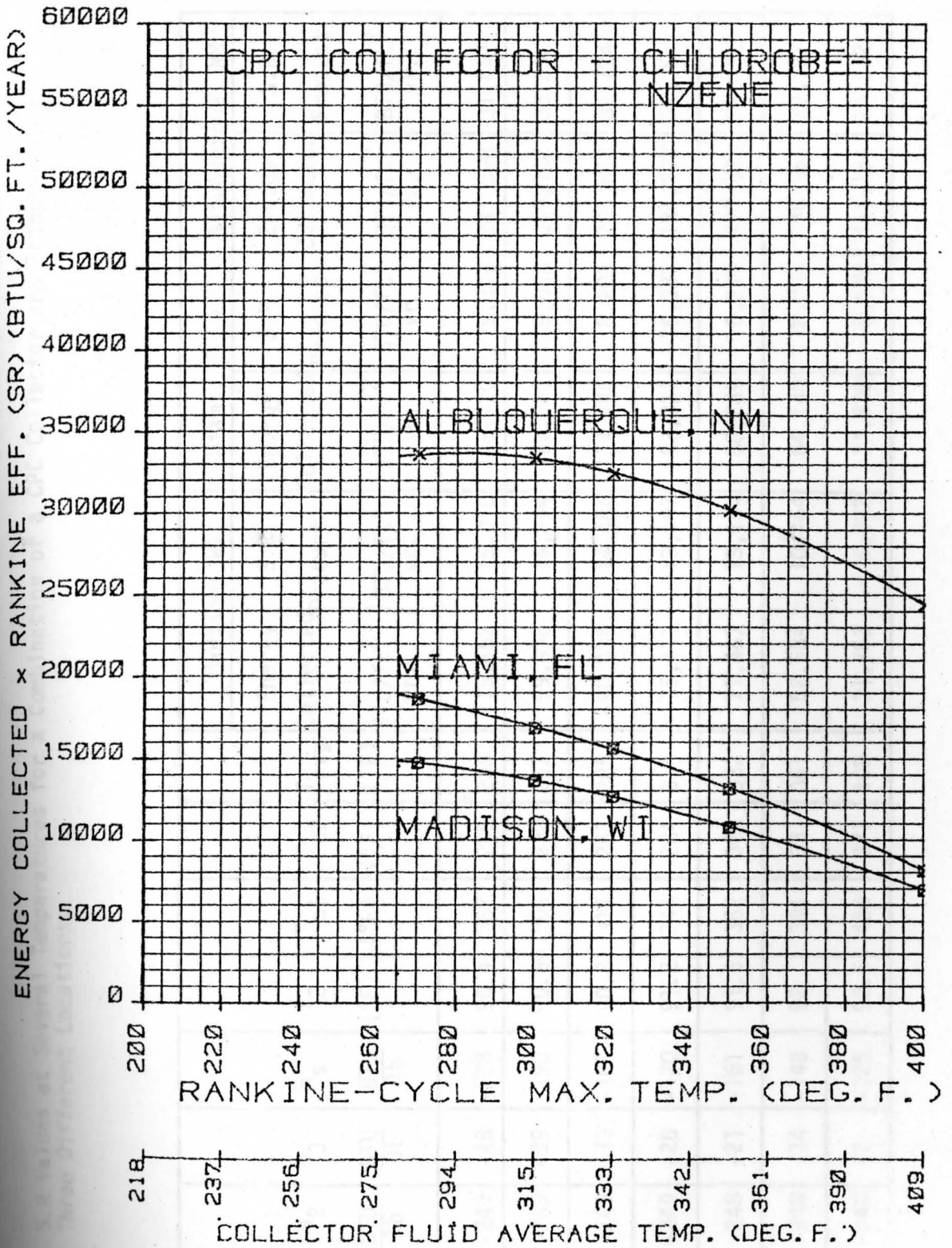


FIGURE 50. Curves of S.R Values vs. Operating Temperature for a Combination of a CPC Collector and Chlorobenzene for Three Locations.

TABLE 29. S.R Values at Several Temperatures for a Combination of a CPC Collector and Thiophene for Three Different Locations.

$T_3$ (°F)	$\eta_R$ (%)	$h_2$ $\frac{BTU}{lb}$	$h_3$ $\frac{BTU}{lb}$	$h_s$ $\frac{BTU}{lb}$	$T_2$ (°F)	$T_{c1}$ (°F)	$T_{c2}$ (°F)	$T_{avg}$ (°F)	Madison, WI		Miami, FL		Albuquerque, NM	
									Energy Collected BTU/ft <sup>2</sup> yr.	S.R Product BTU/ft <sup>2</sup> yr.	Energy Collected BTU/ft <sup>2</sup> yr.	S.R Product BTU/ft <sup>2</sup> yr.	Energy Collected BTU/ft <sup>2</sup> yr.	S.R Product BTU/ft <sup>2</sup> yr.
220	13.0	-249	-48	-208	90.4	267	209	238	115,462	15,010	148,920	19,359	241,898	31,447
250	14.9	-249	-39	-190	90.6	295	238	267	99,958	14,894	127,853	19,050	219,142	32,652
270	15.9	-249	-33	-182	90.8	314	257	285	90,486	14,486	114,486	18,203	205,812	32,724
300	17.5	-249	-26	-170	91.2	344	284	314	75,411	13,197	93,322	16,331	184,292	32,251
320	18.4	-248	-21	-161	91.5	362	303	332	71,487	13,154	88,289	16,245	177,839	32,722
350	19.9	-248	-14	-148	92	391	331	361	52,584	10,464	64,140	12,764	146,669	29,187
400	21.8	-248	-2	-125	93.5	438	377	408	31,753	6,922	37,330	8,138	111,154	24,232

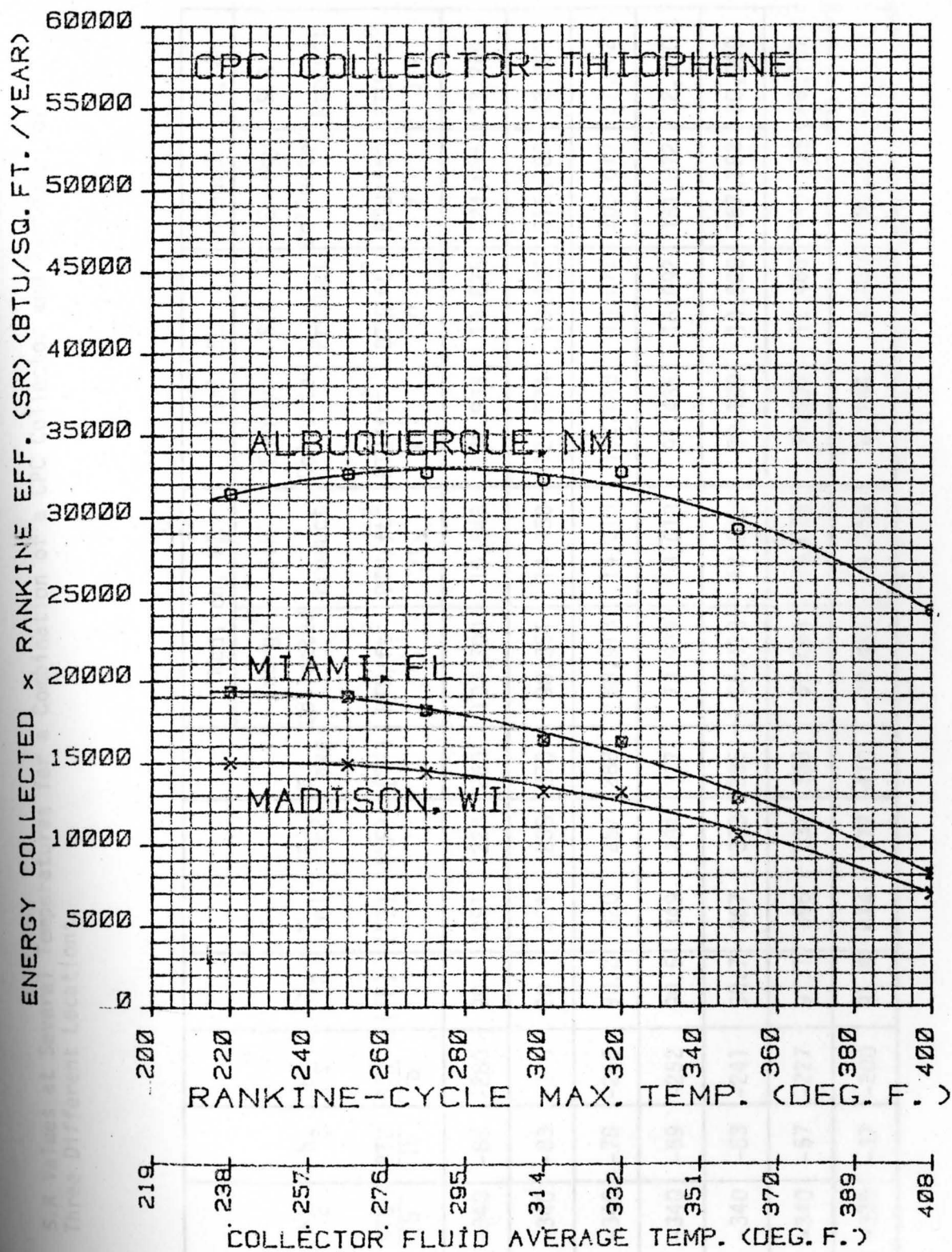


FIGURE 51. Curves of S.R. Values vs. Operating Temperature for a Combination of CPC Collector and Thiophene for Three Locations.



TABLE 30. S.R Values at Several Temperatures for a Combination of a CPC Collector and Pyridine for Three Different Locations.

T <sub>3</sub> (°F)	η <sub>R</sub> (%)	h <sub>2</sub> BTU/lb	h <sub>3</sub> BTU/lb	h <sub>s</sub> BTU/lb	T <sub>2</sub> (°F)	T <sub>c1</sub> (°F)	T <sub>c2</sub> (°F)	T <sub>avg</sub> (°F)	Madison, WI		Miami, FL		Albuquerque, NM	
									Energy Collected BTU/ft <sup>2</sup> yr.	S.R Product BTU/ft <sup>2</sup> yr.	Energy Collected BTU/ft <sup>2</sup> yr.	S.R Product BTU/ft <sup>2</sup> yr.	Energy Collected BTU/ft <sup>2</sup> yr.	S.R Product BTU/ft <sup>2</sup> yr.
240	14.8	-340	-86	-280	90	291	228	260	103,700	15,348	132,938	19,675	224,635	33,246
250	15.2	-340	-83	-275	90	301	238	270	98,354	14,950	125,674	19,102	216,788	32,952
270	16.1	-340	-78	-266	90.2	320	257	288	88,913	14,315	112,248	18,072	203,617	32,782
300	17.6	-340	-69	-252	90.5	349	284	317	73,939	13,013	91,435	16,092	181,872	32,010
320	18.5	-340	-63	-241	90.7	367	303	335	65,110	12,045	80,109	14,820	167,353	30,960
350	19.8	-340	-57	-227	91.1	396	331	363	51,644	10,226	62,953	12,465	145,108	28,731
400	21.7	-339	-37	-200	91.9	444	377	410	30,952	6,716	36,264	7,869	109,723	23,810

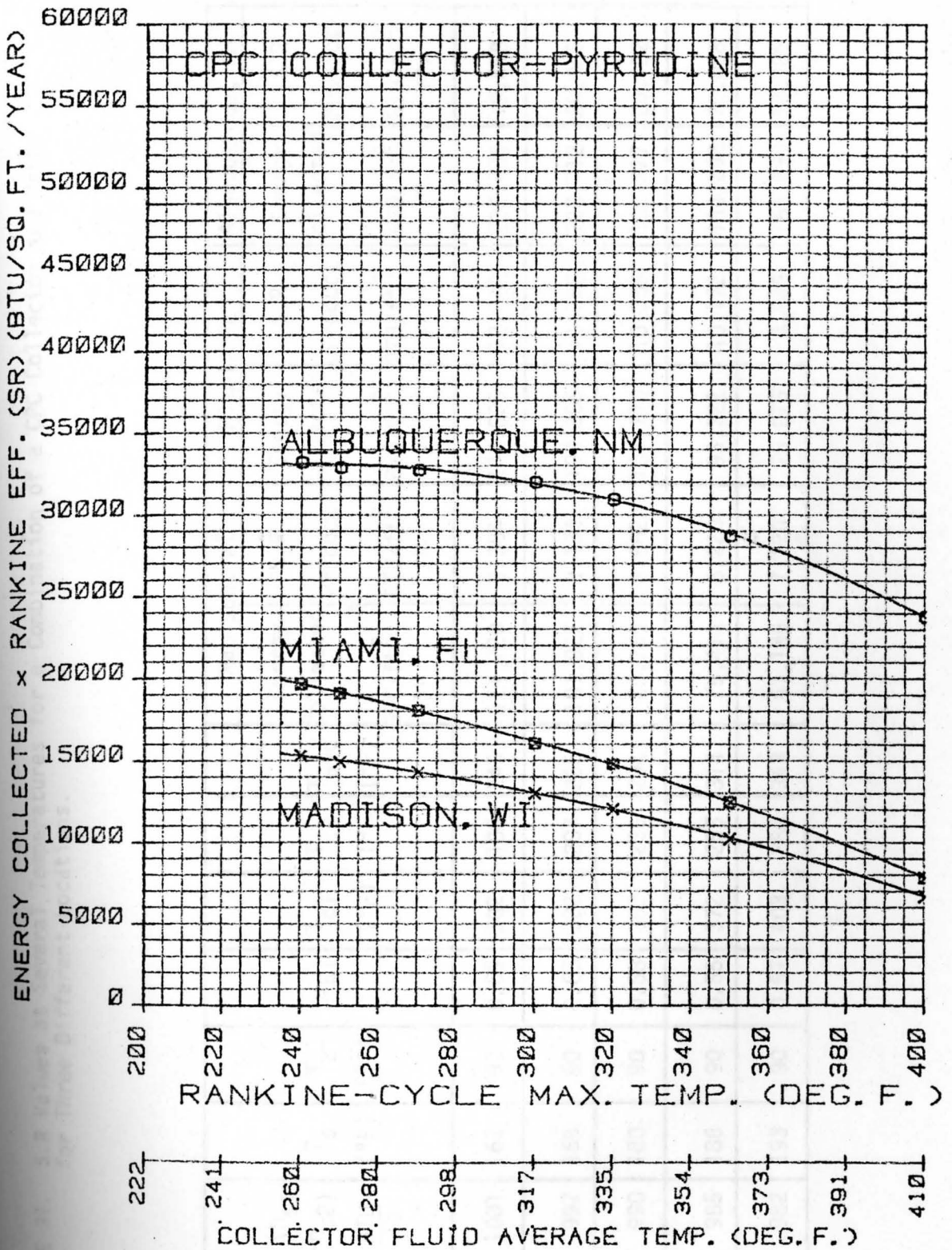


FIGURE 52. Curves of S.R Values vs. Operating Temperature for a Combination of a CPC Collector and Pyridine for Three Locations.

TABLE 31. S.R Values at Several Temperatures for a Combination of a CPC Collector and Water for Three Different Locations.

$T_3$ (°F)	$\eta_R$ (%)	$(h_{s1} - h_{s2})$ $\frac{BTU}{lb}$	$T_s$ (°F)	$T_2$ (°F)	$\epsilon_{B1}$	$T_{c1}$ (°F)	$T_{c2}$ (°F)	$T_{avg}$ (°F)	Madison, WI		Miami, FL		Albuquerque, NM	
									Energy Collected BTU/ft <sup>2</sup> yr.	S.R Product BTU/ft <sup>2</sup> yr.	Energy Collected BTU/ft <sup>2</sup> yr.	S.R Product BTU/ft <sup>2</sup> yr.	Energy Collected BTU/ft <sup>2</sup> yr.	S.R Product BTU/ft <sup>2</sup> yr.
300	8.4	1001	162	90	0.69	302	188	245	111,720	9,384	143,835	12,082	236,406	19,858
320	9.1	997	169	90	0.65	322	207	265	101,027	9,134	129,306	11,768	220,712	20,085
350	10.1	990	180	90	0.58	352	235	294	85,765	8,662	107,773	10,885	199,227	20,122
370	10.9	985	186	90	0.55	372	255	314	75,411	8,220	93,322	10,172	184,292	20,088
400	11.8	982	193	90	0.51	403	284	343	61,186	7,220	75,075	8,869	160,899	18,986

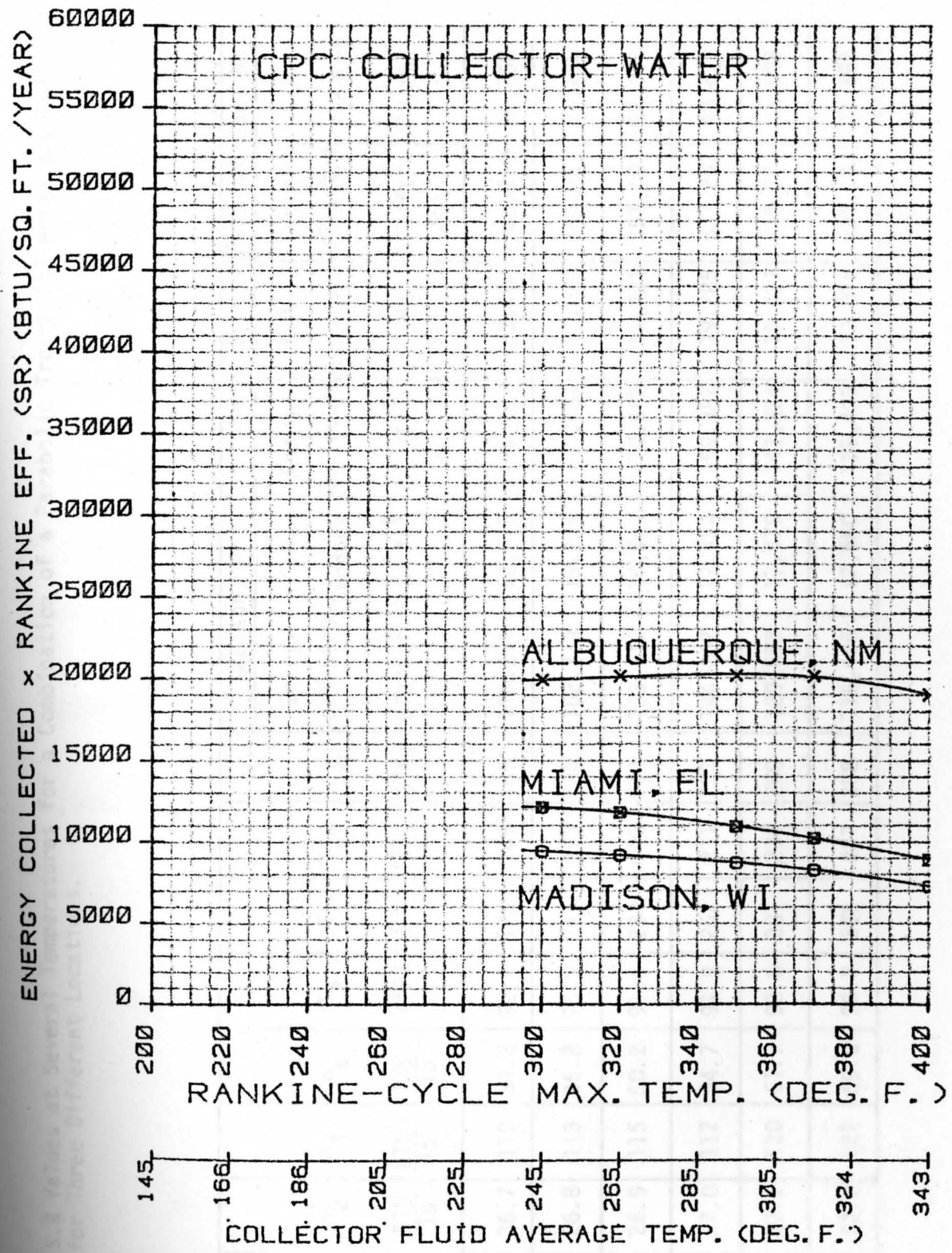


FIGURE 53. Curves of S.R Values vs. Operating Temperature for a Combination of a CPC Collector and Water for Three Locations.

TABLE 32. S.R Values at Several Temperatures for a Combination of a Parabolic Trough Collector and R-11 for Three Different Locations.

T <sub>3</sub> (°F)	η <sub>R</sub> (%)	h <sub>2</sub> BTU/lb	h <sub>3</sub> BTU/lb	h <sub>s</sub> BTU/lb	T <sub>2</sub> (°F)	T <sub>c1</sub> (°F)	T <sub>c2</sub> (°F)	T <sub>avg</sub> (°F)	Madison, WI		Miami, FL		Albuquerque, NM	
									Energy Collected BTU/ft <sup>2</sup> yr.	S.R Product BTU/ft <sup>2</sup> yr.	Energy Collected BTU/ft <sup>2</sup> yr.	S.R Product BTU/ft <sup>2</sup> yr.	Energy Collected BTU/ft <sup>2</sup> yr.	S.R Product BTU/ft <sup>2</sup> yr.
150	6.8	26.7	110	39.3	90.4	185	145	165	176,693	12,015	198,237	13,480	386,290	26,268
180	9.4	26.8	113	45.8	90.9	214	173	194	162,329	15,259	181,164	17,029	364,763	34,288
200	10.8	26.9	115	50.2	91.4	233	192	212	153,413	16,569	170,568	18,421	351,401	37,951
220	12.1	27.0	117	54.7	91.9	252	211	231	144,002	17,424	159,382	19,285	337,297	40,813
250	13.8	27.2	120	61.7	92.8	281	239	260	129,558	17,879	142,224	19,627	315,274	43,508
280	15.2	27.3	122	69.0	93.3	308	267	288	115,465	17,550	125,499	19,076	293,103	44,552

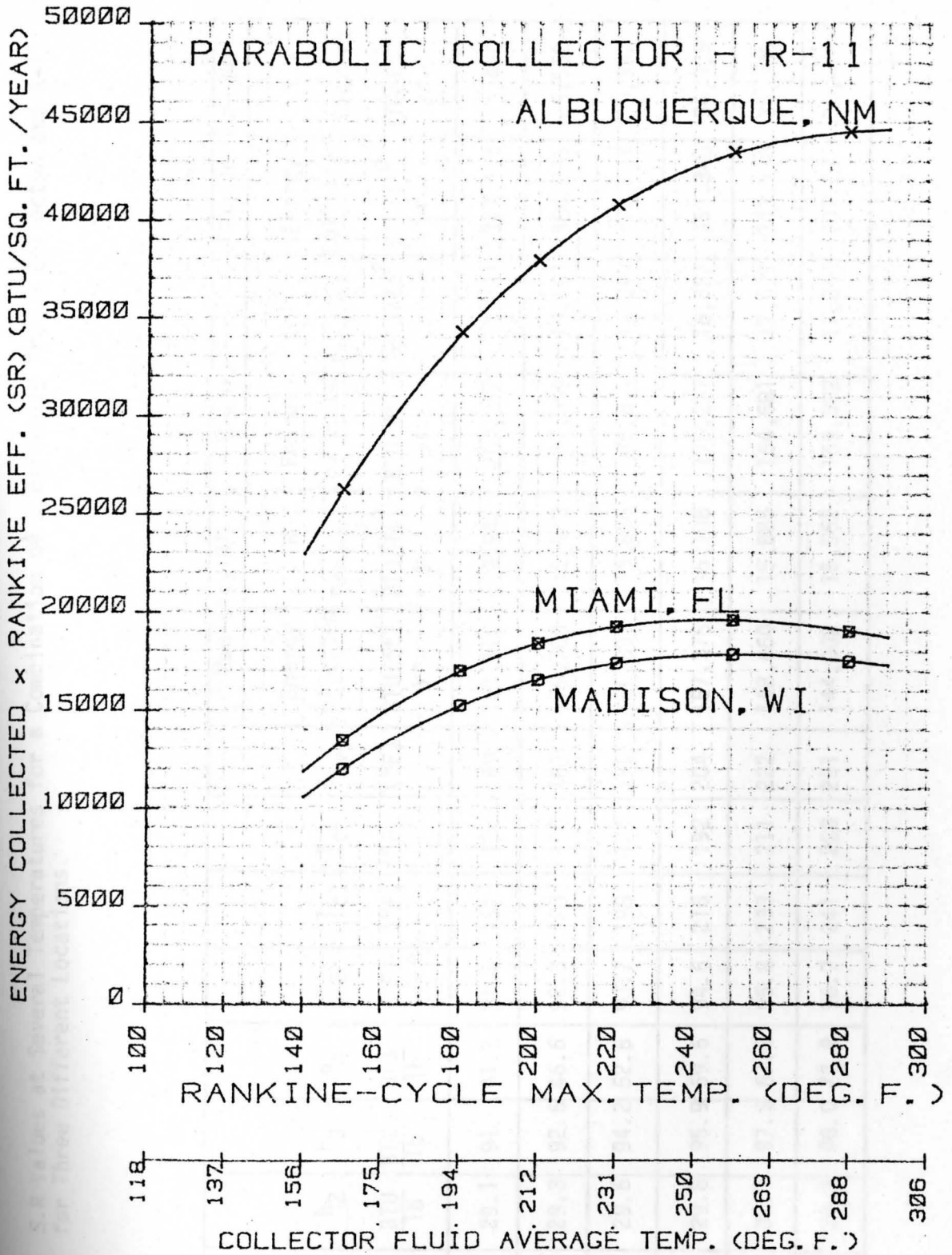


FIGURE 54. Curves of S.R. Values vs. Operating Temperature for a Combination of a Parabolic Trough Collector and R-11 for Three Locations.

TABLE 33. S.R Values at Several Temperatures for a Combination of a Parabolic Trough Collector and R-12 for Three Different Locations.

$T_3$ (°F)	$\eta_R$ (%)	$h_2$ $\frac{BTU}{lb}$	$h_3$ $\frac{BTU}{lb}$	$h_s$ $\frac{BTU}{lb}$	$T_2$ (°F)	$T_{c1}$ (°F)	$T_{c2}$ (°F)	$T_{avg}$ (°F)	Madison, WI		Miami, FL		Albuquerque, NM	
									Energy Collected BTU/ft <sup>2</sup> yr.	S.R Product BTU/ft <sup>2</sup> yr.	Energy Collected BTU/ft <sup>2</sup> yr.	S.R Product BTU/ft <sup>2</sup> yr.	Energy Collected BTU/ft <sup>2</sup> yr.	S.R Product BTU/ft <sup>2</sup> yr.
140	5.4	29.1	91	41.2	91.6	161	136	149	184,110	9,942	207,050	11,181	397,410	21,460
160	6.9	29.3	92.6	46.6	92.5	180	155	167	175,703	12,123	197,059	13,597	384,806	26,552
180	8.2	29.6	94.2	52.6	93.7	198	174	186	166,291	13,636	185,874	15,242	370,701	30,397
200	9.6	29.8	95.9	59.6	94.6	216	192	204	157,376	15,108	175,277	16,827	357,340	34,305
220	10.7	30.1	97.5	67.3	95.8	233	211	222	148,460	15,885	164,681	17,621	343,978	36,806
230	10.8	30.3	98.0	72.9	96.7	241	220	231	144,002	15,552	159,382	17,213	337,297	36,428

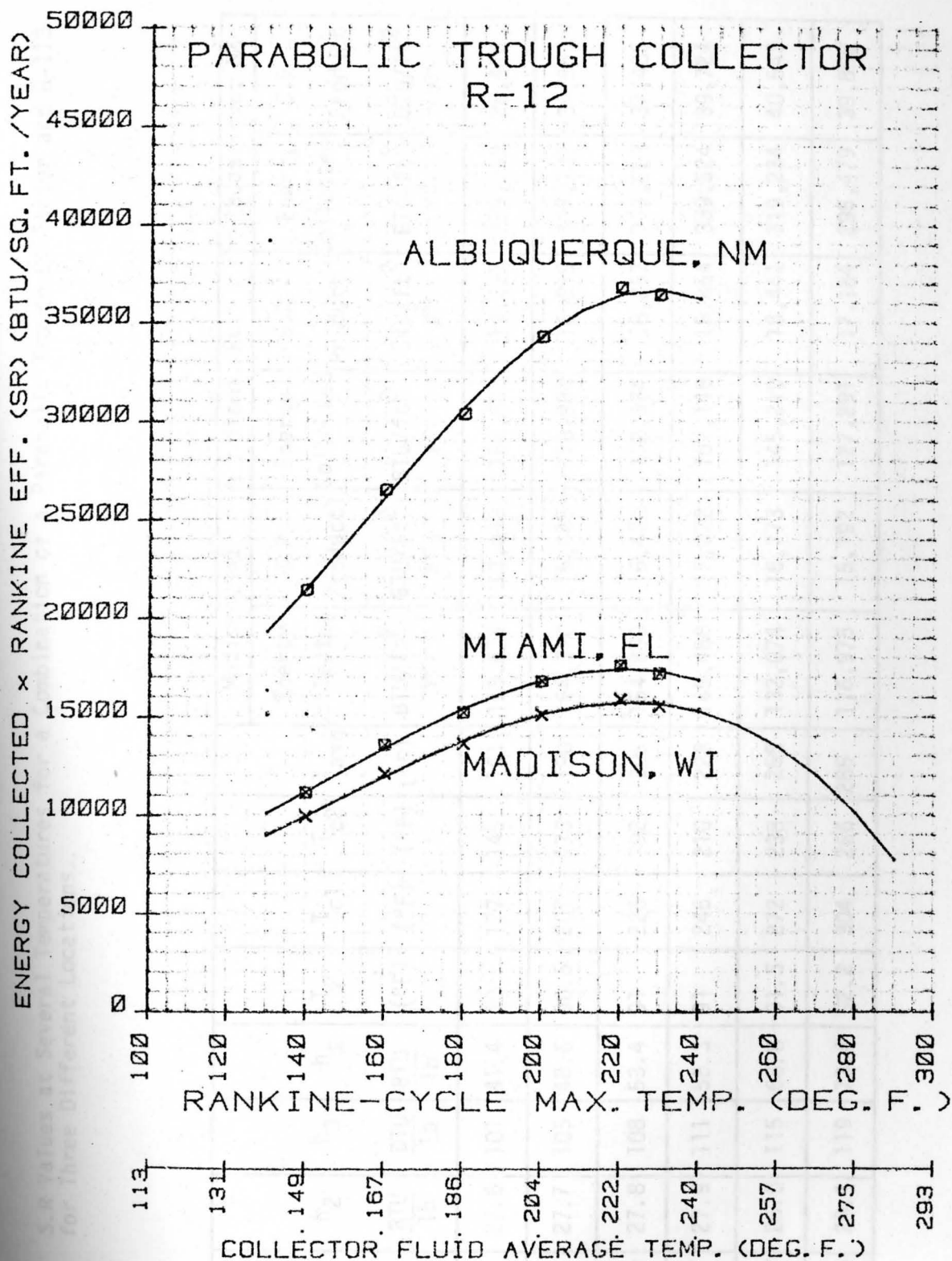


FIGURE 55. Curves of S.R Values vs. Operating Temperature for a Combination of a Parabolic Trough Collector and R-12 for Three Locations.



TABLE 34. S.R Values at Several Temperatures for a Combination of a Parabolic Trough Collector and R-113 for Three Different Locations.

T <sub>3</sub> (°F)	η <sub>R</sub> (%)	h <sub>2</sub> BTU/lb	h <sub>3</sub> BTU/lb	h <sub>s</sub> BTU/lb	T <sub>2</sub> (°F)	T <sub>c1</sub> (°F)	T <sub>c2</sub> (°F)	T <sub>avg</sub> (°F)	Madison, WI		Miami, FL		Albuquerque, NM	
									Energy Collected BTU/ft <sup>2</sup> yr.	S.R Product BTU/ft <sup>2</sup> yr.	Energy Collected BTU/ft <sup>2</sup> yr.	S.R Product BTU/ft <sup>2</sup> yr.	Energy Collected BTU/ft <sup>2</sup> yr.	S.R Product BTU/ft <sup>2</sup> yr.
150	7.3	27.6	101	41.4	90	177	145	161	178,674	13,043	182,695	13,337	389,259	28,416
180	9.4	27.7	105	48.6	90.5	207	173	190	164,310	15,445	178,930	16,819	367,732	34,567
200	10.6	27.8	108	53.4	91	226	192	209	154,899	16,420	172,334	18,267	353,628	37,485
220	11.7	27.9	111	58.3	91	246	210	228	145,488	17,022	161,148	18,854	339,524	39,724
250	12.7	28.0	115	68.8	91.5	272	238	255	132,074	16,773	145,210	18,441	319,234	40,543
280	13.5	28.1	119	73.4	92.2	304	266	285	116,975	15,792	127,291	17,184	295,479	39,890

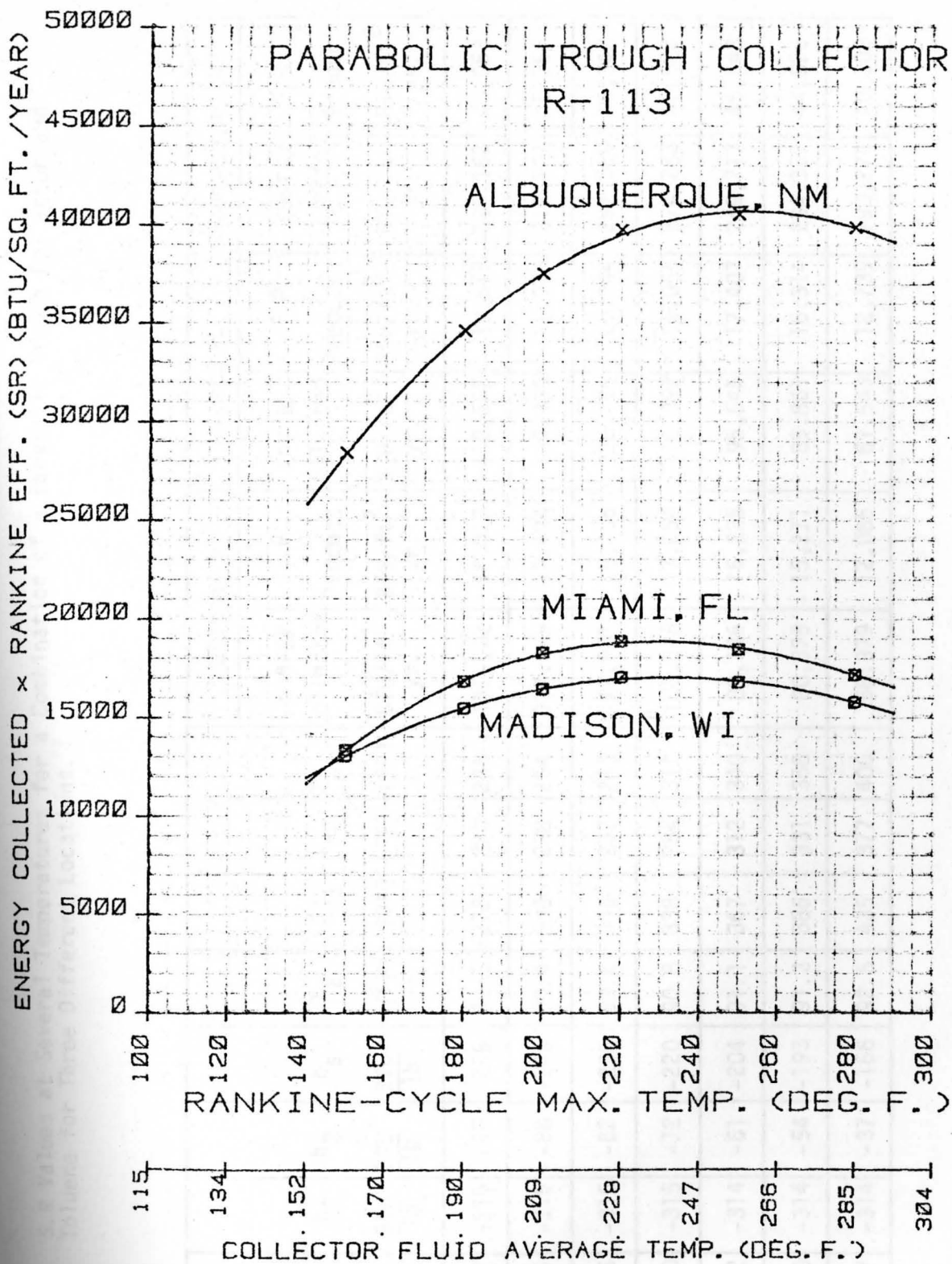


FIGURE 56. Curves of S.R Values vs. Operating Temperature for a Combination of a Parabolic Trough Collector and R-113 for Three Locations.

TABLE 35. S.R Values at Several Temperatures for a Combination of a Parabolic Trough Collector and Toluene for Three Different Locations.

T <sub>3</sub> (°F)	η <sub>R</sub> (%)	h <sub>2</sub> $\frac{\text{BTU}}{\text{lb}}$	h <sub>3</sub> $\frac{\text{BTU}}{\text{lb}}$	h <sub>s</sub> $\frac{\text{BTU}}{\text{lb}}$	T <sub>2</sub> (°F)	T <sub>c1</sub> (°F)	T <sub>c2</sub> (°F)	T <sub>avg</sub> (°F)	Madison, WI		Miami, FL		Albuquerque, NM	
									Energy Collected BTU/ft <sup>2</sup> yr.	S.R Product BTU/ft <sup>2</sup> yr.	Energy Collected BTU/ft <sup>2</sup> yr.	S.R Product BTU/ft <sup>2</sup> yr.	Energy Collected BTU/ft <sup>2</sup> yr.	S.R Product BTU/ft <sup>2</sup> yr.
230	13.2	-315	-95	-256	90.3	272	220	246	136,572	18,028	150,552	19,873	326,162	43,053
250	14.5	-315	-88	-245	90.4	290	238	264	127,545	18,494	139,835	20,276	312,107	45,256
270	15.6	-315	-82	-235	90.6	309	257	283	117,981	18,405	128,485	20,044	297,062	46,342
300	17.0	-315	-72	-220	90.8	338	284	311	103,848	17,654	112,092	19,056	274,283	46,628
330	18.2	-314	-61	-204	91.1	367	312	340	89,146	16,225	95,645	17,407	249,717	45,448
350	19.0	-314	-54	-193	91.3	386	331	358	80,375	15,271	85,861	16,314	234,357	44,528
400	20.7	-314	-37	-166	92.5	435	377	406	58,379	12,085	61,543	12,739	193,274	40,008

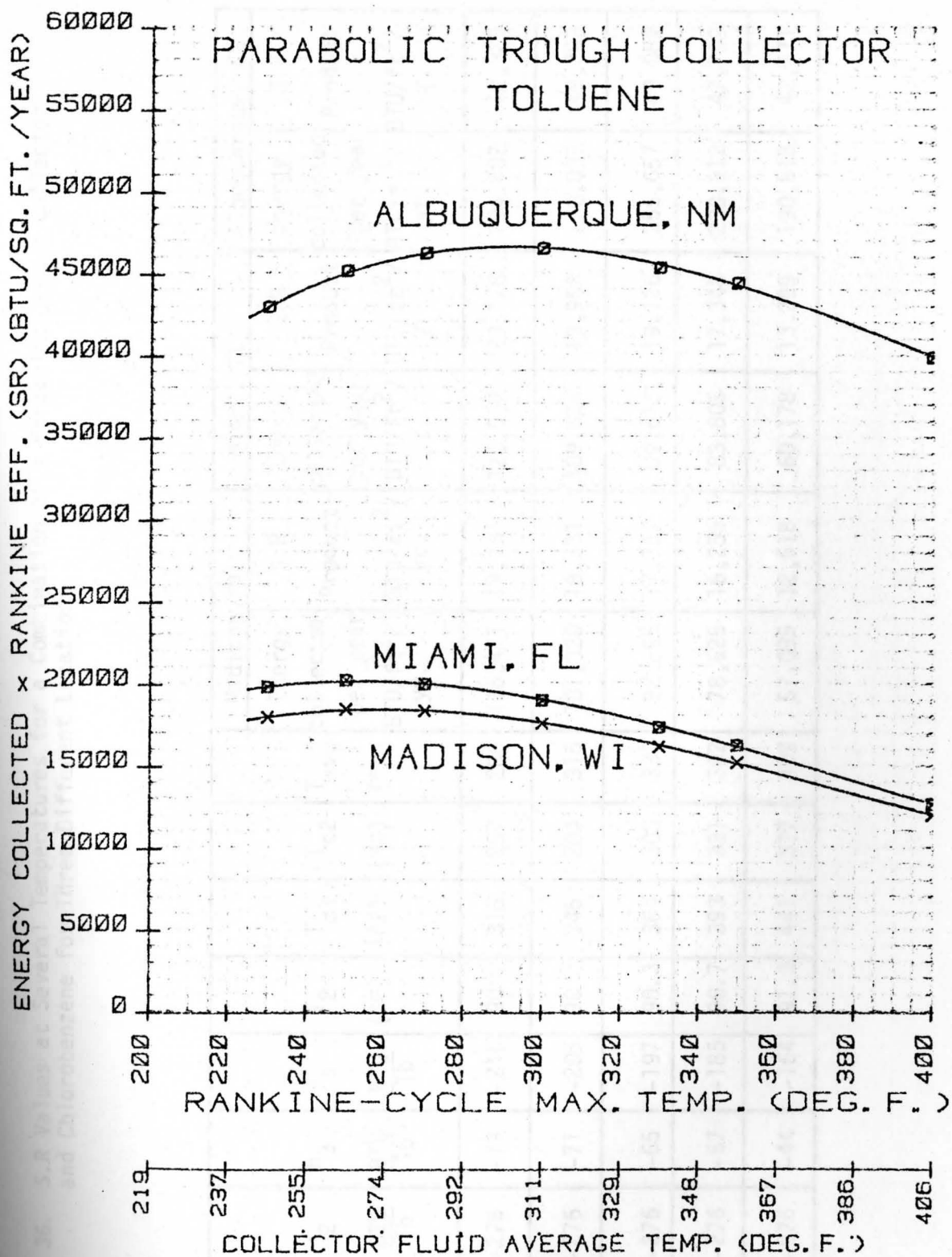


FIGURE 57. Curves of S.R Values vs. Operating Temperature for a Combination of a Parabolic Trough Collector and Toluene for Three Locations.

TABLE 36. S.R Values at Several Temperatures for a Combination of a Parabolic Trough Collector and Chlorobenzene for Three Different Locations.

T <sub>3</sub> (°F)	η <sub>R</sub> (%)	h <sub>2</sub> BTU/lb	h <sub>3</sub> BTU/lb	h <sub>s</sub> BTU/lb	T <sub>2</sub> (°F)	T <sub>c1</sub> (°F)	T <sub>c2</sub> (°F)	T <sub>avg</sub> (°F)	Madison, WI		Miami, FL		Albuquerque, NM	
									Energy collected per year BTU/ft <sup>2</sup> /yr.	S.R Product BTU/ft <sup>2</sup> /yr.	Energy collected per year BTU/ft <sup>2</sup> /yr.	S.R Product BTU/ft <sup>2</sup> /yr.	Energy collected per year BTU/ft <sup>2</sup> /yr.	S.R Product BTU/ft <sup>2</sup> /yr.
270	16.4	-276	-79	-216	90	316	257	286	116,471	19,101	126,693	20,778	294,687	48,329
300	18.2	-276	-71	-205	90	345	284	315	101,820	18,531	109,824	19,988	270,895	49,303
320	19.2	-276	-65	-197	90.3	364	303	333	92,695	17,797	99,615	19,126	255,657	49,084
350	20.7	-276	-57	-185	90.7	393	331	362	78,525	16,255	83,805	17,348	230,912	47,799
400	22.1	-276	-44	-164	91.3	441	377	409	57,095	12,618	60,178	13,299	190,818	42,171

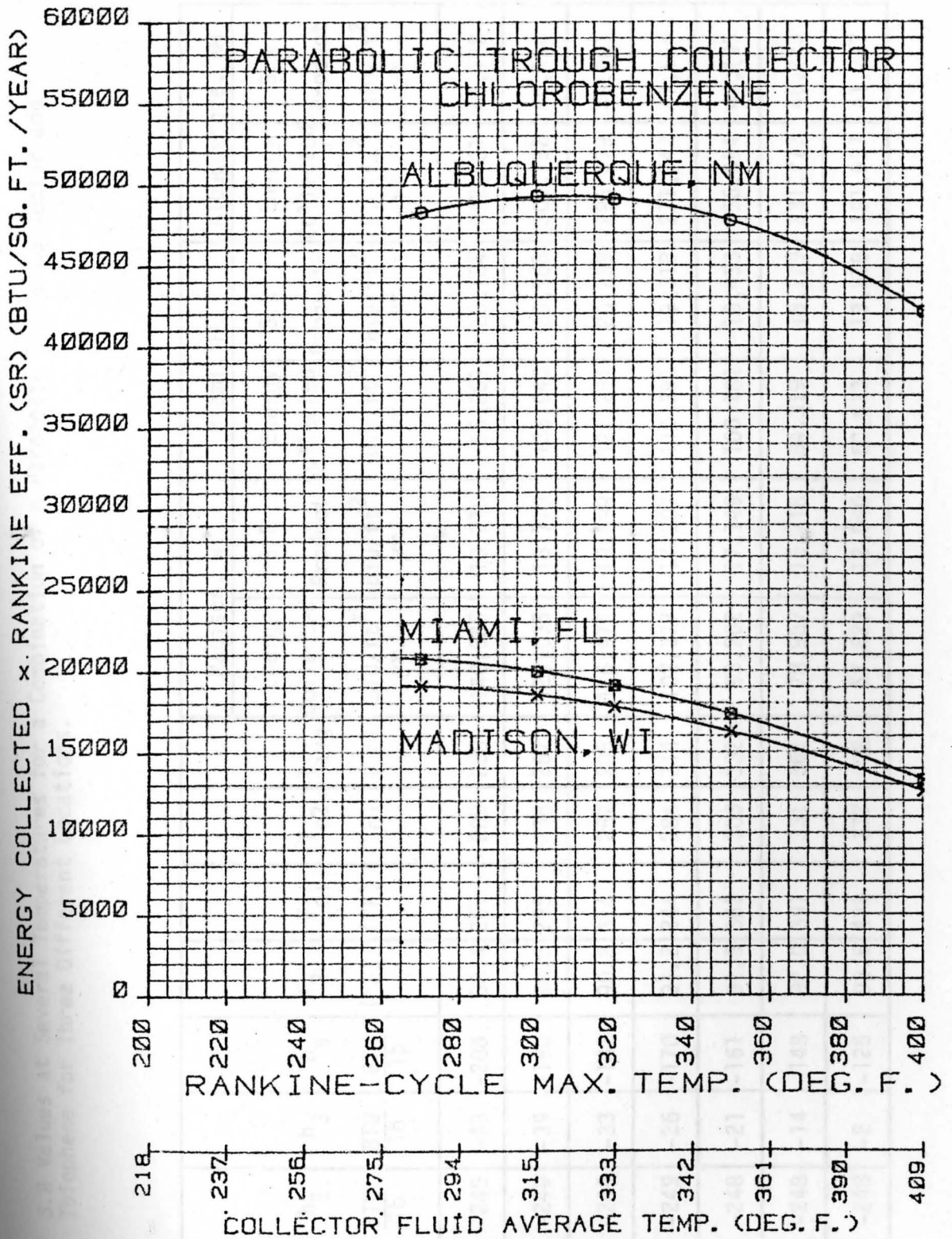


FIGURE 58. Curves of S.R Values vs. Operating Temperature for a Combination of a Parabolic Trough Collector and Chlorobenzene for Three Locations.

TABLE 37. S.R Values at Several Temperatures for a Combination of a Parabolic Trough Collector and Thiophene for Three Different Locations.

$T_3$ (°F)	$\eta_R$ (%)	$h_2$ BTU/lb	$h_3$ BTU/lb	$h_s$ BTU/lb	$T_2$ (°F)	$T_{c1}$ (°F)	$T_{c2}$ (°F)	$T_{avg}$ (°F)	Madison, WI		Miami, FL		Albuquerque, NM	
									Energy Collected BTU/ft <sup>2</sup> yr.	S.R Product BTU/ft <sup>2</sup> yr.	Energy Collected BTU/ft <sup>2</sup> yr.	S.R Product BTU/ft <sup>2</sup> yr.	Energy Collected BTU/ft <sup>2</sup> yr.	S.R Product BTU/ft <sup>2</sup> yr.
220	13.0	-249	-48	-208	90.4	267	209	238	140,535	18,270	155,261	20,184	332,101	43,173
250	14.9	-249	-39	-190	90.6	295	238	267	126,035	18,779	138,043	20,568	309,732	46,150
270	15.9	-249	-33	-182	90.8	314	257	285	116,975	18,599	127,291	20,239	295,479	46,981
300	17.5	-249	-26	-170	91.2	344	284	314	102,327	17,907	110,391	19,318	271,742	47,554
320	18.4	-248	-21	-161	91.5	362	303	332	93,202	17,149	100,181	18,433	256,494	47,195
350	19.9	-248	-14	-148	92.0	391	331	361	78,987	15,718	84,319	16,779	231,773	46,123
400	21.8	-248	-2	-125	93.5	438	377	408	57,523	12,540	60,633	13,218	191,637	41,777

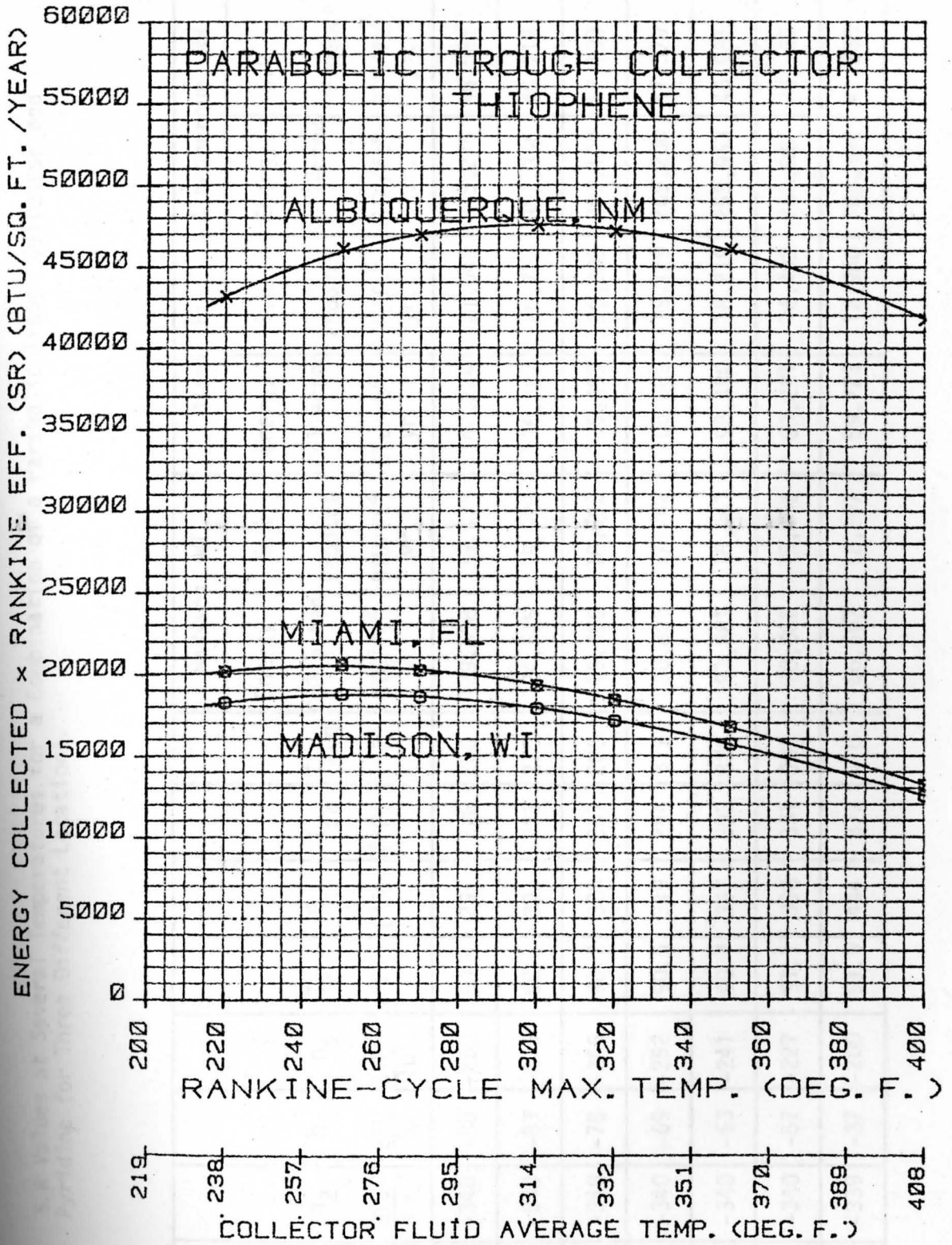


FIGURE 59. Curves of S.R Values vs. Operating Temperature for a Combination of Parabolic Trough Collector and Thiophene for Three Locations.



TABLE 38. S.R Values at Several Temperatures for a Combination of a Parabolic Trough Collector and Pyridine for Three Different Locations.

$T_3$ (°F)	$\eta_R$ (%)	$h_2$ BTU/lb	$h_3$ BTU/lb	$h_s$ BTU/lb	$T_2$ (°F)	$T_{c1}$ (°F)	$T_{c2}$ (°F)	$T_{avg}$ (°F)	Madison, WI		Miami, FL		Albuquerque, NM	
									Energy	S.R	Energy	S.R	Energy	S.R
									Collected BTU/ft <sup>2</sup> yr.	Product BTU/ft <sup>2</sup> yr.	Collected BTU/ft <sup>2</sup> yr.	Product BTU/ft <sup>2</sup> yr.	Collected BTU/ft <sup>2</sup> yr.	Product BTU/ft <sup>2</sup> yr.
240	14.8	-340	-86	-280	90	291	228	260	129,558	19,175	142,224	21,049	315,275	46,661
250	15.2	-340	-83	-275	90	301	238	270	124,525	18,928	136,251	20,710	307,356	46,718
270	16.1	-340	-78	-266	90.2	320	257	288	115,465	18,590	125,499	20,205	293,103	47,190
300	17.6	-340	-69	-252	90.5	349	284	317	100,806	17,742	108,689	19,129	269,200	47,379
320	18.5	-340	-63	-241	90.7	367	303	335	91,681	16,961	98,480	18,219	253,953	46,981
350	19.8	-340	-57	-227	91.1	396	331	363	78,062	15,456	83,291	16,492	230,051	45,550
400	21.7	-339	-37	-200	91.9	444	377	410	56,667	12,297	59,723	12,960	189,999	41,230

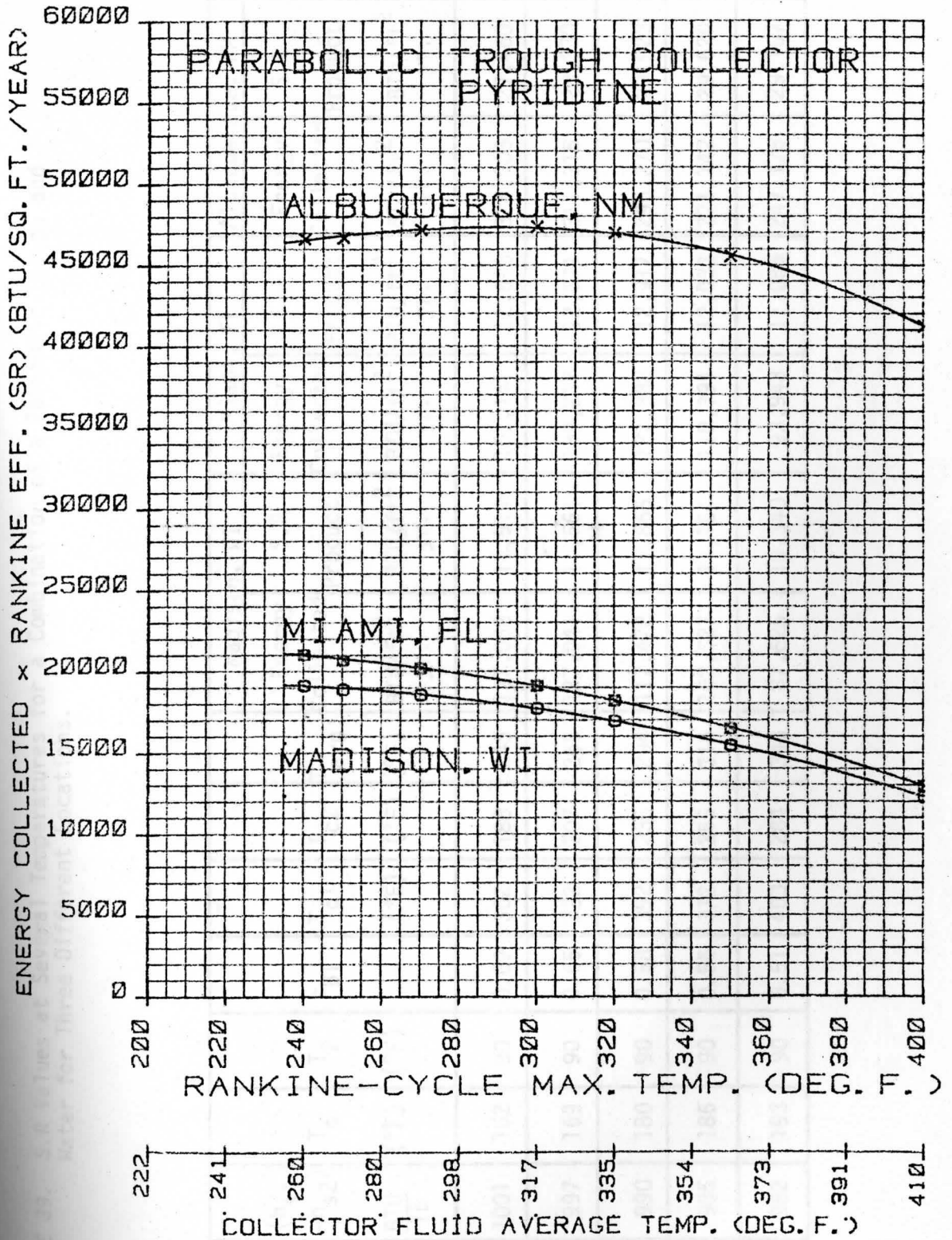


FIGURE 60. Curves of S.R. Values vs. Operating Temperature for a Combination of a Parabolic Trough Collector and Pyridine for Three Locations.

TABLE 39. S.R Values at Several Temperatures for a Combination of a Parabolic Trough and Water for Three Different Locations.

$T_3$ (°F°)	$\eta_R$ (%)	$(h_{s1} - h_{s2})$ BTU/Tb	$T_s$ (°F)	$T_2$ (°F)	$\epsilon_{B1}$	$T_{c1}$ (°F)	$T_{c2}$ (°F)	$T_{avg}$ (°F)	Madison, WI		Miami, FL		Albuquerque, NM	
									Energy Collected BTU/ft <sup>2</sup> . yr.	S.R Product BTU/ft <sup>2</sup> . yr.	Energy Collected BTU/ft <sup>2</sup> . yr.	S.R Product BTU/ft <sup>2</sup> . yr.	Energy Collected BTU/ft <sup>2</sup> . yr.	S.R Product BTU/ft <sup>2</sup> . yr.
300	8.4	1001	162	90	0.69	302	188	245	137,068	11,514	151,141	12,696	326,905	27,460
320	9.1	997	169	90	0.65	322	207	265	127,041	11,561	139,237	12,671	311,315	28,330
350	10.1	990	180	90	0.58	352	235	294	117,478	11,865	127,888	12,917	296,270	29,923
370	10.9	985	186	90	0.55	372	255	314	102,327	11,154	110,391	12,033	271,742	29,620
400	11.8	982	193	90	0.51	403	284	343	87,625	10,340	93,943	11,085	247,176	29,167

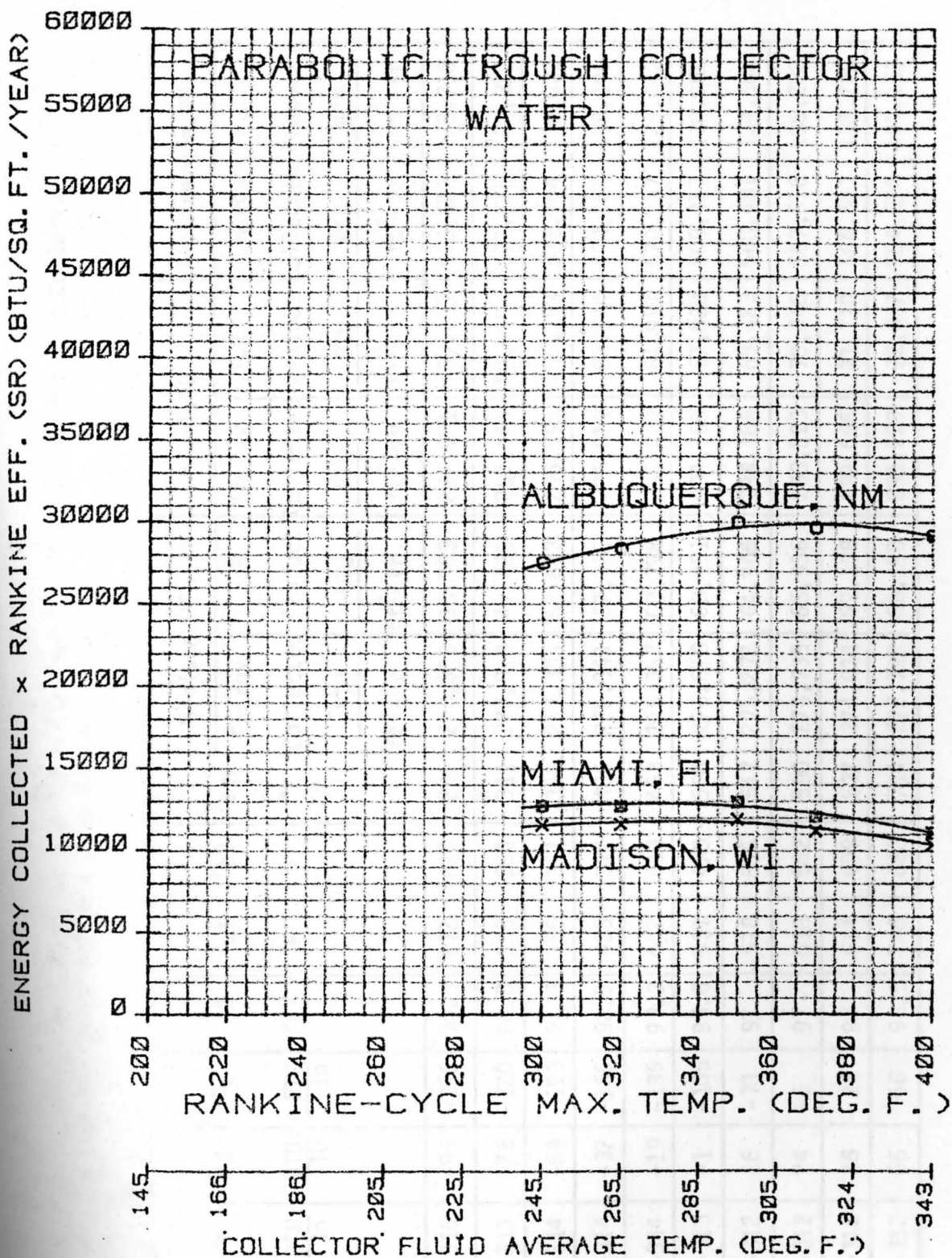


FIGURE 61. Curves of S.R. Values vs. Operating Temperature for a Combination of a Parabolic Trough Collector and Water for Three Locations.

TABLE 10. S.R Values at Several Temperatures for a Combination of a Paraboloid Disc Collector and Toluene for Three Different Locations.

T <sub>3</sub> °F	η <sub>R</sub> (%)	h <sub>2</sub> BTU lb	h <sub>3</sub> BTU lb	h <sub>s</sub> BTU lb	T <sub>2</sub> °F	T <sub>c1</sub> °F	T <sub>c2</sub> °F	T <sub>avg</sub> °F	Madison, WI		Miami, FL		Albuquerque, NM	
									Energy	S.R	Energy	S.R	Energy	S.R
									Collected	Product	Collected	Product	Collected	Product
									BTU	BTU	BTU	BTU	BTU	BTU
									ft <sup>2</sup> -yr	ft <sup>2</sup> -yr	ft <sup>2</sup> -yr	ft <sup>2</sup> -yr	ft <sup>2</sup> -yr	ft <sup>2</sup> -yr
230	13.2	-315	-95	-256	90.3	272	220	246	278,508	36,763	297,981	39,333	573,622	75,718
300	17.0	-315	-72	-220	90.8	338	284	311	277,818	47,229	297,166	50,518	572,525	97,329
350	19.0	-314	-54	-193	91.3	386	331	353	277,334	52,693	296,595	56,353	571,754	108,633
400	20.7	-314	-37	-166	92.5	435	377	406	276,840	57,306	296,011	61,274	570,968	118,190
450	22.0	-314	-19	-135	93.3	482	423	453	276,357	60,798	295,439	64,997	570,197	125,443
500	23.0	-313	-1	-105	95.0	531	470	500	275,873	63,451	294,868	67,820	569,427	130,968
550	23.6	-312	16	-70	97	578	516	547	275,278	64,966	294,166	69,423	568,481	134,162
600	24.0	-312	24	-5	97	618	562	590	274,735	65,936	293,523	70,446	567,616	136,228
650	24.5	-312	26	26	97	664	609	637	274,034	67,138	292,696	71,710	566,501	138,793
730	25.0	-312	66	66	98.5	746	683	714	272,792	68,198	291,229	72,807	564,524	141,131

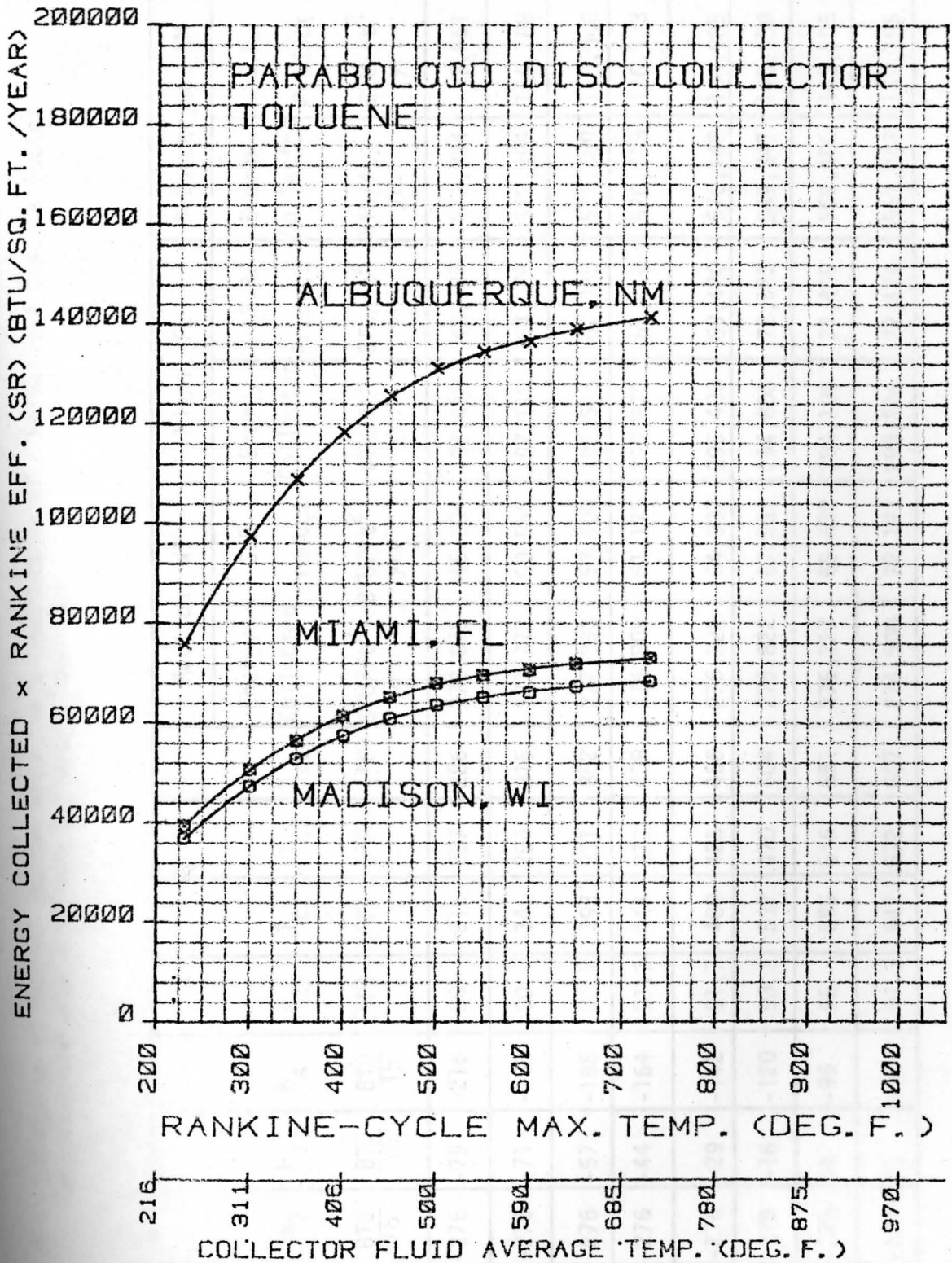


FIGURE 62. Curves of S.R Values vs. Operating Temperature for a Combination of a Paraboloid Disc Collector and Toluene for Three Locations.

TABLE 41. S.R Values at Several Temperatures for a Combination of a Paraboloid Disc Collector and Chlorobenzene for Three Different Locations.

T <sub>3</sub> (°F)	η <sub>R</sub> (%)	h <sub>2</sub> BTU/lb	h <sub>3</sub> BTU/lb	h <sub>s</sub> BTU/lb	T <sub>2</sub> (°F)	T <sub>c1</sub> (°F)	T <sub>c2</sub> (°F)	T <sub>avg</sub> (°F)	Madison, WI		Miami, FL		Albuquerque, NM	
									Energy Collected BTU/ft <sup>2</sup> yr.	S.R Product BTU/ft <sup>2</sup> yr.	Energy Collected BTU/ft <sup>2</sup> yr.	S.R. Product BTU/ft <sup>2</sup> yr.	Energy Collected BTU/ft <sup>2</sup> yr.	S.R Product BTU/ft <sup>2</sup> yr.
270	16.4	-276	-79	-216	90	316	257	286	278,075	45,604	297,470	48,785	572,934	93,961
300	18.2	-276	-71	-205	90	345	284	315	277,777	50,555	297,118	54,075	572,459	104,188
350	20.7	-276	-57	-185	90.7	393	331	362	277,293	57,400	296,546	61,385	571,689	118,340
400	22.1	-276	-44	-164	91.3	441	377	409	276,809	61,175	295,975	65,410	570,918	126,173
450	23.5	-276	-29	-142	91.7	489	423	456	276,325	64,937	295,403	69,420	570,148	133,985
500	24.6	-275	-16	-120	93.3	537	470	504	275,822	67,852	294,808	72,523	549,347	140,059
550	25.3	-275	-2	-95	95	585	516	551	275,227	69,632	294,106	74,409	568,400	143,805
610	26.3	-274	13	-64	97.3	642	572	607	274,500	72,193	293,246	77,124	567,242	149,185

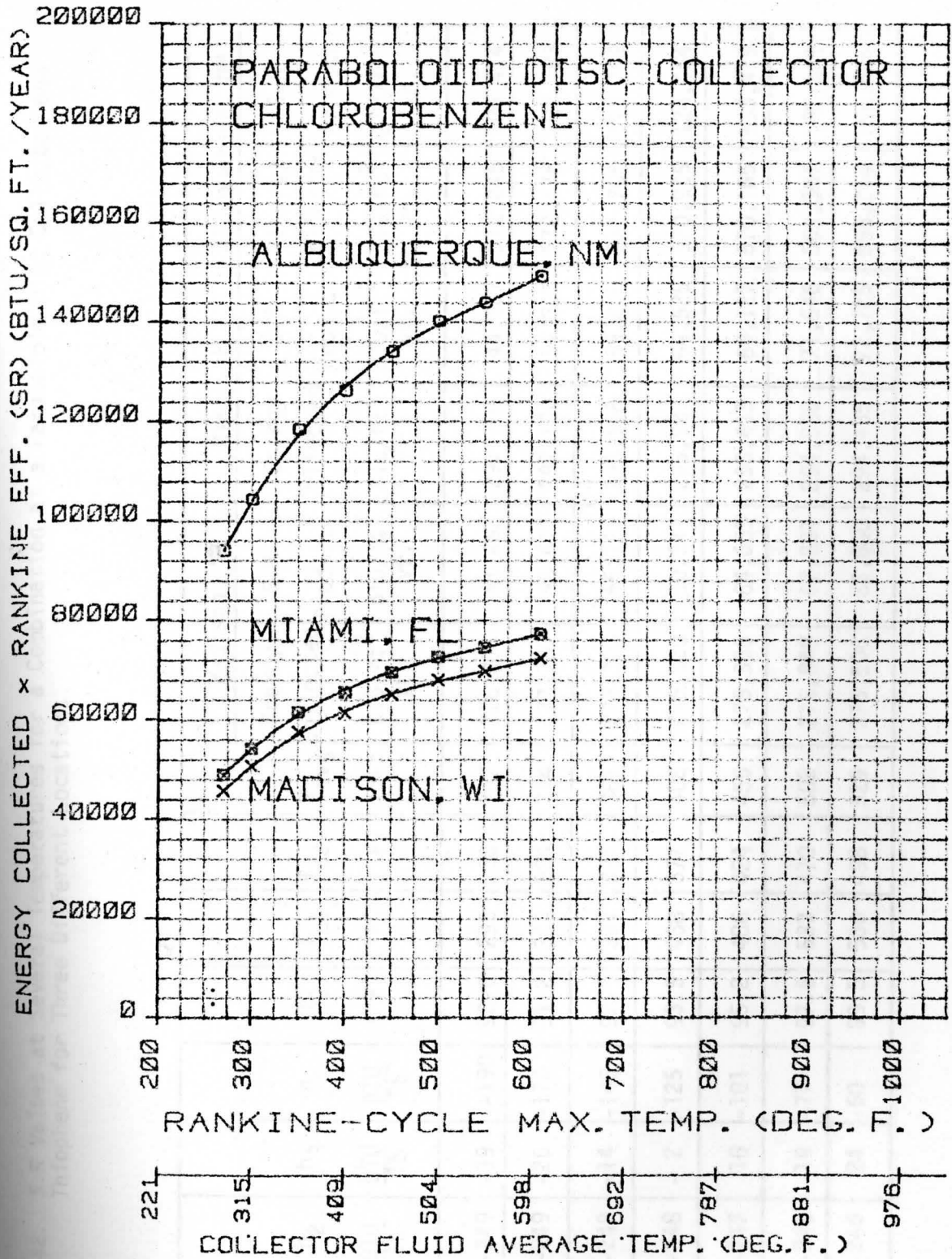


FIGURE 63. Curves of S.R. Values vs. Operating Temperature for a Combination of a Paraboloid Disc Collector and Chlorobenzene for Three Locations.



TABLE 42. S.R Values at Several Temperatures for a Combination at a Paraboloid Disc Collector and Thiophene for Three Different Locations.

T <sub>3</sub> (°F)	η <sub>R</sub> (%)	h <sub>2</sub> BTU T <sub>b</sub>	h <sub>3</sub> BTU T <sub>b</sub>	h <sub>s</sub> BTU T <sub>b</sub>	T <sub>2</sub> (°F)	T <sub>c1</sub> (°F)	T <sub>c2</sub> (°F)	T <sub>avg</sub> (°F)	Madison, WI		Miami, FL		Albuquerque, NM	
									Energy Collected BTU/ft <sup>2</sup> yr.	S.R Product BTU/ft <sup>2</sup> yr.	Energy Collected BTU/ft <sup>2</sup> yr.	S.R Product BTU/ft <sup>2</sup> yr.	Energy Collected BTU/ft <sup>2</sup> yr.	S.R Product BTU/ft <sup>2</sup> yr.
250	14.9	-249	-39	-190	90.6	295	238	267	278,271	41,462	297,701	44,357	573,246	85,414
300	17.5	-249	-26	-170	91.2	344	284	314	277,787	48,613	297,130	51,998	572,476	100,183
350	19.9	-248	-14	-148	92	391	331	361	277,303	55,783	296,558	59,015	571,705	113,769
400	21.8	-248	- 2	-125	93.5	438	377	408	276,820	60,347	295,987	64,525	570,935	124,464
450	23.4	-247	10	-101	95.2	486	424	455	276,336	64,663	295,415	69,127	570,165	133,419
500	24.3	-246	19	-77	97.5	533	470	502	275,848	67,031	294,838	71,646	569,387	138,361
530	24.7	-246	24	-60	99.5	560	498	529	275,506	68,050	294,435	72,725	568,844	140,504

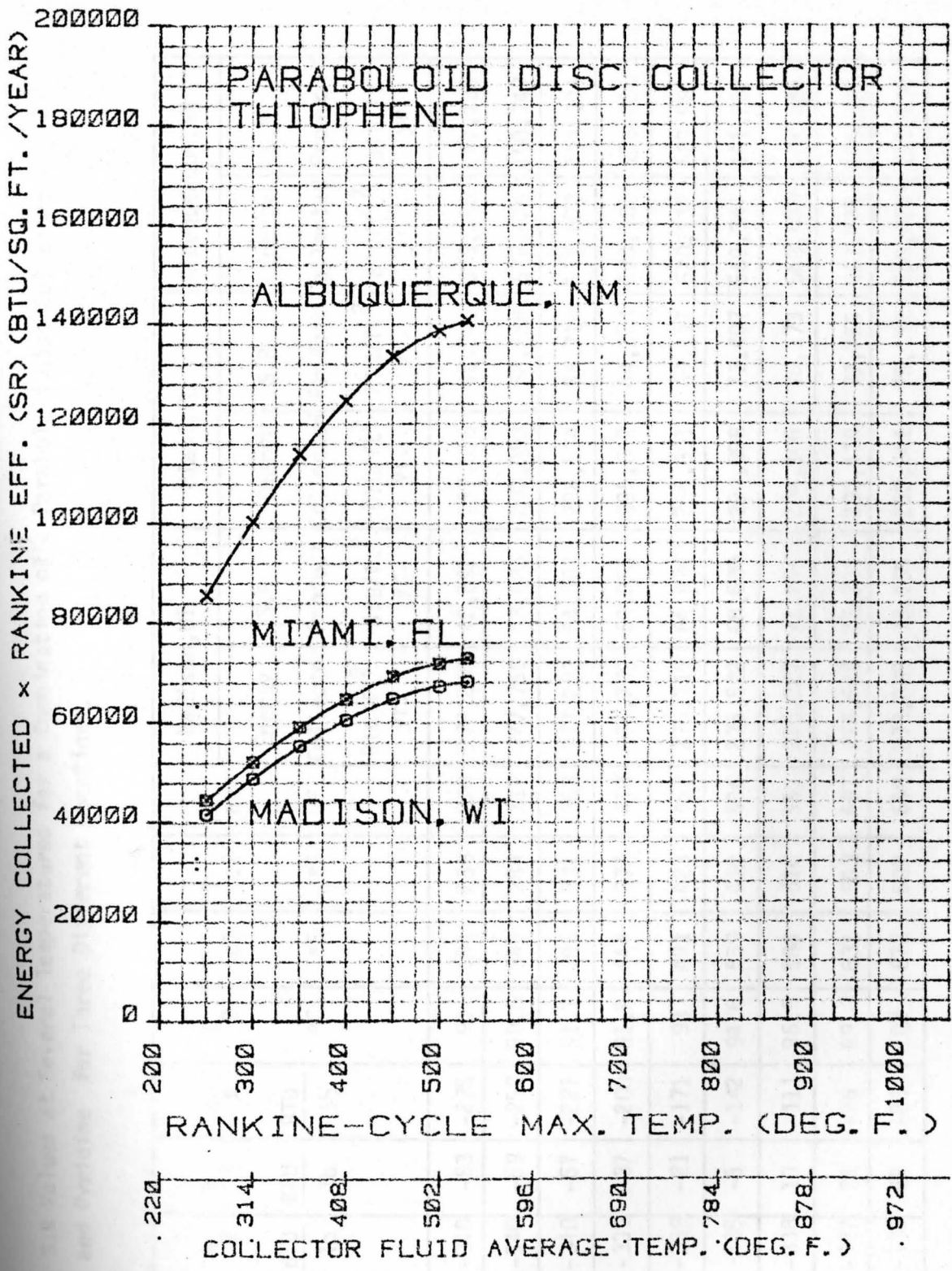


FIGURE 64. Curves of S.R Values vs. Operating Temperature for a Combination of a Paraboloid Disc Collector and Thiophene for Three Locations.

TABLE 43. S.R Values at Several Temperatures for a Combination of a Paraboloid Disc Collector and Pvridine for Three Different Locations.

T <sub>3</sub> °F	η <sub>R</sub> (%)	h <sub>2</sub> BTU/lb	h <sub>3</sub> BTU/lb	h <sub>s</sub> BTU/lb	T <sub>2</sub> °F	T <sub>c1</sub> °F	T <sub>c2</sub> °F	T <sub>avg</sub> °F	Madison, WI		Miami, FL		Albuquerque, NM	
									Energy Collected BTU/ft <sup>2</sup> yr.	S.R Product BTU/ft <sup>2</sup> yr.	Energy Collected BTU/ft <sup>2</sup> yr.	S.R Product BTU/ft <sup>2</sup> yr.	Energy Collected BTU/ft <sup>2</sup> yr.	S.R Product BTU/ft <sup>2</sup> yr.
250	15.2	-340	-83	-275	90	301	238	270	278,240	42,292	297,665	45,245	573,196	87,126
300	17.6	-340	-69	-252	90.5	349	284	317	277,756	48,835	297,093	52,288	572,426	100,747
350	19.8	-340	-57	-227	91.1	396	331	363	277,282	54,902	296,534	58,714	571,672	113,191
400	21.7	-339	-37	-200	91.9	444	377	410	276,799	60,065	295,962	64,224	570,902	123,896
450	23.5	-339	-21	-171	93	491	423	457	276,315	64,934	295,391	69,417	570,132	133,981
500	24.9	-338	-5	-142	94.6	539	470	504	275,822	68,680	294,808	73,407	569,347	141,767
550	25.9	-338	10	-111	96.5	586	516	551	275,227	71,284	294,106	76,173	568,400	147,216
600	26.5	-337	21	-76	99.3	631	563	597	274,646	72,781	293,419	77,756	567,475	150,381
650	26.7	-336	66	-20	102	672	609	640	273,983	73,155	292,641	78,135	566,427	151,236

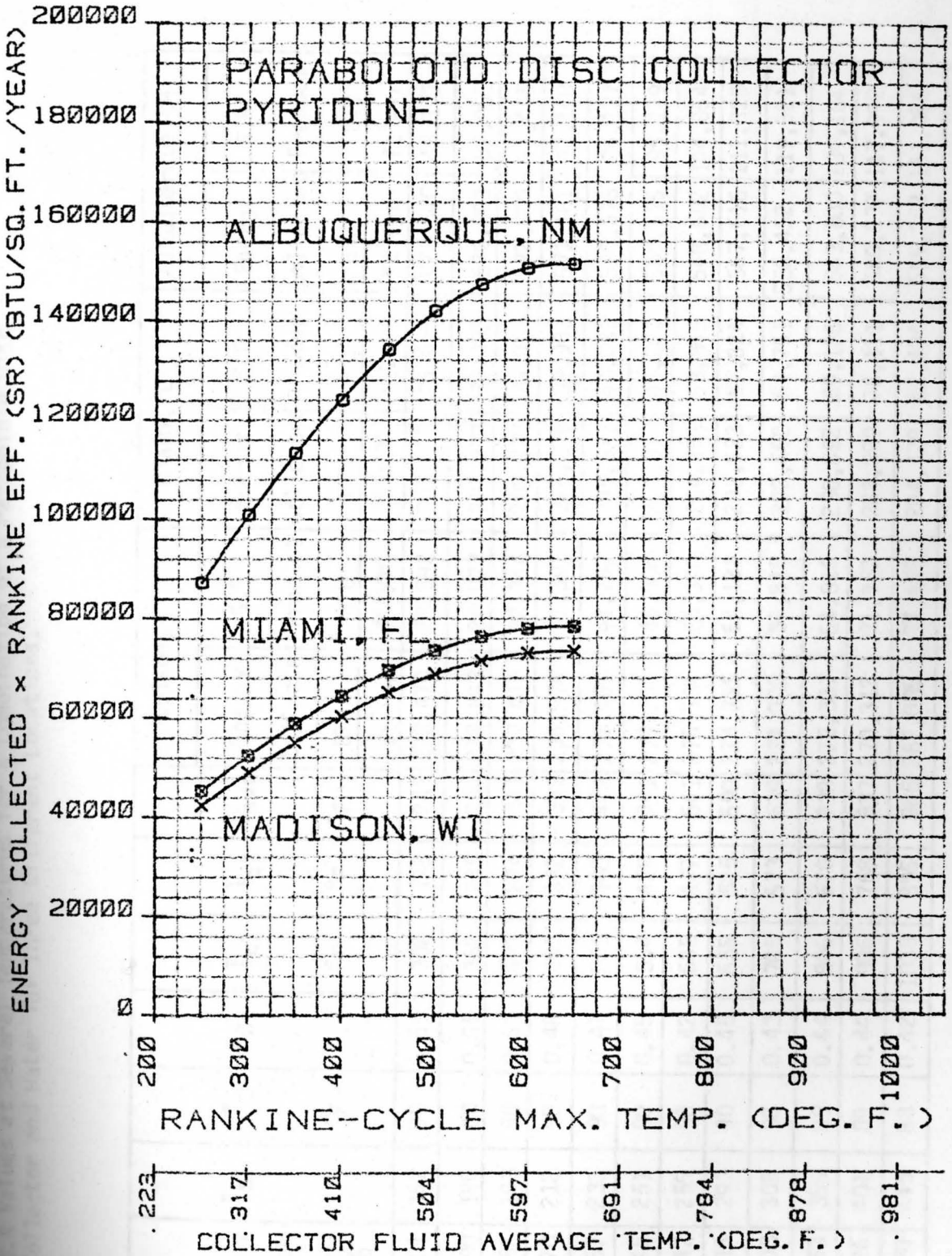


FIGURE 65. Curves of S.R. Values vs. Operating Temperature for a Combination of a Paraboloid Disc Collector and Pyridine for Three Locations.

TABLE 44. S.R Values at Several Temperatures for a Combination of a Paraboloid Disc Collector and Water for Three Different Locations.

T <sub>3</sub> °F	η <sub>R</sub> (%)	(h <sub>sv</sub> -h <sub>sw</sub> ) BTU lb	T <sub>s</sub> °F	T <sub>2</sub> °F	ε <sub>B1</sub>	T <sub>c1</sub> °F	T <sub>c2</sub> °F	T <sub>avg</sub> °F	Madison, WI		Miami, FL		Albuquerque, NM	
									Energy Collected	S.R Product	Energy Collected	S.R Product	Energy Collected	S.R Product
									BTU ft <sup>2</sup> -yr	BTU ft <sup>2</sup> -yr	BTU ft <sup>2</sup> -yr	BTU ft <sup>2</sup> -yr	BTU ft <sup>2</sup> -yr	BTU ft <sup>2</sup> -yr
300	8.4	1001	162	90	0.69	302	188	245	278,470	23,392	297,920	25,025	573,540	48,177
350	10.1	990	180	90	0.58	352	235	294	277,993	28,077	297,373	30,035	572,803	57,853
400	11.8	982	193	90	0.51	403	284	343	277,489	32,744	296,777	35,020	572,000	67,496
450	13.5	970	212	90	0.48	453	332	393	276,974	37,391	296,196	39,983	571,181	77,109
500	15.1	957	233	90	0.47	503	380	442	276,469	41,747	295,573	44,632	570,378	86,127
550	16.7	945	251	90	0.45	554	428	491	275,996	46,086	294,977	49,261	569,575	95,119
600	18.3	942	255	90	0.42	605	477	541	275,534	50,390	294,255	53,849	568,602	104,054
650	19.7	915	293	90	0.45	655	525	590	274,735	54,123	293,523	57,824	567,616	111,820
700	21.1	903	309	90	0.43	705	573	639	274,003	57,815	292,660	61,751	566,452	119,521
800	23.8	863	359	89	0.44	806	670	738	272,337	64,816	290,692	69,185	563,800	134,184
900	26.4	826	401	89	0.44	906	768	837	270,312	71,362	288,299	76,111	560,577	147,992
1030	29.0	780	445	88	0.42	1038	895	966	267,035	77,440	284,429	82,484	555,362	161,055

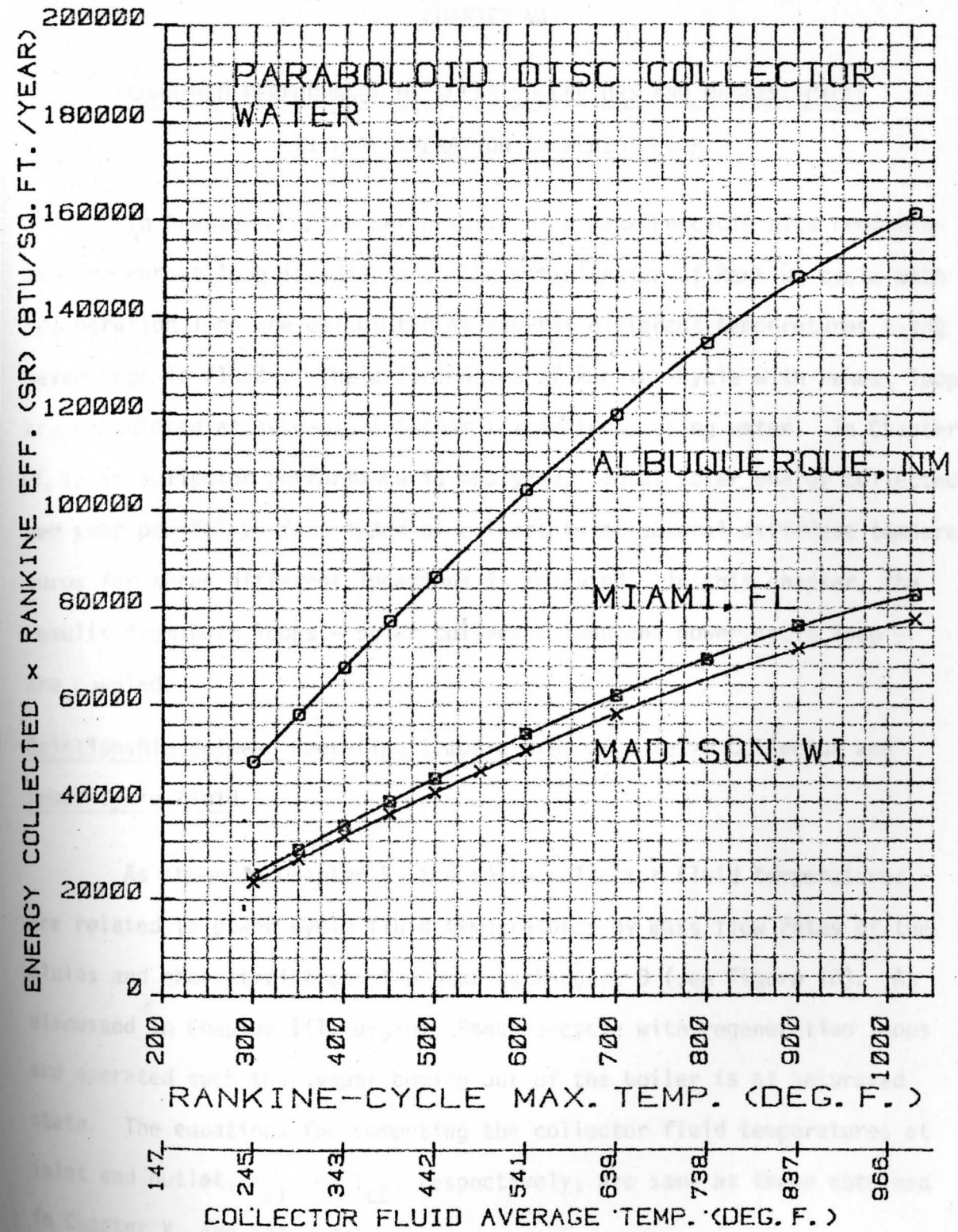


FIGURE 66. Curves of S.R Values vs. Operating Temperature for a Combination of a Paraboloid Disc Collector and Water for Three Locations.

## CHAPTER VI

COMBINED PERFORMANCE OF SOLAR COLLECTORS AND RANKINE-CYCLE  
WITH REGENERATION OR REHEAT LOOP

In Chapter III, the performance of a Rankine-cycle with regeneration or reheat loop is analyzed. The efficiencies of Rankine-cycle with regeneration loop are calculated at several different temperatures using seven organic fluids. The efficiencies of Rankine-cycle with reheat loop are calculated at several different temperatures using water. In Chapter IV, solar collector performance is analyzed. Total solar energy collected per year per  $\text{ft}^2$  by four types of collectors at several different temperatures for three different locations is computed. In this chapter, the results from both loops – solar collector loop and power cycle loop – are coupled.

Relationship Between Operating Temperatures of a Solar Collector and  
Power Cycle Fluid.

As shown in Chapter V, the solar collector fluid temperatures are related to power cycle fluid temperatures by mass flow rates of the fluids and characteristics of a heat exchanger, B (see Figure 18). As discussed in Chapter III, organic Rankine-cycle with regeneration loops are operated such that vapor coming out of the boiler is at saturated state. The equations for computing the collector fluid temperatures at inlet and outlet,  $T_{c1}$  and  $T_{c2}$ , respectively, are same as those obtained in Chapter V, and they are:

$$T_{c1} = T_{2a} + (T_3 - T_{2a}) \left\{ 1.025 + 0.1 \times \frac{(h_3 - h_s)}{(h_3 - h_{2a})} \right\} \quad (74)$$

$$T_{c2} = T_{2a} + 0.925 (T_3 - T_{2a}) \quad (75)$$

where,  $T_{2a}$  = temperature of the power-cycle fluid coming out of the regenerator.

$h_{2a}$  = enthalpy of the fluid at state point 2a. (See Figure 18).

$T_{2a}$  is related to the temperature of the fluid coming out of the power-cycle pump,  $T_2$  by,

$$T_{2a} = \frac{h_{2a} - h_2}{C_{PR}} (1 - \eta_p) + T_2 \quad (76)$$

where,

$h_2$  = enthalpy of the fluid at state point 2. (See Figure 18)

$C_{PR}$  = specific heat of the power-cycle fluid.

The case of a water/steam reheat cycle requires an additional heat exchanger for reheating the steam (Figure 67) compared to the water/steam Rankine-cycle.

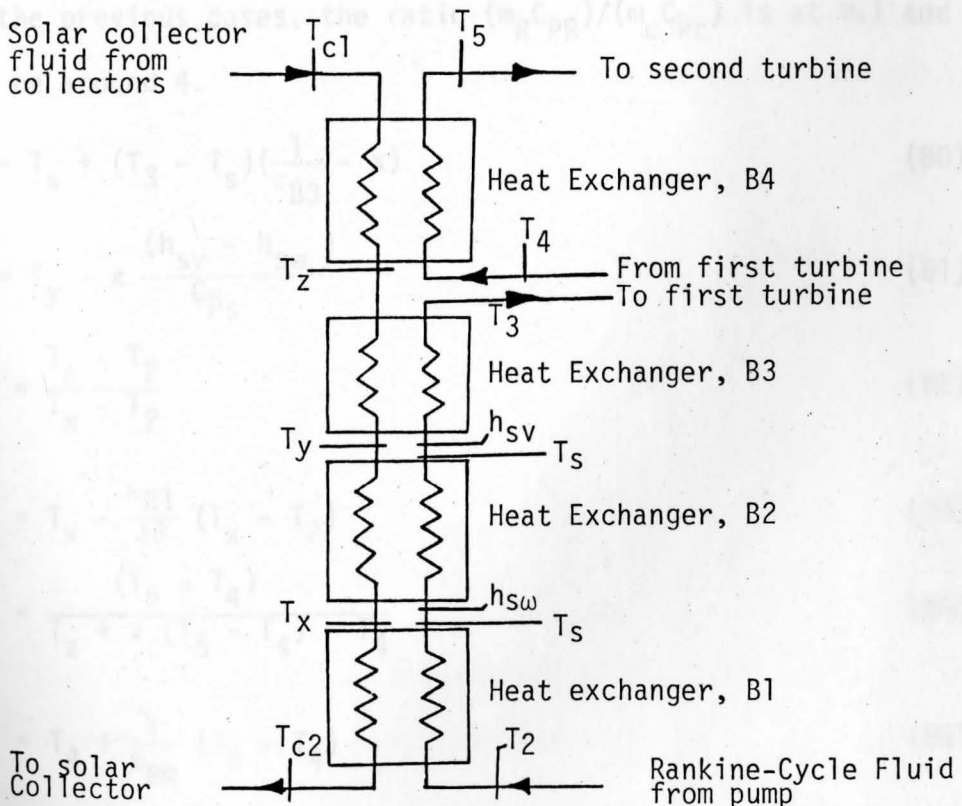


FIGURE 67. Boiler-Heat Exchanger in a Water/Steam Reheat Cycle with Different Heat Transfer Processes Separated.



Following the procedure as discussed in Chapter V, the expressions

for  $T_{c1}$  and  $T_{c2}$  are obtained, as shown below;

$$T_z = \frac{1}{\epsilon_{B3}} (T_3 - T_s) + T_s \quad (77)$$

$$\epsilon_{B3} \leq \frac{1 - e^{-(1-x)NTU_{\max}}}{1 - x \cdot e^{-(1-x)NTU_{\max}}} \quad \text{constrained by the requirement that} \quad (78)$$

$$\epsilon_{B1} \leq \epsilon_{B3}$$

where,

$$x = \frac{\dot{m}_R C_{Ps}}{\dot{m}_C C_{Pc}} \quad (79)$$

$$= \frac{\dot{m}_R C_{PR}}{\dot{m}_C C_{Pc}} \cdot \frac{C_{Ps}}{C_{PR}}$$

where  $C_{Ps}$  = heat capacity of steam

$C_{PR}$  = heat capacity of water

Similar to the previous cases, the ratio  $(\dot{m}_R C_{PR})/(\dot{m}_C C_{Pc})$  is at 0.1 and  $(NTU)_{\max}$  to be around 4.

$$T_y = T_s + (T_3 - T_s) \left( \frac{1}{\epsilon_{B3}} - x \right) \quad (80)$$

$$T_x = T_y - x \frac{(h_{sv} - h_{sw})}{C_{Ps}} \quad (81)$$

$$\epsilon_{B1} = \frac{T_s - T_2}{T_x - T_2} \quad (82)$$

$$T_{c2} = T_x - \frac{\epsilon_{B1}}{10} (T_x - T_2) \quad (83)$$

$$\epsilon_{B4} = \frac{(T_5 - T_4)}{T_z + x(T_5 - T_4) - T_4} \quad (84)$$

$$T_{c1} = T_4 + \frac{1}{\epsilon_{B4}} (T_5 - T_4) \quad (85)$$

Thus, for a given power-cycle maximum temperature, the collector fluid temperatures entering and leaving the collector —  $T_{c2}$  and  $T_{c1}$ , respectively — are computed at several different temperatures using Equations (74) and (75) in case of organic fluids and Equations (77) through (85) in case of water/steam reheat cycle. The results are tabulated in Tables 21 to 44.

As in Chapter V, an average temperature  $T_{avg}$  of  $T_{c1}$  and  $T_{c2}$  is obtained. Solar energy collected at an average fluid temperature is obtained from results obtained in Chapter IV. A product of efficiency of a Rankine-cycle with regeneration or reheat loop at a constant heat source temperature and solar energy collected per year per  $ft^2$  at the corresponding collector fluid average temperature is obtained. This product will be referred to as  $S.R_e$  value.

The  $S.R_e$  value is directly proportional to the net electrical production per year per unit area of a solar collector at a certain operating temperature ( $T_{avg} \equiv T_3$ ).

$$\left( \frac{\text{Solar energy collected by the collector}}{\text{yr. ft}^2} \times \text{Power Cycle Efficiency} \right)_{T_{avg}} \times \left( \frac{\text{Net electrical energy production}}{\text{yr. ft}^2} \right)_{T_{avg}} \quad (86)$$

$$(S.R_e)_{T_{avg}} = k_2 \cdot \left( \frac{\text{Net electrical energy production}}{\text{yr. ft}^2} \right)_{T_{avg}} \quad (87)$$

where  $k_2$  is a constant of proportionality.  $k_2$  takes into account the generator efficiency and certain parasite losses in the system, such as, friction losses, heat losses, etc. The value of  $k_2$  is less than 1. It has approximately the same value in all cases which makes the evaluation

of the optimum operating temperature possible by comparing the  $S.R_e$  values obtained at several different operating temperatures.

The results of  $S.R_e$  values at different operating temperatures for each possible combination of solar collector and power cycle working fluid are shown graphically indicating the variation of  $S.R_e$  value vs. collector fluid average temperature or power-cycle maximum temperature. A peak corresponds to the maximum net solar-to-electrical conversion. Figures 68 to 91 show the graphs of  $S.R_e$  value vs. collector fluid average temperature and power cycle maximum temperature for all possible combinations.

Comparing the maximum  $S.R_e$  values obtained in the combinations of each type of solar collector and all power cycle working fluids gives the fluid best suited for that collector. Thus, an optimum power-cycle working fluid for each type of solar collector is obtained.

TABLE 45. S.Re Values at Several Temperatures for a Combination of a Flat Plate Collector and R-11 for Three Different Locations.

T <sub>3</sub> (°F)	η <sub>Re</sub> (%)	h <sub>2</sub> BTU/lb	h <sub>3</sub> BTU/lb	h <sub>s</sub> BTU/lb	T <sub>2a</sub> (°F)	T <sub>c1</sub> (°F)	T <sub>c2</sub> (°F)	T <sub>avg</sub> (°F)	Madison, WI		Miami, FL		Albuquerque, NM	
									Energy Collected BTU/ft <sup>2</sup> yr.	S.R Product BTU/ft <sup>2</sup> yr.	Energy Collected BTU/ft <sup>2</sup> yr.	S.R Product BTU/ft <sup>2</sup> yr.	Energy Collected BTU/ft <sup>2</sup> yr.	S.R Product BTU/ft <sup>2</sup> yr.
150	6.8	26.7	110	39.3	90.4	185	145	165	123,844	8,421	184,744	12,562	263,940	17,948
180	9.4	26.8	113	45.8	90.9	214	173	194	88,360	8,306	133,885	12,585	209,930	19,733
200	11.0	26.9	115	50.2	91.4	233	192	212	68,511	7,536	104,466	11,491	178,344	19,618
220	12.4	29.4	117	54.7	103.	252	211	231	50,398	6,249	77,215	9,575	146,314	18,143
250	14.3	30.0	120	61.7	106.	280	239	260	26,695	3,817	40,744	5,826	101,071	14,453
280	15.8	30.7	122	69.0	110.	308	267	288	9,103	1,438	15,287	2,415	60,211	9,513

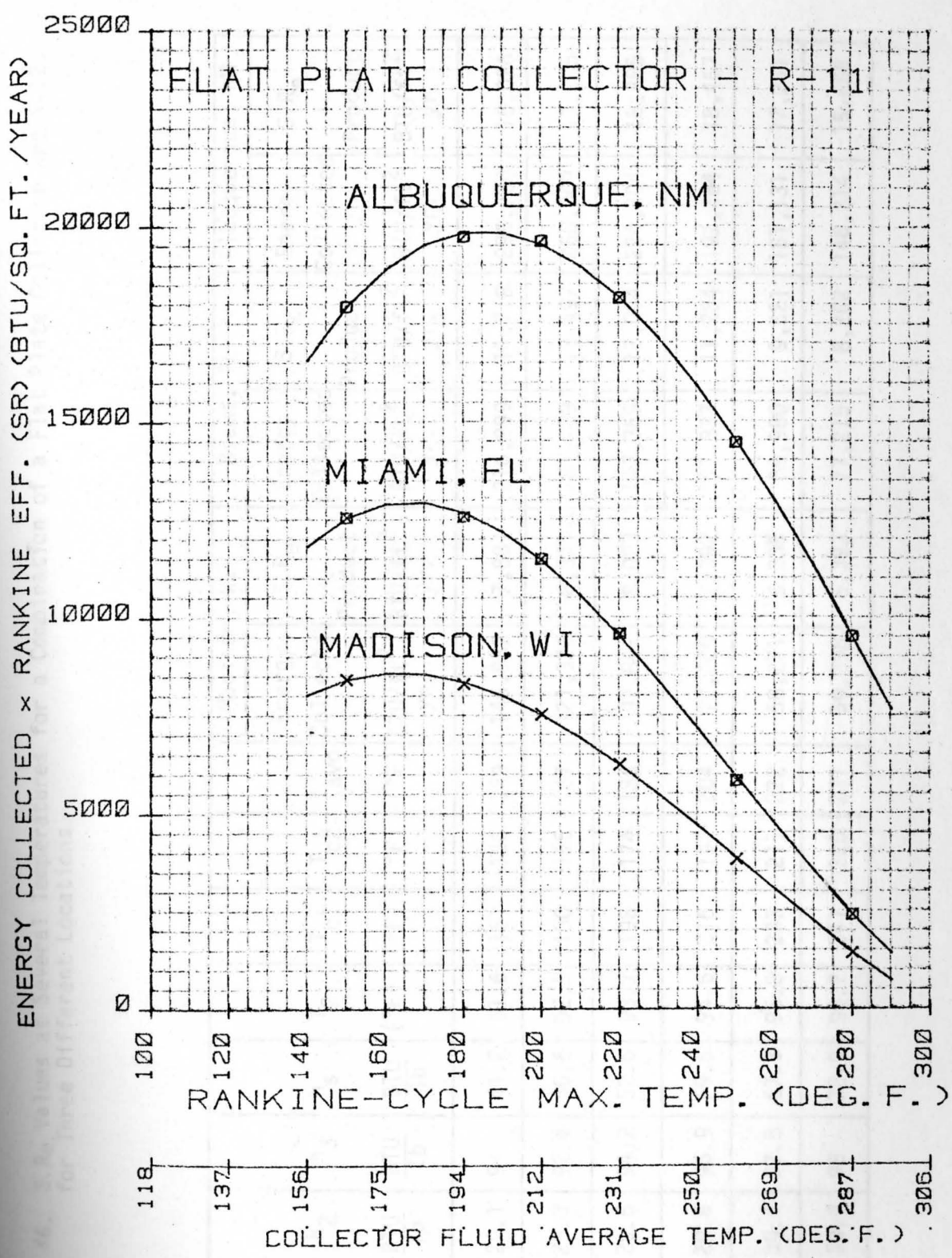


FIGURE 68. Curves of  $S.R_e$  Values vs. Operating Temperature for a Combination of a Flat Plate Collector and R-11 for Three Locations.

TABLE 46. S.Re Values at Several Temperatures for a Combination of a Flat Plate Collector and R-12 for Three Different Locations.

T <sub>3</sub> (°F)	η <sub>Re</sub> (%)	h <sub>2</sub> BTU/Tb	h <sub>3</sub> BTU/Tb	h <sub>s</sub> BTU/Tb	T <sub>2</sub> (°F)	T <sub>c1</sub> (°F)	T <sub>c2</sub> (°F)	T <sub>avg</sub> (°F)	Madison, WI		Miami, FL		Albuquerque, NM	
									Energy Collected BTU/ft <sup>2</sup> yr.	S.Re Product BTU/ft <sup>2</sup> yr.	Energy Collected BTU/ft <sup>2</sup> yr.	S.Re Product BTU/ft <sup>2</sup> yr.	Energy Collected BTU/ft <sup>2</sup> yr.	S.Re Product BTU/ft <sup>2</sup> yr.
140	5.4	29.1	91	41.2	91.6	161	136	149	145,939	7,881	216,999	11,718	296,780	16,026
160	6.9	29.3	92.6	46.6	92.5	180	155	167	121,326	8,371	181,109	12,497	260,069	17,945
180	8.2	29.6	94.2	52.6	93.7	198	174	186	97,842	8,023	147,369	12,084	224,204	18,385
200	9.6	29.8	95.9	59.6	94.6	216	192	204	77,000	7,392	117,337	11,264	192,264	18,457
220	10.7	30.1	97.5	67.3	95.8	233	211	222	58,271	6,235	88,980	9,521	161,131	17,241
230	10.8	30.3	98	72.9	96.7	241	220	231	50,398	5,393	77,215	8,262	146,314	15,656

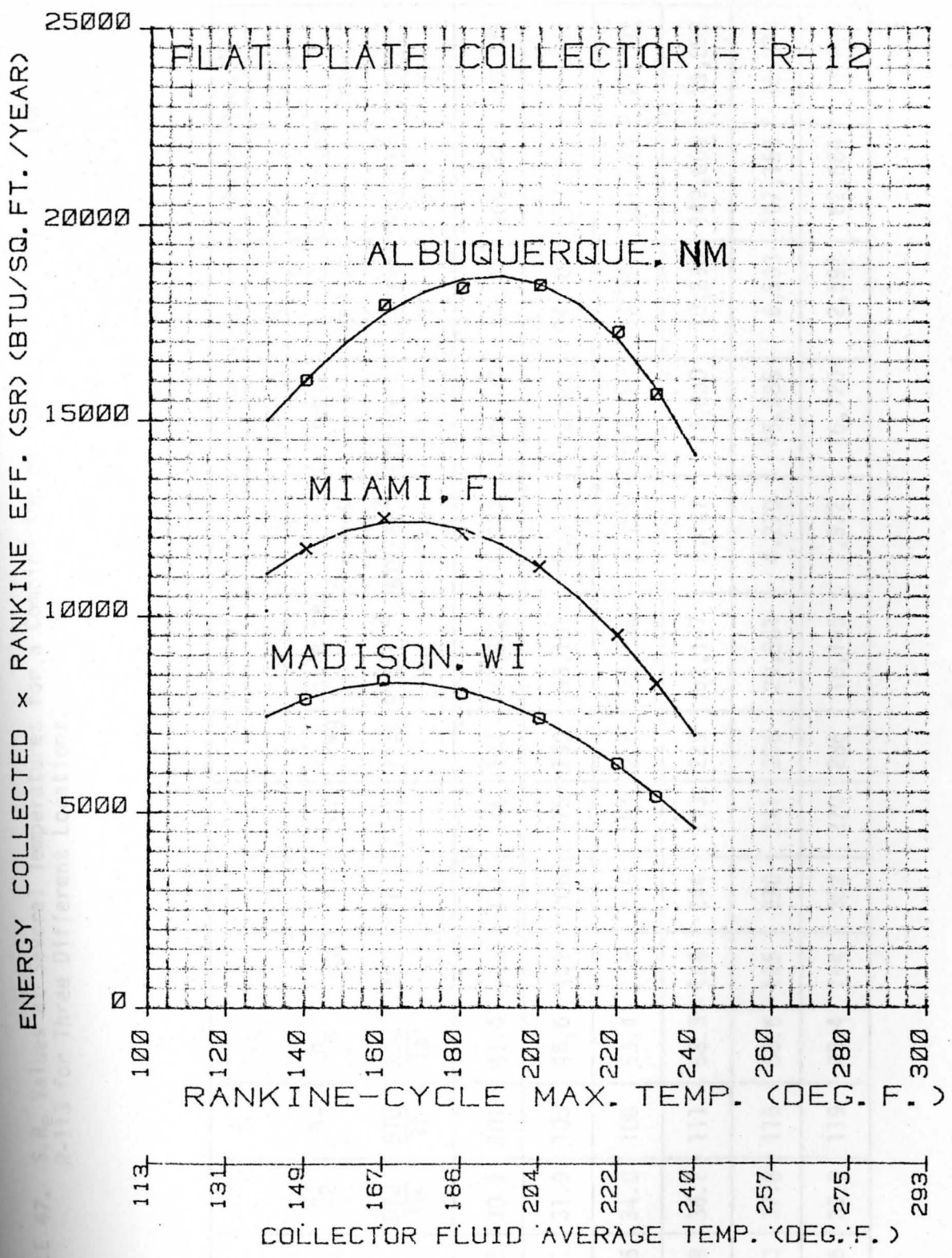


FIGURE 69. Curves of  $S.R_e$  Values vs. Operating Temperature for a Combination of a Flat Plate Collector and R-12 for Three Locations.

TABLE 47.  $S.R_e$  Values at Several Temperatures for a Combination of a Flat Plate Collector and R-113 for Three Different Locations.

$T_3$ (°F)	$\eta_{Re}$ (%)	$h_2$ BTU Tb	$h_3$ BTU Tb	$h_s$ BTU Tb	$T_{2a}$ (°F)	$T_{c1}$ (°F)	$T_{c2}$ (°F)	$T_{avg}$ (°F)	Madison, WI		Miami, FL		Albuquerque, NM	
									Energy Collected BTU/ft <sup>2</sup> yr.	$S.R_e$ Product BTU/ft <sup>2</sup> yr.	Energy Collected BTU/ft <sup>2</sup> yr.	$S.R_e$ Product BTU/ft <sup>2</sup> yr.	Energy Collected BTU/ft <sup>2</sup> yr.	$S.R_e$ Product BTU/ft <sup>2</sup> yr.
150	7.5	30.2	101	41.4	102	177	146	162	127,622	9,572	190,197	14,265	269,746	20,231
180	10.1	31.9	105	48.6	109	206	175	190	93,101	9,403	140,627	14,203	217,067	21,924
200	11.6	34.0	108	53.4	118	225	194	210	70,634	8,194	107,684	12,491	181,824	21,092
220	12.9	36.2	111	58.3	128	244	213	229	52,147	6,727	79,830	10,298	149,606	19,299
250	14.3	37.8	115	68.6	135	270	241	256	29,861	4,270	45,685	6,533	107,156	15,323
280	15.5	39.9	119	73.4	144	302	270	286	10,145	1,572	16,720	2,592	62,664	9,713



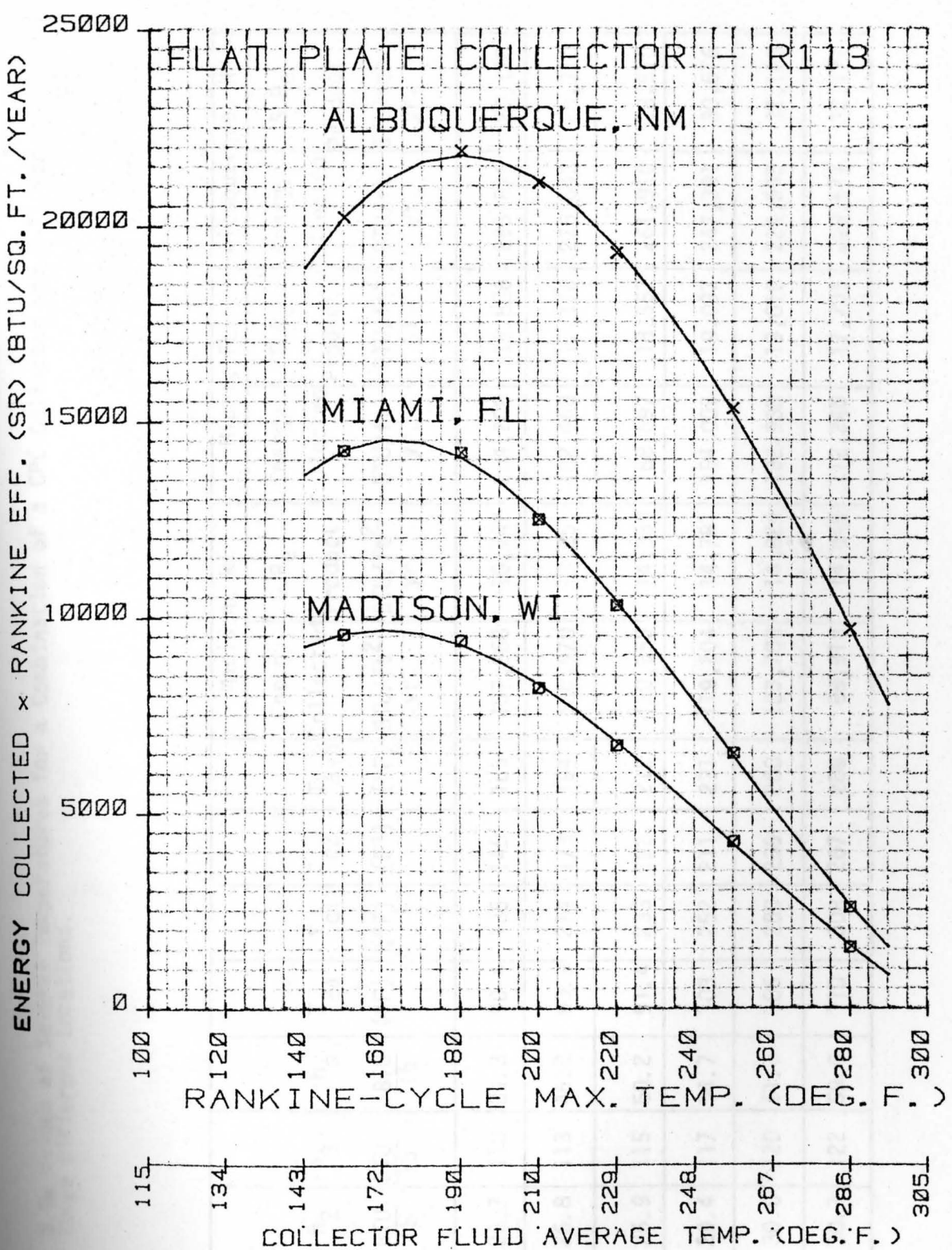


FIGURE 70. Curves of  $S.R_e$  Values vs. Operating Temperature for a Combination of a Flat Plate Collector and R-113 for Three Locations.

TABLE 48. S.Re Values at Several Temperatures for a Combination of a CPC Collector and R-11 for Three Different Locations.

T <sub>3</sub> (°F)	η <sub>Re</sub> (%)	h <sub>2</sub> $\frac{\text{BTU}}{\text{lb}}$	h <sub>3</sub> $\frac{\text{BTU}}{\text{lb}}$	h <sub>s</sub> $\frac{\text{BTU}}{\text{lb}}$	T <sub>2a</sub> (°F)	T <sub>c1</sub> (°F)	T <sub>c2</sub> (°F)	T <sub>avg</sub> (°F)	Madison, WI		Miami, FL		Albuquerque, NM	
									Energy Collected BTU/ft <sup>2</sup> yr.	S.Re Product BTU/ft <sup>2</sup> yr.	Energy Collected BTU/ft <sup>2</sup> yr.	S.Re Product BTU/ft <sup>2</sup> yr.	Energy Collected BTU/ft <sup>2</sup> yr.	S.Re Product BTU/ft <sup>2</sup> yr.
150	6.8	26.7	110	39.3	90.4	185	145	165	157,968	10,742	204,208	13,886	295,878	20,120
180	9.4	26.8	113	45.8	90.9	214	173	194	140,970	13,251	182,663	17,170	275,643	25,910
200	11.0	26.9	115	50.2	91.4	233	192	212	130,355	14,339	168,697	18,557	261,910	28,810
220	12.4	29.4	117	54.7	103	252	211	231	119,204	14,781	154,005	19,097	247,391	30,676
250	14.3	30.0	120	61.7	106	280	239	260	103,700	14,829	132,938	19,010	224,635	32,123
280	15.8	30.7	122	69.0	110	308	267	288	88,913	14,048	112,248	17,735	203,617	32,171

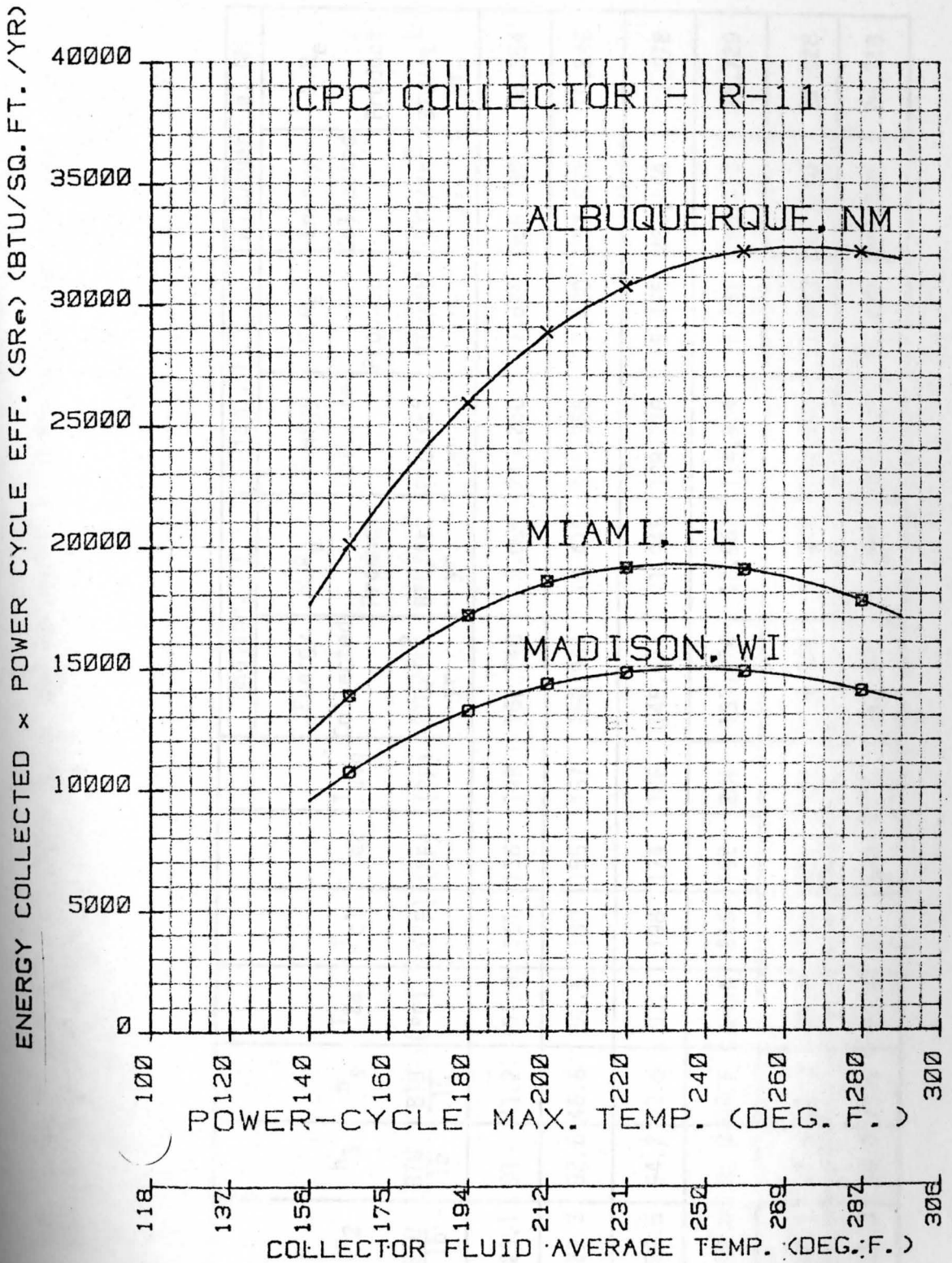


FIGURE 71. Curves of  $S.R_e$  Values vs. Operating Temperature for a Combination of a CPC Collector and R-11 for Three Locations.

TABLE 49.  $S.R_e$  Values at Several Temperatures for a Combination of a CPC Collector and R-12 for Three Different Locations.

$T_3$ (°F)	$\eta_{Re}$ (%)	$h_2$ $\frac{BTU}{lb}$	$h_3$ $\frac{BTU}{lb}$	$h_s$ $\frac{BTU}{lb}$	$T_{2a}$ (°F)	$T_{c1}$ (°F)	$T_{c2}$ (°F)	$T_{avg}$ (°F)	Madison, Wi		Miami, FL		Albuquerque, NM	
									Energy Collected BTU/ft <sup>2</sup> yr.	$S.R_e$ Product BTU/ft <sup>2</sup> yr.	Energy Collected BTU/ft <sup>2</sup> yr.	$S.R_e$ Product BTU/ft <sup>2</sup> yr.	Energy Collected BTU/ft <sup>2</sup> yr.	$S.R_e$ Product BTU/ft <sup>2</sup> yr.
140	5.4	29.1	91	41.2	91.6	161	136	149	166,740	9,004	215,260	11,624	306,180	16,354
160	6.9	29.3	92.6	46.6	92.5	180	155	167	150,941	10,415	195,356	13,480	287,630	19,846
180	8.2	29.6	94.2	52.6	93.7	198	174	186	145,671	11,945	188,718	15,475	281,444	23,078
200	9.6	29.8	95.9	59.6	94.6	216	192	204	135,074	12,967	174,904	16,791	268,013	25,729
220	10.7	30.1	97.5	67.3	95.8	233	211	222	124,457	13,317	160,938	17,220	254,280	27,028
230	10.8	30.3	98.0	72.9	96.6	241	220	231	119,204	12,874	154,005	16,632	247,391	26,718

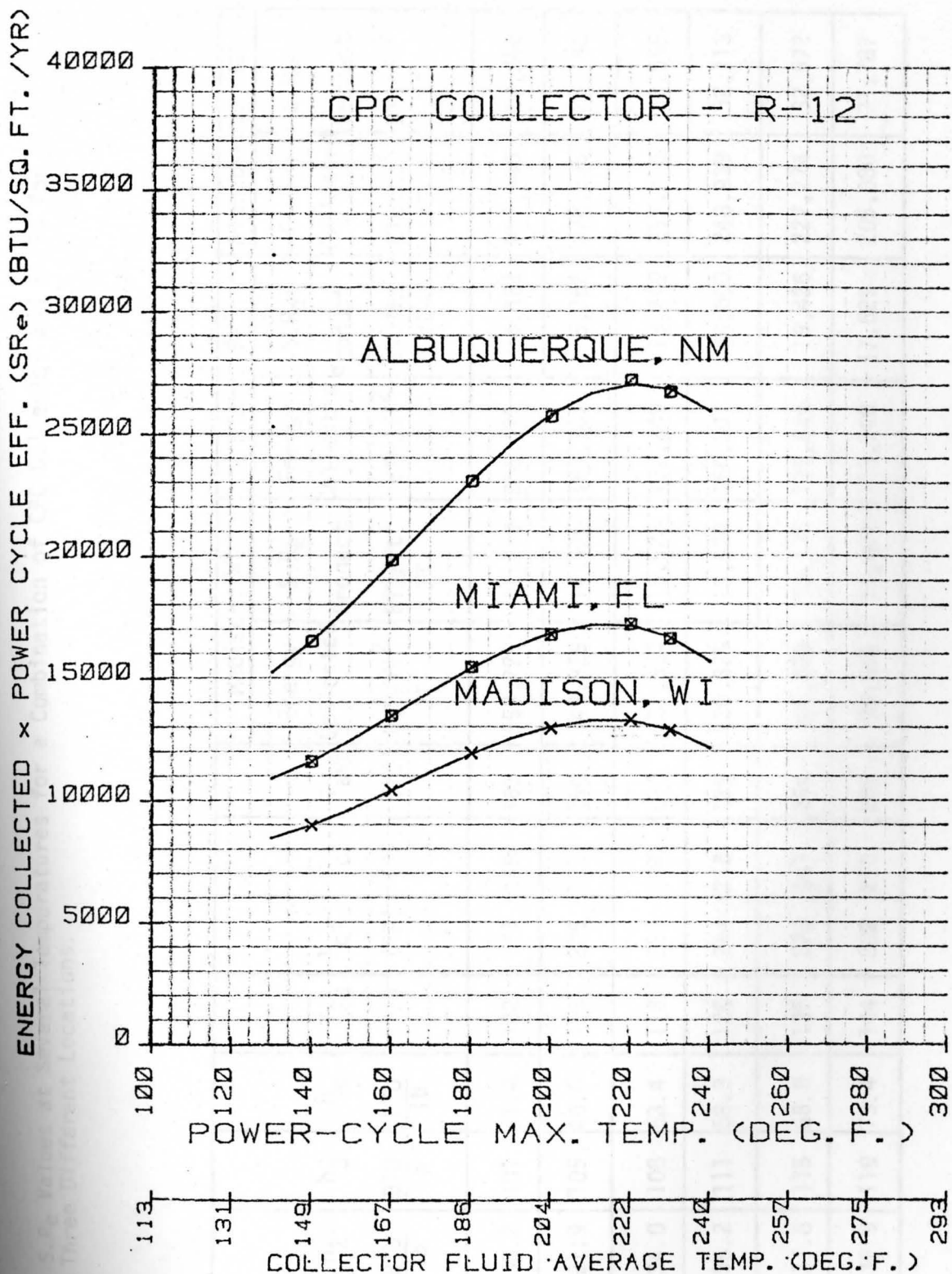


FIGURE 72. Curves of  $S.R_e$  Values vs. Operating Temperature for a Combination of a CPC Collector and R-12 for Three Locations.

TABLE 50.  $S.R_e$  Values at Several Temperatures for a Combination of CPC Collector and R-113 for Three Different Locations.

$T_3$ (°F)	$\eta_{Re}$ (%)	$h_2$ BTU/lb	$h_3$ BTU/lb	$h_s$ BTU/lb	$T_{2a}$ (°F)	$T_{c1}$ (°F)	$T_{c2}$ (°F)	$T_{avg}$ (°F)	Madison, WI		Miami, FL		Albuquerque, NM	
									Energy Collected BTU/ft <sup>2</sup> yr.	$S.R_e$ Product BTU/ft <sup>2</sup> yr.	Energy Collected BTU/ft <sup>2</sup> yr.	$S.R_e$ Product BTU/ft <sup>2</sup> yr.	Energy Collected BTU/ft <sup>2</sup> yr.	$S.R_e$ Product BTU/ft <sup>2</sup> yr.
150	7.5	30.2	101	41.4	102	177	146	162	159,725	11,979	206,421	15,482	297,940	22,346
180	10.1	31.9	105	48.6	109	206	175	190	143,329	14,476	185,767	18,762	278,695	28,148
200	11.6	34.0	108	53.4	118	225	194	210	131,534	15,528	170,249	19,749	263,436	30,559
220	12.9	36.2	111	58.3	128	244	213	229	120,329	15,522	155,507	20,060	248,939	32,113
250	14.3	37.8	115	68.8	135	270	241	256	105,839	15,135	135,844	19,426	227,774	32,572
280	15.5	39.9	119	73.4	144	302	270	286	89,962	13,944	113,740	17,629	205,080	31,787

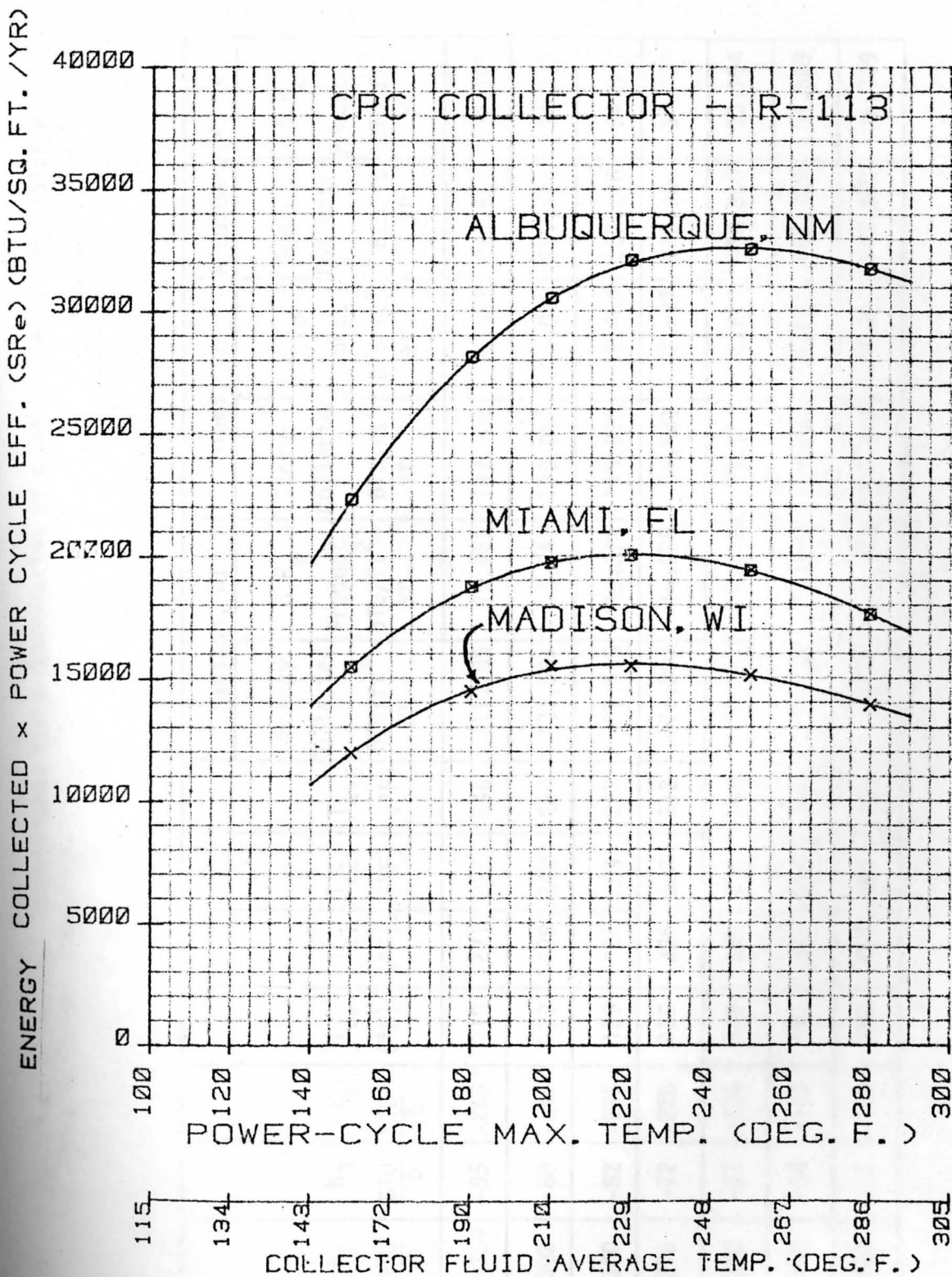


FIGURE 73. Curves of  $S.R_e$  Values vs. Operating Temperature for a Combination of a CPC Collector and R-113 for Three Locations.

TABLE 51.  $S.R_e$  Values at Several Temperatures for a Combination of a CPC Collector and Toluene for Three Different Locations.

$T_3$ (°F)	$\eta_{R_e}$ (%)	$h_2$ BTU Tb	$h_3$ BTU Tb	$h_s$ BTU Tb	$T_{2a}$ (°F)	$T_{c1}$ (°F)	$T_{c2}$ (°F)	$T_{avg}$ (°F)	Madison, WI		Miami, FL		Albuquerque, NM	
									Energy Collected BTU/ft <sup>2</sup> yr.	$S.R_e$ Product BTU/ft <sup>2</sup> yr.	Energy Collected BTU/ft <sup>2</sup> yr.	$S.R_e$ Product BTU/ft <sup>2</sup> yr.	Energy Collected BTU/ft <sup>2</sup> yr.	$S.R_e$ Product BTU/ft <sup>2</sup> yr.
230	13.9	-304	-95	-256	118	271	222	246	111,185	15,455	143,108	19,892	235,621	32,751
250	15.4	-302	-88	-245	123	288	240	264	101,562	15,641	130,032	20,025	221,496	34,110
270	16.8	-300	-82	-235	129	307	259	283	91,535	15,378	115,978	19,484	207,276	34,882
300	18.7	-296	-72	-220	139	336	288	312	76,392	14,285	94,581	17,687	185,906	34,764
330	20.3	-292	-61	-204	149	364	316	340	62,657	12,719	76,963	15,623	163,320	33,154
350	21.5	-288	-54	-193	157	383	336	359	53,523	11,508	65,327	14,045	148,229	31,869
400	23.6	-297	-37	-166	180	427	383	405	32,954	7,777	38,929	9,187	113,302	26,739



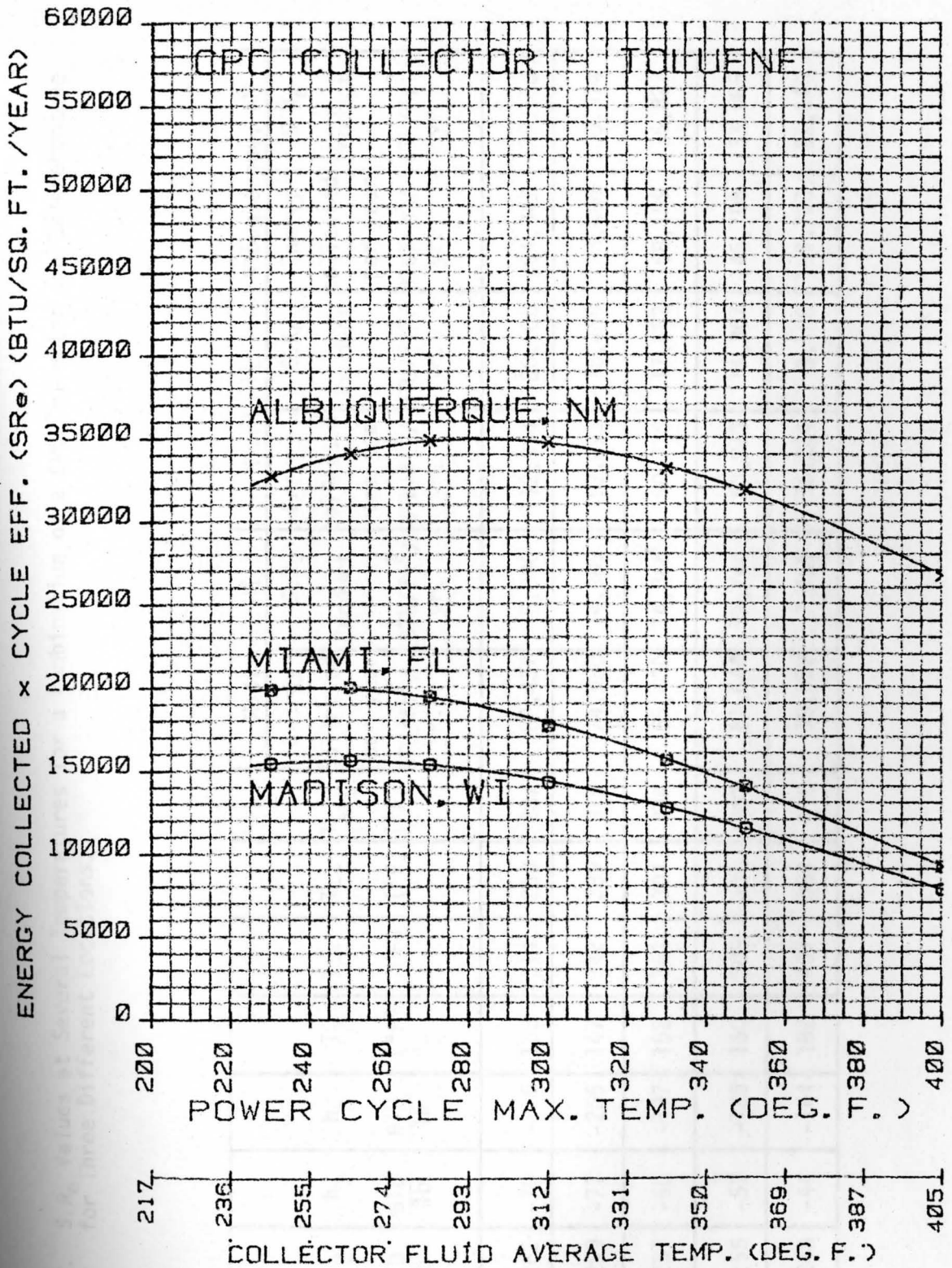


FIGURE 74. Curves of  $S.R_e$  Values vs. Operating Temperature for a Combination of a CPC Collector and Toluene for Three Locations.

TABLE 52.  $S.R_e$  Values at Several Temperatures for a Combination of a CPC Collector and Chlorobenzene for Three Different Locations.

$T_3$ (°F)	$\eta_R$ (%)	$h_2$ BTU/lb	$h_3$ BTU/lb	$h_s$ BTU/lb	$T_2$ (°F)	$T_{c1}$ (°F)	$T_{c2}$ (°F)	$T_{avg}$ (°F)	Madison, WI		Miami, FL		Albuquerque, NM	
									Energy Collected per year BTU/ft <sup>2</sup> /yr.	$S.R_e$ Product BTU/ft <sup>2</sup> /yr.	Energy collected per year BTU/ft <sup>2</sup> /yr.	$S.R_e$ Product BTU/ft <sup>2</sup> /yr.	Energy collected per year BTU/ft <sup>2</sup> /yr.	$S.R_e$ Product BTU/ft <sup>2</sup> /yr.
270	17.7	-262	-79	-216	138	314	260	287	89,437	15,830	112,994	20,000	204,349	36,170
300	19.9	-259	-71	-205	147	342	289	315	74,920	14,909	92,693	18,446	183,486	36,514
320	21.9	-257	-65	-197	152	361	307	334	65,600	14,366	80,738	17,682	168,159	36,827
350	22.8	-255	-57	-185	160	389	336	363	51,644	11,744	63,013	14,367	145,108	33,085
400	25.1	-248	-44	-164	182	437	384	410	30,952	7,769	36,264	9,102	109,723	27,540

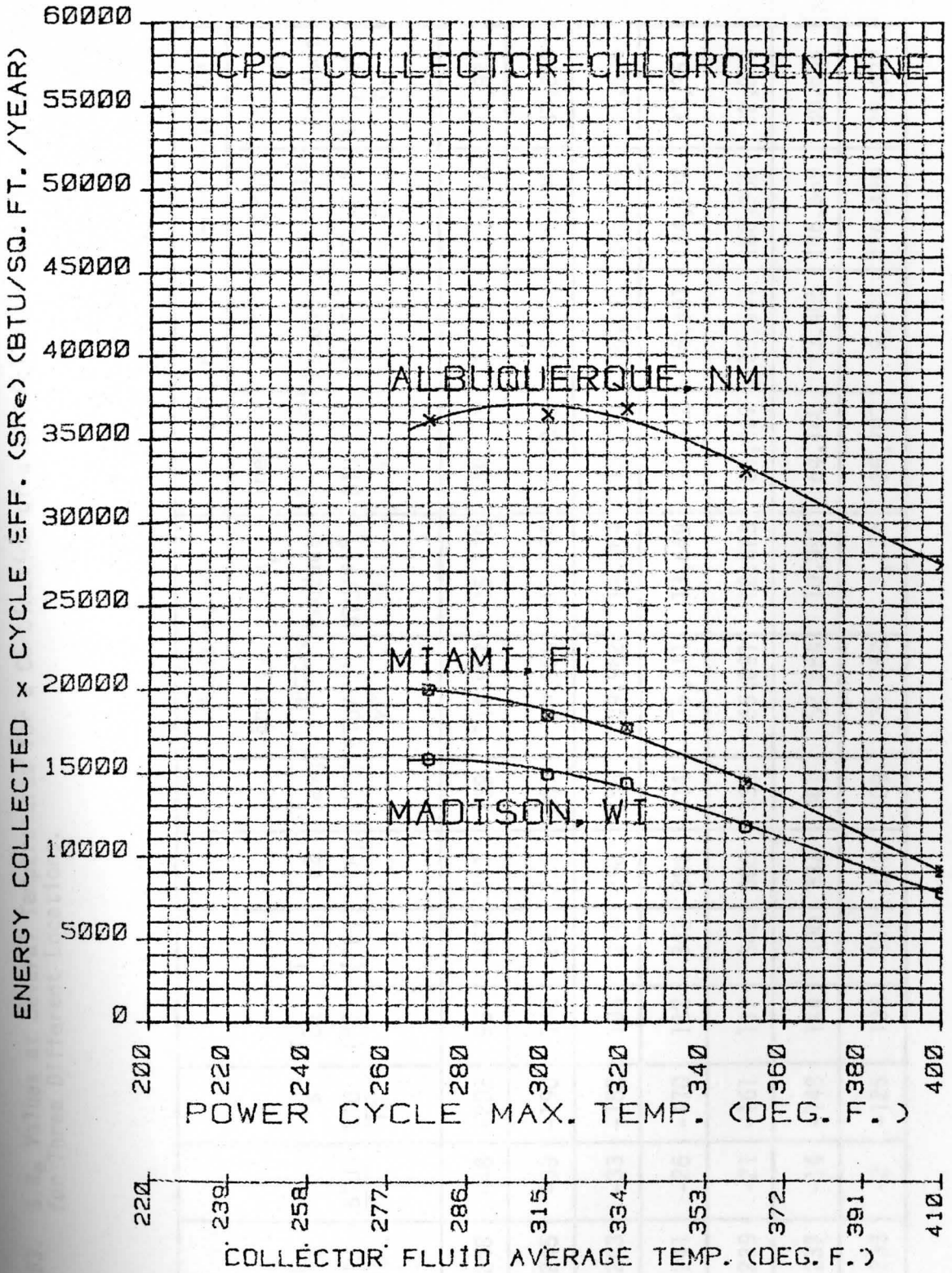


FIGURE 75. Curves of  $S.R_e$  Values vs. Operating Temperature for a Combination of a CPC Collector and Chlorobenzene for Three Locations.

TABLE 53.  $S.R_e$  Values at Several Temperatures for a Combination of a CPC Collector and Thiophene for Three Different Locations.

$T_3$ (°F)	$\eta_{R_e}$ (%)	$h_2$ BTU/lb	$h_3$ BTU/lb	$h_s$ BTU/lb	$T_{2a}$ (°F)	$T_{c1}$ (°F)	$T_{c2}$ (°F)	$T_{avg}$ (°F)	Madison, WI		Miami, FL		Albuquerque, NM	
									Energy Collected BTU/ft <sup>2</sup> yr.	$S.R_e$ Product BTU/ft <sup>2</sup> yr.	Energy Collected BTU/ft <sup>2</sup> yr.	$S.R_e$ Product BTU/ft <sup>2</sup> yr.	Energy Collected BTU/ft <sup>2</sup> yr.	$S.R_e$ Product BTU/ft <sup>2</sup> yr.
220	13.2	-248	-48	-202	96	267	211	239	114,927	15,170	148,193	19,561	241,114	31,827
250	15.2	-245	-39	-190	102	295	239	267	99,958	15,194	127,853	19,434	219,142	33,310
270	16.3	-243	-33	-182	106	314	258	286	89,962	14,664	113,740	18,540	205,080	33,428
300	18.1	-241	-26	-170	112	343	286	314	75,411	13,649	93,322	16,891	184,292	33,357
320	19.1	-239	-21	-161	117	362	305	333	66,091	12,623	81,367	15,541	168,966	32,273
350	20.9	-237	-14	-148	124	390	333	361	52,584	10,990	64,140	13,405	146,669	30,654
400	23.2	-233	-2	-125	136	437	380	409	31,352	7,274	36,797	8,537	110,439	25,622

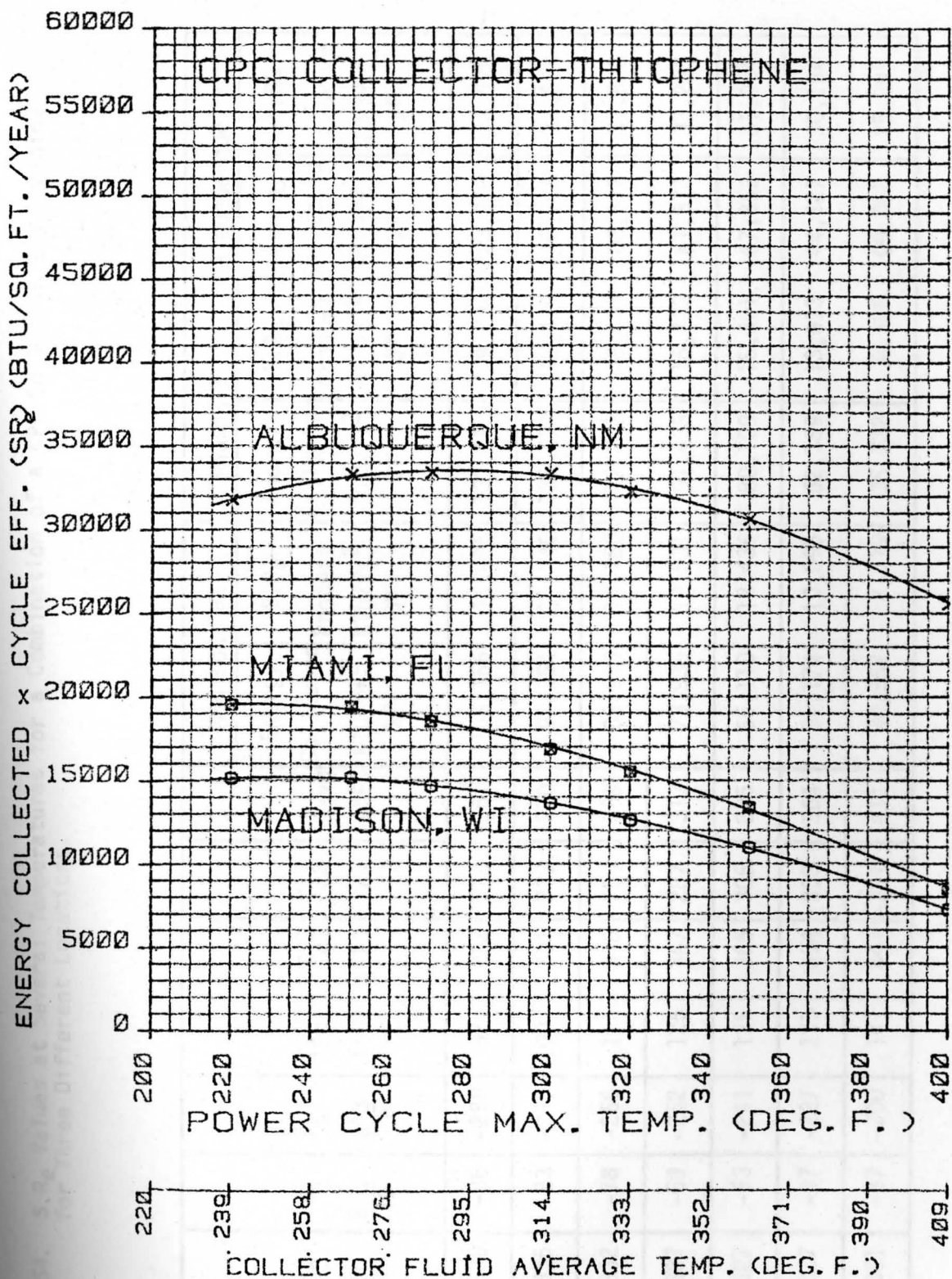


FIGURE 76. Curves of S.R. Values vs. Operating Temperature for a Combination<sup>e</sup> of a CPC Collector and Thiophene for Three Locations.

TABLE 54. S.R<sub>e</sub> Values at Several Temperatures for a Combination of a CPC Collector and Pyridine for Three Different Locations.

T <sub>3</sub> (°F)	η <sub>Re</sub> (%)	h <sub>2</sub> BTU/lb	h <sub>3</sub> BTU/lb	h <sub>s</sub> BTU/lb	T <sub>2a</sub> (°F)	T <sub>c1</sub> (°F)	T <sub>c2</sub> (°F)	T <sub>avg</sub> (°F)	Madison, WI		Miami, FL		Albuquerque, NM	
									Energy Collected BTU/ft <sup>2</sup> yr.	S.R <sub>e</sub> Product BTU/ft <sup>2</sup> yr.	Energy Collected BTU/ft <sup>2</sup> yr.	S.R <sub>e</sub> Product BTU/ft <sup>2</sup> yr.	Energy Collected BTU/ft <sup>2</sup> yr.	S.R <sub>e</sub> Product BTU/ft <sup>2</sup> yr.
240	15.0	-338	-86	-280	97	292	229	261	103,166	15,475	132,212	19,832	223,850	33,578
250	15.5	-336	-83	-275	100	301	239	270	98,354	15,245	125,674	19,479	216,788	33,602
270	16.6	-332	-78	-266	115	318	258	288	88,913	14,760	112,248	18,633	203,617	33,800
300	18.3	-327	-69	-252	125	347	287	317	73,939	13,531	91,435	16,733	181,872	33,283
320	19.1	-327	-63	-241	125	365	305	335	65,110	12,436	80,109	15,301	167,353	31,964
350	20.9	-327	-57	-227	125	394	333	364	51,174	10,695	62,359	13,033	144,327	30,164
400	23.3	-321	-37	-200	141	441	381	411	30,552	7,119	35,732	8,325	109,008	25,399

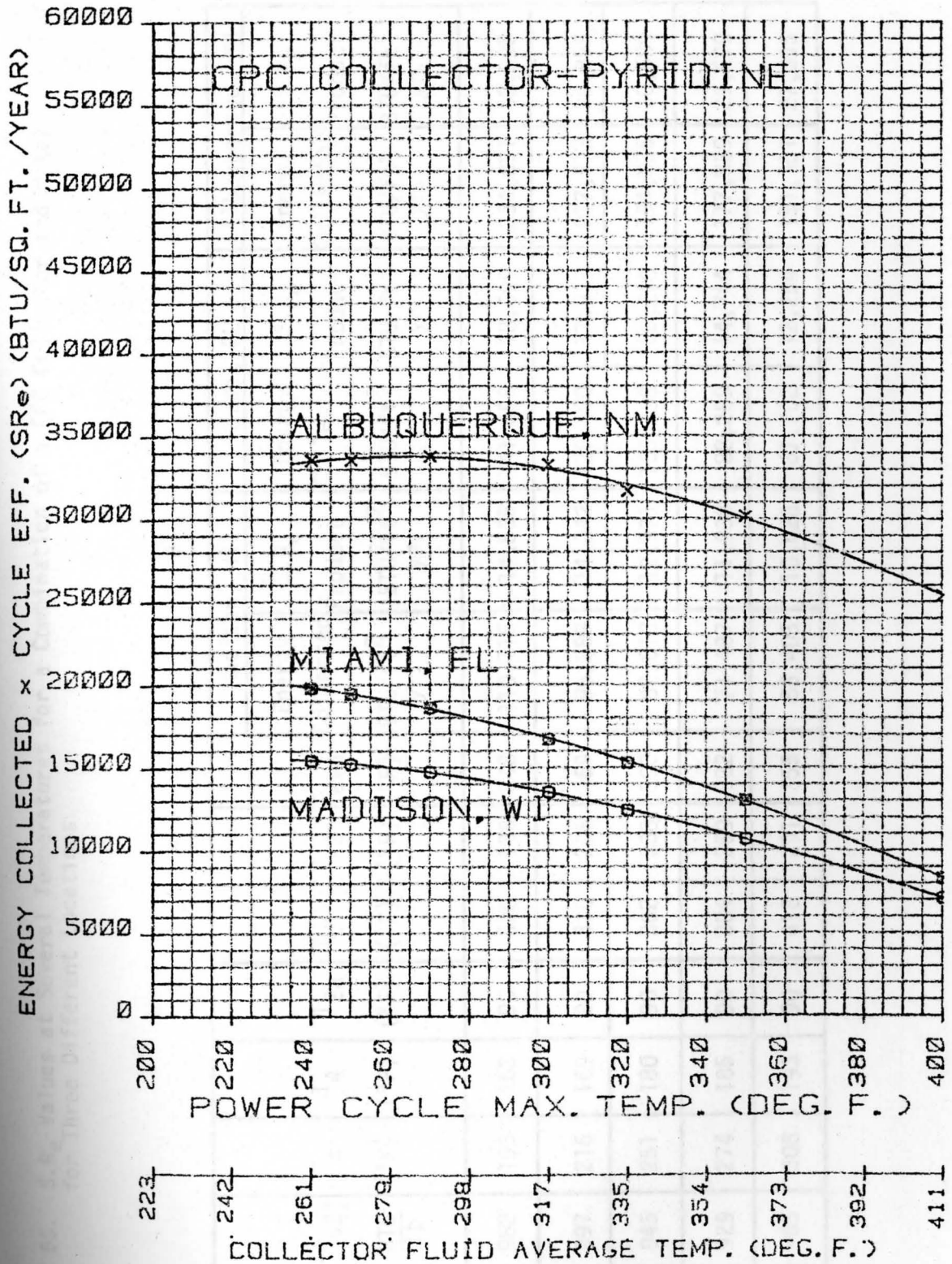


FIGURE 77. Curves of  $S.R_e$  Values vs. Operating Temperature for a Combination of a CPC Collector and Pyridine for Three Locations.

TABLE 55.  $S.R_e$  Values at Several Temperatures for a Combination of a CPC Collector and Water for Three Different Locations.

$T_3$ (°F)	$\eta_R$ (%)	$(h_{s1} - h_{s2})$ $\frac{BTU}{lb}$	$T_s$ (°F)	$T_4$ (°F)	$T_{2a}$ (°F)	$T_{c1}$ (°F)	$T_{c2}$ (°F)	$T_{avg}$ (°F)	Madison, WI		Miami, FL		Albuquerque, NM	
									Energy Collected BTU/ft <sup>2</sup> yr.	$S.R_e$ Product BTU/ft <sup>2</sup> yr.	Energy Collected BTU/ft <sup>2</sup> yr.	$S.R_e$ Product BTU/ft <sup>2</sup> yr.	Energy Collector BTU/ft <sup>2</sup> yr.	$S.R_e$ Product BTU/ft <sup>2</sup> yr.
300	13.2	982	193	162	90	308	188	248	110,116	14,535	141,655	18,699	234,051	30,895
320	14.2	997	216	169	90	330	208	269	98,889	14,042	126,400	17,949	217,573	30,895
350	15.7	945	251	180	90	362	238	300	82,618	12,971	103,298	16,218	194,836	30,589
370	16.7	929	274	185	90	384	259	322	71,487	11,938	88,289	14,744	177,839	29,699
400	18.1	905	308	193	90	418	291	355	55,403	10,028	67,702	12,254	151,351	27,395



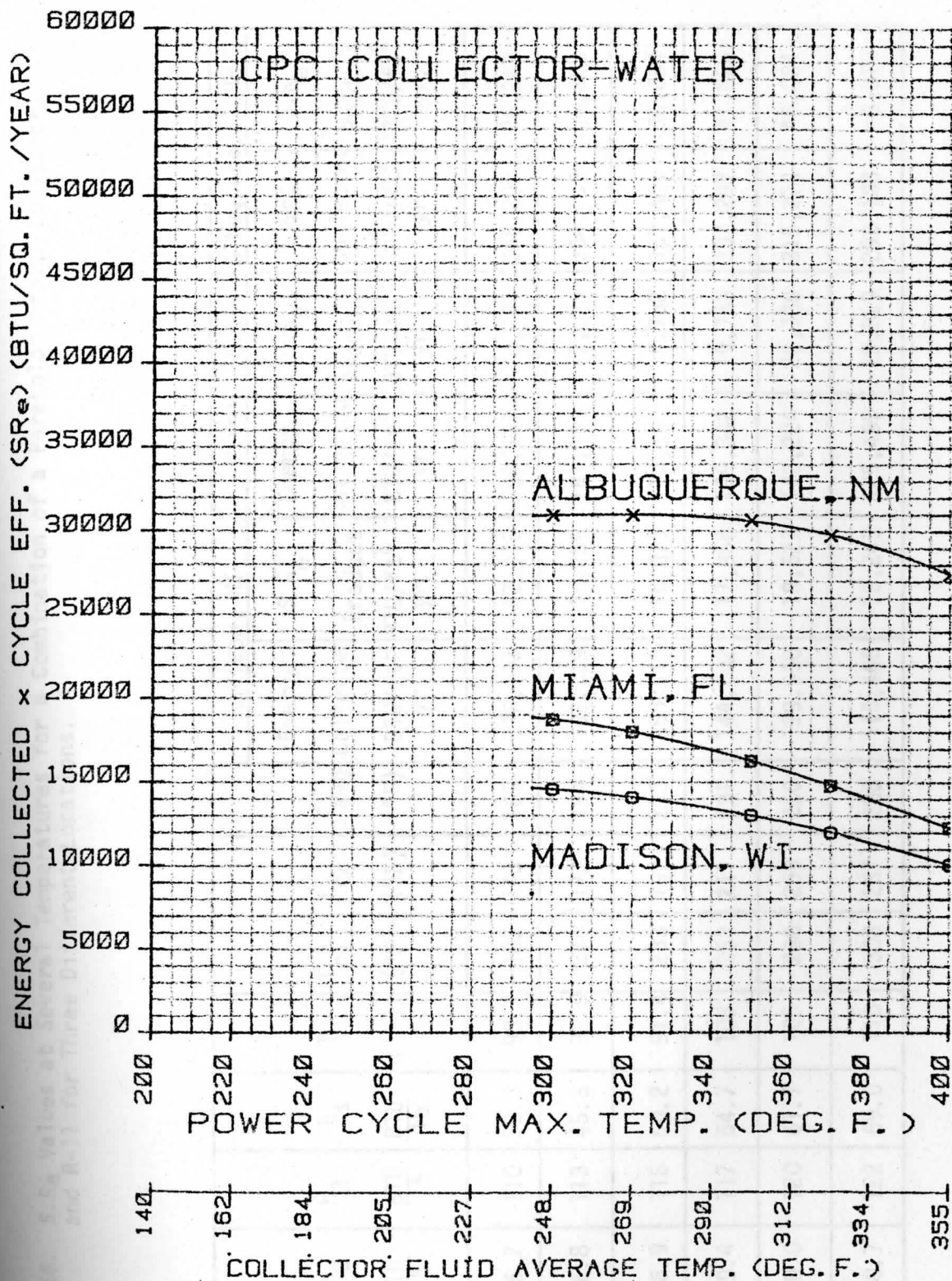


FIGURE 78. Curve of  $S.R_e$  Values vs. Operating Temperature for a Combination of a CPC Collector and Water for Three Locations.

TABLE 56.  $S.R_e$  Values at Several Temperatures for a Combination of a Parabolic Trough Collector and R-11 for Three Different Locations.

$T_3$ (°F)	$\eta_{R_e}$ (%)	$h_2$ BTU/lb	$h_3$ BTU/lb	$h_s$ BTU/lb	$T_2$ (°F)	$T_{c1}$ (°F)	$T_{c2}$ (°F)	$T_{avg}$ (°F)	Madison, WI		Miami, FL		Albuquerque, NM	
									Energy Collected BTU/ft <sup>2</sup> yr.	$S.R_e$ Product BTU/ft <sup>2</sup> yr.	Energy Collected BTU/ft <sup>2</sup> yr.	$S.R_e$ Product BTU/ft <sup>2</sup> yr.	Energy Collected BTU/ft <sup>2</sup> yr.	$S.R_e$ Product BTU/ft <sup>2</sup> yr.
150	6.8	26.7	110	39.3	90.4	185	145	165	176,693	12,015	198,237	13,480	386,290	26,268
180	9.4	26.8	113	45.8	90.9	214	173	194	162,329	15,259	181,164	17,029	364,763	34,288
200	11.0	26.9	115	50.2	91.4	233	192	213	153,413	16,875	170,568	18,762	351,401	38,654
220	12.4	29.4	117	54.7	103	252	211	231	144,002	17,856	159,382	19,763	337,297	41,825
250	14.3	30.0	120	61.7	106	280	239	260	129,558	18,527	142,224	20,338	315,274	45,084
280	15.8	30.7	122	69.0	110	308	267	288	115,465	18,243	125,499	19,829	293,103	46,310

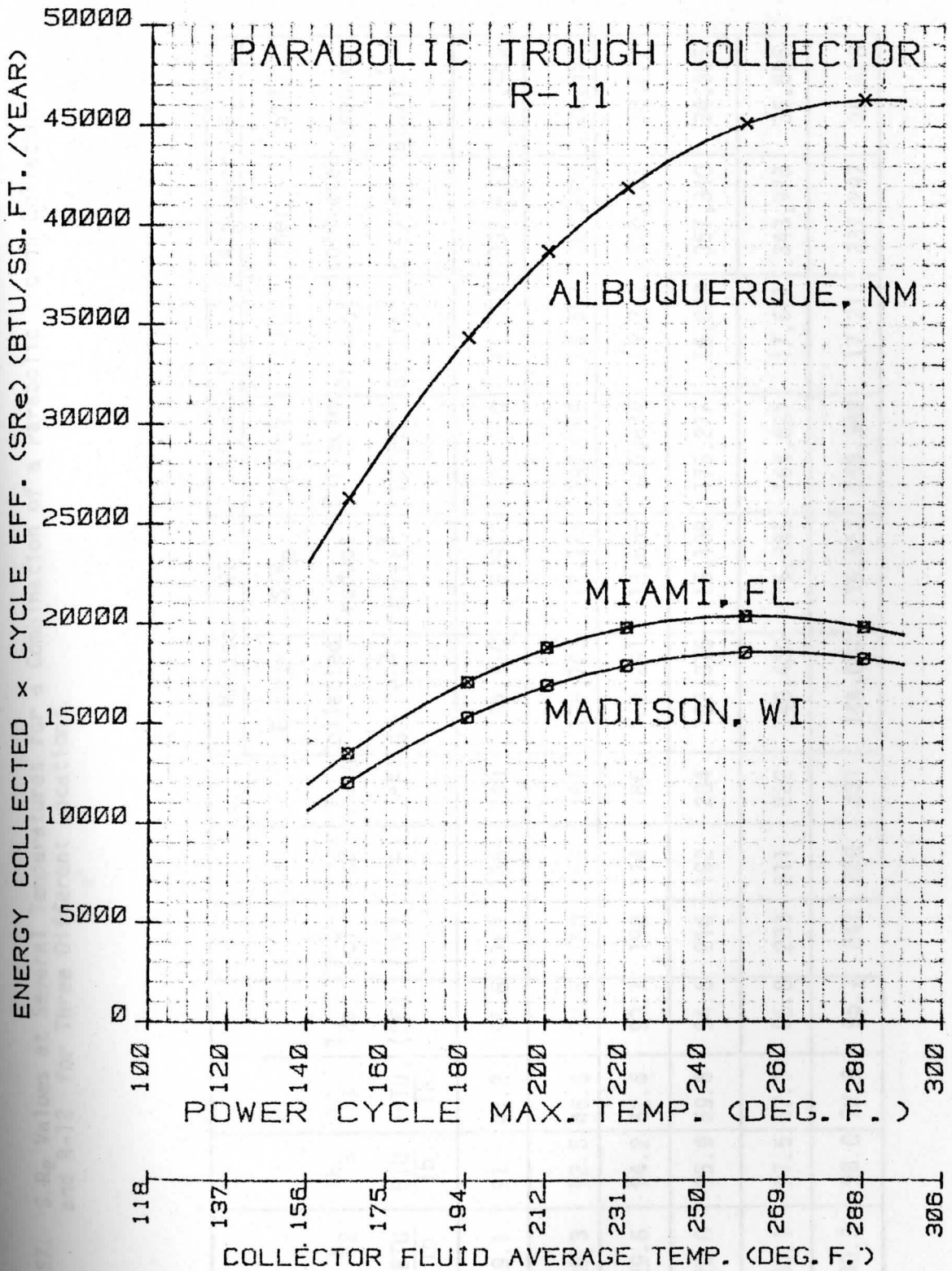


FIGURE 79. Curves of  $SRe$  Values vs. Operating Temperature for a Combination of a Parabolic Trough Collector and R-11 for Three Locations.

TABLE 57.  $S.R_e$  Values at Several Temperatures for a Combination of a Parabolic Trough Collector and R-12 for Three Different Locations.

$T_3$ (°F)	$\eta_{Re}$ (%)	$h_2$ BTU/lb	$h_3$ BTU/lb	$h_s$ BTU/lb	$T_{2a}$ (°F)	$T_{c1}$ (°F)	$T_{c2}$ (°F)	$T_{avg}$ (°F)	Madison, WI		Miami, FL		Albuquerque, NM	
									Energy Collected BTU/ft <sup>2</sup>	$S.R_e$ Product BTU/ft <sup>2</sup>	Energy Collected BTU/ft <sup>2</sup>	$S.R_e$ Product BTU/ft <sup>2</sup>	Energy Collected BTU/ft <sup>2</sup>	$S.R_e$ Product BTU/ft <sup>2</sup>
140	5.4	29.1	91	41.2	91.6	161	136	149	184,110	9,942	207,050	11,181	397,410	21,460
160	6.9	29.3	92.5	46.6	92.5	180	155	167	175,703	12,123	197,059	13,597	384,806	26,552
180	8.2	29.6	94.2	52.6	93.7	198	174	186	166,291	13,636	185,874	15,242	370,701	30,397
200	9.6	29.8	95.9	59.6	94.6	216	192	204	157,376	15,108	175,277	16,827	357,340	34,305
220	10.7	30.1	97.5	67.3	95.8	233	211	222	148,460	15,885	164,681	17,621	343,978	36,806
230	10.8	30.3	98.0	72.9	96.7	241	220	231	144,002	15,552	159,382	17,213	337,297	36,428

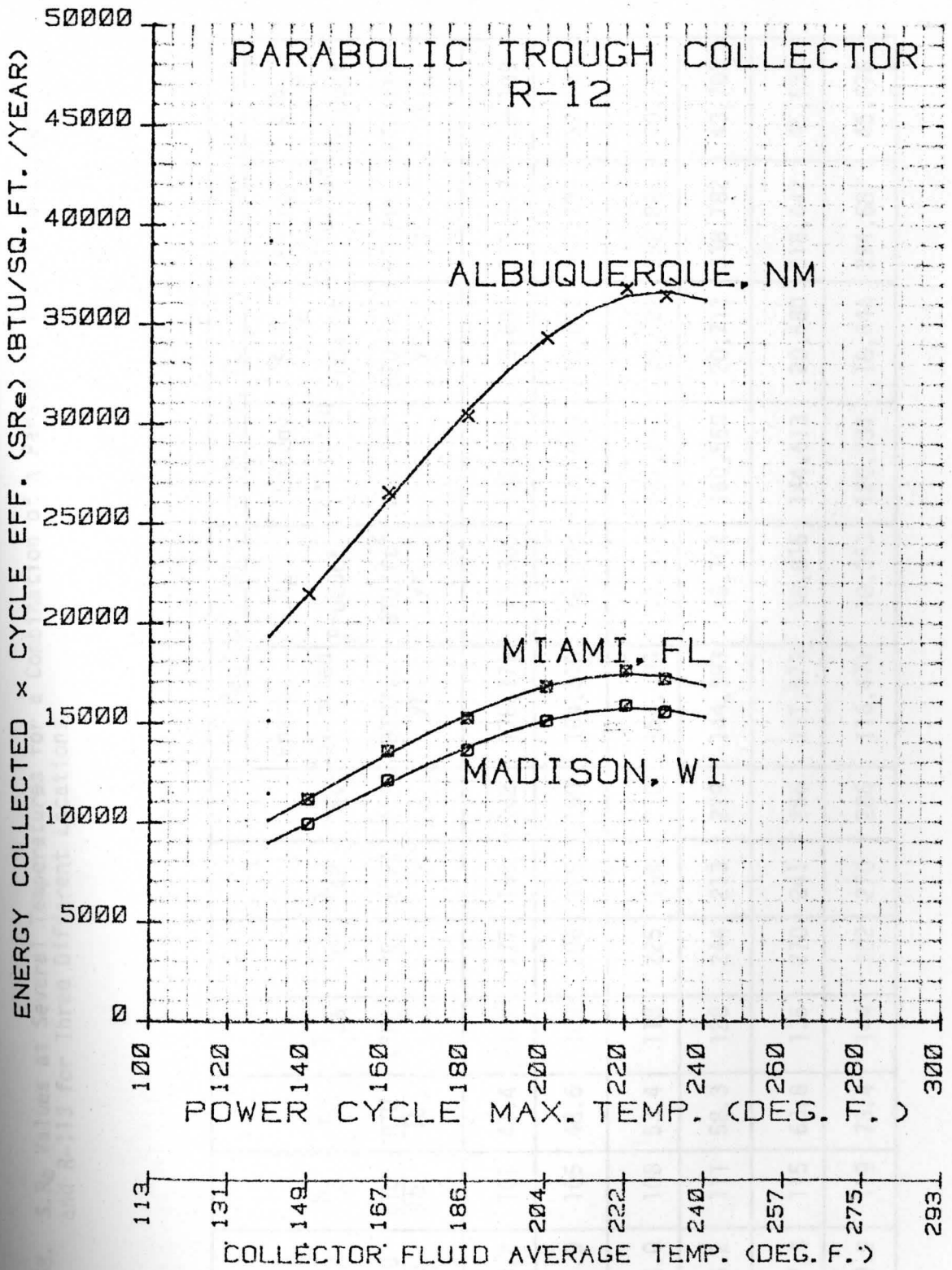


FIGURE 80. Curves of  $S.R_e$  Values vs. Operating Temperature for a Combination of a Parabolic Trough Collector and R-12 for Three Locations.

TABLE 58.  $S.R_e$  Values at Several Temperatures for a Combination of a Parabolic Trough Collector and R-113 for Three Different Locations.

$T_3$ (°F)	$\eta_{Re}$ (%)	$h_2$ BTU/lb	$h_3$ BTU/lb	$h_s$ BTU/lb	$T_{2a}$ (°F)	$T_{c1}$ (°F)	$T_{c2}$ (°F)	$T_{avg}$ (°F)	Madison, WI		Miami, FL		Albuquerque, NM	
									Energy Collected BTU/ft <sup>2</sup> yr.	$S.R_e$ Product BTU/ft <sup>2</sup> yr.	Energy Collected BTU/ft <sup>2</sup> yr.	$S.R_e$ Product BTU/ft <sup>2</sup> yr.	Energy Collected BTU/ft <sup>2</sup> yr.	$S.R_e$ Product BTU/ft <sup>2</sup> yr.
150	7.5	30.2	101	41.4	102	177	146	162	178,179	13,363	182,565	13,692	388,517	29,139
180	10.1	31.9	105	48.6	109	206	175	190	164,310	16,595	178,930	18,072	367,732	37,141
200	11.6	34.0	108	53.4	118	225	194	210	154,404	17,911	171,745	19,922	352,886	40,935
220	12.9	36.2	111	58.3	128	244	213	229	144,993	18,704	160,560	20,712	338,782	43,703
250	14.3	37.8	115	68.8	135	270	241	256	131,571	18,815	144,613	20,680	318,442	45,537
280	15.5	39.9	119	73.4	144	302	270	286	116,471	18,053	120,281	18,644	294,687	45,676

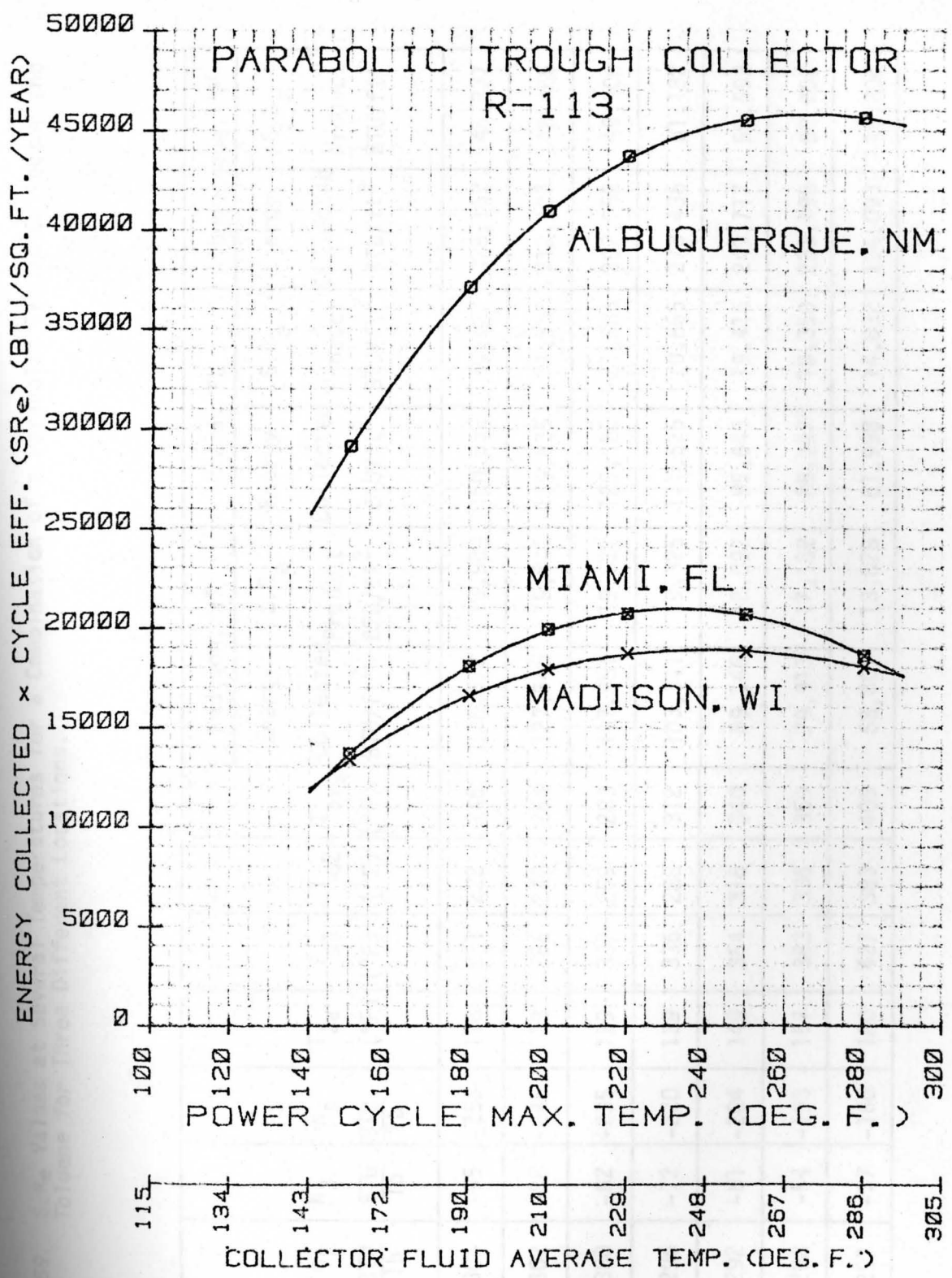


FIGURE 81. Curves of S.R<sub>e</sub> Values vs. Operating Temperature for a Combination of a Parabolic Trough Collector and R-113 for Three Locations.

TABLE 59. S.Re Values at Several Temperatures for a Combination of a Parabolic Trough Collector and Toluene for Three Different Locations.

T <sub>3</sub> (°F)	η <sub>Re</sub> (%)	h <sub>2</sub> BTU/lb	h <sub>3</sub> BTU/lb	h <sub>s</sub> BTU/lb	T <sub>2a</sub> (°F)	T <sub>c1</sub> (°F)	T <sub>c2</sub> (°F)	T <sub>avg</sub> (°F)	Madison, WI		Miami, FL		Albuquerque, NM	
									Energy Collected BTU/ft <sup>2</sup>	S.Re Product BTU/ft <sup>2</sup>	Energy Collected BTU/ft <sup>2</sup>	S.Re Product BTU/ft <sup>2</sup>	Energy Collected BTU/ft <sup>2</sup>	S.Re Product BTU/ft <sup>2</sup>
230	13.9	-304	-95	-256	118	271	222	246	136,572	18,984	150,552	20,927	326,162	45,337
250	15.4	-302	-88	-245	123	288	240	264	127,545	19,642	139,835	21,535	312,107	48,065
270	16.8	-300	-82	-235	129	307	259	283	117,981	19,821	128,485	21,586	297,062	49,906
300	18.7	-296	-72	-220	139	336	288	312	103,341	19,325	111,525	20,855	273,436	51,132
330	20.3	-292	-61	-204	149	364	316	340	89,146	18,097	95,645	19,416	249,717	50,693
350	21.5	-288	-54	-193	157	383	336	359	79,913	17,182	85,347	18,350	233,496	50,202
400	23.6	-297	-37	-166	180	427	383	405	58,807	13,878	61,998	14,632	194,093	45,806



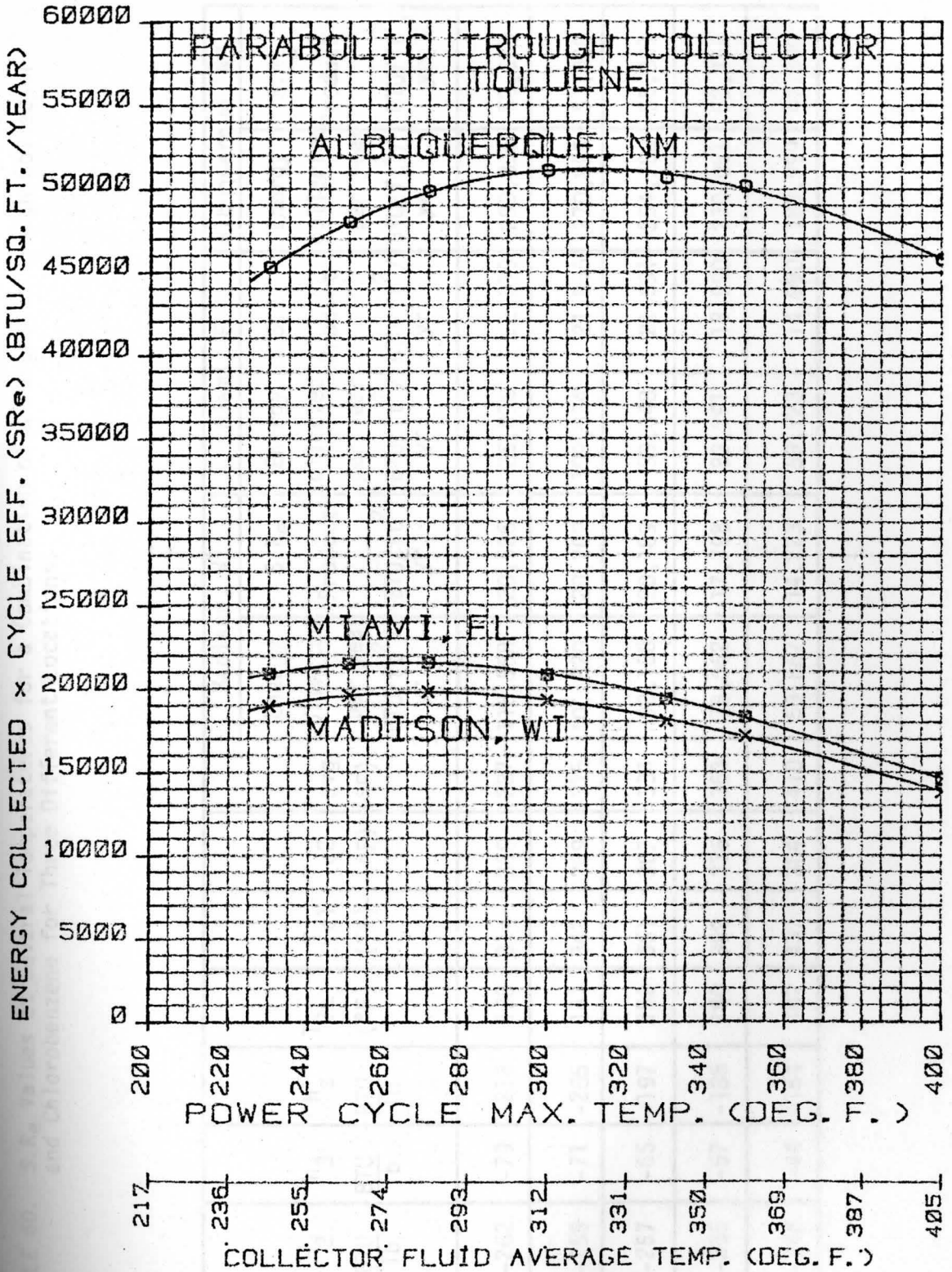


FIGURE 82. Curves of  $S.R_e$  Values vs. Operating Temperature for a Combination of a Parabolic Trough Collector and Toluene for Three Locations.

TABLE 60.  $S.R_e$  Values at Several Temperatures for a Combination of a Parabolic Trough Collector and Chlorobenzene for Three Different Locations.

$T_3$ (°F)	$\eta_{Re}$ (%)	$h_2$ BTU/lb	$h_3$ BTU/lb	$h_s$ BTU/lb	$T_{2a}$ (°F)	$T_{c1}$ (°F)	$T_{c2}$ (°F)	$T_{avg}$ (°F)	Madison, WI		Miami, FL		Albuquerque, NM	
									Energy collected per year BTU/ft <sup>2</sup> /yr.	$S.R_e$ Product BTU/ft <sup>2</sup> /yr.	Energy collected per year BTU/ft <sup>2</sup> /yr.	$S.R_e$ Product BTU/ft <sup>2</sup> /yr.	Energy collected per year BTU/ft <sup>2</sup> /yr.	$S.R_e$ Product BTU/ft <sup>2</sup> /yr.
270	17.7	-262	-79	-216	138	314	260	287	115,968	20,526	126,096	22,319	293,895	52,019
300	19.9	-259	-71	-205	147	342	289	315	101,820	20,262	109,824	21,855	270,895	53,908
320	21.9	-257	-65	-197	152	361	307	334	92,188	20,189	99,048	21,691	254,780	55,801
350	22.8	-255	-57	-185	160	389	336	363	78,062	17,798	83,291	18,990	230,051	52,452
400	25.1	-248	-44	-164	182	437	384	410	56,667	14,223	59,723	14,990	189,999	47,690

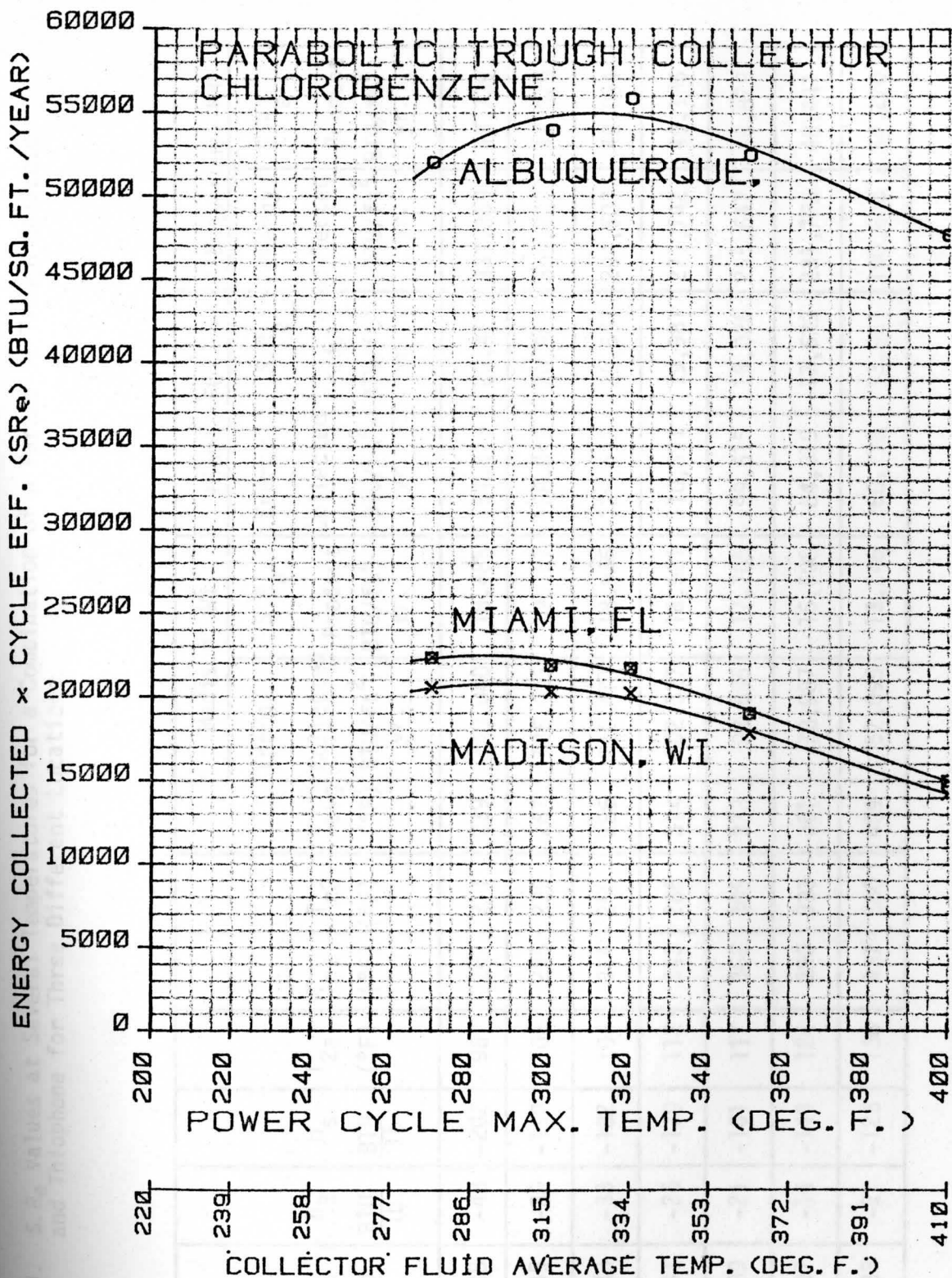


FIGURE 83. Curves of  $S.R_e$  Values vs. Operating Temperature for a Combination of a Parabolic Trough Collector and Chlorobenzene for Three Locations.

TABLE 61.  $S.R_e$  Values at Several Temperatures for a Combination of a Parabolic Trough Collector and Thiophene for Three Different Locations.

$T_3$ (°F)	$\eta_{Re}$ (%)	$h_2$ $\frac{BTU}{lb}$	$h_3$ $\frac{BTU}{lb}$	$h_s$ $\frac{BTU}{lb}$	$T_{2a}$ (°F)	$T_{c1}$ (°F)	$T_{c2}$ (°F)	$T_{avg}$ (°F)	Madison, Wi		Miami, FL		Albuquerque, NM	
									Energy Collected BTU/ft <sup>2</sup> yr.	$S.R_e$ Product BTU/ft <sup>2</sup> yr.	Energy Collected BTU/ft <sup>2</sup> yr.	$S.R_e$ Product BTU/ft <sup>2</sup> yr.	Energy Collected BTU/ft <sup>2</sup> yr.	$S.R_e$ Product BTU/ft <sup>2</sup> yr.
220	13.2	-248	-48	-202	96	267	211	239	140,040	18,485	154,673	20,417	331,359	43,739
250	15.2	-245	-39	-190	102	295	239	267	126,035	19,157	138,043	20,982	309,732	47,079
270	16.3	-243	-33	-182	106	314	258	286	116,471	18,985	126,693	20,651	294,687	48,034
300	18.1	-241	-26	-170	112	343	286	314	102,327	18,521	110,391	19,981	271,742	49,185
320	19.1	-239	-21	-161	117	362	305	333	92,695	17,705	99,615	19,026	255,647	48,829
350	20.9	-237	-14	-148	124	390	333	361	78,987	16,508	84,319	17,623	231,773	48,441
400	23.2	-233	-2	-125	136	437	380	409	57,095	13,246	60,178	13,961	190,818	44,270

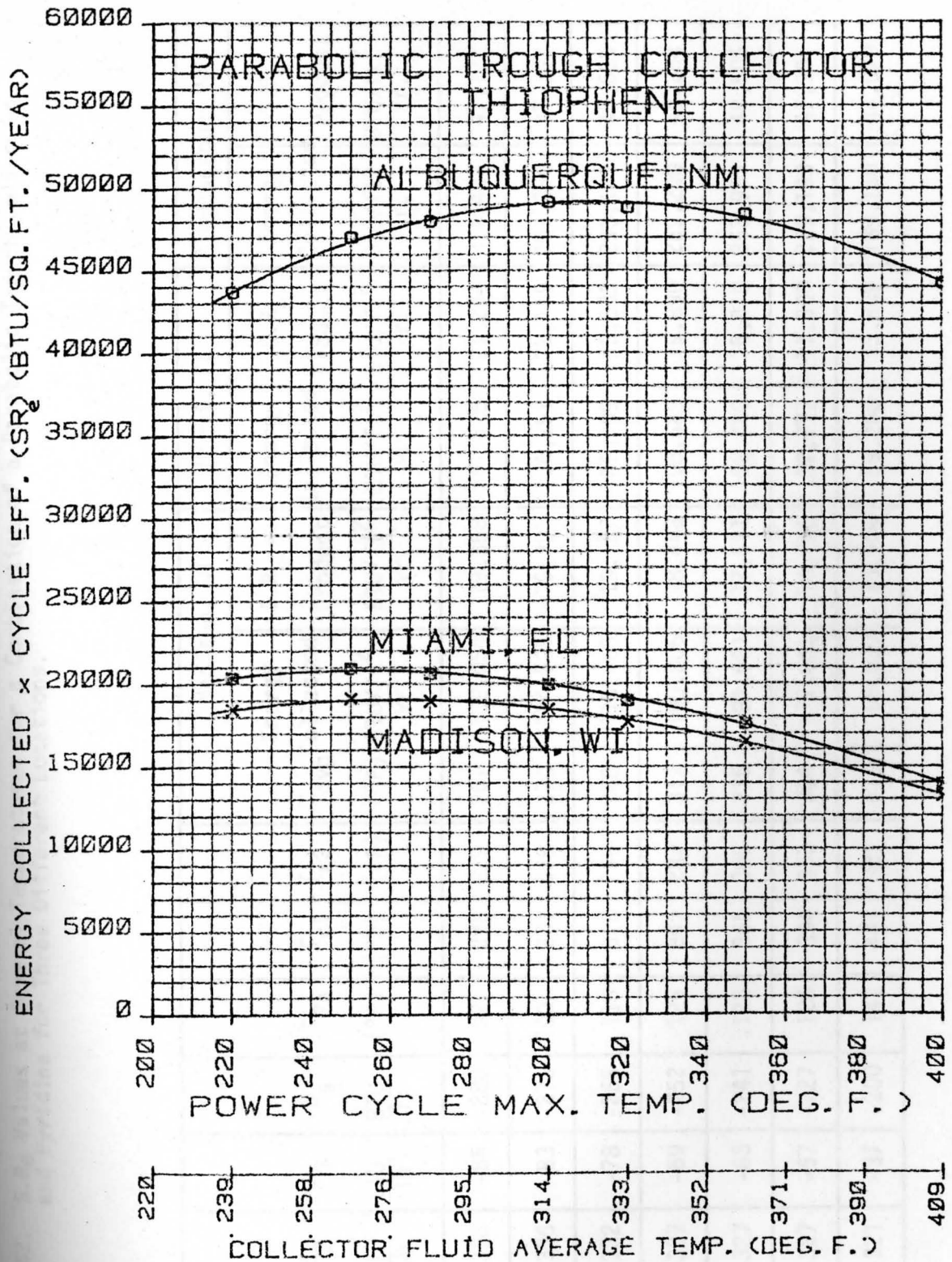


FIGURE 84. Curves of  $SR_e$  Values vs. Operating Temperature for a Combination of a Parabolic Trough Collector and Thiophene for Three Locations.

TABLE 62.  $S.R_e$  Values at Several Temperatures for a Combination of a Parabolic Trough Collector and Pyridine for Three Different Locations.

$T_3$ (°F)	$\eta_{Re}$ (%)	$h_2$ BTU/lb	$h_3$ BTU/lb	$h_s$ BTU/lb	$T_{2a}$ (°F)	$T_{c1}$ (°F)	$T_{c2}$ (°F)	$T_{avg}$ (°F)	Madison, WI		Miami, FL		Albuquerque, NM	
									Energy Collected BTU/ft <sup>2</sup> yr.	$S.R_e$ Product BTU/ft <sup>2</sup> yr.	Energy Collected BTU/ft <sup>2</sup> yr.	$S.R_e$ Product BTU/ft <sup>2</sup> yr.	Energy Collected BTU/ft <sup>2</sup> yr.	$S.R_e$ Product BTU/ft <sup>2</sup> yr.
240	15.0	-338	-86	-280	97	292	229	261	129,054	19,358	141,626	21,244	314,483	47,172
250	15.5	-336	-83	-275	100	301	229	270	124,525	19,301	136,251	21,119	307,356	47,641
270	16.6	-332	-78	-266	115	318	258	288	115,465	19,167	125,499	20,833	293,103	48,655
300	18.3	-327	-69	-252	125	347	287	317	100,806	18,448	108,689	19,890	269,200	49,264
320	19.1	-327	-63	-241	125	365	305	335	91,681	17,511	98,480	18,810	253,953	48,505
350	20.9	-327	-57	-227	125	394	333	364	77,600	16,218	82,777	17,300	229,190	47,901
400	23.3	-321	-37	-200	141	441	381	411	56,239	13,104	59,268	13,809	189,180	44,079

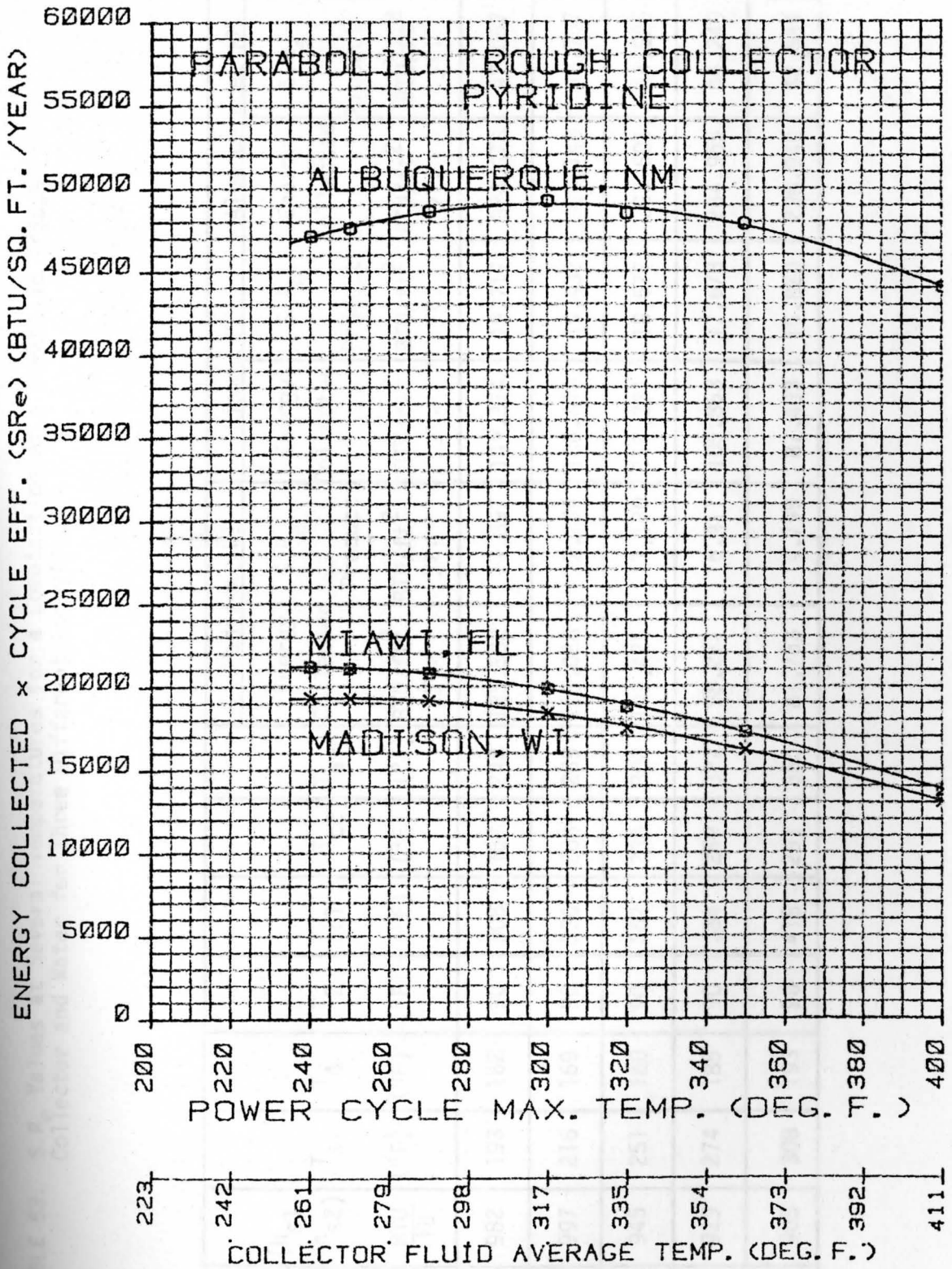


FIGURE 85. Curves of  $S.R_e$  Values vs. Operating Temperature for a Combination of a Parabolic Trough Collector and Pyridine for Three Locations.

TABLE 63. S.R<sub>e</sub> Values at Several Temperatures for a Combination of a Parabolic Trough Collector and Water for Three Different Locations.

T <sub>5</sub> or T <sub>3</sub> (°F)	η <sub>R</sub> (%)	(h <sub>s1</sub> -h <sub>s2</sub> ) BTU/Tb	T <sub>s</sub> (°F)	T <sub>4</sub> (°F)	T <sub>2</sub> (°F)	T <sub>c1</sub> (°F)	T <sub>c2</sub> (°F)	T <sub>avg</sub> (°F)	Madison, WI		Miami, FL		Albuquerque, NM	
									Energy Collected BTU/ft <sup>2</sup> yr.	S.R <sub>e</sub> Product BTU/ft <sup>2</sup> yr.	Energy Collected BTU/ft <sup>2</sup> yr.	S.R <sub>e</sub> Product BTU/ft <sup>2</sup> yr.	Energy Collected BTU/ft <sup>2</sup> yr.	S.R <sub>e</sub> Product BTU/ft <sup>2</sup> yr.
300	13.2	982	193	162	90	308	188	248	135,582	17,897	149,374	19,717	324,678	42,857
320	14.2	997	216	169	90	330	208	269	125,028	17,754	136,848	19,432	308,148	43,757
350	15.7	945	251	180	90	362	238	300	109,425	17,180	118,331	18,577	283,601	44,525
370	16.7	929	274	185	90	384	259	322	98,271	16,411	105,853	17,678	264,965	44,249
400	18.1	905	308	193	90	418	291	355	81,763	14,799	87,403	15,820	236,940	42,886



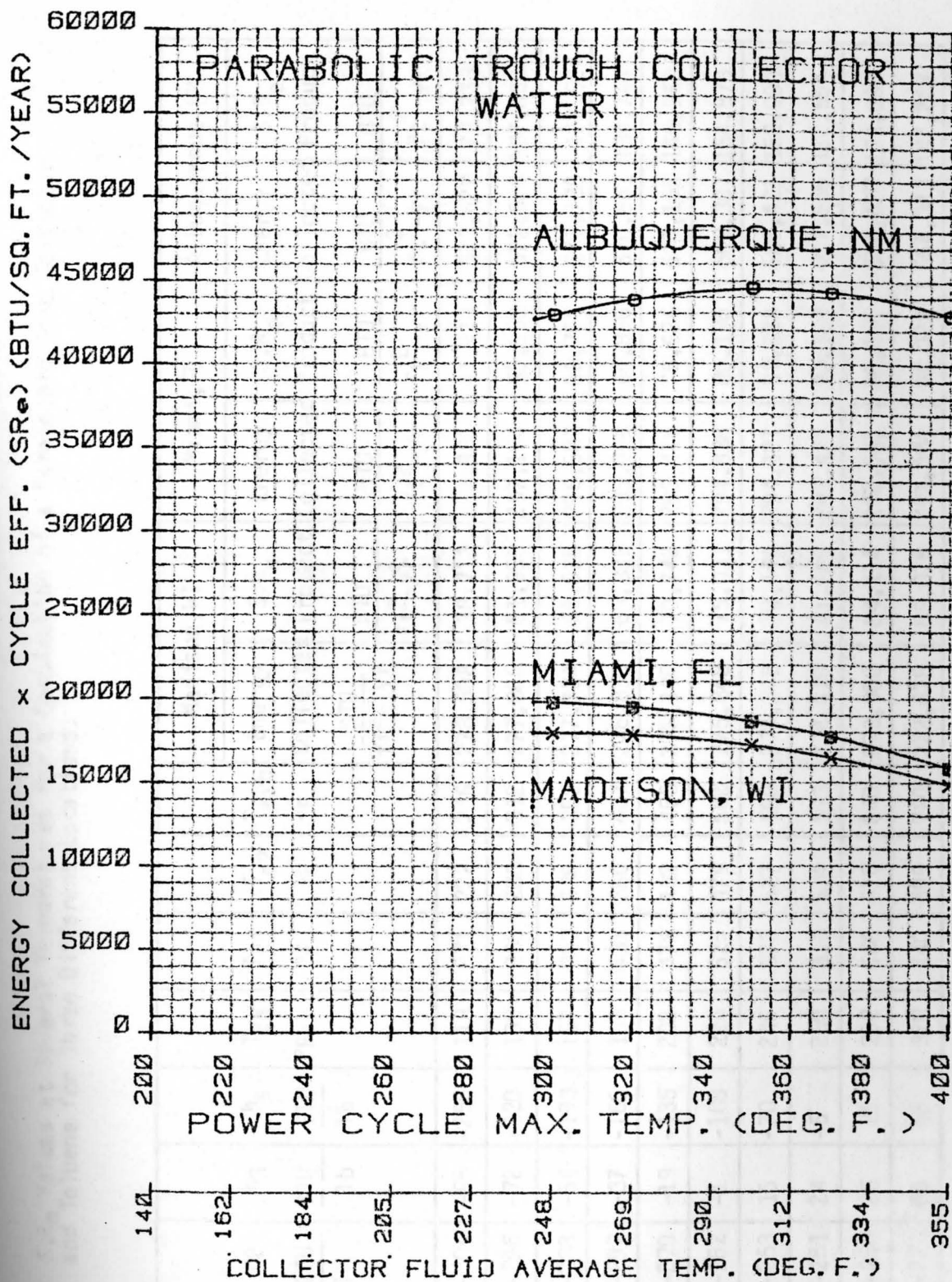


FIGURE 86. Curves of  $S.R._e$  Values vs. Operating Temperature for a Combination of a Parabolic Trough Collector and Water for Three Locations.

TABLE 64. S.R<sub>e</sub> Values at Several Temperatures for a Combination of a Paraboloid Disc Collector and Toluene for Three Different Locations.

T <sub>3</sub> °F	η <sub>Re</sub> (%)	h <sub>2</sub> BTU 1b	h <sub>3</sub> BTU 1b	h <sub>s</sub> BTU 1b	T <sub>2a</sub> °F	T <sub>c1</sub> °F	T <sub>c2</sub> °F	T <sub>avg</sub> °F	Madison, WI		Miami, FL		Albuquerque, NM	
									Energy Collected	S.R <sub>e</sub> Product	Energy Collected	S.R <sub>e</sub> Product	Energy Collected	S.R <sub>e</sub> Product
									$\frac{\text{BTU}}{\text{ft}^2\text{-yr}}$	$\frac{\text{BTU}}{\text{ft}^2\text{-yr}}$	$\frac{\text{BTU}}{\text{ft}^2\text{-yr}}$	$\frac{\text{BTU}}{\text{ft}^2\text{-yr}}$	$\frac{\text{BTU}}{\text{ft}^2\text{-yr}}$	$\frac{\text{BTU}}{\text{ft}^2\text{-yr}}$
230	13.9	-304	-95	-256	118	271	222	246	278,508	38,713	297,981	41,419	573,622	79,733
300	18.7	-296	-72	-220	139	336	288	312	277,808	51,950	297,154	55,568	572,508	107,059
350	21.5	-288	-54	-193	157	383	336	359	277,324	59,625	296,583	63,765	571,738	122,924
400	23.6	-297	-37	-166	134	433	380	407	276,830	65,332	295,999	69,856	570,951	134,744
450	25.6	-270	-19	-135	202	478	432	455	276,336	70,742	295,415	75,626	570,165	145,962
500	27.2	-262	-1	-105	224	525	479	502	275,848	75,031	294,838	80,196	569,387	154,873
550	28.5	-253	16	-70	246	572	527	550	275,241	78,444	294,121	83,824	568,421	162,000
600	29.7	-251	24	-5	250	613	574	593	274,670	81,585	293,479	87,164	567,556	168,564
650	30.7	-250	26	26	252	660	620	640	273,988	84,114	292,641	89,841	566,427	173,893
730	32.3	-223	66	66	320	740	699	720	272,678	88,075	291,094	94,023	564,343	182,283

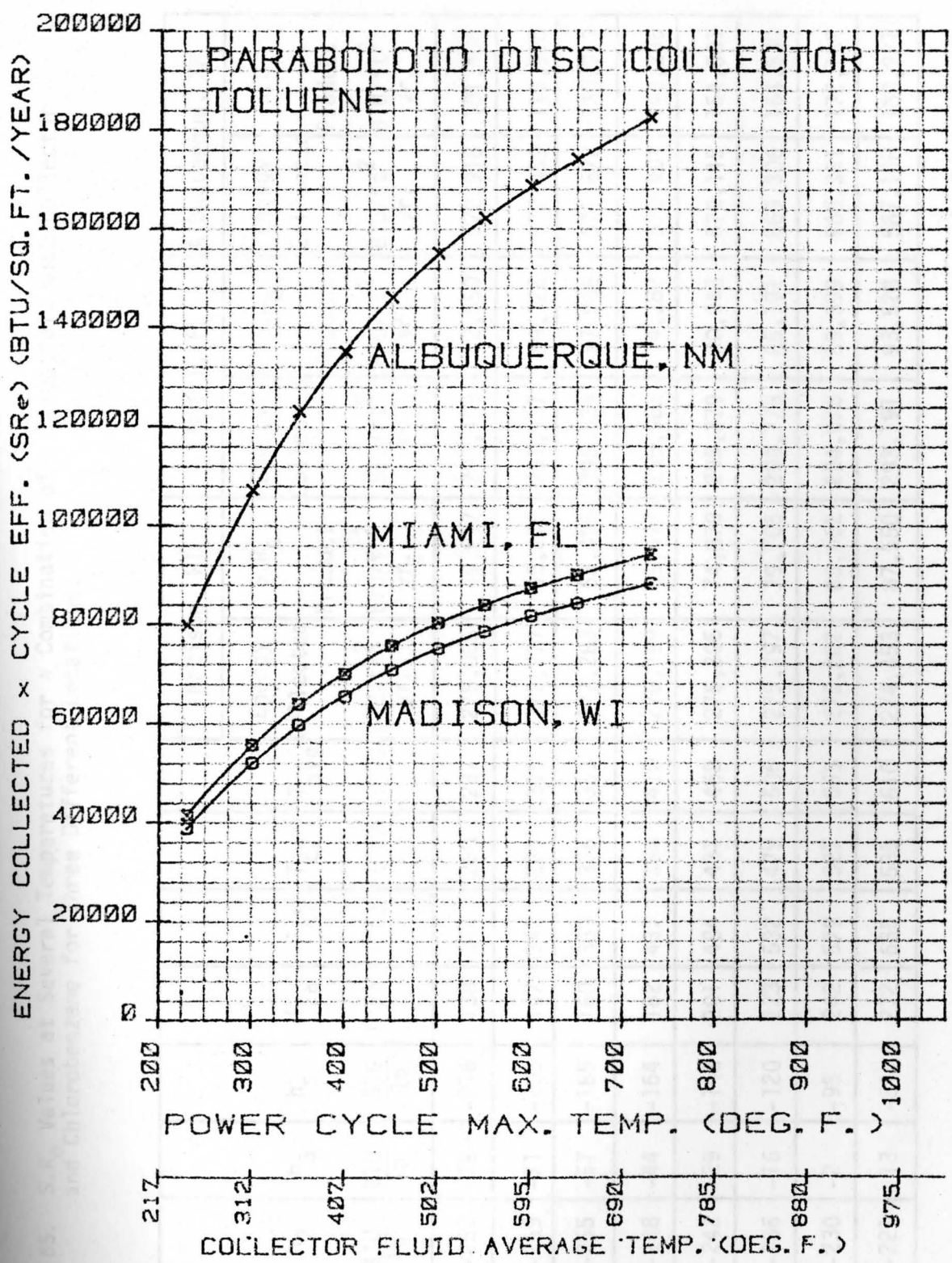


FIGURE 87. Curves of  $S.R_e$  Values vs. Operating Temperature for a Combination of a Paraboloid Disc Collector and Toluene for Three Locations.

TABLE 65. S.R<sub>e</sub> Values at Several Temperatures for a Combination of a Paraboloid Disc Collector and Chlorobenzene for Three Different Locations.

T <sub>3</sub> (°F)	η <sub>Re</sub> (%)	h <sub>2</sub> BTU/Tb	h <sub>3</sub> BTU/Tb	h <sub>s</sub> BTU/Tb	T <sub>2a</sub> (°F)	T <sub>c1</sub> (°F)	T <sub>c2</sub> (°F)	T <sub>avg</sub> (°F)	Madison, WI		Miami, FL		Albuquerque, NM	
									Energy Collected BTU/ft <sup>2</sup> yr.	S.R <sub>e</sub> Product BTU/ft <sup>2</sup> yr.	Energy Collected BTU/ft <sup>2</sup> yr.	S.R <sub>e</sub> Product BTU/ft <sup>2</sup> yr.	Energy Collected BTU/ft <sup>2</sup> yr.	S.R <sub>e</sub> Product BTU/ft <sup>2</sup> yr.
270	17.7	-262	-79	-216	138	314	260	287	278,065	49,217	297,458	52,650	572,918	101,406
300	19.9	-259	-71	-205	147	342	289	315	277,777	55,278	297,117	59,126	572,459	113,918
350	22.9	-255	-57	-185	160	389	336	363	277,283	63,498	296,534	67,906	571,672	130,913
400	25.1	-248	-44	-164	182	437	384	410	276,799	69,477	295,962	74,287	570,902	143,296
450	27.1	-242	-29	-142	201	484	431	458	276,305	74,879	295,379	80,048	570,115	154,501
500	28.9	-236	-16	-120	223	532	479	506	275,797	79,705	294,778	85,191	569,306	164,530
550	30.4	-230	-2	-95	242	579	527	553	275,202	83,662	294,076	89,399	568,361	172,782
610	31.9	-221	13	-64	272	635	585	610	274,453	87,550	293,191	93,528	567,168	180,927

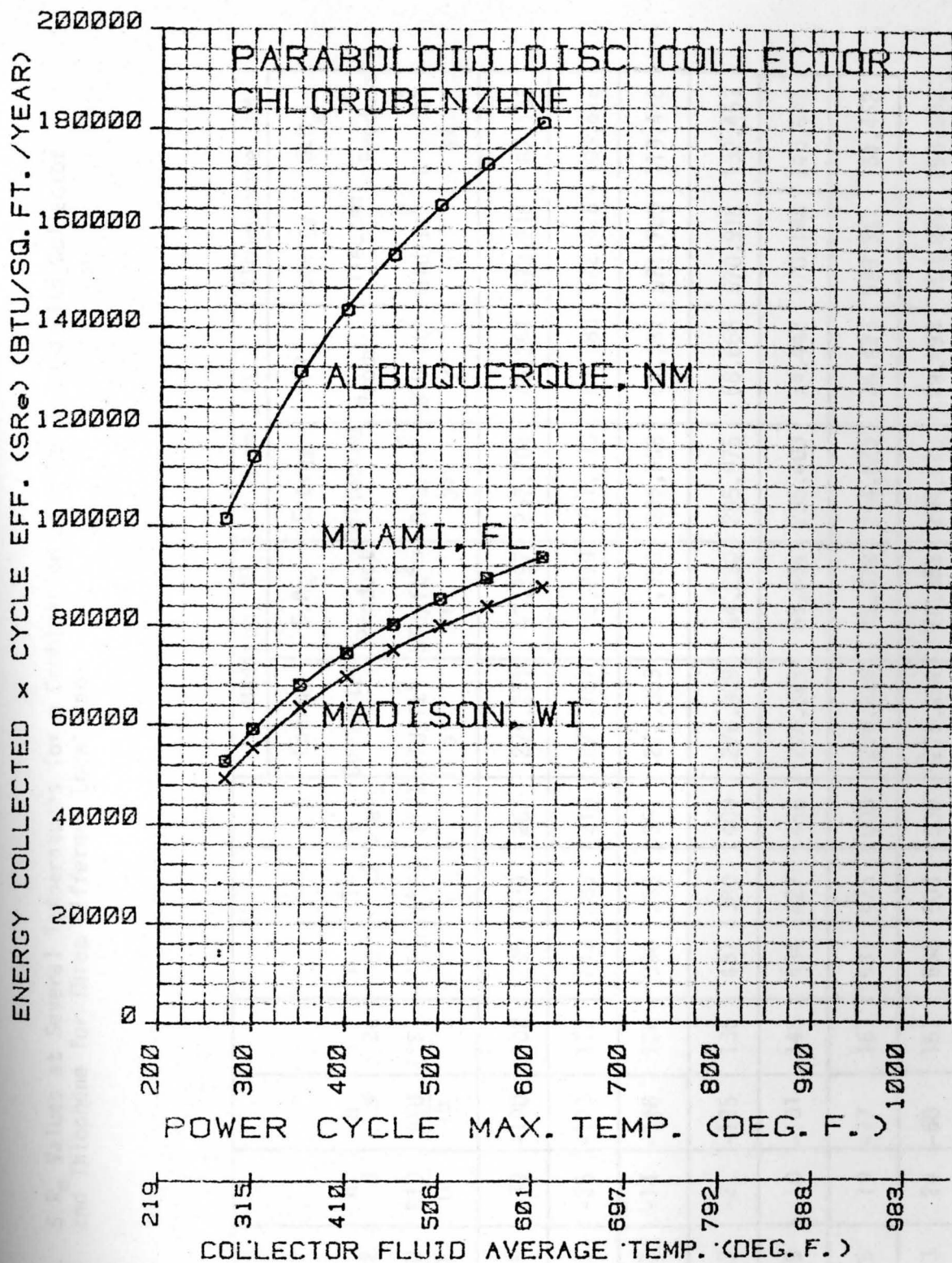


FIGURE 88. Curves of  $S.R_e$  Values vs. Operating Temperature for a Combination of a Paraboloid Disc Collector and Chlorobenzene for Three Locations.

TABLE 66.  $S.R_e$  Values at Several Temperatures for a Combination of a Paraboloid Disc Collector and Thiophene for Three Different Locations.

$T_3$ (°F)	$\eta_{R_e}$ (%)	$h_2$ BTU/lb	$h_3$ BTU/lb	$h_s$ BTU/lb	$T_{2a}$ (°F)	$T_{c1}$ (°F)	$T_{c2}$ (°F)	$T_{avg}$ (°F)	Madison, WI		Miami, FL		Albuquerque, NM	
									Energy Collected BTU/ft <sup>2</sup> yr.	$S.R_e$ Product BTU/ft <sup>2</sup> yr.	Energy Collected BTU/ft <sup>2</sup> yr.	$S.R_e$ Product BTU/ft <sup>2</sup> yr.	Energy Collected BTU/ft <sup>2</sup> yr.	$S.R_e$ Product BTU/ft <sup>2</sup> yr.
250	15.2	-245	-39	-190	102	295	239	267	278,271	42,297	297,701	45,251	573,246	87,133
300	18.1	-241	-26	-170	112	243	286	314	277,787	50,279	297,130	53,780	572,476	103,618
350	20.9	-237	-14	-148	124	390	333	361	277,303	57,956	296,558	61,981	571,705	119,486
400	23.2	-233	-2	-125	136	437	380	409	276,809	64,220	295,975	68,666	570,918	132,453
450	25.2	-229	10	-101	148	484	427	456	276,325	69,634	295,403	74,442	570,148	143,677
500	26.6	-225	19	-77	161	531	475	503	275,835	73,372	294,823	78,423	569,367	151,452
530	27.0	-223	24	-60	167	558	503	530	275,494	74,383	294,420	79,493	568,823	153,582

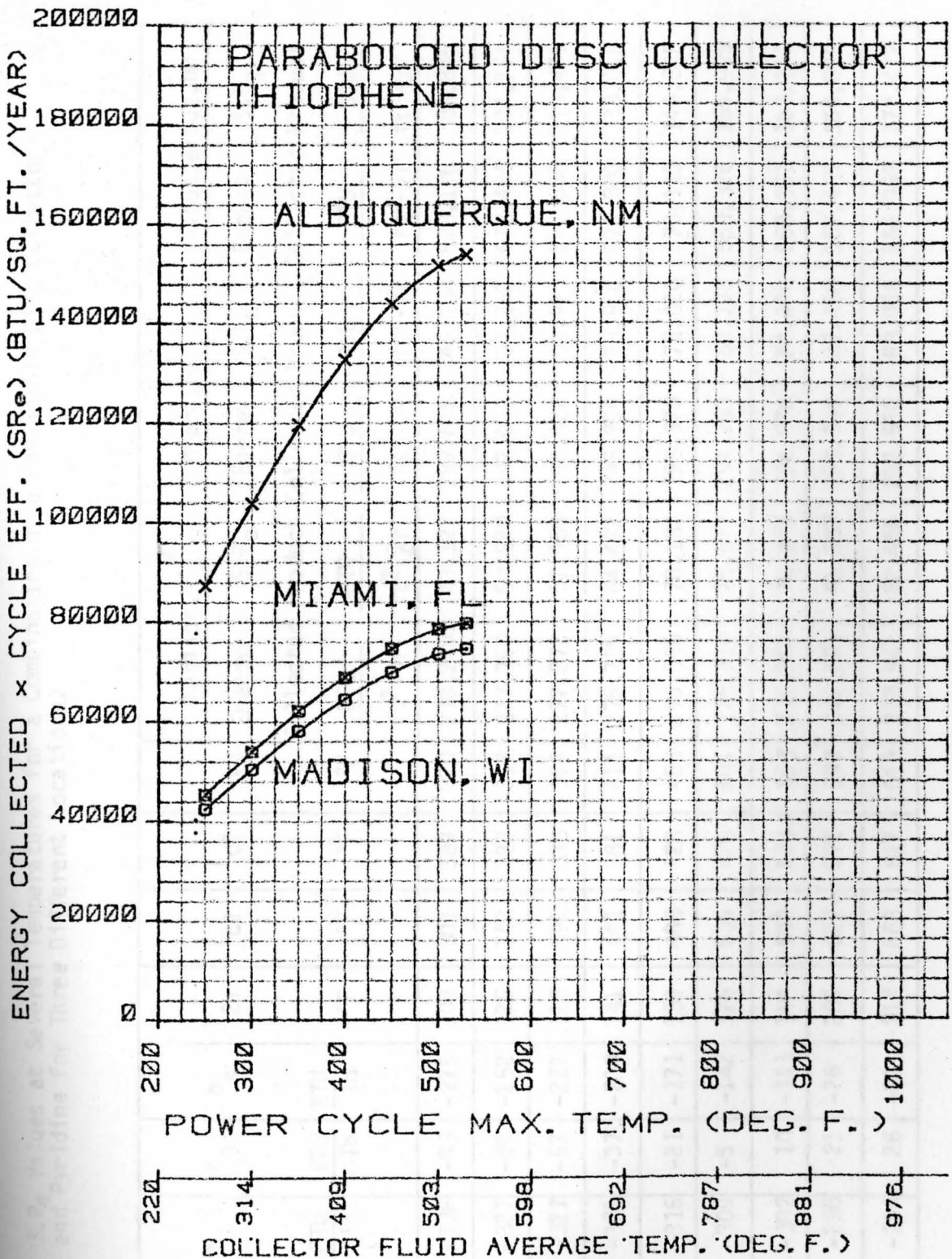


FIGURE 89. Curves of S.R.<sub>e</sub> Values vs. Operating Temperature for a Combination of a Paraboloid Disc Collector and Thiophene for Three Locations.

TABLE 67.  $S.R_e$  Values at Several Temperatures for a Combination of a Paraboloid Disc Collector and Pyridine for Three Different Locations.

$T_3$	$\eta_{Re}$	$h_2$	$h_3$	$h_s$	$T_{2a}$	$T_{c1}$	$T_{c2}$	$T_{avg}$	Madison, WI		Miami, FL		Albuquerque, NM	
									Energy	$S.R_e$	Energy	$S.R_e$	Energy	$S.R_e$
									Collected	Product	Collected	Product	Collected	Product
									$\frac{BTU}{ft^2-yr}$	$\frac{BTU}{ft^2-yr}$	$\frac{BTU}{ft^2-yr}$	$\frac{BTU}{ft^2-yr}$	$\frac{BTU}{ft^2-yr}$	$\frac{BTU}{ft^2-yr}$
°F	(%)	$\frac{BTU}{lb}$	$\frac{BTU}{lb}$	$\frac{BTU}{lb}$	°F	°F	°F	°F	°F	°F	°F	°F	°F	°F
250	15.5	-336	-83	-275	100	301	389	270	278,240	43,127	297,665	46,138	573,196	88,845
300	18.3	-327	-69	-252	125	347	287	317	277,756	50,829	297,093	54,368	572,426	104,754
350	20.9	-327	-57	-227	125	394	333	364	277,272	57,950	296,522	61,973	571,656	119,476
400	23.3	-321	-37	-200	141	441	381	411	276,789	64,492	295,950	68,956	570,886	133,016
450	25.4	-315	-21	-171	159	488	428	458	276,305	70,182	295,379	75,026	570,115	144,808
500	27.4	-309	-5	-142	176	535	476	505	275,810	75,572	294,793	80,773	569,326	155,995
550	28.7	-302	10	-111	194	582	523	553	275,202	78,983	294,076	84,400	568,361	163,120
600	29.8	-296	21	-76	209	627	571	599	274,621	81,337	293,389	87,430	567,435	169,096
650	30.1	-294	26	-20	214	668	617	643	273,941	82,456	292,586	88,068	566,353	170,472



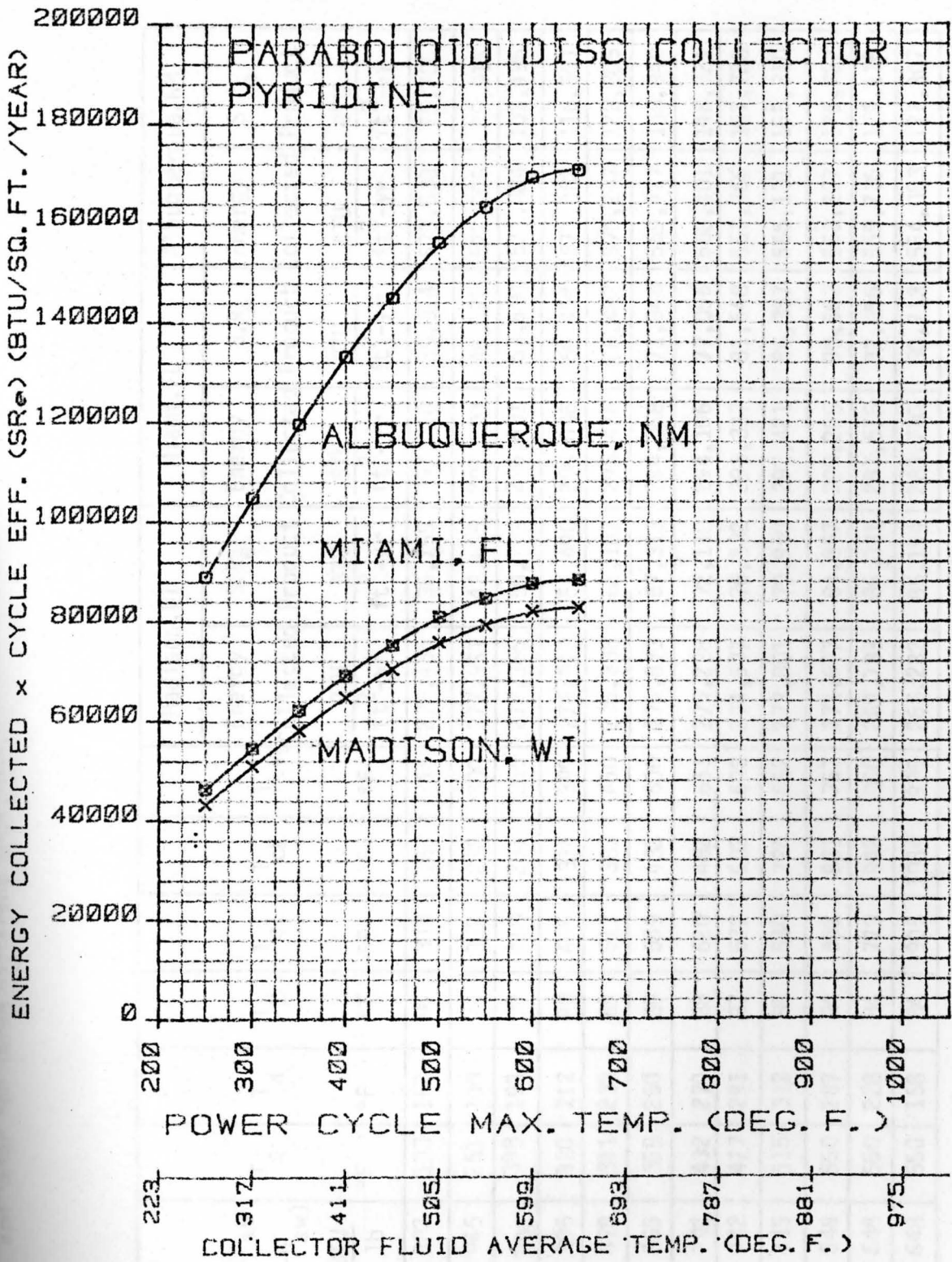


FIGURE 90. Curves of  $S.R_e$  Values vs. Operating Temperature for a Combination of a Paraboloid Disc Collector and Pyridine for Three Locations.

TABLE 63. S:Re Values at Several Temperatures for a Combination of a Parabolic Disc Collector and Water for Three Different Locations.

T <sub>3</sub> or T <sub>5</sub>  °F	η <sub>Re</sub>  (%)	(h <sub>sv</sub> -h <sub>sw</sub> )  BTU lb	T <sub>s</sub>  °F	T <sub>4</sub>  °F	T <sub>2</sub>  °F	T <sub>c1</sub>  °F	T <sub>c2</sub>  °F	T <sub>avg</sub>  °F	Madison, WI		Miami, FL		Albuquerque, NM	
									Energy Collected	S.R <sub>e</sub> Product	Energy Collected	S.R <sub>e</sub> Product	Energy Collected	S.R <sub>e</sub> Product
									$\frac{\text{BTU}}{\text{ft}^2\text{-yr}}$	$\frac{\text{BTU}}{\text{ft}^2\text{-yr}}$	$\frac{\text{BTU}}{\text{ft}^2\text{-yr}}$	$\frac{\text{BTU}}{\text{ft}^2\text{-yr}}$	$\frac{\text{BTU}}{\text{ft}^2\text{-yr}}$	$\frac{\text{BTU}}{\text{ft}^2\text{-yr}}$
300	13.2	982	193	162	90	303	183	248	278,450	36,755	297,910	39,324	573,530	75,706
350	15.7	945	251	180	90	362	233	300	277,931	43,635	297,300	46,676	572,705	89,915
400	18.1	905	308	193	90	413	291	355	277,365	50,203	296,631	53,690	571,804	103,496
450	20.4	895	320	212	90	465	334	399	276,912	56,490	296,096	60,404	571,082	116,501
500	22.5	878	341	233	89	517	383	450	276,388	62,187	295,476	66,482	570,247	128,305
550	24.4	855	369	250	89	569	432	500	275,873	67,313	294,868	71,948	569,427	138,940
600	26.2	792	432	270	88	620	482	551	275,228	72,110	294,106	77,056	568,401	148,921
650	27.8	742	477	291	87	672	532	602	274,577	76,332	293,337	81,548	567,366	157,728
700	29.2	715	515	312	85	580	724	652	273,801	79,950	292,421	85,387	566,131	165,310
800	31.2	648	550	287	84	682	831	757	271,977	84,857	290,266	90,563	563,227	175,727
900	32.0	648	550	228	84	779	942	860	269,783	86,331	287,675	92,056	559,736	179,115
1030	32.0	648	550	158	84	905	1084	995	266,232	85,194	283,780	90,713	554,083	177,307

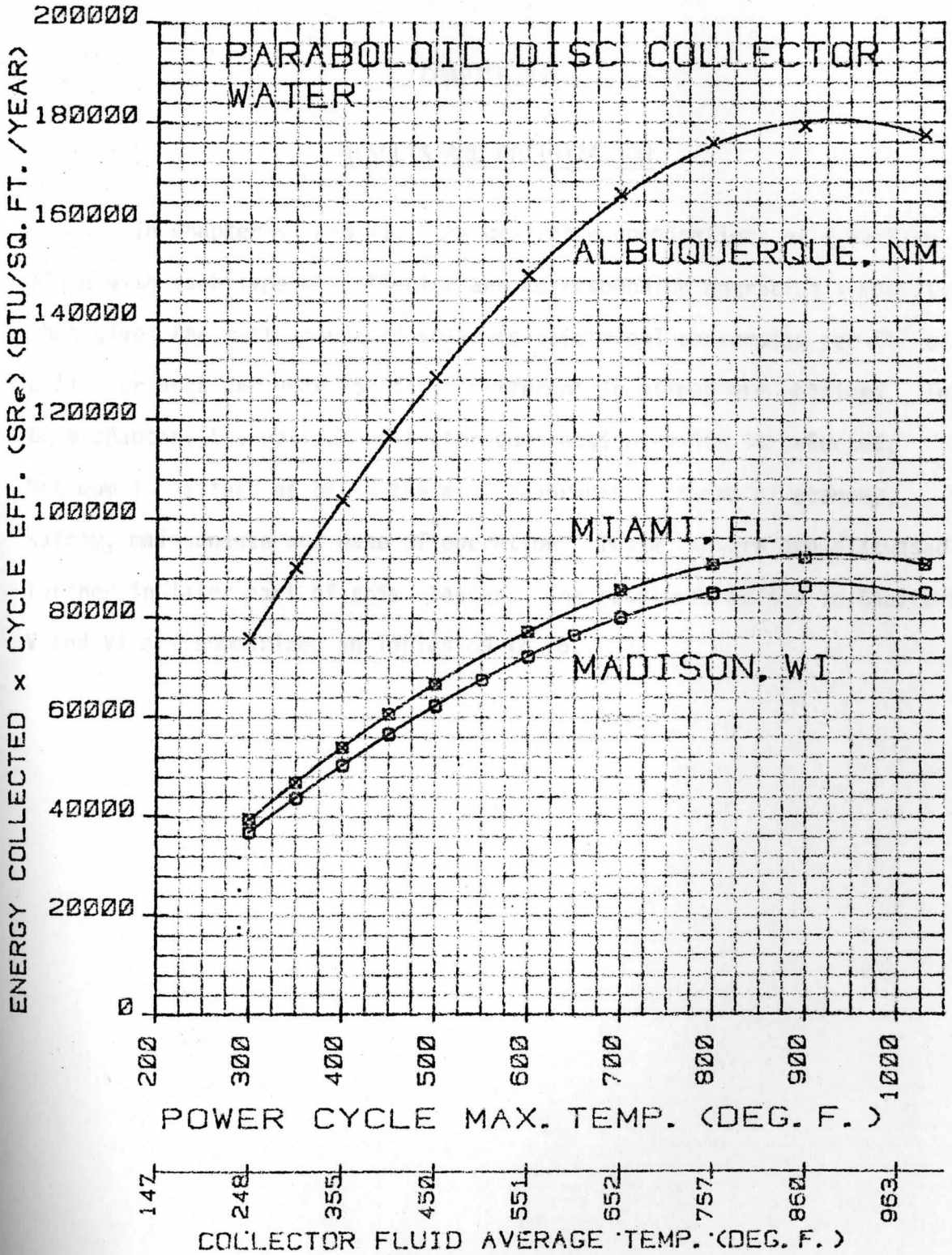


FIGURE 91. Curves of S.R<sub>e</sub> Values vs. Operating Temperature for a Combination of a Paraboloid Disc Collector and Water for Three Locations.

CHAPTER VII

RESULTS AND OPTIMIZATION

In Chapter V and VI, the desirable combinations of a working fluid with each type of collector and corresponding operating temperature that gives the most amount of solar-to-electrical conversion per ft<sup>2</sup> of collector area per year for three different locations are obtained. In this chapter, the optimum collector combination system is selected. Optimum is defined as being the most favorable in terms of economy, safety, maintenance and ease of operation. These factors are discussed further in later part of this chapter. The results obtained in Chapters V and VI are summarized in Tables 69 to 76.

Collector	Fluid	Temp (°C)	Area (ft <sup>2</sup> )	Output (kWh)	Efficiency (%)
Flat-plate	Toluene	240	74,700	770	15,940
	Dichlorobenzene	230	74,800	715	15,700
	Thiophene	210	75,000	710	15,350
	Pyridine	235	75,000	735	15,650
	Water	300	75,000	740	17,100
	R-11	255	75,000	730	15,100
	R-12	275	75,000	720	17,250
	R-113	230	75,000	730	16,400
	Toluene	250	75,000	740	16,250
	Dichlorobenzene	245	75,000	700	20,000
Cylindrical	Thiophene	255	75,000	740	21,000
	Pyridine	230	75,000	730	21,000
	Water	300	75,000	750	17,300
	R-11	250	75,000	730	17,300
	R-12	270	75,000	730	17,300
	R-113	230	75,000	730	16,400
	Toluene	250	75,000	740	16,250
	Dichlorobenzene	245	75,000	700	20,000
	Thiophene	255	75,000	740	21,000
	Pyridine	230	75,000	730	21,000

TABLE 69. Summary of Maximum S.R. Values and Corresponding Optimum Temperature for all Possible Combinations Using Rankine-Cycle.

Type of Collector	Rankine-Cycle Working Fluid	Madison WI		Miami FL		Albuquerque NM	
		Optimum Temperature °F	(S.R) BTU/ft <sup>2</sup> -yr	Optimum Temperature °F	(S.R) BTU/ft <sup>2</sup> -yr	Optimum Temperature °F	(S.R) BTU/ft <sup>2</sup> -yr
Flat Plate Collector	R-11	160	8550	165	12,900	180	19,733
	R-12	165	8250	170	12,400	190	18,600
	R-113	150	9400	150	14,000	170	20,450
CPC Collector	R-11	230	14,500	230	18,700	260	31,100
	R-12	210	13,300	210	17,200	220	27,000
	R-113	220	14,150	210	18,300	235	29,200
	Toluene	240	14,700	230	18,900	270	32,350
	Chlorobenzene	239	14,800	239	18,700	280	33,700
	Thiophene	220	15,000	220	19,350	270	32,900
	Pyridine	239	15,500	239	19,850	239	33,100
Water	300	9,500	300	12,100	350	20,300	
Parabolic Trough Collector	R-11	255	17,900	240	19,700	280	44,550
	R-12	225	15,700	220	17,400	230	36,500
	R-113	230	17,100	230	18,900	255	40,700
	Toluene	260	18,500	250	20,250	290	46,700
	Chlorobenzene	269	19,100	269	20,800	310	49,200
	Thiophene	255	18,800	245	20,600	300	47,600
	Pyridine	239	19,200	239	21,050	290	47,350
Water	330	11,800	325	12,000	370	30,000	
Paraboloid disc Collector	Toluene	730	68,200	730	72,800	730	141,130
	Chlorobenzene	610	72,200	610	77,125	610	149,200
	Thiophene	530	68,050	530	72,725	530	140,500
	Pyridine	650	73,155	650	78,135	650	151,236
	Water	1030	77,400	1030	82,500	1030	161,000

TABLE 70. Optimum Working Fluid and Corresponding Rankine-Cycle Maximum Temperature for Each Type of Collector Using Rankine-Cycle for Madison, WI.

Type of Collector	Optimum Rankine-Cycle Working Fluid	Maximum S.R. Value (BTU/ft <sup>2</sup> /yr)	Corresponding Rankine-Cycle Max. Temp. (°F)
Flat Plate	R-113	9,400	150
CPC	Pyridine	15,500	239
Parabolic Trough	Pyridine	19,200	239
Paraboloid Disc	Water	77,400	1030

TABLE 71. Optimum Working Fluid and Corresponding Rankine-Cycle Maximum Temperature for Each Type of Collector Using Rankine-Cycle for Miami, FL.

Type of Collector	Optimum Rankine-Cycle Working Fluid	Maximum S.R. Value (BTU/ft <sup>2</sup> /yr)	Corresponding Rankine-Cycle Max. Temp. (°F)
Flat Plate	R-113	14,000	150
CPC	Pyridine	19,850	239
Parabolic Trough	Pyridine	21,050	239
Paraboloid Disc	Water	82,500	1030

TABLE 72. Optimum Working Fluid and Corresponding Rankine-Cycle Maximum Temperature for Each Type of Collector Using Rankine-Cycle for Albuquerque, NM.

Type of Collector	Optimum Rankine-Cycle Working Fluid	Maximum S.R. Value (BTU/ft <sup>2</sup> /yr)	Corresponding Rankine-Cycle Max. Temp. (°F)
Flat Plate	R-113	20,450	170
CPC	Chlorobenzene	33,700	280
Parabolic Trough	Chlorobenzene	49,200	310
Paraboloid Disc	Water	161,000	1030

TABLE 73. Summary of Maximum  $S.R_e$  Values and Corresponding Optimum Temperature for all Possible Combinations Using Rankine-Cycle with Regeneration or Reheat Loop.

Type of Collector	Rankine-Cycle Working Fluid	Madison WI		Miami FL		Albuquerque NM	
		Optimum Temperature °F	$S.R_e$ Value BTU/ft <sup>2</sup> -Yr.	Optimum Temperature °F	$S.R_e$ Value BTU/ft <sup>2</sup> -Yr.	Optimum Temperature °F	$S.R_e$ Value BTU/ft <sup>2</sup> -Yr.
Flat Plate Collector	R-11	165	8,550	170	12,950	185	19,850
	R-12	165	8,250	170	12,400	190	18,600
	R-113	160	9,650	160	14,500	180	21,750
CPC Collector	R-11	235	14,900	230	19,200	265	32,200
	R-12	210	13,300	210	17,200	220	27,000
	R-113	220	15,600	215	20,000	245	32,600
	Toluene	250	15,650	240	20,000	280	35,000
	Chlorobenzene	275	15,800	269	20,000	295	37,000
	Thiophene	235	15,200	230	19,600	275	33,600
	Pyridine	239	15,500	239	19,900	265	33,800
Water	300	14,600	300	18,800	310	31,000	
Parabolic Trough Collector	R-11	260	18,600	255	20,350	280	46,300
	R-12	225	15,700	220	17,400	230	36,500
	R-113	240	19,000	230	21,000	265	45,900
	Toluene	270	19,800	260	21,600	310	51,200
	Chlorobenzene	290	20,800	285	22,500	310	55,000
	Thiophene	260	19,100	250	20,900	310	49,200
	Pyridine	240	19,360	240	21,250	300	49,000
Water	300	18,000	300	19,800	355	44,600	
Paraboloid disc Collector	Toluene	730	88,100	730	94,000	730	182,300
	Chlorobenzene	610	87,550	610	93,528	610	180,927
	Thiophene	530	74,383	530	79,493	530	153,382
	Pyridine	650	82,456	650	88,068	650	170,472
	Water	925	87,000	950	93,000	925	180,500

TABLE 74. Optimum Working Fluid and Corresponding Power-Cycle Maximum Temperature for Each Type of Collector Using Rankine-Cycle with Regenerator or Reheat Loop for Madison, WI

Type of Collector	Optimum Working Fluid	Maximum S.R. <sub>e</sub> Value (BTU/ft <sup>2</sup> /yr)	Corresponding Power-Cycle Max. Temperature (°F)
Flat Plate	R-113	9,650	160
CPC	Chlorobenzene	15,800	275
Parabolic Trough	Chlorobenzene	20,800	290
Paraboloid Disc	Toluene	88,100	730

TABLE 75. Optimum Working Fluid and Corresponding Power-Cycle Maximum Temperature for Each Type of Collector Using Rankine-Cycle with Regenerator or Reheat Loop for Miami, FL.

Type of Collector	Optimum Working Fluid	Maximum S.R. <sub>e</sub> Value (BTU/ft <sup>2</sup> /yr)	Corresponding Power-Cycle Max. Temperature (°F)
Flat Plate	R-113	14,500	160
CPC	Toluene	20,000	240
Parabolic Trough	Chlorobenzene	22,500	285
Paraboloid Disc	Toluene	94,000	730

TABLE 76. Optimum Working Fluid and Corresponding Power-Cycle Maximum Temperature for Each Type of Collector Using Rankine-Cycle with Regeneration or Reheat Loop for Albuquerque, NM.

Type of Collector	Optimum Working Fluid	Maximum S.R. <sub>e</sub> Value (BTU/ft <sup>2</sup> /yr)	Corresponding Power-Cycle Max. Temperature (°F)
Flat Plate	R-113	21,750	180
CPC	Chlorobenzene	37,000	295
Parabolic Trough	Chlorobenzene	55,000	310
Paraboloid Disc	Toluene	182,300	730



These results (Tables 69 to 76) are now compared with each other in terms of economy, safety, maintenance and ease of operation, which are now discussed in more detail.

### Economics

It is not intended here to compare economics of a solar system with a conventional system. Rather, economics of one collector combination system (given in Tables 70 to 72) are compared with that of others to arrive at the least expensive system for a unit power output.

In a solar system, the main cost factors involved are:

- 1) capital cost of the system for a unit power output and,
- 2) maintenance cost every year for a unit power output.

Other minor factors, such as, tax credit, salvation value, etc. can be neglected as their values will be almost the same in each case and thus need not be considered for a relative comparison. The life expectancy of all four types of collectors considered here is 20 years.

The first cost of the system is made of

- 1) the cost of the Rankine-cycle components and,
- 2) the cost of the solar collectors.

According to Alvis, the cost of the Rankine-cycle in production will be on the average less than 15% of the total system cost for small scale power units of about 100 KW.<sup>15</sup> Cost of the solar collectors will make up more than 85% of the total system cost. For a certain power

---

<sup>15</sup>R.L. Alvis, "Solar Irrigation Program Status Report", Oct. 1977, Sandia Report SAND 78-0049.

output system, Rankine-cycle components for all systems will be the same except few minor changes as might be required to make system adaptable to a particular working fluid. As the cost of the Rankine-cycle is only 15% of the total system cost, these slight variations in cost can be neglected. Thus, the cost of the Rankine-cycle components is the same in all cases and need not be considered for a relative comparison of different systems.

Maintenance requirements of the Rankine-cycle components will be almost the same in each case and as life expectancy of the system is also the same, making this cost to be common and thus, it need not be considered for a relative comparison. Maintenance cost of the collectors as it relates to routine cleaning of the collector arrays is practically the same for all types of collectors and so it is common in all cases and thus need not be considered for a relative comparison. Maintenance cost, as it relates to breakage or malfunction in the tracking mechanism of collector arrays, differs considerably from one type of collector to the other. Parabolic trough and paraboloid disc collectors, because of their tracking requirements, have greater maintenance cost than stationary mounted flat plate or CPC collectors. However, a well designed collector system having adequate automatic controls will have very low maintenance cost compared to their first cost. Since the solar industry is relatively a new industry, these maintenance costs have not been well established. Therefore, this factor is not quantitatively analyzed. It is only subjectively treated along with the other factors, such as, the ease of operation, as discussed later in this chapter.

Thus, economics of system combinations given in Table 70 to 72 and Tables 74 to 76 can be compared by comparing only the first cost of the collectors per unit power output. The first cost of the collectors

varies considerably depending upon the quantity of collectors purchased. The average costs of different collectors as of March 1981, for quantity requirements of about 50 KW peak power output unit are:

Flat plate collector	\$17/ft <sup>2</sup>
CPC collector	\$28/ft <sup>2</sup>
Parabolic trough	\$40/ft <sup>2</sup>
Paraboloid disc	\$65/ft <sup>2</sup>

$$\frac{\text{Capital cost of the collector}}{\text{power output}} = \left( \frac{\text{Capital cost of the collector}}{\text{ft}^2} \right) \times \left( \frac{\text{year unit area}}{\text{Energy collected by the collector}} \times \text{Rankine-cycle efficiency} \right)_{\text{optimum}}$$

$$= \left( \frac{\text{Capital cost of the collector}}{\text{ft}^2} \right) \times \left( \frac{1}{(\text{S.R.}) \text{ value}} \right)_{\text{optimum}}$$

For a system that produces say, 5000 KWH of net energy per year, (average electrical consumption of a family in the United States), the first cost of collectors is computed for all systems that are given in Tables 70 to 72 and Tables 74 to 76. These costs are shown in Tables 77 and 78.

TABLE 77. First Cost of Different Types of Collectors Using Rankine-Cycle for 5000 KWH Output Per Year at Three Different Locations. (\$)

Type of Collector	Madison WI	Miami FL	Albuquerque NM
Flat Plate	30,862	20,722	14,186
CPC	30,827	24,072	14,179
Parabolic Trough	35,552	32,428	13,874
Paraboloid Disc	14,331	13,445	6,000

TABLE 78. First Cost of Different Types of Collectors Using Rankine-Cycle with Regeneration or Reheat Loop for 5000 KWH Output Per Year at Three Different Locations (\$

Type of Collector	Madison WI	Miami FL	Albuquerque NM
Flat Plate	30,063	20,007	13,338
CPC	30,242	23,891	12,914
Parabolic Trough	32,817	30,338	12,411
Paraboloid Disc	12,590	11,800	6,085

Thus, for all locations, paraboloid disc has the least cost per unit power output among all collectors. Although economy is the most important factor, certain other tradeoffs mentioned below need to be considered before choosing one over the rest.

#### Safety (as it Relates to the Use of a Working Fluid)

Refrigerants R-11, R-12 and R-113 are non-flammable, but toxic to a degree and have low disintegration temperatures. They have high proven performance in refrigeration cycles. Chlorobenzene, Thiophene, Toluene and Pyridine are flammable, more toxic than refrigerents and have high disintegration temperature. They do not have much proven performance in power cycles. Water is non-inflammable, non-toxic, has a very high disintegration temperature and proven performance in power cycles for many decades.

As the system is a closed type, safety can be assumed by safety devices and proper care in design and fabrication of the system.

### Maintenance and Ease of Operation.

Flat plate collectors are simplest in their operation, have least maintenance requirements and also have the highest proven performance among all collectors. CPC collectors are simple in their operation, have low maintenance requirements, but do not have high performance records. Parabolic trough collectors due to diurnal tracking requirements are little more complex and have more maintenance requirements than flat plate or CPC collectors. Paraboloid disc collectors due to two axes diurnal tracking requirements are the most complex, have the most maintenance requirements and have the least proven performance among all collectors.

All collectors are provided with automatic controls and so do not require constant attention. In a well designed system, the maintenance cost as it relates to collectors and its tracking mechanism is a very small fraction of the first cost.

Thus, the factors, such as, — safety, maintenance and ease of operation — will have to be treated only subjectively; their influence is dependent upon the end use and how one weighs different factors.

Thus, a selection of a particular system for use in particular location can be made mainly based upon the economics presented in Tables 77 and 78 and after the subjective evaluation of the other factors.

## CHAPTER VIII

### DISCUSSIONS AND CONCLUSIONS

This thesis dealt with the thermal analysis of a Solar Rankine-Cycle System for solar-to-electrical conversion. This system basically consists of solar collectors for energy collection and Rankine-cycle for thermal to electrical (or mechanical) energy conversion. In this analysis four different types of solar collectors and eight different Rankine-cycle working fluids with two different power cycles for three climatically different cities are considered. The objective of the analysis was aimed at obtaining the optimum combinations of solar collector, Rankine-cycle working fluid and the operating temperature for a given climatic location. The results of optimum sets of combinations are presented in Table 69 through 78 in the previous chapter.

On observing the results of these analyses, it is evident that economically, the paraboloid disc collectors are the best among all collectors for solar-to-electrical conversion for any location. They have far lower first cost per unit power output than any other type of solar collector and for any location (See Tables 77 and 78). On average, the first cost per unit power output for paraboloid disc collector is less than half of that of other collectors. The following are the two main factors that contribute towards high efficiency of a paraboloid disc collector.

- i) The receiver area in a paraboloid disc collector is far less than the receiver area in a flat plate collector. It has therefore, lower heat losses and thus can attain high efficiency even at high temperatures. Besides, the Rankine-cycle efficiency is higher at higher available heat source tempera-

tures as can be readily available from paraboloid disc collectors. Thus, the combination of a high collector efficiency and high power cycle efficiency results in the highest overall solar-to-electrical conversion.

- ii) By virtue of the two axes diurnal tracking, paraboloid disc collectors always face normal to the sun, intercepting the most amount of possible radiation for a given collector area. Other collectors make certain angle,  $\theta$ , with sunrays, thus reducing solar radiation incident on the collector plane by a factor of  $\cos \theta$ . The significance of this effect can be seen from the comparison of the results of solar energy collected by parabolic trough collector and paraboloid disc collector. For example, at Albuquerque, NM, for collector fluid average temperature of  $400^{\circ}\text{F}$ , parabolic trough collector can collect 198,188 BTU per  $\text{ft}^2$  area per year compared to 571,066 BTU per  $\text{ft}^2$  area per year by paraboloid disc collector. (See Figures 38, 39, 40)

The additional cost involved in paraboloid disc collectors is the cost of the structure and controls for two axes diurnal tracking. The simple economic analysis points out that this additional cost is far outweighed by the additional energy collected.

The paraboloid disc collectors are therefore recommended for solar-to-electrical conversion. However, because of the complexity of these collectors, they are not well accepted among people and consequently not much used for solar-to-electrical conversion. As such, these collectors are now commercially available and quite similar to other collectors, equipped with controls for a complete automatic operation. Maintenance

cost, although certainly higher in paraboloid disc collectors than in non-tracking collectors, the advantage of increased efficiency will far outweigh the additional maintenance costs.

As expected, the other three collectors — flat plate, CPC and parabolic trough — produce higher solar-to-electrical conversion efficiency in the increasing order of concentration. (See Tables 69 and 73) However, the average cost of the collectors increases at about the same rate and consequently, there is not much difference in the cost per unit power output. (See Tables 77 and 78)

If paraboloid disc collectors are not to be used, it is recommended to use flat plate solar collectors since their cost is lower or compares very well to the other two types of collectors. The flat plate collectors are simple in their operation and has low maintenance cost due to no-tracking requirements. For a sunny location, such as, Albuquerque, NM, the CPC and parabolic trough collectors are slightly better in terms of economics than flat plate collectors. (See Tables 77 and 78) However, the other advantages of flat plate collector will easily outweigh the economic disadvantage.

At high temperatures, the performance of water as a power cycle working fluid exceeds or compares very well to organic fluids. (See Tables 69 and 73) The use of organic fluids is limited by their disintegration temperatures. Also, after the heat source temperature exceeds their critical temperature (different from disintegration temperature) their ability to increase cycle efficiency levels off. Water then holds an advantageous position because of its high disintegration temperature and high critical pressure.

Water is therefore, recommended to be used as a power cycle working fluid with paraboloid disc collectors, either in a Rankine or reheat cycle



Toluene offers about 1.5% higher  $S.R_e$  value than water. (See Table 73) However, the superior physical qualities of water compared to organic fluids — toluene — will easily outweigh the slight higher  $S.R_e$  value offered by Toluene.

With low temperature collectors, such as, CPC and parabolic trough collectors, water is far inferior to organics in a simple Rankine-cycle. (See Table 69) On average, water produces 40% less S.R values compared to that by an organic fluid.

The difference in the performance among most of the organic fluids is very little — about 4%. (See Tables 69 and 73) Consequently, the other properties of the fluids such as, specific heat, viscosity, relative toxicity, flash point temperature, relative cost and saturation pressure at the heat source will have significant influence on the final decision.

The efficiency of a Rankine-cycle (or Rankine-cycle with regeneration or reheat loop) is a complex function of many of the properties of the working fluid. However, a certain trend in the efficiency results can be observed that can be related to the strong influence of two properties: a) saturation pressure at the available heat sink temperature (i.e. at the condenser) and b) the slope of the saturation vapor line on a T-s diagram. For low condenser pressures and high positively sloped saturation vapor line at the heat sink temperature, high power cycle efficiencies are observed. However, at lower heat sink pressure at an available heat sink temperature, the lower will be the saturation pressure at the available heat source temperature (i.e turbine pressure). As mentioned earlier, turbines require certain minimum pressure to function. So fluids may be constrained by a certain minimum heat source temperature that corresponds to a minimum requirement of the turbine pressure. This is the reason why

toluene, chlorobenzene, pyridine and thiophene will not be competitive with refrigerant fluids with flat plate collectors. Thus, a general conclusion regarding the use of organic fluids with the Rankine-cycle can be reached with some precautions. Among all available candidate working fluids that can produce high enough saturation pressure at the optimum heat source temperature, the fluid having a combination of low saturation pressure at the available heat sink temperature and high positive (or low negative) saturation vapor line slope is likely to give the highest power cycle efficiency. However, it must be understood that many other properties of the fluid also influence the overall cycle efficiency. Nevertheless, as revealed in the results, the difference would be very small and as mentioned earlier, many of the other qualities of the fluid will have a significant influence over the final decision.

Regeneration cycle certainly produces better results with organics. However, the difference is significant only at high temperatures. As can be seen in the results, for locations having low solar insolation such as, Madison, WI, and Miami, FL, the optimum operating temperature is relatively low, so the improvement that regeneration makes is very small. However, for a sunny and dry location, such as, Albuquerque, NM, the optimum operating temperature is relatively higher and regeneration is very beneficial. The one-step reheat cycle is very effective in increasing the overall efficiency of the water/steam power cycle. It puts water in a very competitive position. Evaluating the results shown in Table 73, it can be seen that the  $S.R_e$  values obtained by use of water are comparable to that of organic fluids especially for cloudy locations. For example, the  $S.R_e$  value for a CPC collector at Madison, WI, using water ( $14,600 \text{ BTU/ft}^2\text{-hr}$ ) is about 7.5% lower than that obtained by the optimum fluid-chlorobenzene

(15800 BTU/ft<sup>2</sup>-year). The final decision after considering many of the good qualities of water may very well shift in favor of using water and a reheat cycle even at low temperatures available by use of CPC and parabolic trough collectors. Finally, it is to be noted that only three climatically different locations are considered. However, evaluation of the results suggests that the results can be extended for any location since there is no significant change in the optimum sets of combinations from one location to the other. At low temperatures, the choice of an optimum fluid shifts from one organic fluid to the other, but, the difference is very small. It can also be seen that the optimum operating temperature decreases slightly as the location gets cloudier. If absolute S.R or S.R<sub>e</sub> values are desired for any other location, they can be obtained by comparing the average solar insolation, K<sub>T</sub> value of the location and the average ambient temperature with those of the above three locations considered here.

### Recommendation

The thermal and frictional losses in this study are neglected. As mentioned earlier, in arriving at the optimum sets of combinations, this has very little effect since the losses are almost the same and has no effect in relative comparison. However, this study can be extended to include economic comparison with conventional fuels. The absolute values of overall solar-to-electrical conversion would then be necessary; frictional and thermal losses must be then considered.

The pump power is a function of the viscosity and specific heat of the fluid. Some of the organic fluids have very high viscosity at low temperatures. As the pump power is very small compared to turbine power output in a Rankine-cycle, the variation in these properties will have

no significant effect on the optimum. However, this study can be refined to include the effect of these properties and obtain absolute values of overall solar-to-electrical conversion, so that solar economics can be compared to conventional fuels.

The transient effect of the system components is not considered here. This study can be refined to include the transient effect of solar collectors, storage tanks, heat exchangers, etc.

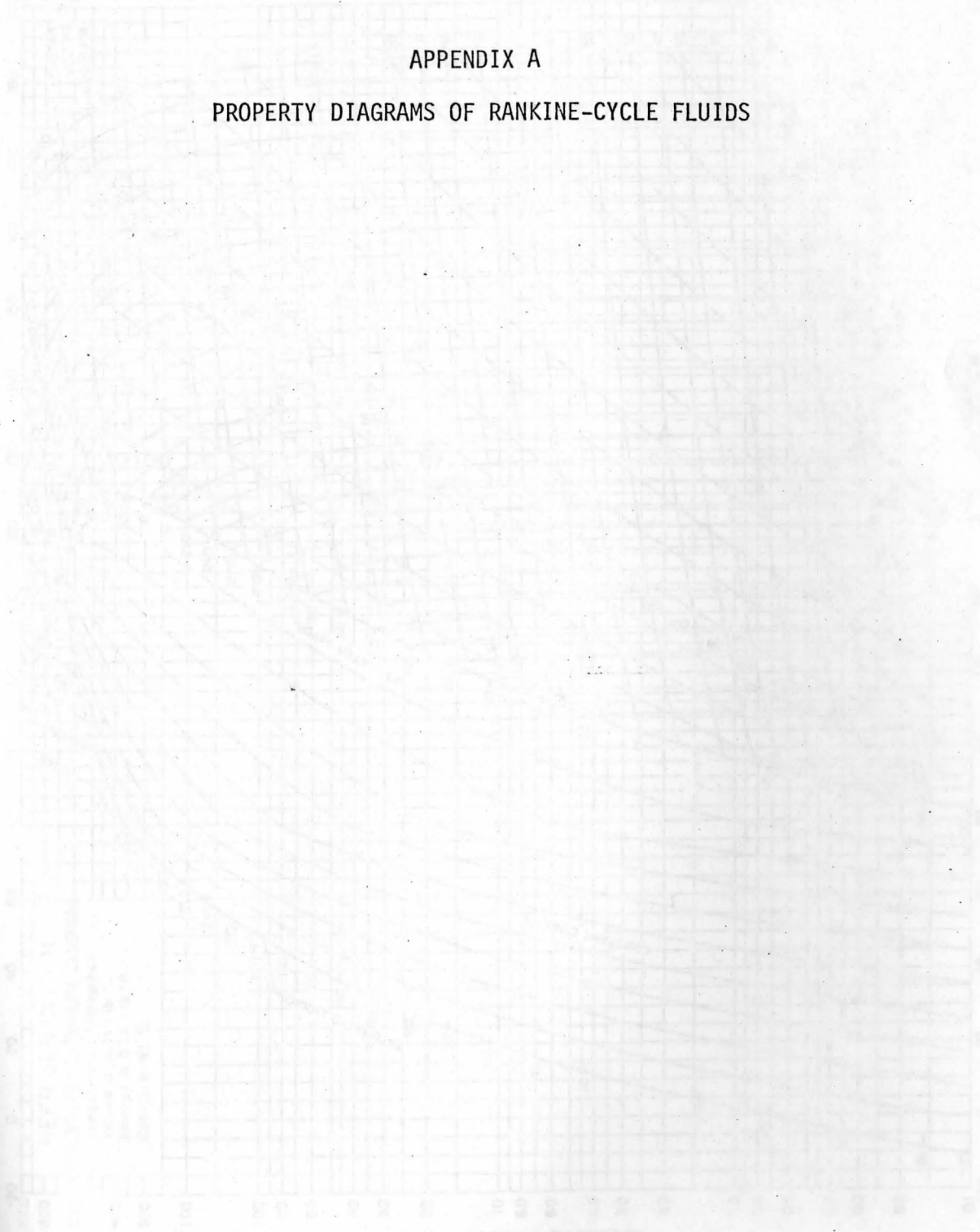
A computer program called 'TRNSYS' (Transient System Simulation) has been developed by the University of Wisconsin to analyze the transient response of many of the solar system components. Use of this program is highly recommended for better accuracy.

In this study, the effect of the condenser cooling fluid temperature is not considered; this temperature is fixed at 90°F throughout the year. However, it is envisaged from the results obtained here that the condenser temperature may have significant effect on the absolute values of the overall solar-to-electrical conversion. Again, 'TRNSYS' program can be used to determine the effect of condenser fluid temperature on the absolute values of overall solar-to-electrical conversion.

Further studies can be oriented toward the development of organic fluids for power cycles that are non-flammable, non-toxic, low in cost and having high disintegration temperature and high positive sloped saturation vapor line curve on a T-s diagram similar to the way refrigerant fluids were developed.

APPENDIX A

PROPERTY DIAGRAMS OF RANKINE-CYCLE FLUIDS



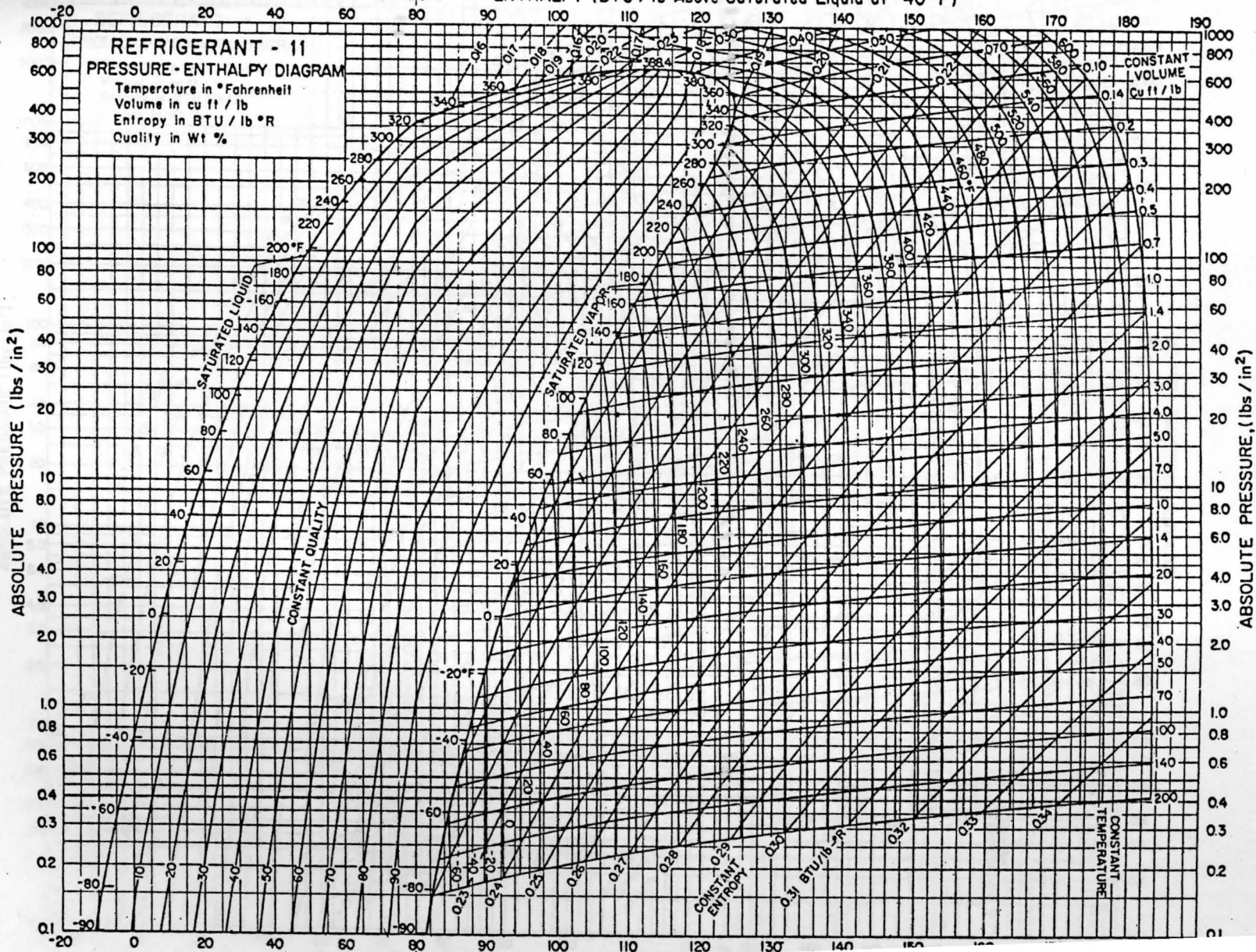
Pressure-Enthalpy Diagram for H<sub>2</sub>O

SCALE CHANGE

ENTHALPY (BTU/lb Above Saturated Liquid at -40°F)

**REFRIGERANT - 11**  
**PRESSURE-ENTHALPY DIAGRAM**

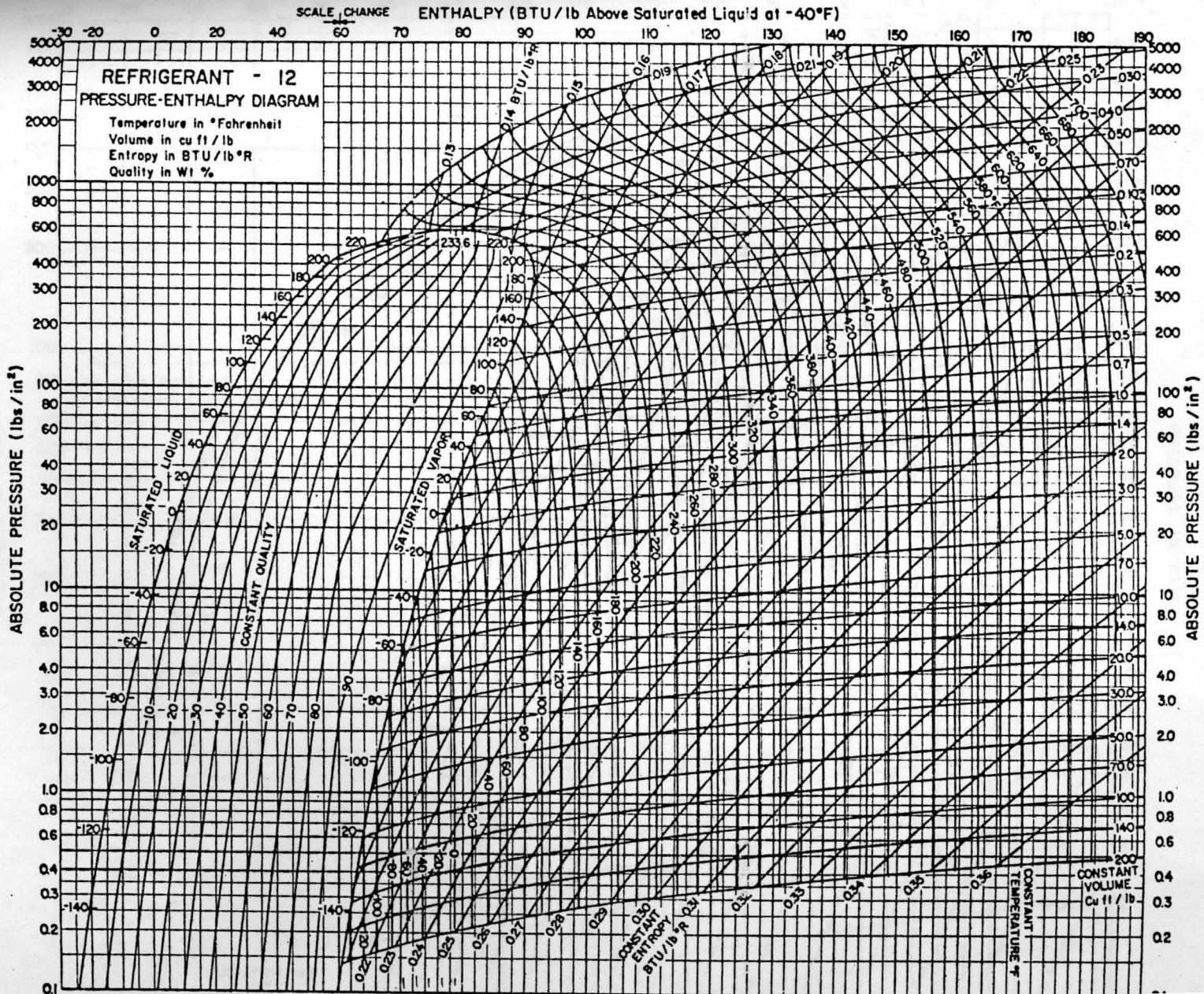
Temperature in °Fahrenheit  
Volume in cu ft / lb  
Entropy in BTU / lb °R  
Quality in Wt %



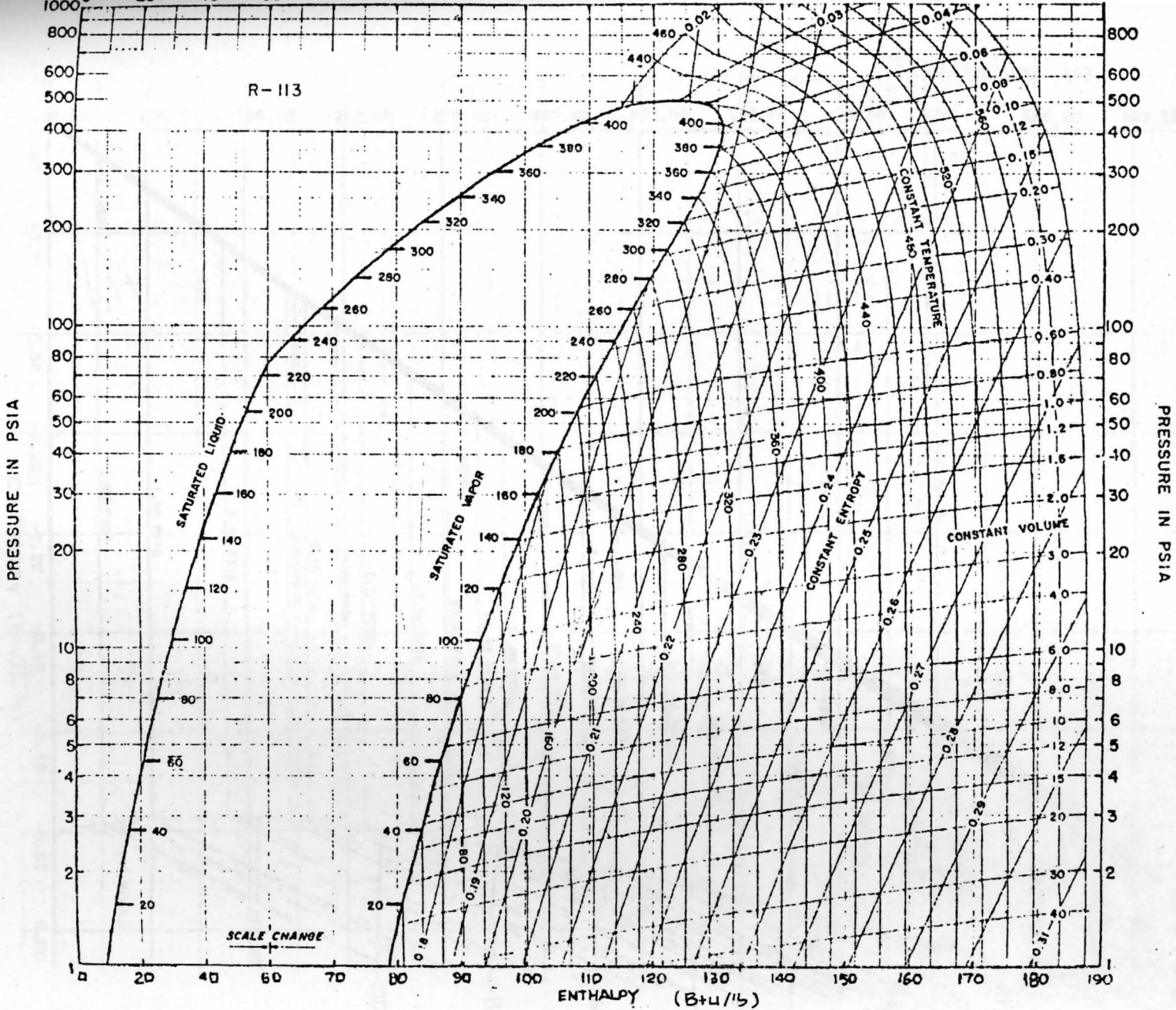
Pressure-Enthalpy Diagram for R-11

ABSOLUTE PRESSURE, (lbs / in<sup>2</sup>)

Pressure-Enthalpy Diagram for R-12

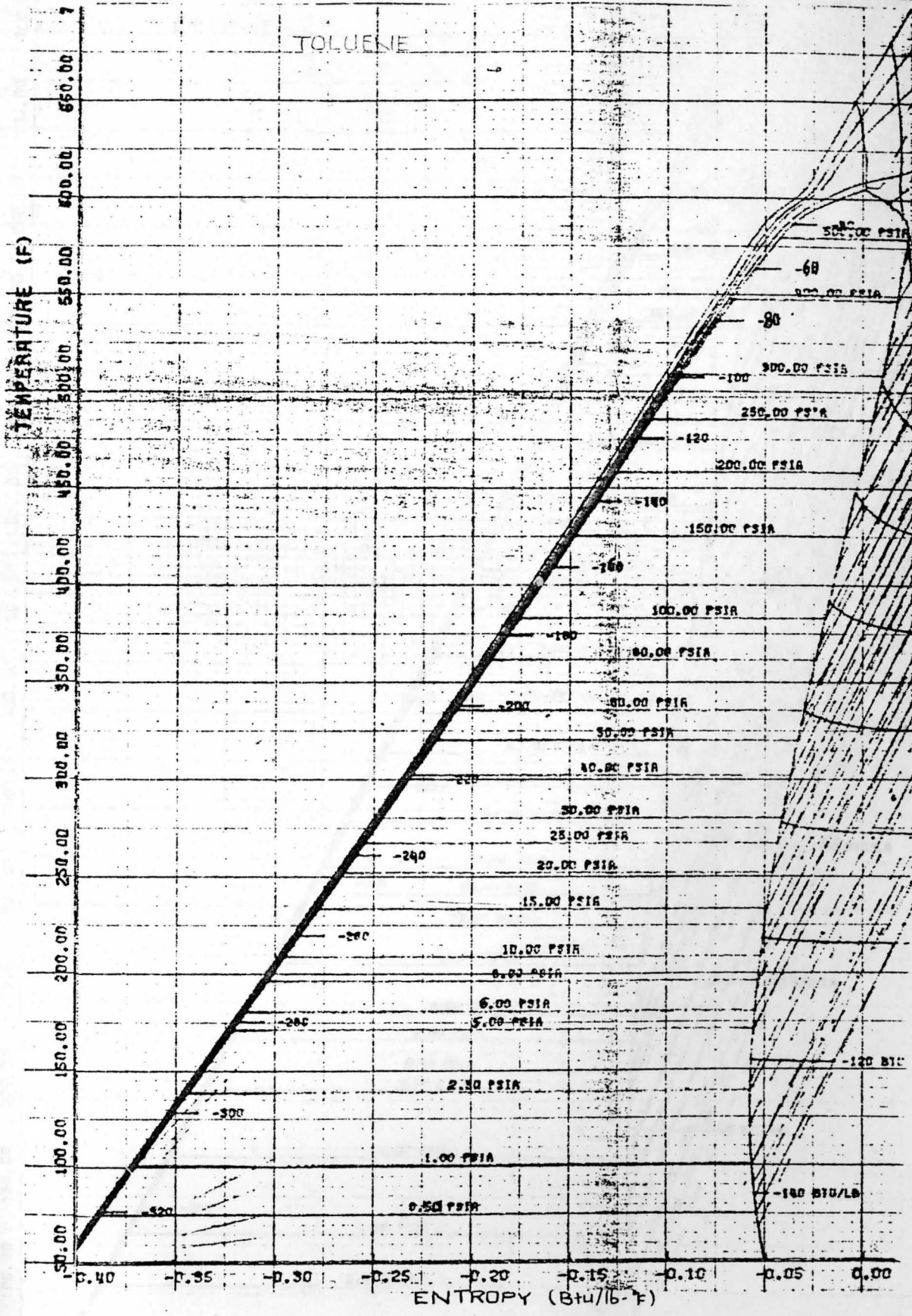


Pressure-Enthalpy Diagram for R-113





# TOLUENE

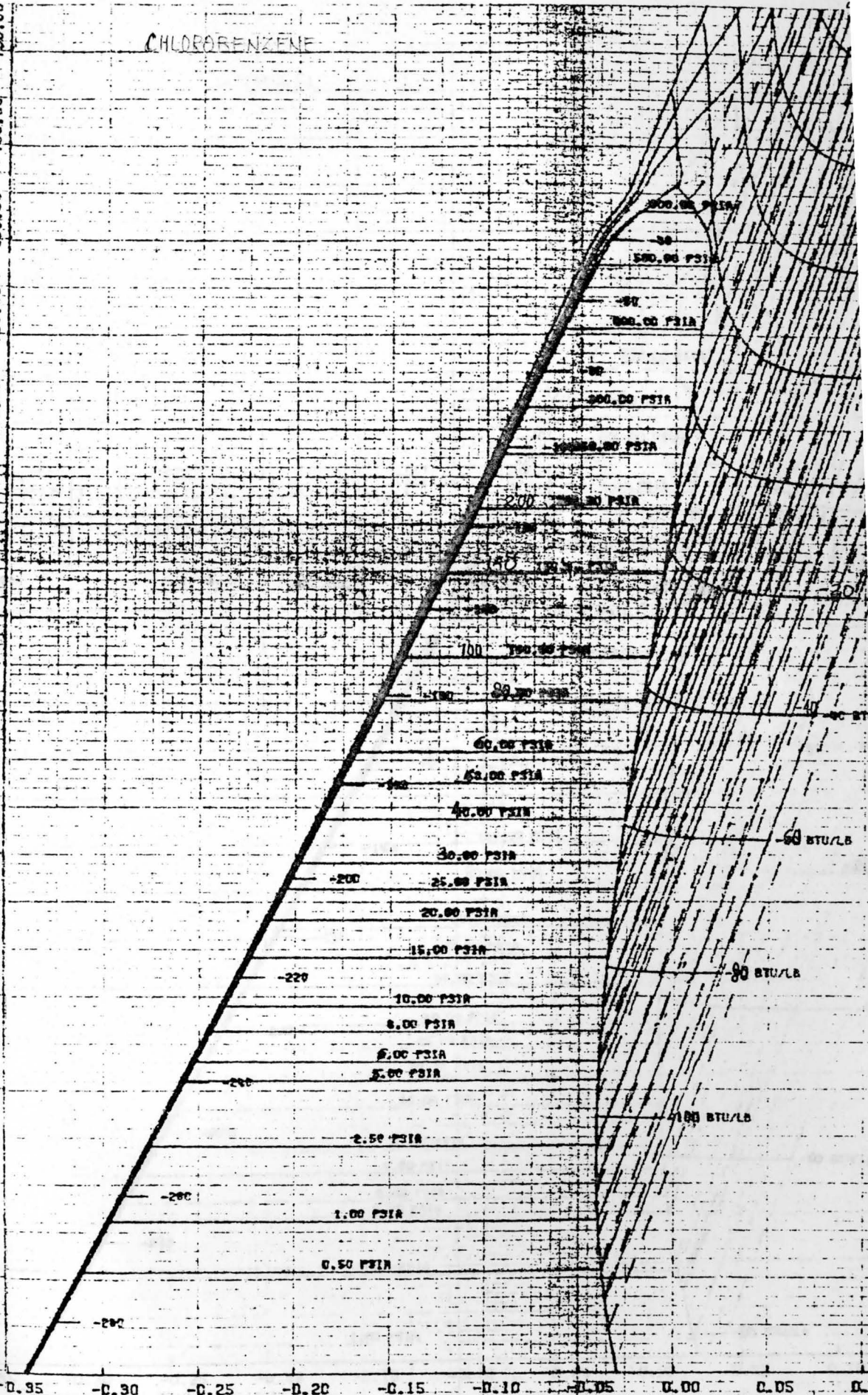


Temperature-Entropy Diagram for Toluene

CHLOROBENZENE

TEMPERATURE (°F)

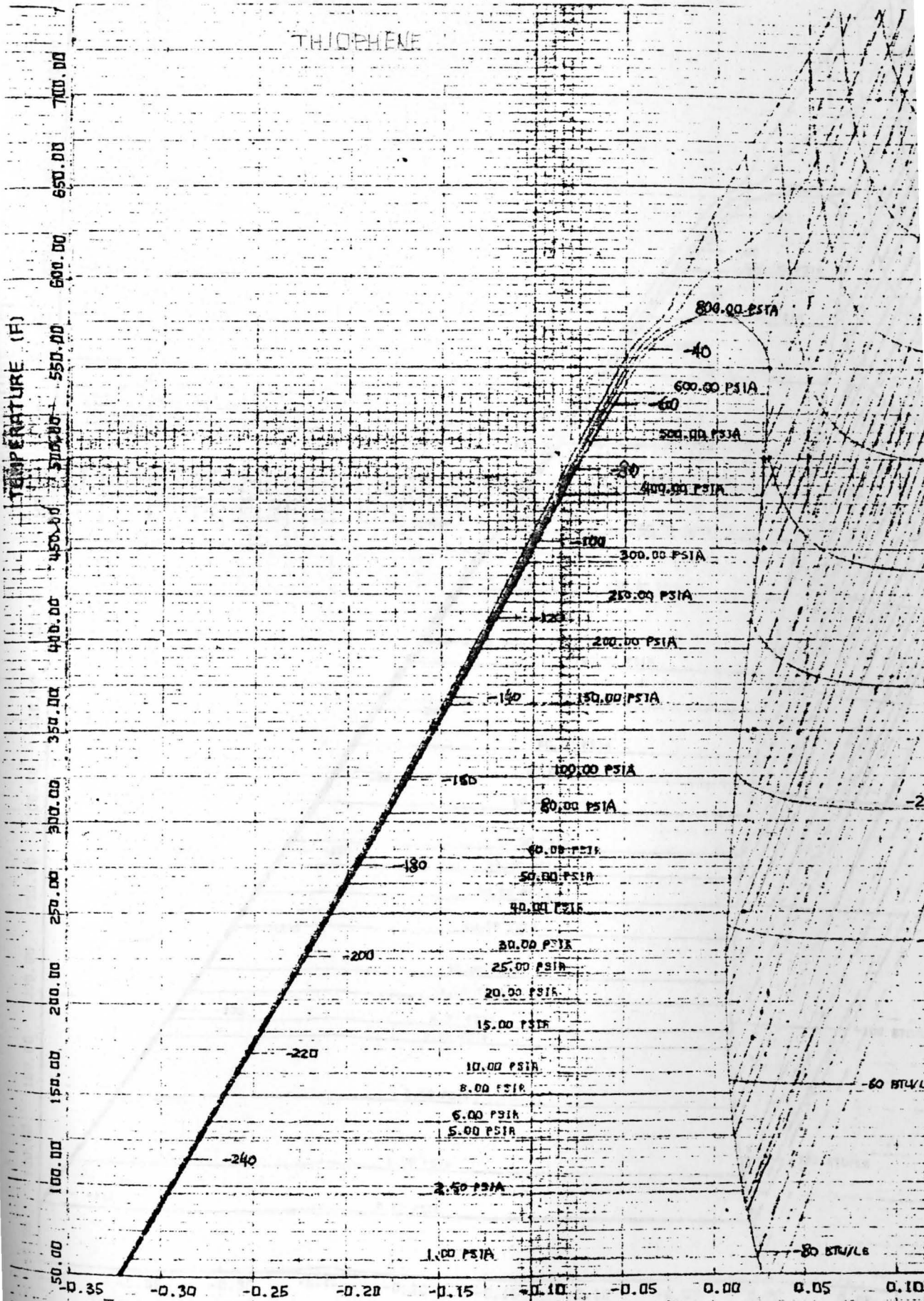
750.00  
700.00  
650.00  
600.00  
550.00  
500.00  
450.00  
400.00  
350.00  
300.00  
250.00  
200.00  
150.00  
100.00  
50.00



-0.95 -0.90 -0.25 -0.20 -0.15 -0.10 -0.05 0.00 0.05 0.10

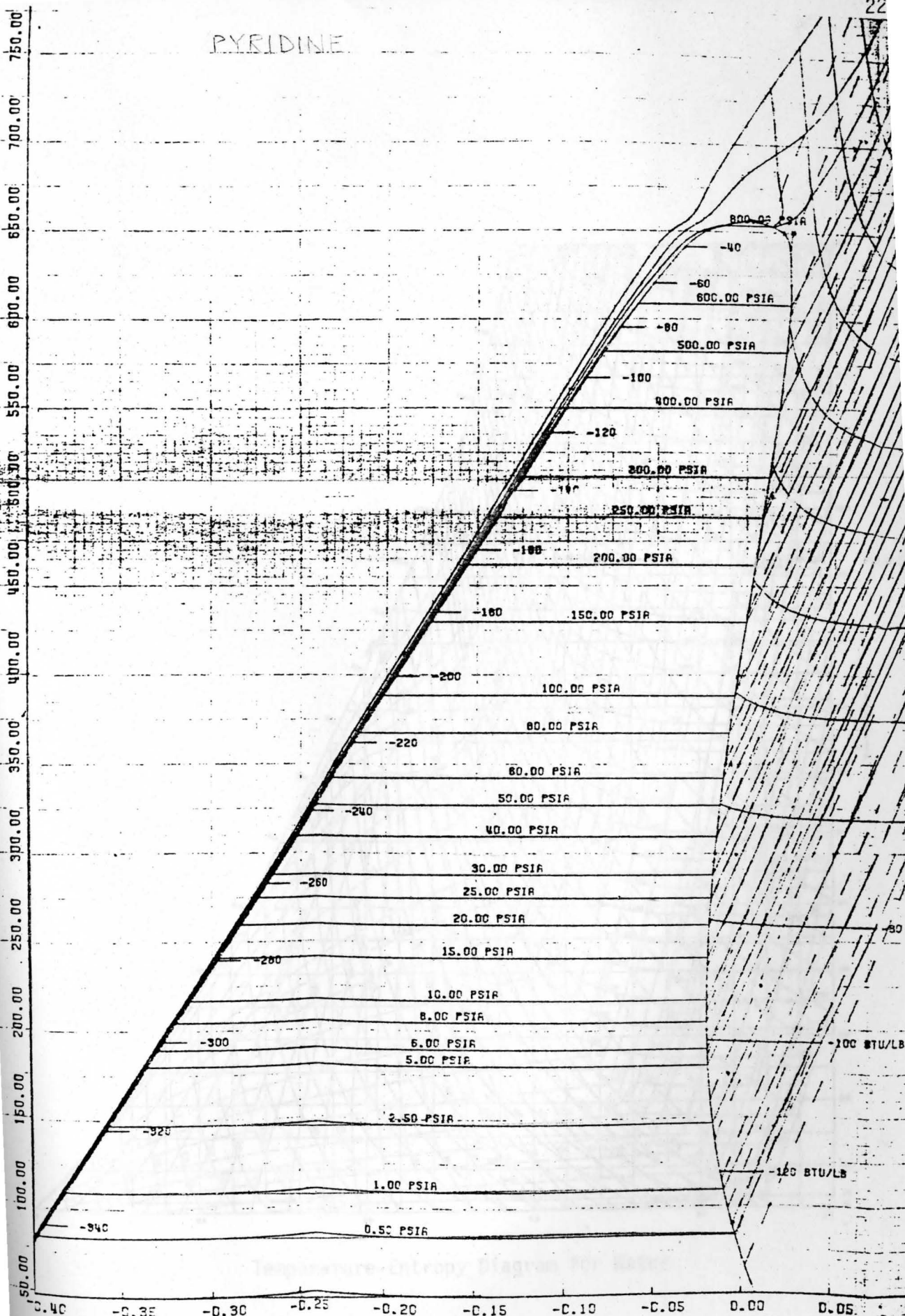
Temperature Entropy Diagram

THIOPHENE



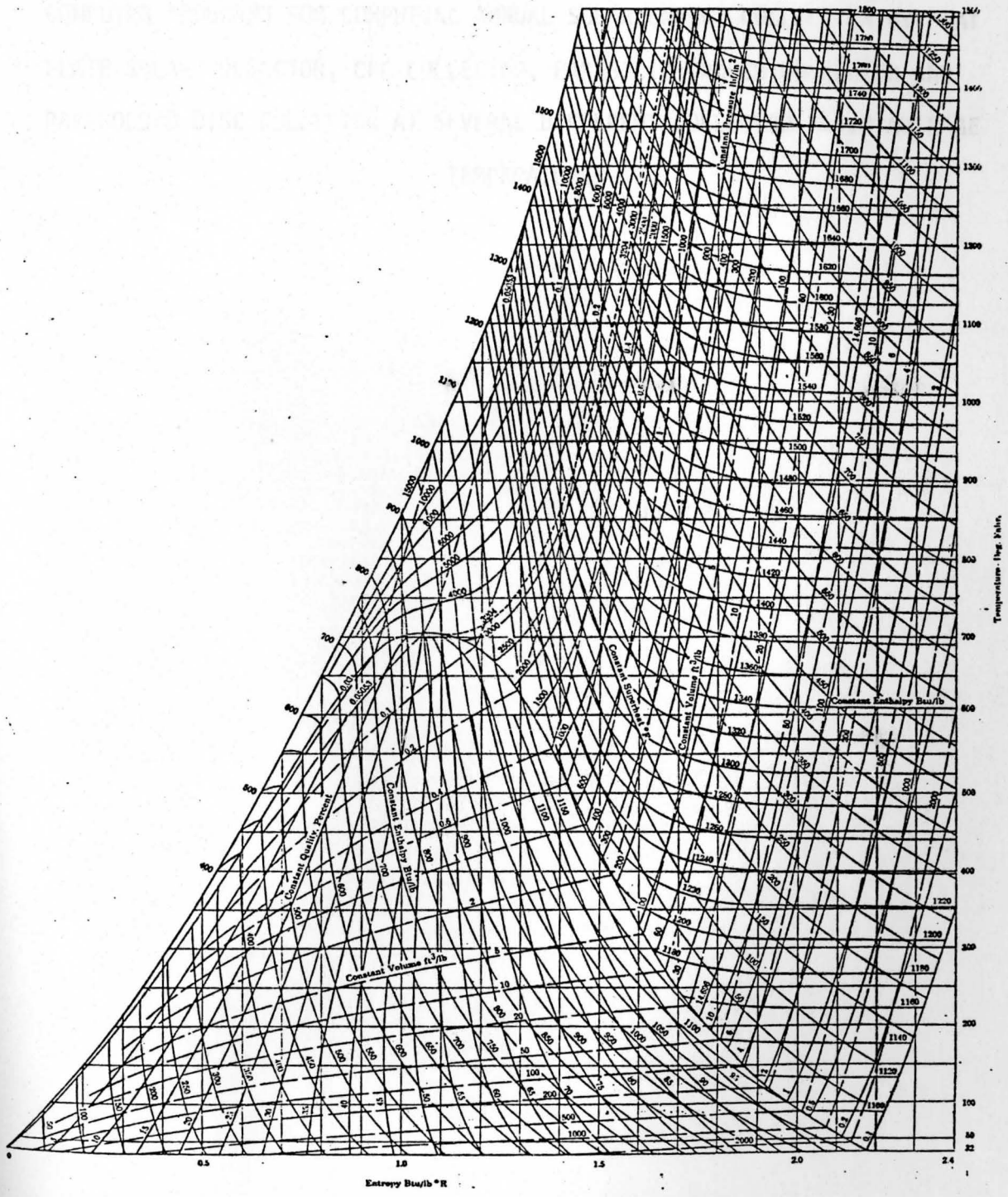
Temperature-Entropy Diagram

PYRIDINE



Temperature-Entropy Diagram

ENTROPY (BTU/LB)



Temperature-Entropy Diagram for Water

APPENDIX B

COMPUTER PROGRAMS FOR COMPUTING ANNUAL SOLAR ENERGY COLLECTION BY FLAT  
PLATE SOLAR COLLECTOR, CPC COLLECTOR, PARABOLIC TROUGH COLLECTOR AND  
PARABOLOID DISC COLLECTOR AT SEVERAL DIFFERENT COLLECTOR FLUID AVERAGE  
TEMPERATURES.

## FLAT-PLATE SOLAR COLLECTOR

```

FORTRAN IV G1  RELEASE 2-0          MAIN          DATE = 81103          19/22/11

      C   THIS PROGRAM ANALYZES THE PERFORMANCE OF A TYPICAL LIQUID TYPE
      C   FLAT PLATE COLLECTOR HAVING TWO GLASS COVERS AND A COPPER ABSORBER
      C   PLATE COATED WITH A SELECTIVE SURFACE. IT CALCULATES THE COLLECTOR
      C   EFFICIENCY AND ENERGY COLLECTED EVERY HOUR OF THE YEAR FOR AVERAGE
      C   COLLECTOR TEMP. OF 140,160,180,200,220,240,260,280 AND 300 DEG.
      C   F. THE SOLAR RADIATION AND AMBIENT TEMP. DATA ARE TAKEN FROM
      C   'SOLMET' WEATHER TAPE. THE RESULTS ARE INTEGRATED OVER A DAY,
      C   MONTH AND YEAR. ONLY THE RESULTS FOR SOLAR ENERGY COLLECTED PER
      C   MONTH AND PER YEAR ARE PRINTED OUT.
0001      DIMENSION SUDAY(90),SUMNTH(90),SUYEAR(90),TAVG(90),SUH8(90),H(90),
      C   +D(90),T(90)
0002      DELTA=0.-0.40163
0003      RN=1.
0004      INDAY=0
0005      PI=3.14159
0006      FI=43.*PI/180.
0007      BETA=FI
0008      FRTA=0.647
0009      FRUL=0.666
0010      450  CONTINUE
0011      DO 100 J=1,24
0012      READ(5,150)IWBAN,MONTH,IDAY,IPHOUR,IDIRNL,ITOTHL,ITAMB
      C   DATA ARE READ FROM 'SOLMET' TAPE
      C   IWBAN=WEATHER STATION NUMBER, IDAY=DAY NUMBER, IPHOUR=HOUR NUMBER
      C   IDIRNL=HOURLY DIRECT SOLAR INSOLATION ON A NORMAL SURFACE(KJ/M**2)
      C   ITOTHL=HOURLY TOTAL INSOLATION ON A HORIZONTAL SURFACE (KJ/M**2)
      C   ITAMB=TEN TIMES THE AMBIENT TEMP. IN CENTIGRADE.
0013      150  FORMAT(1I6,3X,3I3,3I5)
0014      HOUR=IPHOUR-0.5
0015      TAMB=ITAMB*0.18+32.
      C   TAMB=AMBIENT TEMP. IN DEG. F.
0016      SDIRNL=IDIRNL/11.35
      C   SDIRNL =DIRECT SOLAR INSOLATION ON A NORMAL SURFACE(BTU/SQ. FT./HR)
0017      STOTHL=ITOTHL/11.35
0018      OMEGA=ABS(HOUR-12.)*PI/12.
0019      COSZ=COS(DELTA)*COS(FI)*COS(OMEGA)+SIN(DELTA)*SIN(FI)
0020      SDIRHL=SDIRNL*COSZ
      C   SDIRHL=DIRECT INSOLATION ON A HORIZONTAL SURFACE(BTU/SQ. FT./HR)
0021      SSCHL=STOTHL-SDIRHL
      C   SSCHL=SCATTERED INSOLATION ON A HORIZONTAL SURFACE(BTU/SQ.FT./HR)
0022      COSTHE=COS(DELTA)*COS(OMEGA)
0023      STOTPL=SDIRNL*COSTHE+SSCHL
0024      TAVG(1)=140.
0025      DO 110 K=1,9
0026      IF(IDAY-INDAY)60,60,50
0027      60  INDAY=0
0028      DO 130 M=1,9
0029      SUYEAR(M)=SUYEAR(M)+SUMNTH(M)
0030      RMONTH=MONTH-1
0031      WRITE(6,700)RMONTH,TAVG(M),SUMNTH(M)
0032      700  FORMAT(1X,'MONTH=',I3.0,9X,'AVG. TEMP.=',I7.2,10X,'SOLAR COLL./M
      C   +ONTH=',I8.2)
0033      SUMNTH(M)=0.
0034      130  CONTINUE
0035      WRITE(6,701)
0036      701  FORMAT(//)
0037      50  CONTINUE
0038      IF(STOTPL-50.120,10,10)

```

```

0039      20  SUHR(K)=0.
0040      GO TO 55
0041      10  CONTINUE
0042      TEFF=0.
0043      DO 106 K2=1,3
0044      TIN=TAVG(K)+(K2-2.5)*10.0
0045      EFF1=ERTI-ERUL*(TIN-TAMB)/STOTPL
0046      TEFF=TEFF+EFF1
0047      106  CONTINUE
0048      EFF=TEFF/3.
0049      C    COLLECTOR EFFICIENCY(EFF) IS AVERAGED OVER THREE TEMPERATURES
0050      C    SUHR(K)=EFF*STOTPL
0051      IF(EFF1 .LE. 0.0)SUHR(K)=0.0
0052      40  SUDAY(K)=SUDAY(K)+SUHR(K)
0053      55  CONTINUE
0054      TAVG(K+1)=TAVG(K)+20.
0055      110  CONTINUE
0056      100  CONTINUE
0057      INDAY=IDAY
0058      RN=RN+1.
0059      DELTA=(23.45*PI/180.)*SIN(2.*PI*(284.+RN)/365.0)
0060      DO 120 L=1,9
0061      SUMNTH(L)=SUMNTH(L)+SUDAY(L)
0062      SUDAY(L)=0.
0063      120  CONTINUE
0064      IF(MONTH .NE. 12)GO TO 320
0065      IF(IDAY .NE. 31)GO TO 320
0066      GO TO 900
0067      320  CONTINUE
0068      GO TO 450
0069      900  CONTINUE
0070      DO 131 N=1,9
0071      SUYEAR(N)=SUYEAR(N)+SUMNTH(N)
0072      WRITE(6,702)MONTH,TAVG(N),SUMNTH(N)
0073      FORMAT(1X,'MONTH=',113 ,9X,'AVG. TEMP.=',1F7.2,10X,'SOLAR COLL./M
+ONTH=',1F8.2)
0074      SUMNTH(N)=0.
0075      131  CONTINUE
0076      DO 132 N1=1,9
0077      WRITE(6,703)TAVG(N1),SUYEAR(N1)
0078      FORMAT(///,1X,'COLLECTOR FLUID AVERAGE TEMP.=',F6.0,1X,'DEG. F.',1
+OX,'SOLAR ENERGY COLLECTED/YEAR=',F11.2,2X,'BTU/SQ. FT./YEAR')
0079      132  CONTINUE
0080      IF(IWBAN .NE. 23050) GO TO 11
0081      WRITE(6,806)
0082      806  FORMAT(//,30 X,'ALBUQUERQUE, NM')
0083      11  IF(IWBAN .NE. 14837)GO TO 12
0084      WRITE(6,807)
0085      807  FORMAT(//,30 X,'MADISON,WI')
0086      12  IF(IWBAN .NE. 12839)GO TO 13
0087      WRITE(6,808)
0088      808  FORMAT(//,30 X,'MIAMI,FLORIDA')
0089      13  CONTINUE
0090      STOP
0091      END

```



OUTPUT: Annual Solar Energy Collection by Flat-Plate Solar Collector.

COLLECTOR FLUID AVERAGE TEMP.= 140. DEG. F.	SOLAR ENERGY COLLECTED/YEAR= 158864.31 BTU/SQ. FT./YEAR
COLLECTOR FLUID AVERAGE TEMP.= 160. DEG. F.	SOLAR ENERGY COLLECTED/YEAR= 130140.50 BTU/SQ. FT./YEAR
COLLECTOR FLUID AVERAGE TEMP.= 180. DEG. F.	SOLAR ENERGY COLLECTED/YEAR= 104954.31 BTU/SQ. FT./YEAR
COLLECTOR FLUID AVERAGE TEMP.= 200. DEG. F.	SOLAR ENERGY COLLECTED/YEAR= 81248.12 BTU/SQ. FT./YEAR
COLLECTOR FLUID AVERAGE TEMP.= 220. DEG. F.	SOLAR ENERGY COLLECTED/YEAR= 60019.63 BTU/SQ. FT./YEAR
COLLECTOR FLUID AVERAGE TEMP.= 240. DEG. F.	SOLAR ENERGY COLLECTED/YEAR= 42524.70 BTU/SQ. FT./YEAR
COLLECTOR FLUID AVERAGE TEMP.= 260. DEG. F.	SOLAR ENERGY COLLECTED/YEAR= 26694.86 BTU/SQ. FT./YEAR
COLLECTOR FLUID AVERAGE TEMP.= 280. DEG. F.	SOLAR ENERGY COLLECTED/YEAR= 13268.76 BTU/SQ. FT./YEAR
COLLECTOR FLUID AVERAGE TEMP.= 300. DEG. F.	SOLAR ENERGY COLLECTED/YEAR= 2854.61 BTU/SQ. FT./YEAR

MADISON, WI

## CPC SOLAR COLLECTOR

```

C THIS PROGRAM ANALYZES THE PERFORMANCE OF A TYPICAL COMPOUND
C PARABOLIC CONCENTRATING COLLECTOR. IT CALCULATES THE COLLECTOR
C EFFICIENCY AND ENERGY COLLECTED EVERY HOUR OF THE YEAR FOR AVERAGE
C TEMP. OF 150, 190, 230, 270, 310, 350, 390, 430, AND 470 DEG.
C F. THE SOLAR RADIATION AND AMBIENT TEMP. DATA ARE TAKEN FROM
C 'SOLMET' WEATHER TAPE. THE RESULTS ARE INTEGRATED OVER A DAY,
C MONTH AND YEAR. ONLY THE RESULTS FOR SOLAR ENERGY COLLECTED PER
C MONTH AND PER YEAR ARE PRINTED OUT.
0001 DIMENSION SUDAY(90),SUMNTH(90),SUYEAR(90),TAVG(90),SUHR(90),H(90),
+D(90),J(90)
0002 DELTA=0.-0.40163
0003 RN=1.
0004 INDAY=0
0005 PI=3.14159
0006 FI=43.*PI/180.
0007 BETA=FI
0008 450 CONTINUE
0009 DO 100 J=1,24
0010 READ(5,150)IWBAN,MONTH,IDAY,IPHOUR,DIRNL,ITOTHL,ITAMB
C DATA ARE READ FROM 'SOLMET' TAPE
C IWBAN=WEATHER STATION NUMBER, IDAY=DAY NUMBER, IPHOUR=HOURLY NUMBER
C DIRNL=HOURLY DIRECT SOLAR INSOLATION ON A NORMAL SURFACE(KJ/H**2)
C ITOTHL=HOURLY TOTAL INSOLATION ON A HORIZONTAL SURFACE (KJ/M**2)
C ITAMB=TEN TIMES THE AMBIENT TEMP. IN CENTIGRADE.
0011 150 FORMAT(1I6,3X,3I3,3I5)
0012 HOUR=IPHOUR-0.5
0013 TAMB=ITAMB*0.18+32.
C TAMB=AMBIENT TEMP. IN DEG. F.
0014 SDIRNL=DIRNL/11.35
C SDIRNL=DIRECT SOLAR INSOLATION ON A NORMAL SURFACE(BTU/SQ. FT./HR)
0015 OMEGA=ABS(HOUR-12.)*PI/12.
0016 COSTHE=COS(DELTA)*COS(OMEGA)
0017 STOTHL=ITOTHL/11.35
0018 COSZ=COS(DELTA)*COS(FI)*COS(OMEGA)+SIN(DELTA)*SIN(FI)
0019 SDIRHL=SDIRNL*COSZ
C SDIRHL=DIRECT INSOLATION ON A HORIZONTAL SURFACE(BTU/SQ. FT./HR)
0020 SSCHL=STOTHL-SDIRHL
C SSCHL=SCATTERED INSOLATION ON A HORIZONTAL SURFACE(BTU/SQ.FT./HR)
0021 Z=ARCOS(COSZ)
0022 GAMA=ATAN(SIN(OMEGA)/(SIN(FI)*COS(OMEGA)-COS(FI)*TAN(DELTA)))
0023 ALFA=ATAN(TAN(Z)*COS(GAMA))
0024 IF(ALFA .LT. (BETA-98.*PI/180.))GO TO 105
0025 IF(ALFA .GT. (BETA+98.*PI/180.))GO TO 105
0026 F=1.0
0027 GO TO 107
0028 105 F=0.
0029 107 SDIRPL=F*SDIRNL*COSTHE
C SDIRPL=DIRECT INSOLATION ON A COLLECTOR PLANE(BTU/SQ.FT./HR)
0030 SSCPL=0.75*SSCHL
C SSCPL=SCATTERED SOLAR INSOLATION ON A COLLECTOR (BTU/SQ.FT.HR)
0031 STOTPL=SDIRPL+SSCPL
0032 TAVG(1)=150.
0033 DO 110 K=1,9
0034 IF(IDAY-INDAY)60,60,50
0035 60 INDAY=0
0036 DO 130 M=1,9
0037 SUYEAR(M)=SUYEAR(M)+SUMNTH(M)
0038 RMONTH=MONTH-1

```

```

0039      WRITE(6,700)RMONTH,TAVG(M),SUMNTH(M)
0040      700  FORMAT(1X,'MONTH=',1F3.0,9X,'AVG. TEMP.=',1F7.2,10X,'SOLAR COLL./M
+ONTH=',1F8.2)
0041      SUMNTH(M)=0.
0042      130  CONTINUE
0043      WRITE(6,701)
0044      701  FORMAT(//)
0045      50   CONTINUE
0046      IF(STOTPL-50.120,10,10)
0047      20   SUHR(K)=0.
0048      GO TO 55
0049      10   CONTINUE
0050      TEFF=0.
0051      DO 106 K2=1,3
0052      TIN=TAVG(K)+(K2-2.5)*20.0
0053      EFF1=.499-.104*(TIN-TAMB)/STOTPL-0.098*((TIN-TAMB)/STOTPL)**2
0054      TEFF=TEFF+EFF1
0055      106  CONTINUE
0056      EFF=TEFF/3.
0057      SUHR(K)=EFF*STOTPL
C      SUHR=SOLAR ENERGY COLLECTED PER HOUR.
0058      IF(EFF1 .LE. 0.0)SUHR(K)=0.0
0059      IF(EFF-.15)20,40,40
0060      40   SUDAY(K)=SUDAY(K)+SUHR(K)
0061      55   CONTINUE
0062      TAVG(K+1)=TAVG(K)+40.
0063      110  CONTINUE
0064      100  CONTINUE
0065      INDAY=IDAY
0066      RN=RN+1.
0067      DELTA=(23.45*PI/180.)*SIN(2.*PI*(284.+RN)/365.0)
0068      DO 120 L=1,9
0069      SUMNTH(L)=SUMNTH(L)+SUDAY(L)
0070      SUDAY(L)=0.
0071      120  CONTINUE
0072      IF(MONTH .NE. 12)GO TO 320
0073      IF(IDAY .NE. 31)GO TO 320
0074      GO TO 900
0075      320  CONTINUE
0076      GO TO 450
0077      900  CONTINUE
0078      DO 131 N=1,9
0079      SUYEAR(N)=SUYEAR(N)+SUMNTH(N)
0080      WRITE(6,702)MONTH,TAVG(N),SUMNTH(N)
0081      702  FORMAT(1X,'MONTH=',1I3 ,9X,'AVG. TEMP.=',1F7.2,10X,'SOLAR COLL./M
+ONTH=',1F8.2)
0082      SUMNTH(N)=0.
0083      131  CONTINUE
0084      DO 132 N1=1,9
0085      WRITE(6,703)TAVG(N1),SUYEAR(N1)
0086      703  FORMAT(///,1X,'COLLECTOR FLUID AVERAGE TEMP.=',F6.0,1X,'DEG. F.',1
+0X,'SOLAR ENERGY COLLECTED/YEAR=',F11.2,2X,'BTU/SQ. FT./YEAR')
0087      132  CONTINUE
0088      IF(IWBAN .NE. 23050) GO TO 11
0089      WRITE(6,806)
0090      806  FORMAT(//,30 X,'ALBUQUERQUE, NM')
0091      11   IF(IWBAN .NE. 14837)GO TO 12
0092      WRITE(6,807)

```

FORTRAN IV G1 RELEASE 2.0

MAIN

DATE = 81103

19/38/40

```

0093      807  FORMAT(//,30 X,'MADISON,WI')
0094      12   IF(IWBAN .NE. 12839)GO TO 13
0095      WRITE(6,808)
0096      808  FORMAT(//,30 X,'MIAMI,FLORIDA')
0097      13   CONTINUE
0098      STOP
0099      END

```

OUTPUT: Annual Solar Energy Collection by CPC Collector

COLLECTOR FLUID AVERAGE TEMP.= 150. DEG. F.	SOLAR ENERGY COLLECTED/YEAR= 166752.44 BTU/SQ. FT./YEAR
COLLECTOR FLUID AVERAGE TEMP.= 190. DEG. F.	SOLAR ENERGY COLLECTED/YEAR= 143328.74 BTU/SQ. FT./YEAR
COLLECTOR FLUID AVERAGE TEMP.= 230. DEG. F.	SOLAR ENERGY COLLECTED/YEAR= 119738.81 BTU/SQ. FT./YEAR
COLLECTOR FLUID AVERAGE TEMP.= 270. DEG. F.	SOLAR ENERGY COLLECTED/YEAR= 98353.25 BTU/SQ. FT./YEAR
COLLECTOR FLUID AVERAGE TEMP.= 310. DEG. F.	SOLAR ENERGY COLLECTED/YEAR= 77373.44 BTU/SQ. FT./YEAR
COLLECTOR FLUID AVERAGE TEMP.= 350. DEG. F.	SOLAR ENERGY COLLECTED/YEAR= 57751.55 BTU/SQ. FT./YEAR
COLLECTOR FLUID AVERAGE TEMP.= 390. DEG. F.	SOLAR ENERGY COLLECTED/YEAR= 38958.02 BTU/SQ. FT./YEAR
COLLECTOR FLUID AVERAGE TEMP.= 430. DEG. F.	SOLAR ENERGY COLLECTED/YEAR= 22945.71 BTU/SQ. FT./YEAR <i>Youngstown, Pa</i>
COLLECTOR FLUID AVERAGE TEMP.= 470. DEG. F.	SOLAR ENERGY COLLECTED/YEAR= 9314.93 BTU/SQ. FT./YEAR

MADISON, WI

## PARABOLIC TROUGH COLLECTOR

```

C      THIS PROGRAM ANALYZES THE PERFORMANCE OF A TYPICAL PARABOLIC
C      TROUGH CONCENTRATING COLLECTOR. THE COLLECTOR IS ORIENTED
C      NORTH-SOUTH AND IT TRACKS EAST-WEST. THE COLLECTOR EFFICIENCY AND
C      ENERGY COLLECTED IS CALCULATED FOR EVERY HOUR OF THE YEAR FOR
C      COLLECTOR FLUID AVERAGE TEMP. OF 200,250,300,350,400,450,500,550 AND
C      600 F THE SOLAR RADIATION AND AMBIENT TEMP. DATA ARE TAKEN FROM
C      *SOLMET* WEATHER TAPE. THE RESULTS ARE INTEGRATED OVER A DAY,
C      MONTH AND YEAR. ONLY THE RESULTS FOR SOLAR ENERGY COLLECTED PER
C      MONTH AND PER YEAR ARE PRINTED OUT.
0001      DIMENSION SUDAY(90),SUMNTH(90),SUYEAR(90),TAVG(90),SUHR(90),H(90),
          +D(90),T(90)
0002      DELTA=0.-0.40163
0003      RN=1.
0004      INDAY=0
0005      PI=3.14159
0006      FI=43.*PI/180.
0007      450 CONTINUE
0008      DO 100 J=1,24
0009      READ(5,150)INBAN,MONTH,IDAY,IPHOUR,DIRNL,ITOTHL,ITAMB
C      DATA ARE READ FROM *SOLMET* TAPE
C      INBAN=WEATHER STATION NUMBER, IDAY=DAY NUMBER, IPHOUR=HOUR NUMBER
C      DIRNL=HOURLY DIRECT SOLAR INSOLATION ON A NORMAL SURFACE(KJ/M**2)
C      ITOTHL=HOURLY TOTAL INSOLATION ON A HORIZONTAL SURFACE (KJ/M**2)
C      ITAMB=TEN TIMES THE AMBIENT TEMP. IN CENTIGRADE.
0010      150 FORMAT(116,3X,313,315)
0011      HOUR=IPHOUR-0.5
0012      TAMB=ITAMB*0.18+32.
C      TAMB=AMBIENT TEMP. IN DEG. F.
0013      SDIRNL=DIRNL/11.35
C      SDIRNL =DIRECT SOLAR INSOLATION ON A NORMAL SURFACE(BTU/SQ. FT.-HR)
0014      STOTHL=ITOTHL/11.35
0015      OMEGA=ABS(HOUR-12.)*PI/12.
0016      COSTHE=(1.0-(COS(DELTA)*SIN(OMEGA))**2)**0.5
0017      THETA=ARCOS(COSTHE)
0018      STOTPL=SDIRNL*COSTHE
0019      TAVG(1)=200.
0020      DO 110 K=1,9
0021      IF(IDAY-INDAY)60,60,50
0022      60 INDAY=0
0023      DO 130 M=1,9
0024      SUYEAR(M)=SUYEAR(M)+SUMNTH(M)
0025      RMONTH=MONTH-1
0026      WRITE(6,700)RMONTH,TAVG(M),SUMNTH(M)
0027      700 FORMAT(11X,'MONTH=',1F3-0,9X,'AVG. TEMP.=',1F7.2,10X,'SOLAR COLL./M
          +ONTH=',1F8.2)
0028      SUMNTH(M)=0.
0029      130 CONTINUE
0030      WRITE(6,701)
0031      701 FORMAT(//)
0032      50 CONTINUE
0033      IF(STOTPL-50.)20,10,10
0034      20 SUHR(K)=0.
0035      GO TO 55
0036      10 CONTINUE
0037      TEFF=0.
0038      DO 106 K2=1,3
0039      TOUTI=TAVG(K)+(K2-1.5)*20.
0040      EFF1=0.694-0.052*(TOUTI-TAMB)/STOTPL-.119*((TOUTI-TAMB)/STOTPL)**2

```

```

0041      TEFF=TEFF+EFF1
0042      106 CONTINUE
0043      EFF=TEFF/3.
C      COLLECTOR EFFICIENCY(EFF) IS AVERAGED OVER THREE TEMPERATURES
0044      SUHR(K)=EFF*(STOTPL-3.0*TAN(THETA)/80.0)
C      SUHR=SOLAR ENERGY COLLECTED PER HOUR.
0045      IF(EFF.LE.0.0)SUHR(K)=0.0
0046      IF(EFF-.15)20,40,40
0047      40 SUDAY(K)=SUDAY(K)+SUHR(K)
0048      55 CONTINUE
0049      TAVG(K+1)=TAVG(K)+50.
0050      110 CONTINUE
0051      100 CONTINUE
0052      INDAY=IDAY
0053      RN=RN+1.
0054      DELTA=(23.45*PI/180.)*SIN(2.*PI*(284.+RN)/365.0)
0055      DO 120 L=1,9
0056      SUMNTH(L)=SUMNTH(L)+SUDAY(L)
0057      SUDAY(L)=0.
0058      120 CONTINUE
0059      IF(MONTH.NE.12)GO TO 320
0060      IF(IDAY.NE.31)GO TO 320
0061      GO TO 900
0062      320 CONTINUE
0063      GO TO 450
0064      900 CONTINUE
0065      DO 131 N=1,9
0066      SUYEAR(N)=SUYEAR(N)+SUMNTH(N)
0067      WRITE(6,702)MONTH,TAVG(N),SUMNTH(N)
0068      702 FORMAT(1X,'MONTH=',113 ,9X,'AVG. TEMP.=',1F7.2,10X,'SOLAR COLL./M
+QNTH=',1F8.2)
0069      SUMNTH(N)=0.
0070      131 CONTINUE
0071      DO 132 N1=1,9
0072      WRITE(6,703)TAVG(N1),SUYEAR(N1)
0073      703 FORMAT(///,1X,'COLLECTOR FLUID AVERAGE TEMP.=',F6.0,1X,'DEG. F.',1
+0X,'SOLAR ENERGY COLLECTED/YEAR=',F11.2,2X,'BTU/SQ. FT./YEAR')
0074      132 CONTINUE
0075      IF(IWBAN.NE.23050)GO TO 11
0076      WRITE(6,806)
0077      806 FORMAT(//,30 Y,'ALBUQUERQUE, NM')
0078      11 IF(IWBAN.NE.14837)GO TO 12
0079      WRITE(6,807)
0080      807 FORMAT(//,30 X,'MADISON,MI')
0081      12 IF(IWBAN.NE.12839)GO TO 13
0082      WRITE(6,808)
0083      808 FORMAT(//,30 X,'MIAMI,FLORIDA')
0084      13 CONTINUE
0085      STOP
0086      END

```

OUTPUT: Annual Solar Energy Collection by Parabolic Trough Collector.

COLLECTOR FLUID AVERAGE TEMP.= 200. DEG. F.	SOLAR ENERGY COLLECTED/YEAR= 159357.37 BTU/SQ. FT./YEAR
COLLECTOR FLUID AVERAGE TEMP.= 250. DEG. F.	SOLAR ENERGY COLLECTED/YEAR= 134591.37 BTU/SQ. FT./YEAR
COLLECTOR FLUID AVERAGE TEMP.= 300. DEG. F.	SOLAR ENERGY COLLECTED/YEAR= 109425.00 BTU/SQ. FT./YEAR
COLLECTOR FLUID AVERAGE TEMP.= 350. DEG. F.	SOLAR ENERGY COLLECTED/YEAR= 84075.94 BTU/SQ. FT./YEAR
COLLECTOR FLUID AVERAGE TEMP.= 400. DEG. F.	SOLAR ENERGY COLLECTED/YEAR= 60944.50 BTU/SQ. FT./YEAR
COLLECTOR FLUID AVERAGE TEMP.= 450. DEG. F.	SOLAR ENERGY COLLECTED/YEAR= 39551.01 BTU/SQ. FT./YEAR
COLLECTOR FLUID AVERAGE TEMP.= 500. DEG. F.	SOLAR ENERGY COLLECTED/YEAR= 22663.37 BTU/SQ. FT./YEAR
COLLECTOR FLUID AVERAGE TEMP.= 550. DEG. F.	SOLAR ENERGY COLLECTED/YEAR= 9063.04 BTU/SQ. FT./YEAR
COLLECTOR FLUID AVERAGE TEMP.= 600. DEG. F.	SOLAR ENERGY COLLECTED/YEAR= 1419.22 BTU/SQ. FT./YEAR

MADISON, MI

## Paraboloid Disc Collector

```

C THIS PROGRAM ANALYZES THE PERFORMANCE OF A TYPICAL POINT FOCUSING-
C TWO AXES TRACKING- PARABOLIC DISC CONCENTRATING COLLECTOR. THE
C COLLECTOR EFFICIENCY AND ENERGY COLLECTED IS CALCULATED FOR EVERY
C HOUR OF THE YEAR FOR AN AVERAGE TEMP. OF 400, 500, 600, 700, 800
C 900, 1000, 1100, AND 1200 DEGREE F.
C THE SOLAR RADIATION AND AMBIENT TEMP. DATA ARE TAKEN FROM
C 'SOLMET' WEATHER TAPE. THE RESULTS ARE INTEGRATED OVER A DAY.
C MONTH AND YEAR. ONLY THE RESULTS FOR SOLAR ENERGY COLLECTED PER
C MONTH AND PER YEAR ARE PRINTED OUT.
0001 DIMENSION SUDAY(90),SUMNTH(90),SUYEAR(90),TAVG(90),SUHR(90),H(90),
+D(90),T(90)
0002 DELTA=0.-0.40163
0003 RN=1.
0004 INDAY=0
0005 PI=3.14159
0006 EI=43.*PI/180.
0007 450 CONTINUE
0008 DO 100 J=1,24
0009 READ(5,150)IWBAN,MONTH,IDAY,IPHOUR,DIRNL,ITOTHL,ITAMB
C DATA ARE READ FROM 'SOLMET' TAPE
C IWBAN=WEATHER STATION NUMBER, IDAY=DAY NUMBER, IPHOUR=HOUR NUMBER
C DIRNL=HOURLY DIRECT SOLAR INSOLATION ON A NORMAL SURFACE (KJ/M**2)
C ITOTHL=HOURLY TOTAL INSOLATION ON A HORIZONTAL SURFACE (KJ/M**2)
C ITAMB=TEN TIMES THE AMBIENT TEMP. IN CENTIGRADE.
0010 15) FORMAT(116,3X,313,315)
0011 HOUR=IPHOUR-0.5
0012 TAMB=ITAMB*0.18+32.
C TAMB=AMBIENT TEMP. IN DEG. F.
0013 SDIRNL=DIRNL/11.35
C SDIRNL =DIRECT SOLAR INSOLATION ON A NORMAL SURFACE(BTU/SQ. FT.HR)
0014 STOTHL=ITOTHL/11.35
0015 STOTPL=SDIRNL
0016 TAVG(1)=400.
0017 DO 110 K=1,9
0018 IF(IDAY-INDAY)60,60,50
0019 60 INDAY=0
0020 DO 130 M=1,9
0021 SUYEAR(M)=SUYEAR(M)+SUMNTH(M)
0022 RMONTH=MONTH-1
0023 WRITE(6,700)RMONTH,TAVG(M),SUMNTH(M)
0024 700 FORMAT(1X,'MONTH=',1F3.0,9X,'AVG. TEMP.=',1F7.2,10X,'SOLAR COLL./M
+ONTH=',1F8.2)
0025 SUMNTH(M)=0.
0026 130 CONTINUE
0027 WRITE(6,701)
0028 701 FORMAT(//)
0029 50 CONTINUE
0030 IF(STOTPL-50.)20,10,10
0031 20 SUHR(K)=0.
0032 GO TO 55
0033 10 CONTINUE
0034 TAVGR=TAVG(K)+460.0
0035 TAMBR=TAMB+460.0
0036 EFF=0.708-(0.15426*10.**((0-8)*(TAVGR **4-TAMBR**4))+2.82*(TAVG(K
+)-TAMB))/(1600.0*SDIRNL)-0.952/SDIRNL
0037 SUHR(K)=EFF*SDIRNL
C SUHR=SOLAR ENERGY COLLECTED PER HOUR.
0038 IF(EFF-.15)20,40,40

```



```

0039      40  SUDAY(K)=SUDAY(K)+SUHR(K)
0040      55  CONTINUE
0041      TAVG(K+1)=TAVG(K)+100.0
0042      110 CONTINUE
0043      100 CONTINUE
0044      INDAY=IDAY
0045      RN=RN+1.
0046      DELTA=(23.45*PI/180.)*SIN(2.*PI*(284.+RN)/365.0)
0047      DO 120 L=1,9
0048      SUMNTH(L)=SUMNTH(L)+SUDAY(L)
0049      SUDAY(L)=0.
0050      120 CONTINUE
0051      IF(MONTH.NE. 12)GO TO 320
0052      IF(IDAY.NE. 31)GO TO 320
0053      GO TO 900
0054      320 CONTINUE
0055      GO TO 450
0056      900 CONTINUE
0057      DO 131 N=1,9
0058      SUYEAR(N)=SUYEAR(N)+SUMNTH(N)
0059      WRITE(6,702)MONTH,TAVG(N),SUMNTH(N)
0060      102 FORMAT(1X,'MONTH=',113 ,9X,'AVG. TEMP.=',1F7.2,10X,'SOLAR COLL./M
+ONTH=',1F8.2)
0061      SUMNTH(N)=0.
0062      131 CONTINUE
0063      DO 132 N1=1,9
0064      WRITE(6,703)TAVG(N1),SUYEAR(N1)
0065      703 FORMAT(///,1X,'COLLECTOR FLUID AVERAGE TEMP.=',F6.0,1X,'DEG. F.',1
+0X,'SOLAR ENERGY COLLECTED/YEAR=',F11.2,2X,'BTU/SQ. FT./YEAR!')
0066      132 CONTINUE
0067      IF(IWBAN.NE. 23050) GO TO 11
0068      WRITE(6,806)
0069      806 FORMAT(//,30 X,'ALBUQUERQUE, NM')
0070      11  IF(IWBAN.NE. 14837)GO TO 12
0071      WRITE(6,807)
0072      807 FORMAT(//,30 X,'MADISON, MI')
0073      12  IF(IWBAN.NE. 12839)GO TO 13
0074      WRITE(6,808)
0075      808 FORMAT(//,30 X,'MIAMI, FLORIDA')
0076      13  CONTINUE
0077      STOP
0078      END

```

OUTPUT: Annual Solar Energy Collection by Paraboloid Disc Collector

COLLECTOR FLUID AVERAGE TEMP.= 400. DEG. F.	SOLAR ENERGY COLLECTED/YEAR= 276902.06 BTU/SQ. FT./YEAR
COLLECTOR FLUID AVERAGE TEMP.= 500. DEG. F.	SOLAR ENERGY COLLECTED/YEAR= 275872.50 BTU/SQ. FT./YEAR
COLLECTOR FLUID AVERAGE TEMP.= 600. DEG. F.	SOLAR ENERGY COLLECTED/YEAR= 274607.81 BTU/SQ. FT./YEAR
COLLECTOR FLUID AVERAGE TEMP.= 700. DEG. F.	SOLAR ENERGY COLLECTED/YEAR= 273056.62 BTU/SQ. FT./YEAR
COLLECTOR FLUID AVERAGE TEMP.= 800. DEG. F.	SOLAR ENERGY COLLECTED/YEAR= 271162.44 BTU/SQ. FT./YEAR
COLLECTOR FLUID AVERAGE TEMP.= 900. DEG. F.	SOLAR ENERGY COLLECTED/YEAR= 268863.56 BTU/SQ. FT./YEAR
COLLECTOR FLUID AVERAGE TEMP.= 1000. DEG. F.	SOLAR ENERGY COLLECTED/YEAR= 266093.25 BTU/SQ. FT./YEAR
COLLECTOR FLUID AVERAGE TEMP.= 1100. DEG. F.	SOLAR ENERGY COLLECTED/YEAR= 262779.75 BTU/SQ. FT./YEAR
COLLECTOR FLUID AVERAGE TEMP.= 1200. DEG. F.	SOLAR ENERGY COLLECTED/YEAR= 258846.06 BTU/SQ. FT./YEAR

*Worcestershire State*

MADISON, WI

## BIBLIOGRAPHY

Books

- American Society of Heating, Refrigeration and Air Conditioning Engineers. ASHRAE Handbook of Fundamentals, Menasha: George Banta Co., Inc., 1974.
- Considine, Douglas M. Energy Technology Handbook. New York: McGraw Hill Book Company, 1977.
- Duffie, John A., et al, Solar Engineering of Thermal Sciences. New York: John Wiley & Sons, 1980.
- Federal Energy Administration. National Energy Outlook, FEA-N-75/713. Washington D.C.: Government Printing Office, 1976.
- Meinel, Adden B. and Meinel, Marjorie P. Applied Solar Energy. Massachusetts: Addison-Wesley Publication Co., 1977.

Articles

- Alvis, R.L. "Solar Irrigation Program Status Report." Oct., 1977, Sandia Report SAND 78-0049.
- Barber R.E. "Solar Rankine Engines -- Examples and Projected Costs." An ASME Publication, 79-Sol-3, 1978.
- Bianacardj, F.R. "Solar Cooling for Buildings," Workshop Proceedings, Solar Cooling for Buildings, Feb. 6-8, 1974, Los Angeles, California, Washington: Government Printing Office, 1974.
- Davis, Jerry. "Solar Rankine Powered Cooling Systems," Workshop Proceedings, Solar Cooling for Buildings, Feb. 6-8, 1974, Los Angeles, California, Washington: Government Printing Office, 1974.
- Miller, D.R. "Rankine-Cycle Working Fluids for Solar-to-Electrical Energy Conversion." Jan, 1974 Sandia Report 58-5556.
- Sons, R.L. "Optimization of a Point-Focusing Distributed Receiver Solar Thermal Electric System." An ASME Publication 79-WA/Sol-11, Aug. 1979.
- Werner, Douglas K. "Design and Test Results of a 63.4 KW(85 HP) Solar Powered Rankine-Cycle." Presented at the 1978 Annual Meeting of the American Section of International Solar Energy Society, Aug. 28-31, Denver, Co.

## REFERENCES

- Bird, S.P., "SOLSTEP — A Computer Model for Predicting the Thermodynamic and Economic Performance of Solar Thermal Power Plants." An ASME Publication, 79-WA/Sol-12, 1979.
- Duffie, John A., et al, Solar Engineering of Thermal Processes, New York: John Wiley & Sons, 1980.
- Holl, R.J., "A Solar Thermal Electric Power Plants with Early Commercial Potential." An ASME Publication, 79-WA/Sol-9, 1979.
- Jones, H.E., et al, "Small Solar Thermal Electric Power Plants with Early Commercial Potential." An ASME Publication, 79-WA/Sol-9, 1979.
- Kreith, Frank, Principles of Heat Transfer, New York: Intext Educational Publishers, 1973.
- Lönnroth, Mans, et al, Solar Versus Nuclear—Choosing Energy Futures, Trans. by P.C. Hogg, Great Britain: Pergamon Press, 1980.
- Sonntag, Richard E. and Van Wylen, Gordon J. Introduction to Thermodynamics: Classical and Statistical, New York: John Wiley & Sons, Inc. 1971.